Biomass Pyrolysis and Optimisation for Bio-bitumen

Master's Thesis

Olga N Kolokolova

University of Canterbury

Department of Chemical and Process Engineering

January 16th, 2014

Acknowledgements

I would like to say an enormous thank you to my mom, Olga Kolokolova, who has supported and encouraged me from day one of this project. My mom was very sympathetic and reassuring, when I had to make a tough call during this project. She constantly had interest in my work and provided me with healthy meals when I had to work incredibly long days. My beautiful mom always had time to listen to my problems and I would have not been able to succeed without her. This Masters achievement is very much hers, as well as mine.

A special thank you goes to my wonderful grandmother, Nina Meshkova, who is an engineer herself and who has been very encouraging and understanding during this project.

I would like to thank my incredibly patient partner Anthony Hills. Anthony had to put up with my long discussions about this project and has put in a tremendous amount of effort towards making our long distance relationship work. Because of this project's intensive workload, I could not come and visit him, and he has continuously made effort and visited me throughout the last two years, while I have been working on this project. I am very lucky to have him in my life.

I would like to show my appreciation to my amazing friend Monique Milne, who has helped keeping me sane during the demanding hours this project.

I acknowledge Shusheng Pang, my university supervisor, for his help and assistance during this project. His valuable input helped me make revisions to the material. Thanks to my second supervisor, Tana Levi, I was able to directly communicate at numerous meetings with Phil Harrington, the client representative from Opus, and other investors, who financially supported this project for CRL Energy.

I am really grateful to both of my supervisors Prof Pang and Dr Levi for your help, encouragement and opportunities you both have made available to me during this project. I have learnt a lot from you both and I value the experience I have gained from working with you.

I would also like to thank Tana Levi, Rodney Brown, Trevor Matheson, Ben Rumsey and all staff at CRL Energy Limited Lower Hutt, for their help and support during the project. Being a part of the Sustainable Energy Technologies team at CRL Energy has defiantly been a learning experience for me.

Abstract

Biomass waste has been recognised as a promising, renewable source for future transport fuels. With 1.7 million hectares of pine plantation forests and 12 million cubic meters of annual residue produced by sawmills and the pulp and paper industries, New Zealand presents a prime location where utilisation of these resources can take the next step towards creating a more environmentally friendly future. In this research, the process of fast pyrolysis was investigated using a laboratory-scale, nitrogen-blown fluidised bed pyrolyser at CRL Energy. This equipment can process 1–1.5 kg/h of woody biomass in a temperature range of 450–550°C. The purpose of this rig was to determine the impact of various processing parameters on bio-oil yields. Next, the pyrolysis liquids (bio-oil and tar) were processed downstream into bio-bitumen. Pyrolysis experiments were carried out on *Pinus Radiata* and *Eucalyptus Nitens* residue sawdust from sawmills and bark feedstock. The properties of the collected products, including pyrolysis liquids (bio-oil and tar), gas and solid biochars, were measured under different operational conditions. Further analysis was also performed to determine pH, volatile content, chemical composition and calorific values of the products. The ultimate goal for this project was to develop a feasible, advanced fast-pyrolysis system for a bio-bitumen production plant using various biomass feedstocks. Additionally, a design for a bio-bitumen production plant was developed, and techno-economic analysis was conducted on a number of plant production yield cases and bio-bitumen manufacture ratios.

Table of Contents

Table of Figures

Chapter 1: Introduction and Outline of the Project

1.1 Project Introduction

Woody biomass has been recognised as a promising renewable source of future transport fuels and chemicals produced through various conversion processes. New Zealand has 1.7 million hectares of *Pinus Radiata* plantation forests, the most common softwood in the country, and annually produces 12 million cubic meters of residue from forest harvesting, wood processing plants and pulp and paper mills (Forest Owners Association, 2012). Both the New Zealand government and industry have targeted utilization of these resources to achieve the goals of the Kyoto and Montreal protocols.

The need for a clean, renewable alternative to fossil fuels and crude oil bitumen has increased in recent years. With fossil fuel reserves decreasing and demand for fuel and power rising, extensive research and development efforts have been directed at energy production using biomass and biosolid wastes. Woody biomass consists mainly of hemicellulose, cellulose and lignin, which can be processed via different technologies to form various products. This research has focused on the pyrolysis of *Pinus Radiata* sawdust and bark.

Pyrolysis of woody biomass and other organic solid wastes is among the thermochemical processes with a promising future. During pyrolysis, feedstock is heated in an oxygen-free environment to between 400°C and 600°C. The products from the pyrolysis include liquids (bio-oil), gases and solid char, the proportions of which depend on the heating rate, operation temperature and residence time. A high temperature, fast heating rate and short residence will increase the production of gases, while a slow heating rate and low temperature will result in more solid char production. This solid char has a high energy density and improved storage and handling properties and can be easily powdered into a pulverised fuel. It can also be used in agricultural industries for sequestering carbon and increasing grain production. With further chemical treatments, the liquid products can be used as fuel or converted into bio-bitumen.

Bitumen is a main component of asphalt and has been used in road construction in New Zealand and across the world. New Zealand produces approximately 160,000 tonnes of bitumen annually, and bitumen prices have increased by 500% in the past 30 years, from $200/tonne in 1982 to $1,200/tonne in 2012 (Herrington, 2012). With higher demand for bitumen and diminishing fossil fuel supplies in the future, bitumen prices will likely keep increasing.

In long-term considerations, potentially environmentally sustainable bitumen has attracted great interest and support from both industry and government. In some industries, it is acceptable to pay a higher price for eco-products. However, other industries operate under the bang-for-your-buck theory. Either approach can be implemented in today's economic market, or the choice between the approaches rests with management teams and investors who typically consider a company's values and ethics code, the amount of financial investment available and the domestic economic environment (i.e., an expansion or regression phase in the economy or business cycle). Based on these trends, bio-bitumen's price per tonne could be higher than regular bitumen in the future. The market attraction of this new product is that is has similar or slightly lower production prices than crude oil bitumen while maintaining excellent quality and offering environmental benefits.

This report consists of two major parts. The first presents the practical work on a smaller-scale research pyrolyser, analysis of the collected data and determination and optimization of the conditions for the design of and feasibility studies for a pilot-scale plant. The second part discusses the preliminary upscale design of the waste to bio-bitumen conversion process and a techno-economic analysis of the preliminary design of a commercial plant.

The biomass feedstock used in the development process is residue from the wood processing industry, including sawdust, chips and barks. In the proposed pilot-plant design, the operations which

transform bulk biomass feedstock into bio-bitumen are divided into four separate sections, each of which uses different technologies.

1.2 Process Description and Products

Biomass consists mainly of hemicellulose, cellulose and lignin, which react and fractionate in thermochemical processes at different temperatures, as shown in Figure 1.1. Wild (2008) tested beech and poplar (representative of deciduous forests), spruce (representative of coniferous forests closely related to the *Pinus Radiata* analysed in this study) and straw (an herbaceous plant representative of agricultural waste). Wild (2008) used different types of forest plants to thoroughly analyse the decomposition steps in different temperature ranges. The mixtures generated at 250–300°C primarily contained hemicellulose degradation products, while the composition of the mixtures obtained at 350–400°C were mostly cellulose. Lignin-derived fragments were found in both temperature ranges

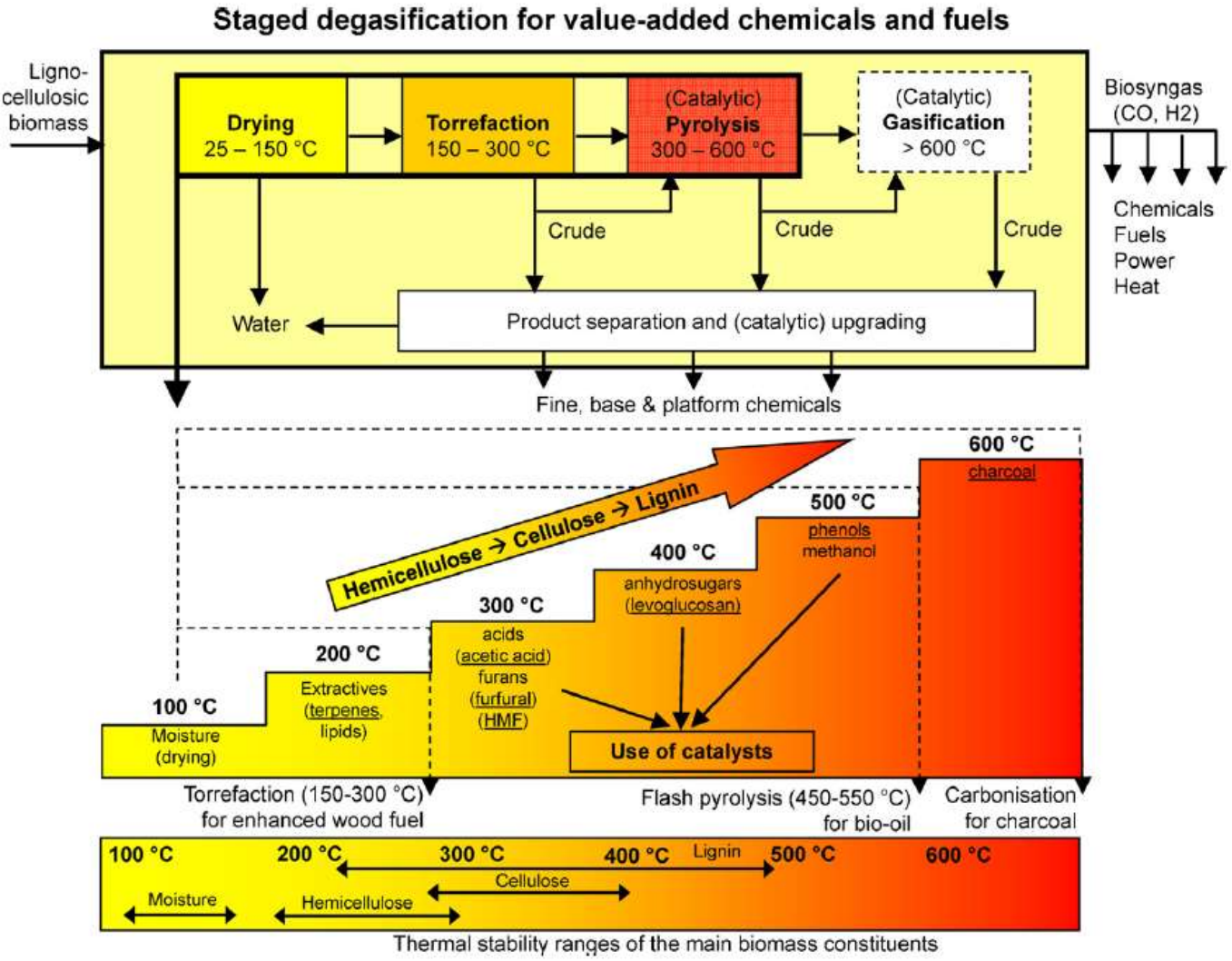

Figure 1.1: Staged degasification for value-added chemicals and fuels. (Wild, 2008)

Zhang and his colleagues (2007) conducted pyrolysis experiments using southern yellow pine, red oak and sweet gum sawdust, focusing on determining the composition of the pyrolysis process products. The experiment set up was similar to the experimental set up used during this project, both using nitrogen gas as carrier gas in the pyrolysis. This makes the data collected from southern yellow pine from the experiments by Zhang relevant to the results from the present study, discussed later in the thesis.

Zhang observed that wood thermal decomposition at 425-557 °C in the absence of oxygen causes extensive depolymerization/fragmentation of the macromolecular structures of the wood, which agreed with that observed by Wild (2008). Primary components of biomass (hemicellulose, cellulose and lignin) when placed in high temperature atmospheres result in 'cracking' to yield lower molecular weight products. Cross-linking via condensation reactions and water loss results in bio-char formation, Zhang (2007). Very high heat transfer rates reduce bio-char formation because volatilization is rapid, minimizing second-order polymerization rates. Whilst, longer vapour residence times at pyrolysis temperatures permit more secondary vapour-phase cracking to gases, water, formic and acetic acids, and other low-molecular-weight products. Thus high speed vapour quenching minimizes the extent of cracking. Here cracking implies high number of short hydro-carbon molecules in the liquid product, due to long chains breaking under specific conditions. From what, it follows, that higher yields of long hydrocarbon chains will result after rapid cooling of the 'pyrolysis gas' (the gas exiting the Fluidised Bed rector before it enters the cyclone). The list of most components in the products from pyrolysis of southern yellow pine sawdust tested by Zhang (2007) can be reviewed in Table 1.1.

Table 1.1: Percent yields of gaseous (left) & liquid (right) products from pyrolysis of southern yellow pine sawdust (Zhang, 2007).

components	538 °C
hydrogen	0.20
carbon monoxide	14.40
methane	2.06
carbon dioxide	8.34
ethylene	0.83
acetylene	BDL
ethane	0.40
propylene	0.60
propane	0.08
1-propyne	0.002
1,2-propadiene	0.26
acetaldehyde	3.27
methanol	1.26
1-butene	0.19
1,2-butadiene	0.09
2-butene	0.06
2-methyl-1-propene	0.03
propanal	0.32
acetone	0.23
2-methyl-1-buten-3-yne	0.18
2-butenal	0.19
3-buten-2-one	0.22
acetic acid ethyl ester	0.12
2-methylpropanal	0.09
sum of gas products	34.74

[1] BDL = below detection limit.

components	538 °C
benzene	0.05
toluene	0.12
ethylbenzene	trace
m- and *p*-xylene	trace
styrene	trace
o-xylene	0.03
ethylmethylbenzene	BDL
cyclopropyl benzene	BDL
phenol	0.18
OC-methylstyrene	BDL
2-methylphenol	0.13
4-methylphenol	0.18
indene	BDL
2,3-dimethylphenol	BDL
2-ethylphenol	BDL
2,4-dimethylphenol	0.12
2,6-dimethylphenol	0.02
4-ethylphenol	0.05
1,2-benzenediol	0.23
naphthalene	BDL
3-(1-methylethyl)phenol	0.01
2-ethyl-5-methylphenol	0.04
4-methyl-1,2-benzenediol	0.04
3-methyl-1,2-benzenediol	0.17
2-(2-propenyl)phenol	0.05
1-methylnaphthalene	BDL
2-methylnaphthalene	BDL
biphenyl	BDL
1,3-dimethylnaphthalene	BDL
acenaphthalene	BDL
fluorene	BDL
anthracene	BDL
phenathrene	BDL
fluoranthene	BDL
pyrene	BDL
sum of C6−C16	1.45
char	17.42
sum of gases	34.74
total mass yield	53.61

Salehi (2011) has performed a study on waste wood sawdust pyrolysis in a fluidised bed reactor with focus on the influence of the pyrolysis temperature, feedstock particle size and residence time in the reactor on the product yield as well as product composition. In the experiments, the feedstock sawdust was sieved into three size sets (<0.59 mm, 0.59-1 mm, 1-1.4 mm) and at the operation temperatures were controlled in the range of 425-550°C. Figure 1.2 shows product distribution versus the pyrolysis temperature.

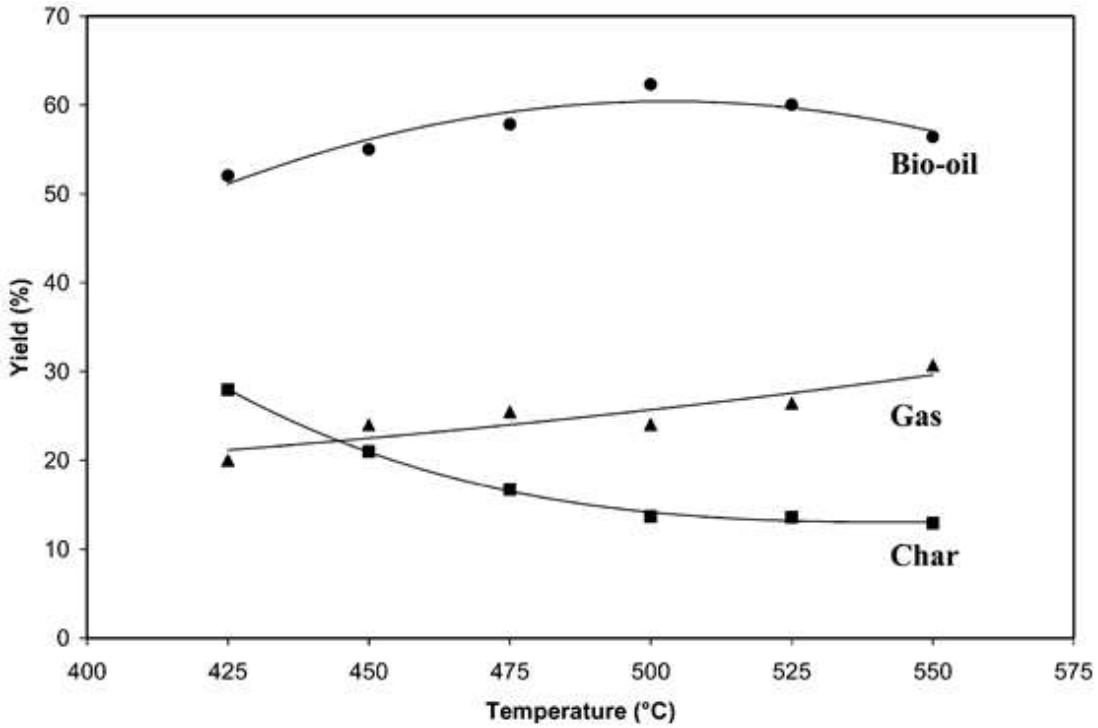

Figure 1.2: Product distribution versus the pyrolysis temperature (Operational conditions: nitrogen gas flow rate, 15 L/min; sawdust particle size, <590μm) (Salehi 2011)

From the experiments of Salehi (2011), it has been found that at the temperature of 425°C, the total bio-char yields was 30% of the feed, the non-condensible gas yield was 20%, and the bio-oil yield was 50%. The product composition varied with the operation temperatures in the researched range as observed in Figure 1.2.

1.3 Project Background: The Bigger Picture

The project presented in this thesis is a part of a large research programme called the National Land Transport Programme (NLTP) run by the New Zealand Transport Agency (NZTA) and Opus International Consultants. The programme contributes to the economic development and sustainability in the roading industry in New Zealand. Its aim is to advance New Zealand roading through the development of new road construction and maintenance technologies and materials. A key objective is to reduce consumption of non-renewable bitumen by replacing it with a non-food biomass bio-bitumen developed from renewable and environmentally friendly resources. The other objectives include developing a new method of roading construction, recycling existing pavement and chip seal materials and extending the lifetime of the road structure (NLTP, 2005).

The NLTP programme, which began in 2005, addresses the issue of high roading construction and maintenance costs. Due to increasing vehicle numbers, there is a clear need to reduce these high costs and to improve the physical performance and long-term environmental sustainability of the roading network in New Zealand. Heavy traffic volumes are predicted to increase by 60% by 2040, leading to more frequent road maintenance and associated road construction costs (New Zealand Ministry of Transport, 2008). This project is considered a step-change in the development of new roading materials (The Allen Consulting Group, 2004).

The cost of bio-bitumen production has been identified as a potential barrier; however, its price is predicted to decrease in the future due to technology improvements. The uptake of bio-bitumen and new road construction methods will benefit the long-term wellbeing of the country.

1.4 Project Objectives

1. The principal objective of this project is to advance the knowledge in biomass conversion to bio-bitumen for roading construction applications.

2. The second objective of the project is to improve the existing pyrolysis system and to optimise the operation conditions for production of a new product that can potentially be used as a partial or complete substitute to petroleum derived bitumen. This part of the project consists of laboratory pyrolysis system development and improvements, for production of target product at the maximum yield. Optimal conditions which maximised yields of high molecular weight organic species ('tar') collected are favoured. Other useful products obtained from the biomass pyrolysis are also subjects of interest as applications of these by-products can be improve the economy or these by-products can before processed for production of bio-bitumen.

3. The third objective of the project is to conduct scale up design and cost analysis using the operation data collected from the experiments.

1.5 Thesis Outline

The second chapter of this thesis is the extensive literature review on pyrolysis process and products. Effects of operation conditions on the product yield and product distribution were also examined. Feedstocks for production of fossil fuel derived bitumen and biomass based bio-bitumen were described and their properties are discussed. Potential applications of bio-char, a by-product from biomass pyrolysis, were also examined.

Chapter three describes the experimental part of the project which includes detail discussion on pyrolysis rig used in the study with particular attention paid to the problems encountered and the im-

provements made to the rig during this investigation. This chapter also covers the experimental methodology and materials used as the feedstock in the experiments. This chapter also described the analysing methods for the biomass pyrolysis products.

Chapter four of this thesis presents the experimental results as well as discussion of these results with regard to the production yields of useful products and examined factors which influence product yields.

Chapters five and six present the description and design of the scale-up pilot plant. Chapter five describes all stages of the process of biomass into bio-bitumen conversion while Process Flow Diagrams (PFDs) and Piping and Instrumentation Diagrams (P&IDs) are included in chapter six.

The seventh chapter of this thesis covers the techno-economic analysis of the commercial plant design which includes design and costing analysis. It additionally contains the sensitivity and the cash flow analyses, which outline the proposed process specifications and commercial value. References Chapter eighth gives the research conclusion and recommendations for design of a commercial bio-bitumen plant.

In the appendices, health and safety aspects, raw data collected and all calculations are presented.

Chapter 2: Literature Review

2.1 Process Background

2.1.0 Specific Terminology used in Chapter 2 cited from The Free Dictionary by Farlex (2013)

Energy density: energy per unit volume.

Flash point of a liquid fuel: the lowest temperature for the vapour above the liquid to be ignited when exposed to a flame.

Lubricity of a liquid fuel: the ability to reduce wear and friction.

Newtonian fluid: fluid in which the state of stress at any point is proportional to the gradient of strain over time at that point.

Pour point of a liquid fuel: the lowest temperature at which a liquid can flow without disturbance.

2.1.1 Biomass Pyrolysis

Fast Pyrolysis is a thermo-chemical process in absent of oxygen which converts biomass feedstock to liquid (bio-oil), gases and solid char (Wild, 2008). The fast pyrolysis is commonly operated as the temperature range of 400-600°C with very rapid heating rates (Sadaka, 2009). Reactions taking place at different stages of pyrolysis and corresponding products under various operation conditions (temperature, pressure and residence time) are presented in Figure 2.1. Short vapour residence time provides high quality products and ethylene-rich gases. Liquid products of the pyrolysis process may be used as fuel or converted into other valuable materials like bio-bitumen (Herrington, 2012). The gas products could be used to produce alcohols or gasoline or directly combusted. The solid products of the process may be used in agricultural industries buried in soil for retaining nutrients or used as a solid fuel (Sadaka, 2009).

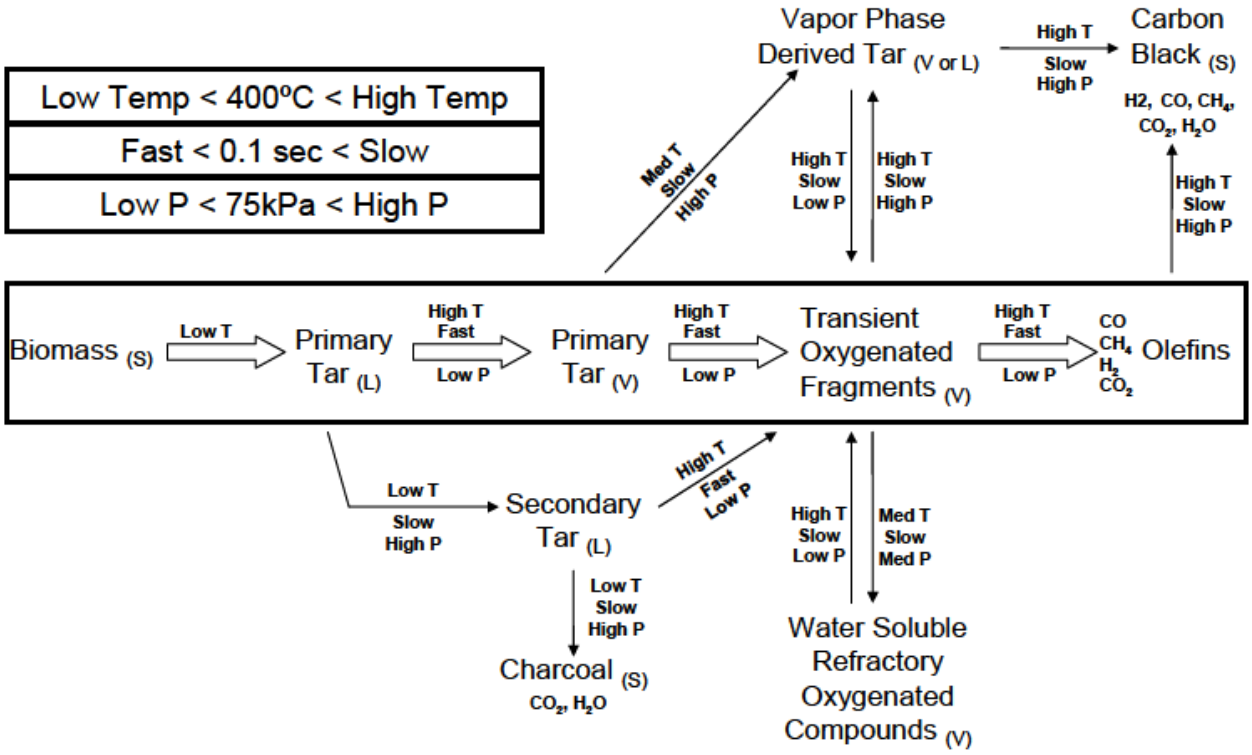

Figure 2.1: Reactions taking place in pyrolysis (Sadaka, 2007)

2.1.2 Formation of Volatiles

During pyrolysis dehydration and fragmentation are the two main reactions occurring, shown in Figure 2.1. Dehydration reaction occurs under slow heat rates and long residence time of the process. During this process bio-char and water vapour are formed. Sadaka (2007) summarised that an increase in the heat rate and temperature, triggers the formation of free radicals and low molecular weight (<105) volatile compounds such as hydrogen, carbon monoxide and carbon dioxide. Dehydration is expected to occur in temperatures below 310°C and typically slow pyrolysis. Fragmentation occurs at temperatures higher 310°C. During fragmentation pyrolysis vapour and bio-char mixture depolymerises to for levoglucosan and tar (Sadaka, 2007), Figure 2.2. Under conditions of rapid heat rate (flash or fast pyrolysis) and high temperatures portion of tars vaporises and oxygenated fragments are produced. These are further cracked to alkenes, carbon monoxide, nitrogen and hydrocarbons like acetol, furfural and aldehydes (Sadaka, 2007).

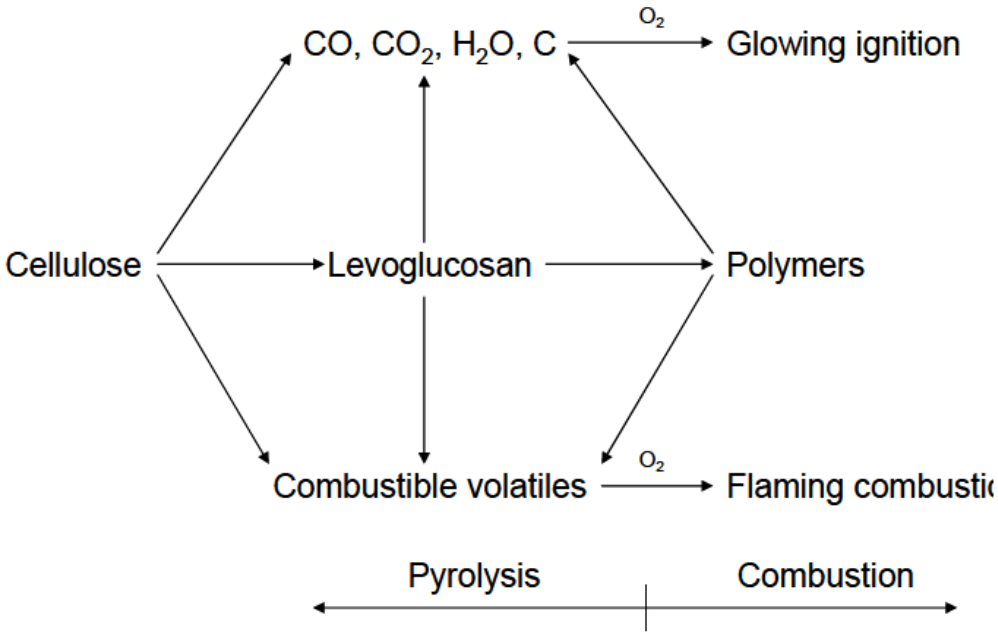

Figure 2.2: Pyrolysis and combustion of cellulose (Sadaka, 2007)

2.1.3 Product Yields - Affecting Factors.

The two key parameters affecting the pyrolysis product composition and the product yield are the operating temperature of the reactor and the residence time of the feed and the product throughout the whole system. Yield of solid product (char) decreases and the solid product energy density increases as the operating temperature and the residence time are increased. However the energy conversion rate decreases as these two parameters increase. Therefore, the pyrolysis process operational conditions can be varied depending on the target chemical and physical qualities of the product from the pyrolysis (Saddawi, 2010).

In his investigations Salehi (2011) found the temperature of the pyrolysis process to be the most influential parameter. Bio-char yield decreased significantly by increasing the pyrolysis temperature. Salehi also found that the bio-oil yield declined as the biomass particle size was increased. With the particle size increasing, the water content in bio-oil also increased (Salehi, 2011).

Qiang (2009) completed a review on the properties and utilization of bio-oils from biomass pyrolysis. High yields of bio-oil are achieved at operating temperature of 500°C, very high heating rates (103–105°C/s), short vapour residence time (<2 s) and rapid quenching of the pyrolysis vapours. Numerous bio-oil properties and bio-oil performance in different applications were examined including homogeneity, microscopic multiphase structure, oxygen composition, water composition, heating value, rheological property, viscosity, ash, flash point, pour point, cloud point, thermal conductivity and stability, distillation and thermogravimetric property, storage, surface tension, combustion, atomization, ignition, lubricity, evaporation, acidity, corrosion, toxicity, and bio-degradability.

In conclusion Qiang (2009) found that homogeneity of bio-oils depends on the initial wood composition. The bio-oils produced from pyrolysis of woody biomass separated into two phases if left for sufficient time: top phase rich in extractives and bottom phase resembling the normal bio-oils. The water in the bio-oils delays the ignition, thus it is important to know the percent of water in the oils produced from the biomass pyrolysis. Additionally, an aquatic phase in oils reduces combustion rates and adiabatic flame temperatures during the combustion process. Bio-oils retain most of the original oxygen composition. Oxygen is known to be the primary reason for the property differences between biomass pyrolysis bio-oils and petroleum derived fuels. Rich in oxygen pyrolysis oils are polar compounds, and thus non-miscible with non-polar petroleum fuels. High oxygen content in the biomass pyrolysis bio-oil is also responsible for the low heating value, corrosiveness and instability of bio-oils as pointed out by Qiang (2009).

The findings of Qiang (2009) are consistent with conclusions made by Wang and Kersten (2005) who stated that removal of oxygen from bio-based fuels for liquid hydrocarbon fuel is needed to increase its energy intensity and stability, and decrease its viscosity. This is one of the issues needed to be addressed in bio-bitumens production research.

As the goal of this project is to achieve high yield of the long hydrocarbon chains with improved product quality, tar is more valuable material than light bio-oil for the production of bio-bitumen. However, it is helpful to understand the properties of all of the bio-oil product from biomass pyrolysis as described by Qiang (2009).

From the review conducted by Qiang (2009), most bio-oils from the pyrolysis of woody biomass behave as Newtonian fluids under 80°C. The flash point of the bio-oils varies from 40 to above 100°C, dependent on light organics composition. The pour point of the bio-oils is in -12°C to 33°C. With storage time, the bio-oil has shown slow increase in viscosity, however, the viscosity decreases fast under heated environment. During distillation under atmospheric pressure, the bio-oils start boiling at temperature of around 100°C and the boiling finishes at temperatures of 250–280°C, leaving 35–50 wt% of residues. The viscosity and surface tension of the bio-oils are higher than those of light petroleum fuels. The review by Qiang (2009) also reported that bio-oil shows a certain extent of lubricity.

Bio-oils contain about 7–12 wt% acids and have a pH of 2-4, therefore, the bio-oils are corrosive to aluminium, mild steel and nickel-based materials. The corrosion rates would be enhanced at elevated temperatures or with the increase in water contents.

Orfao (1999) performed pyrolysis experiments for pine, eucalypt and pine bark using TGA. Peak maxima was identified as the temperature at which the rate of mass loss was the highest. The measured percentage of mass loss over the temperature range can be used to find out the maximum conversion as presented in Table 2.1 for each of the materials tested. The values provided by Orfao (1999) predominantly agree with temperature ranges suggested by Wild (2008) as illustrated in Figure 1.1. However Orfao tested smaller samples, which explains the variation in the peak maxima temperature.

Table 2.1: Peak Maxima and Maximum Conversions of Samples tested by Orfao (1999)

Sample	Peak Maxima (°C)	Maximum Conversion (%)
Cellulose	332	94.9
Xylan	281	79.5
Lignin	363	62.6
Pine Wood	330	82.5
Eucalyptus	331	82.1
Pine Bark	331	61.5

From Table 2.1, it is noticed that cellulose and lignin peak maxima fall within the range of torrefaction temperatures, however, the wood and bark samples have similar peak maxima (330-331°C) although the bark has a lower maximum conversion.

2.2 Summary of Previous Biomass Pyrolysis Studies

Oasmaa (2011) used titration method to investigate the changes in the carbonyl compounds for determination of the bio-oil stability. The change in viscosity is also regarded a measure for the bio-oil stability which is related to the changes in the molecular weight of water insolubles present in the bio-oil. Figure 2.3 shows the results of the bio-oil stability from fast pyrolysis of woody biomass of forestry residues.

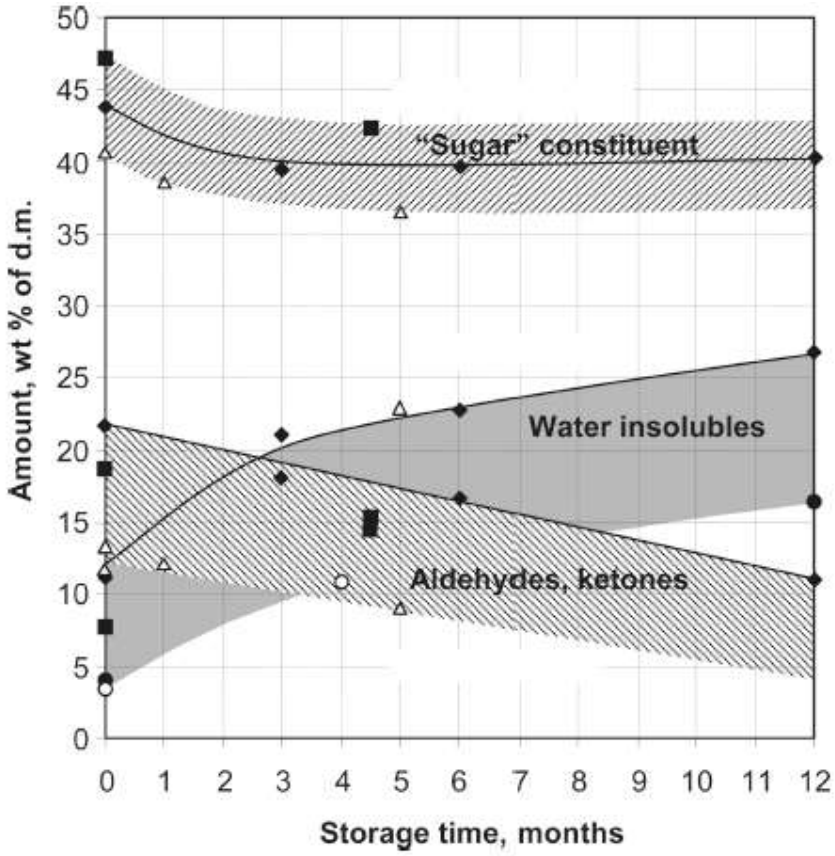

Figure 2.3: Stability test result of bio-oil produced from pyrolysis, presented as changes in sugar constituent, water insolubles and aldehydes/ketones on dry basis with stiorage time (Oasmaa 2011).

The increase in water-insoluble content correlates positively with increased molecular weight distribution and viscosity (Oasmaa, 2011). Boateng (2007) in Agricultural Research Service US developed a fluidised bed fast pyrolyzer unit with capacity to process 2.5 kg/h biomass of switchgrass. The fluidised bed material used was silica sand and the fluidizing gas was Nitrogen. Table 2.2 pre-

sents distribution of pyrolysis product yields at operation temperature of 500°C. From the results in Table, the bio-oil yield is 60.7% and the char yield was 12.9%. The energy conversion efficiency from biomass to the bio-oil yield was about 60% as the heating value of the switchgrass and that of the bio-oil are similar; however the bio-oil has a specific gravity of 1.2-1.3 which is 2.4-2.6 times of that of palletized switchgrass.

Table 2.2: Distribution of product yields from fast pyrolysis of switchgrass biomass at 500°C operating temperature (Boateng, 2007).

	mass, kg	mass, wt %
biomass	1.647	
char	0.212	12.9
noncondensable gas	0.186	11.3
bio-oil	1.000	60.7
difference	0.250	15.2

The energy recovered from the biomass and contained in the bio-oil produced was about 60%. The switchgrass and bio-oil heating values were similar; however the bio-oil had a specific gravity of 1.2-1.3, compared to about 0.5 for densely palletized switchgrass. These findings agree with 60-65% bio-oil yields and 15% bio-char yields observed in the current study.

Oasmaa (2009) developed a pyrolyser for pyrolysis of biomass of agricultural residues and wood at feeding rate of 20 kg/h into PDU (process development unit) and 1 kg/h for the bench scale pyrolysis uni. The bio-oil and gas produced from the pyrolysis were used in a fluidized-bed boiler. Operation temperature was varied between 480-520°C. The correlation of bio-oil yield with the feedstock ash from fast pyrolysis of biomass is shown in Figure 2.4.

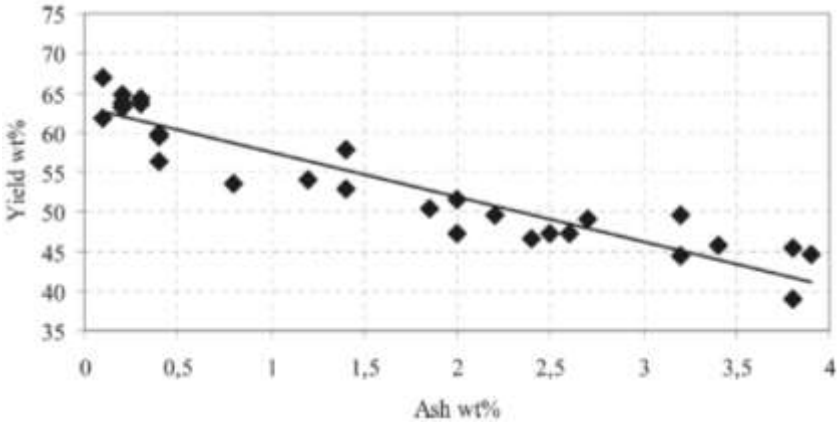

Figure 2.4: Correlation of bio-oil yield with the feedstock ash from fast pyrolysis of biomass (Oasmaa, 2009).

A fixed bed tubular gasifier was used by Salehi (2009) to pyrolysise wood sawdust and to investigate the effects of the sweep gas flow rate, operating temperature and heating rate on the product yields. The feedstock was dried overnight to 10% moisture content. The optimum yield of bio-oil was achieved at a pyrolysis temperature of 500°C, heating rate of 100°C/min and nitrogen flow of 2 L/min. The bio-oil collected contained compounds of aromatic and carbonyl structures, thus had low pH and heating values.

Solantausta (2011) conducted studies in a bubbling fluidised bed pyrolysis reactor with bio-oil and gas produced being used in a conventional fluidised bed boiler. The pyrolysis plant had a capacity of feedstock feeding rate of 7 odt/d (oven-dry tonne per day). In the study of Solantausta (2011), the feestocks were forest residues and sawdust of pine and eycalyptus as well as straw and grass. The pyrolysis temperature was about 480–520°C, and the residence time for pyrolysis vapours was about 0.5–2 s. Figure 2.5 shows the bio-oil yield and composition of organic content and water content from pyrolysis of different feedstocks which had different organic proportion and moisture content.

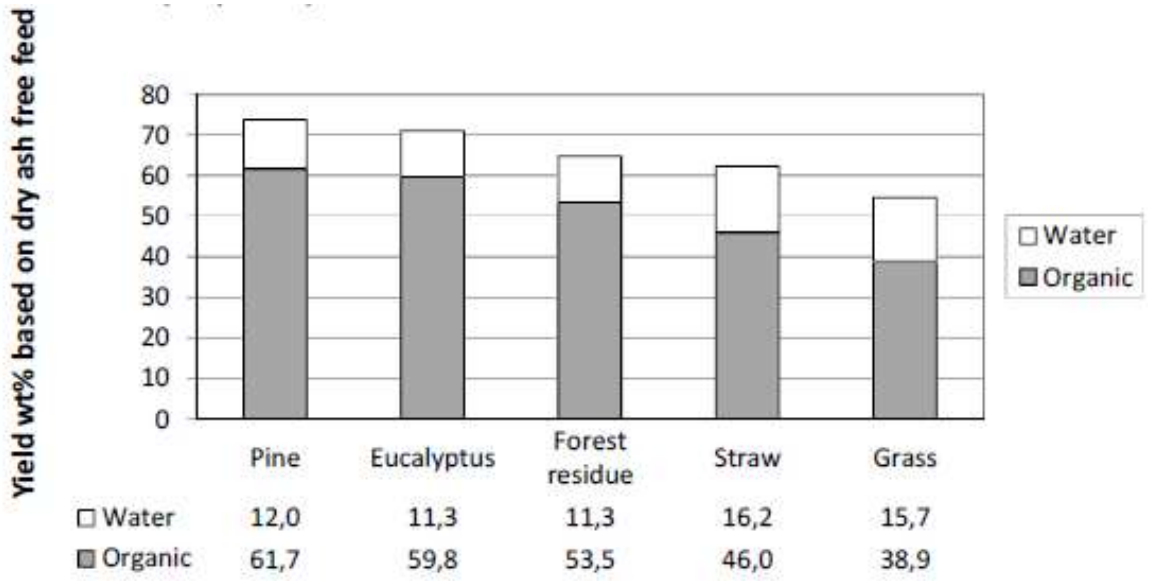

Figure 2.5: Yields and composition of bio-oils from pyrolysis of various types of biomass (Solantausta, 2011).

Some researchers have tried adding a catalyst like HZSM-5 to the pyrolysis reactor to increase valuable products. Atutxa (2005) conducted flash pyrolysis of sawdust at 400°C in a conical spouted bed reactor. HZSM-5 zeolite catalyst was added in the reactor bed which was found to affect the product yields. The yield of gas increased with addition of the catalyst in the system while the yield of liquid decreased. However, the composition of the bio-oil changed with addition of the catalyst with heavy organic fraction being partially transformed to the aqueous fraction due cracking and the aqueous liquid fraction undergoing reactions of dehydration, decarboxylation and decarbonylation. Both reactions contribute to the increase in the generation of CO and CO_2. Therefore, bio-oil obtained by the catalytic pyrolysis has a lower average molecular weight and is less oxygenated than the bio-oil obtained by conventional pyrolysis. Catalytic pyrolysis bio-oil is less viscous, less corrosive and more stable than the bio-oil from the conventional pyrolysis, thus it is a better fuel for use in diesel engines. However, the objective of this project was to maximise the yield of heavy bio-oil tar and thus the ctaalytic pyrolysis will not be investigated in this study.

The conical spouted bed reactor is favoured over fluidised bed reactor in this study due to its capacity for handling solids of irregular texture with suitable gas, the geometry allows for handling mix-

tures of solids of different hydrodynamic properties, nonexistence of gas distributor plate, cyclic movement of the solid, low pressure drop, easy design, and great capacity for being scaled up.

Branca (2006) conducted studies on conventional pyrolysis on sawdust, bark, agricultural residues (straw, olive husks and nut shells) and cellulose. Two liquid fractions, namely A and B, were collected during the experiments and analysed. Fraction A was collected by ice-cooled condensers. It was rich in water and consisted of compounds with relatively low molecular weights. Fraction B was collected as a superficial muddy layer above the water scrubbers. It presumably constituted of extractives and pyrolytic lignin. The aqueous fraction was about 70-76% of the mixture. Higher yields of solid residues (26-35%, dry liquid basis) were found from fraction B, consisting of phenolic compounds and presumably extractives and high-molecular-weight species.

Prins (2006) conducted a study in a quartz fixed bed reactor placed inside an oven which was controlled up to 300°C, with a flow of argon gas as the inert medium. Biomass species tested were beech, willow, larch and straw. In the study of Prins (2006), volatile products were cooled down to -5°C and the final product was split into liquid and gas phase. Due to the low operation tempetrature, the solid yield ranged from 98% at low temperatures to approximately 65% at 300°C. At higher temperatures the yield of formic acid, methanol, lactic acid, furfural, hydroxyl acetone and phenol increased. The yields of non-condensable gases also increased with temperature. The gas yield from pyrolysis of willow (gas yield 10wt%) was found to be greater than that from pyrolysis of larch (gas yield 2-5wt%). The composition of this syngas was mainly carbon dioxide, methane and carbon monoxide. The proportion of carbon monoxide increased with temperature.

Dominguez (2008) observed the thermal stability and pyrolysis kinetics of lignins extracted from *Eucalyptus globulus* samples after TGA. Dominguez showed slow lignin degradation with temperature over a range 200-800°C. No sharply defined peak maxima for the lignin (that is seen with cellulose and hemicelluloses) was observed. The decomposition of lignin over a wide range of tempera-

tures was attributed to the complex structure of lignin resulting in a number of different reactions involved in the degradation requiring different activation energies.

Azeez (2010) performed a series of pyrolysis experiments in a fluidized bed reactor. He aimed to compare the pyrolysis differences between African woods of iroko (*Chlophora excelsa L.*), albizia (*Albizia adianthifolia L.*) and corncob (*Zea mays ssp.*) and some European woods of spruce (*Picea abies L.)* and beech (*Fagus sylvatica L.*). The fluidised bed pyrolysis reactor was operated at 465 to 470°C. Phisicap chemical analysis was carried out prior to the experiment. The tropical African woody biomass was found to be richer in extractives than the European woods. The extractives are defined as phenolic compounds, terpenes, aliphatic acids, chinones and alcohols. Table 2.3 gives the detailed product yields for pyrolysis products and Table 2.4 shows the detailed results of pyrolysis product analysis using different types of woody biomass as mentioned above.

Table 2.3: Analysis results of pyrolysis product yields of different wood species (Azeez, 2010).

	beech	spruce	iroko	albizia	corn cob
reactor temperature	465–470 °C	465–470 °C	465–470 °C	465–470 °C	465–470 °C
total liquid product wt %	70.1	69.9	56.4	61.4	61.3
bio oil wt %	62.7	62.7	50.6	54.7	56.2
condensate wt %	7.4	7.3	5.8	6.7	5.1
organic[b]mf wt %	57.5	57.1	40.4	47.6	43.9
gas[c]	22.6	23.0	23.1	24.3	27.2
char daf %	10.2	10.1	22.8	16.6	14.7
pyrolytic water wt %	9.7	9.8	13.3	11.2	14.0
biomass-to-volatiles wt %	88.7	86.7	77.5	83.3	83.6

Table 2.4: Analysis results of pyrolysis products of different species of woody biomass (Azeez, 2010).

	beech	spruce	iroko	albizia	corn cob
		bio-oil			
water content %	22.2	22.0	32.3	25.1	32.2
viscosity (40 °C) cST	15.2	14.8	-	57.1	6.7
pH	2.5	2.8	2.9	2.9	3.0
solid content %	0.2	0.1	0.2	0.2	0.1
lignin content %	15.0	15.4	14.1	12.2	8.5
carbon %	41.4	42.3	38.2	41.9	38.1
oxygen %[a]	51.2	50.3	54.0	50.1	53.2
hydrogen %	7.1	7.2	7.5	7.4	8.0
nitrogen %	0.2	0.2	0.3	0.6	0.7
HHV MJ/kg	16.9	17.2	15.9	17.4	15.8
carbon mf. wt%	53.3	54.2	56.5	55.9	56.2
oxygen mf. wt%	20.7	19.8	8.5	14.9	7.7
hydrogen mf. wt%	6.0	6.1	5.8	6.2	6.6
nitrogen mf. wt%	0.3	0.3	0.4	0.8	1.0
HHV MJ/kg[b]	23.4	24.0	25.6	25.2	25.6
		condensate			
water content	64.2	66.3	76.6	70.4	74.3
carbon mf wt. %	40.4	44.51	46.0	37.2	42.7
		char (maf wt. %)			
carbon	73.6	72.9	68.4	70.4	67.7
oxygen[a]	6.3	12.8	15.3	15.8	9.2
hydrogen	3.4	3.3	3.4	3.1	3.2
nitrogen	0.2	0.2	0.2	0.4	0.5
HHV MJ/kg[b]	29.1	28.0	26.3	26.6	26.5

[a] By difference. [b] Values calculated according to Boie's equation.

In the above tables, *a* represents by difference*; b* means values calculated according to Boi's equation.

From Tables 2.3 and 2.4, it is found that that the bio-oil from corncob had the lowest lignin content. Additionally, according to Azeez (2010), bio-oil from corncob contained a high concentration of 4-vinylphenol, a lignin derived product. The pyrolysis of African hardwood biomass resulted in lower organic yield, but high pyrolytic water and bio-char contents compared to European biomasses. Azeez (2010) research proved the acetic acid, hydroxyacetaldehyde, hydroxypropanone, and levoglucosan to be the largest individual components in the volatiles. The higher heating value of all bio-oils ranged 16-17 MJ/kg in this study.

Sascha and Kesten (2005) conducted a literature review on biomass pyrolysis with focus on kinetics modelling for a single biomass particle in the pyrolysis. Figure 2.6, cited from Sascha and Kesten

(2005), shows the model predicted product yields and conversion time at different operation temperatures based on various models.

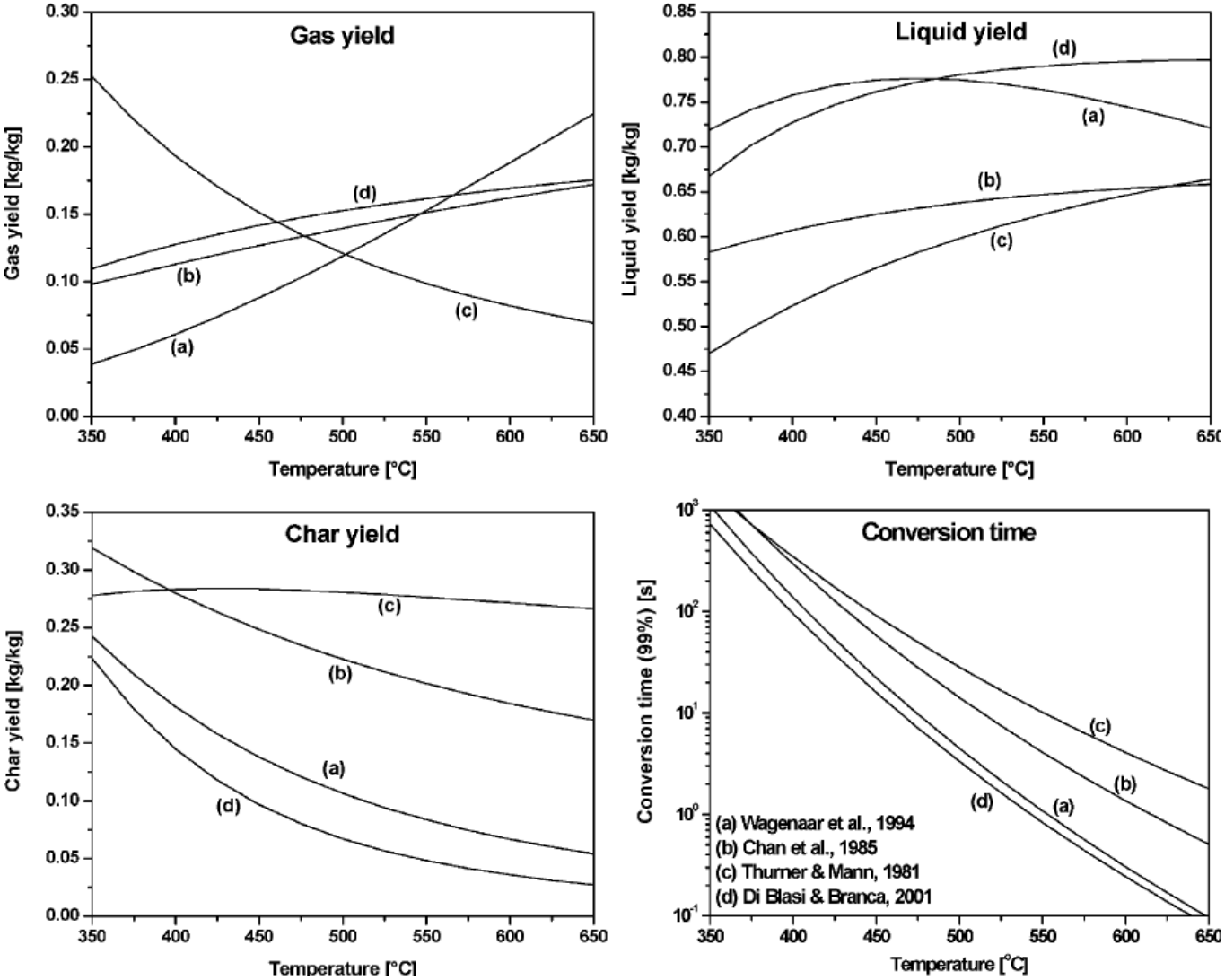

Figure 2.6: Product yields and conversion time (99% conversion) as predicted by the intrinsic kinetic models of (a) Wagenaar et al. (1994), (b) Chan et al. (1985), (c) Thurner and Mann (1981) and (d) Di Blasi and Branca (2001). (cited from Sascha and Kesten, 2005).

In Figure 2.6, the kinetics curves and the conversion time curves were predicted from four different models including a first-order decay reaction (a) Wagenaar), a three parameter nucleation model (b) Chan), a distributed activation energy model (c) Thurner and Mann) and a superposition model based on first-order reactions (d) Di Blasi and Branca). Of these pyrolysis reaction kinetics models, the distributed activation energy model best predicted the yield trends, thus showed the best perfor-

mance. This model was referred to by Sascha and Kersten (2005) and was cited from Stenseng (2001). From the predicted results using the models of Wagenaar et al. (1994) and Di Blasi and Branca (2001), the maximum yield of bio-oil is obtained at the temperature range 425-550°C which is consistent with other published results (Scott (1999), Zaror (1984), Luo (2004)). Therefore, in the present study, the operation temperature will be controlled in this range. Except for the model of Thurner and Mann (1981), all of the model predict that the gas product yield increase while the char product yield decreases with the pyrolysis temperature.

Sascha and Kesten (2005) investigated the effect of particle size and the heating rate in a fixed bed pyrolysis reactor, and found that the product yields did not change with the particle size but the bio-oil yield increased with increase in the heating rate.

Sascha and Kesten (2005) also developed three types of models to predict the conversion time and product yields for pyrolysis of single biomass particles with 5 mm diameter at 527°C. Table 2.5 shows the predicted results from an intrinsic model, a 1D model and a 2D model.

Table 2.5: Model predicted results from three different models for pyrolysis of a wood Particle with d_p=5 mm at 527°C (Sascha and Kesten, 2005).

		2D model			
l_p/d_p permeability	intrinsic kinetics	1 isotropic	1 anisotropic	3 anisotropic	1D model ∞
τ, s	2	22	20	34	35
gas yield, kg/kg	0.14	0.1	0.1	0.09	0.09
liquid yield	0.77	0.77	0.78	0.76	0.76
char yield	0.09	0.13	0.12	0.15	0.15

Wang and his colleagues (2005) conducted experimental studies on pyrolysis of woody biomass in a bubbling fluidised bed reactor, which included pine, beech and bamboo. The particles size tested varied from 0.7 to 17 mm. The vapour's residence time in the pyrolysis reactor was 0.25-6 s. In the experiments, preheated nitrogen gas at a velocity of 0.032 m/s passed through the fluidised bed reac-

tor and silica sand with particle diameter of about 258μm was used as the bed material. The bed temperature was alternated during the experiments and it was found that the maximum bio-oil yield of 65 wt% was achieved at the pyrolysis temperature range of 450-550 °C.

2.3 Bitumen and Bio-bitumen

Natural bitumen is the oil contained in clastic and carbonate reservoir rocks. These are mostly accumulated near the Earth's surface. The clastic rocks are composed of fragments of pre-existing rock (Demirbas, 2010), often referred to as tar sands or oil sands. Natural bitumen is found in 183 identified deposits in 21 countries in 2010. Tar sands contain about 10–15% bitumen, with the remainder being sand or other inorganic materials. The deposits are highly viscous at reservoir temperatures, and have high density (low API gravity), significant contents of nitrogen, oxygen and sulfur compounds as well as heavy-metal contaminants (Rodríguez-Valverde, 2007).

Presently bitumen is commonly produced in petroleum refining industry via non-destructive distillation of crude oil (Lesueur, 2008). However, not all crude oil yields significant amounts of bitumen. The heavier the crude oil, the higher the bitumen yield (Corbett, 1965). It exist as a viscous viscoelastic liquid at room temperature and thus behaves like thermoplastic nature. It has high resistant to water but shows adhesion toward most substances. Bitumen density at room temperature is between 1.01 and 1.04 g/cm^3 (Whiteoak, 2003). Bitumen is a very popular engineering material used in roading industries as a binder in the road construction. Stones and bitumen mixture produces asphalt, also referred to as an asphaltic concrete mixture. During the mixing, the bitumen is heated to around 160°C in order to decrease its viscosity (Lesueur, 2008) and is then mixed with stones at a weight ratio of 5:95 (bitumen: stones). For the roading application, the pre–mixed of bitumen and stones may be applied cold, warm (92-120°C) or hot (150°C) (Wikipedia, 2013).

The world's largest hydrocarbon deposits are located in Alberta (Strausz, 2010). These contain 1.7 trillion barrels deposits of bitumen and 1.7 trillion barrels of heavy oil (Strausz, 2010). Bitumen in

sand rocks and oil sands are located here. 0.86 trillion barrels in carbonate rocks (the carbonate trend resources) were also discovered in Alberta (Strausz, 2010). These bituminous deposits are dense, slightly viscoelastic, semi-solid hydrocarbons with a dark brown to black colour, richly endowed with heteroatoms (N, O, and S), trace level metals, and organometallic compounds (Strausz, 2010).

In New Zealand the Bitumen is supplied by Marsden Point refinery in Whangarei, which is the only refinery in the country. Marsden Supplies approximately 120 000 tonnes of bitumen annually (Hills, 2013). Bitumen is the heaviest form of petroleum with viscosity >104 mP.s and a density >1.000 g/cm^{-3} (Hills, 2013).

Roading industry is highly developed in New Zealand. 11 000 km of country's land area is covered by state highways, with 82 000 km roads linkage between cities and towns with total investment of $12.5 billions (NZTA, 2009). In every 10 to 12 years, the roads in New Zealand need resurfaced, and in every 60 years on average, the roads need to be totally re-built (NZTA, 2009). With 90% of New Zealand roads covered in asphaltic concrete mixture, bitumen is evidently a highly demanded material.

As the present bitumen is derived from fossil resources, it is unsustainable. Therefore, development of bio-bitumen from renewable resources has attracted great interests. However, the bio-bitumen needs to meet the quality requirement for the road construction which will be accepted by industry, possibly with some minor adjustments to the current application technologies. The bio-bitumen is presently a mixture of treated liquid products collected from pyrolysis of woody biomass which can be blended, at a certain ratio, with the conventional crude oil based bitumen. This blended bio-bitumen and traditional bitumen can be sold for a similar or slightly lower price to the construction and roading manufactures. The bio-bitumen has a great potential in New Zealand and may be commercially available on the market in less than 10 years' time (Herrington, 2012).

Prior to commercialization, the product will need to undergo and pass several tests to show compliance with NZTA M/1 New Zealand quality specifications. Various viscosity and aging tests are currently conducted at Opus International Consultants, Wellington, New Zealand.

The pyrolysis liquid products used in bio-bitumen production process are tarry being viscous but pourable, consisting of longer hydrocarbon chains with dark brown or black colour. An overview of the fast pyrolysis bio-oil properties and its elements analysed by Bridgwater (2010) are presented in Table 2.6 for feedstock of woody biomass.

Table 2.6: An overview of the fast pyrolysis bio-oil properties and its elements for feedstock of woody biomass (Bridgwater, 2010).

Moisture Content %	25.00
pH	2.5
Specific Gravity	1.20
HHV MJ/kg	17.00
Viscosity at 40°C cP	40-100
Solids (bio-char) %	0.10
Elemental Analysis	
C wt% db	56.4
H wt% db	6.20
N wt% db	0.1
O wt% db	37.30
Ash %	0.1

2.4 Bio-char

As discussed above, pyrolysis of biomass also generates solid product, bio-char, which is a carbon-rich solid with improved grindability compared to the original biomass due to the breaking down of the biomass chemical structure that provides tenacity. In addition, the bio-char has an improved storage stability and water resistance (Barrow, 2012). Bio-char heating value goes as high as 28-29 GJ per tonne, (Dynamotive, 2009). Pyrolysis bio-char has a higher heating value than many grades of coal (CRL Energy lab tests, 2012). It may be used domestically or shipped off in powder form as export to overseas. Additionally bio-char may be further processed into fuel or activated carbon to be used domestically or export. The average bio-char density is about 250 kg/m^3.

The yield of bio-char from the biomass pyrolysis varies with operation temperature, residence time and heating rate. As pointed out by Oasmaa (2003) and Zhang (2007), wood thermal decomposition at 425-557 °C in oxygen free conditions results in extensive depolymerisation/fragmentation of the macromolecular structures of the wood. Cross-linking via condensation reactions and water loss result in bio-char formation (Zhang, 2007).

Figure 2.7: Picture of pine sawdust compared with bio-char collected from pyrolysis.

Bio-char collected during pyrolysis at temperature less than 550 °C has been proven to have a greater percent of C in its composition (Amonette, 2010). Elements like N, K, and S are reduced in the bio-char substance during higher temperature processes (Keiluweit et al. 2010). The bio-chars collected during the low temperature process are found to have a greater reactivity in soils than higher temperature bio-chars and a better contribution to soil fertility (Steinbeiss et al. 2009). To prove that, Chan *et al.* (2008) conducted a pot and field study mixing soil with bio-char and comparing results with ordinary crops and crops fertilized with bio-char produced above 550°C. It was observed that the bio-chars produced at temperatures less than 500 °C gave higher crop yields than other methods tested (Chan et al. 2008).

Low temperature bio-chars have been blended with minerals and sludges to balance the nutrient content of the soils, and results of pot and field trials can be found in literature (Chia et al. 2010; McHenry 2008). These promising results indicate that bio-char collected during bio-bitumen production is a valuable product which may be applied in agricultural industry, thus supplying extra revenue. There is considerable interest in finding reliable methods of sequestering carbon in agricultural soils to both reduce farm investment risk and cut atmospheric greenhouse gas concentrations, in a timeframe suitable to investors. More studies should be completed on the collected solid bio-char samples prior plant construction.

McBeath and Smemik reported in 2009 that bio-char produced at the lower temperature has a predominantly amorphous C structure, with a lower aromaticity than bio-chars produced at higher temperatures (McBeath and Smemik 2009; Keiluweit et al. 2010). As expected the structure, size, volume, surface area and composition of bio-char solidly depends on the chemical and physical properties of feedstock material. Woody bio-char has the exoskeleton of the tracheids, which are part of the untreated wood structure (Downie et al. 2009).

Antal and Gronli showed that as the temperature of the heat treatment increases the physical, electrical and chemical properties of bio-char change until most of the carbon is in the form of graphite (Antal and Gronli 2003; Amonette 2010). At lower pyrolysis temperatures the biomass material is converted into fused aromatic ring bio-char structures with the loss of carbon dioxide (CO_2), carbon monoxide (CO), water and hydrogen (H_2) (Graetz and Skjemstad, 2003; Demirbas, 2004).

Trials completed by Milne on a smaller scale demonstrated that soil organic carbon levels shape agro-ecosystem function and influence soil fertility and physical properties, such as aggregate stability, water holding capacity and cation exchange capacity (CEC) (Milne et al., 2007). From Wikipedia, CEC is the maximum quantity of total cations that soil is capable of holding at natural conditions and pH. It is a definition of soil's fertility, nutrition retention capacity and ability to protect groundwater from contamination. Milne's research showed the improvement bio-char has on nutrients retention in soil, thus improving the agricultural yields harvested from the treated plantations, Figure 2.8. Lehmann supplied data indicating 500 °C as the optimum bio-char production temperature in terms of carbon recovery and CEC. (Lehmann, 2007). The CEC of freshly produced bio-char is relatively low, although it will increase over a few months when stored between 30 and 70 °C (Lehmann et al., 2003; Lehmann, 2007).

Figure 2.8: On the left crops were planted in soil mixed with an adjusted ratio of bio-char, to the right crops were planted on the ordinary soil. (Rcchar.inc, 2013)

There is a need for further research into the safe level of bio-char application for many soil types. The levels of metal contaminants presented in the original biomass influence the safe level of bio-char addition. Thus, safety testing is required on the collected bio-char. Additional trial runs should be completed on the calculation of the optimum bio-char ratio addition for New Zealand soils. Application may begin from as little as 38 t of bio-char per hectare. Some basics of application may be found in Department of Environmental Protection 2002 and Bridle 2004 publications.

Dynamotive in Vancouver has completed a series of experiments adding bio-char to soil. The practiced application rate for the bio-char was 2.5 tons/acre (5,000 lbs/ acre, or 5,617 kg/hectare or 561 700 kg/km^2) and was spread by an agricultural spreader (Figure 2.9). Bio-char was mixed with the soil in May 2008. Crops were harvested from threated soil in October 2008. Conclusions drawn were: 6-17% crop yield increase, 24% increase in 'plants per area', 68% longer roots in length (also see Figure 2.11), plant height above ground increased by 10%, 13% greater weight per seed, 25% fewer seeds per plant, 22% lower plant leaf temperatures with bio-char soil mixture.

Figure 2.9: Agricultural Spreader used on Bio-char (Dynamotive, 2009).

Collected during bio-bitumen production, bio-char may be sold as is or activated with steam to produce activated carbon. This is another area of this by-product application. The highly developed internal surface area and porosity of activated carbon result in considerable adsorptive abilities

(McHenry, 2008). Activated carbon has a wide range of high value uses that include water and gas treatments, material recovery, catalysts and gas storage applications (Zanzi et al., 2001). In fact Enecon estimated prices for granular activated carbon and CSIRO activated wood pellets are around Australian $3000 per tonne, and prices for powdered activated carbon are approximately Australian $1000 per tonne (Enecon, 2001), with 1NZ$=0.80AU$ based on 2013 ANZ bank conversion (ANZ Bank New Zealand Ltd., 2013). These would be equivalent to 1250NZ$ and 3750NZ$ per tonne. The proposed plant design outlined in following chapters produces 550 tonne a year of bio-char, which would provide a positive income, attractive for investors.

Some potential bio-char regulations have been identified by a series of scientists over the years. Criteria include near-neutral pH, on exchange capacities (CEC and AEC), moderate hydrophobicity to retain organics, and stability to oxidation (CEC - cation exchange capacity, AEC - anion exchange capacity). Low volatile content suggests that the types and rates of interactions between bio-char and soil take place in the soil and depend on the following factors: (i) feedstock composition, in particular the total percentage and specific composition of the mineral fraction; (ii) pyrolysis process conditions; (iii) bio-char particle size and delivery system; and (iv) soil properties and local environmental conditions (Amonette, 2010). Adsorption-desorption, precipitation-dissolution, and redox reactions are different interactions between bio-char and soil and have been studied by Steiner et al. (2007), Bruun et al. (2008), Singh and Cowie (2010), and Kuzyakov et al. (2009).

Based on Bruun's trials, bio-char increases retention of NH^{4+}, K^{+}, Ca^{2+}, Mg^{2+} and P in soil. Some studies suggest that bio-char can be used as a carrier for microbially-based environmental remediation. This means bio-char helps to reduce soil pollution with the help of microorganisms. Microorganisms do not digest bio-char, but simply swallow and 'drop it off' at another location, thus improving the mixing process between bio-char and soil. Addition of bio-char to soil lowers soil's bulk density (Bruun et al., 2008).

A series of reactions occurs between plant roots, microorganisms in the soil and bio-char. Microscopic, chromatographic, and spectroscopic studies of bio-char and root growth in bio-char-amended systems were completed by Amonette et al. in 2010. This study showed that some worm species, termites, larvae, and other insects appear to ingest or live inside bio-char. Microorganisms were observed to break up the bio-char, consequently coating it with organic compounds. Breaking up the bio-char can result in exposed surfaces being oxidised and then reacting with mineral or organic matter. Eckmeier in 2007 noted that earthworms ingest particles <2 mm (but do not digest them) and redistribute them elsewhere in the profile (concentrated at ~0.8 m depth) by excretion. Bioturbation is mixing of sediment, organic materials and soil by microorganisms. From this definition, bioturbation is the first step in the application process - physical mixing of bio-char particles and its redistribution within the soil profile. Studies show that eventually bio-char moves down through the soil profile to areas with lower microbial activity (Major et al., 2009a).

Figure 2.10: On the left crops were planted in soil mixed with an adjusted ratio of bio-char, to the right crops were planted on the ordinary soil (BIOCHAR Farms.org, 2013).

Barrow (2012) analyzed benefits from bio-char bioturbation in soil, such as enhanced plant growth (Figure 2.10), increased crop yields and decreased malnutrition in varies types of soils. Bio-char use in agriculture was additionally observed to reduce phosphate, nitrate and agrochemicals pollution of

streams and groundwater; reduce the need for fertilizer and compost; reduce soil acidity (raise pH); increase soil microbial biomass and support earthworms. Bio-char improves soil moisture retention.

Throughout New Zealand territory the soil differs. Thus the ratio of bio-char to soil will vary dependent on location. Bio-char has been often referred to as 'carbon negative' substance addition to the soil. This means that bio-char production process is one of the energy generation systems that withdraw more carbon than it produces (Massey University, 2013).

One of the industrial examples of bio-char and soil applications is bioremediation through bio-char at Dilmah Tea plantations, Figure 2.10. Bioremediation is a process which uses microorganisms, here via bio-char application, to reduce soil contamination and pollution. This process additionally reduced the amount of fertilizer and other chemicals use during the growth, reproduction and harvesting by at least 50% and increased the land productivity by at least 50%. The project was initiated by the IUCN Sri Lanka in 2008 in partnership with the Tea Research Institute of Sri Lanka (TRI). Subsequently, Dr. J.C. Krishnaratne of Dilmah Conservation has been leading this program to apply bio-char at the Palmadulla field at Kahawatte and Nawalapitiya plantations—chosen for their different agronomic and climatic conditions.

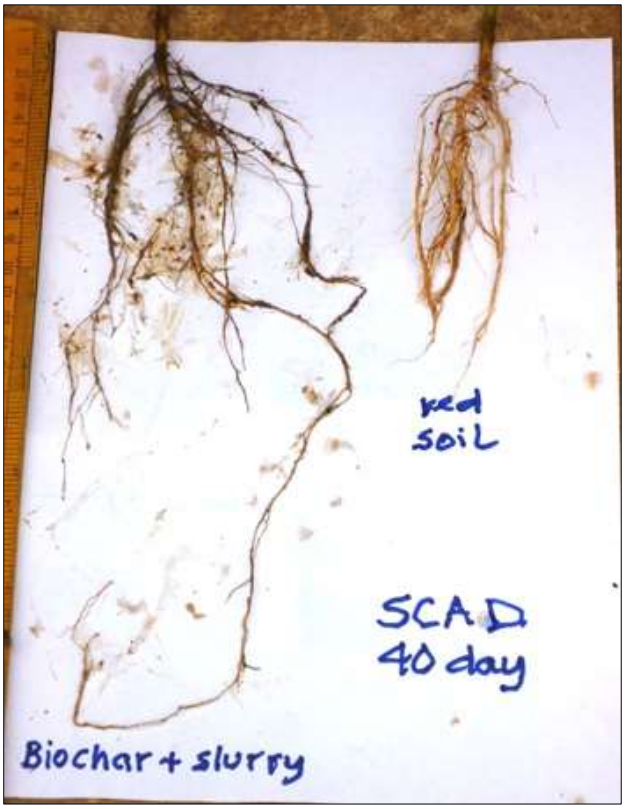

Figure 2.11: The roots of same species grown for 40 days: one grown in Bio-Char injected soil and the other one grown in the same soil without the bio-char in India (International Bio-Char Initiative, 2012).

As presented by Dynamotive 2008-2009 experiments of bio-char mixture with soil is valuable, as it adds up to 10% fertility in soil. The proposed pyrolysis process design uses nitrogen as a carrier gas, which adds even further value to bio-char as an effective fertilizer. Figures 2.8 and 2.10 show a field with two types of plantations. One part with crop plants grown on soil mixed with bio-char and the other part on bio-char untreated soil. Photos provide a visual representation of fertility increase in soil treated with bio-char.

Pelletizing is another method for bio-char (‘the waste product‘ of the process) to be utilized. Bio-char pellets are created using bio-char and a mixer which works as glue. Pellets are used for heating in domestic and industrial markets. Most of the pellets are currently manufactured out of woody sawdust, Nature Flame in New Zealand. Fuel pellets made from bio-char would have a higher energy density than wood pellets.

Bio-char can be transformed into fuels via briquetting, pelletizing or co-gasification and combination with biomass or coal. Combination of pyrolysis bio-char with pelletisation is more economically feasible, than the pelletisation of original wood. Uslu (2008) found heat treatment process to be 92% efficient, reducing to 90.8% when pelletisation is performed after heat treatment. The pelletisation process on its own was found to be 84-87% efficient and the pyrolysis process was 66-70% efficient.

One of the biggest commercial competitors of the heat treated biomass fuel use is sawdust woody pellets. Due to high density and next to zero MC, woody pellets are a very popular biomass fuel source. However, within seconds of contact with water wood pellets literally 'fall apart' and even consequent drying of the wetted pellets does not return them to the original product with the similar properties. The chemical and physical properties of pine originated bio-char are unaffected by wetting as well as long term water contact. This unique retention property allows bio-char to be a good fuel choice for humid climate locations, eliminating storage issues associated with biomass pellets storage.

Chapter 3: Experimental

3.1 Laboratory Scale Equipment

3.1.1 Pilot Rig Process Description and Materials

The laboratory-scale fluidised bed pyrolyzer at CRL Energy Ltd., Lower Hutt, Wellington, shown in Figure 3.1, was used for fast pyrolysis tests in the present study. The flow diagram of the rig is shown in Figure 3.2. In the experiments, nitrogen gas was used as fluidization agent and gas carrier in the pyrolysis reactor. The experiments conducted investigated the impact of processing parameters (reactor temperature, feed rate, feed particle size) and types of feedstocks on liquid yield and bio-char yield in the fast pyrolysis. Additionally the results are used to help define the specifications and parameters for scale up design.

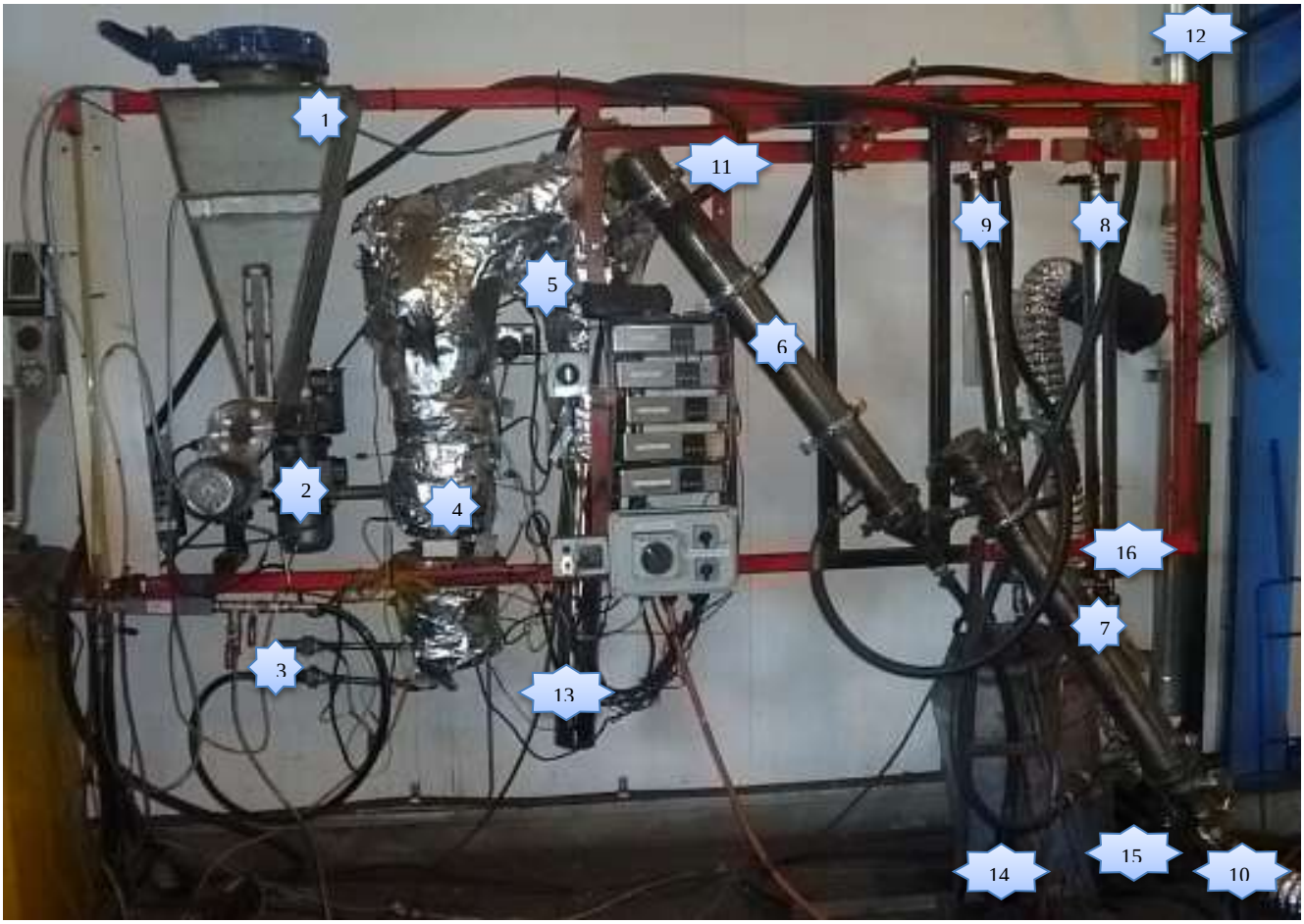

Note. (1- feed hopper, 2- injection augers, 3- nitrogen injection heaters, 4- fuidised bed reactor, 5- cyclone, 6- heat exchanger 1, 7- heat exchanger 2, 8-mesh condenser, 9-condenser, 10- water injection point, 11-water outlet point, 12- exhaust gas outlet, 13- bio-char collection point, 14- bio-oil collection point, 15- tar collection point 1, 16- tar collection point 2)

Figure 3.1: CRL fluidized bed pyrolysis unit (‘rig’) used for this experimental research.

The feedstocks used for the pyrolysis experiments were *Eucalyptus Nitens* and *Pinus Radiata* barks, sawdust and the mixture of sawdust and barks with different mixing ratios. The sawdust sizes were between 0.5 mm and 0.05 mm samples (both wood types) and the bark size was about 0.4 mm. The full description of the feedstocks will be given in Section 3.3 of this chapter.

In the experiments, the feedstock was firstly stored in a hopper with a horizontal internal rotary auger at the bottom which feeds the biomass into a drop tube (see Figure 3.1 and Figure 3.2). The drop tube is attached to an injection auger that feeds the biomass into the pyrolyser (Figure 3 and Figure 4). The rotary augor regulates the biomass feeding rate and is controlled by a variable speed drive motor. The second injection auger is used to prevent the backflow of the gas from the pyrolyser to the hopper and to force the biomass into the pyrolyzer as quickly as possible.

Once the biomass has entered the pyrolysis reactor, it is fluidized by the nitrogen gas and heated by external electrical band heaters attached on the reactor outer walls. The fluidised bed reactor with the external heaters on it was purchased from TEMPCO, USA. The heaters were controlled by the PID controllers, with a set point in the reactor specified for each run, ranging from 450 to 580°C. There are five K-type thermocouples inside the reactor at different locations for temperature measurement and control. These thermocouples ensure that the process is continuously running at the desired conditions.

At the controlled temperatures (450-580°C), the biomass is decomposed into gases and solid chars (bio-char). The bio-char is separated from the gases in the cyclone and collected from the cyclone bottom. The gas stream, flowing out of the cyclone from the cyclone top, is cooled down in the cooler where condensate is generated to form the liquid product. The non-condensable gas is then vented through the extraction system to atmosphere. Back pressure of the system is measured by a monometer. It has been aware that this non-condensable gas contains light hydrocarbon and CO, thus should be used for energy recovery in a large scale plant.

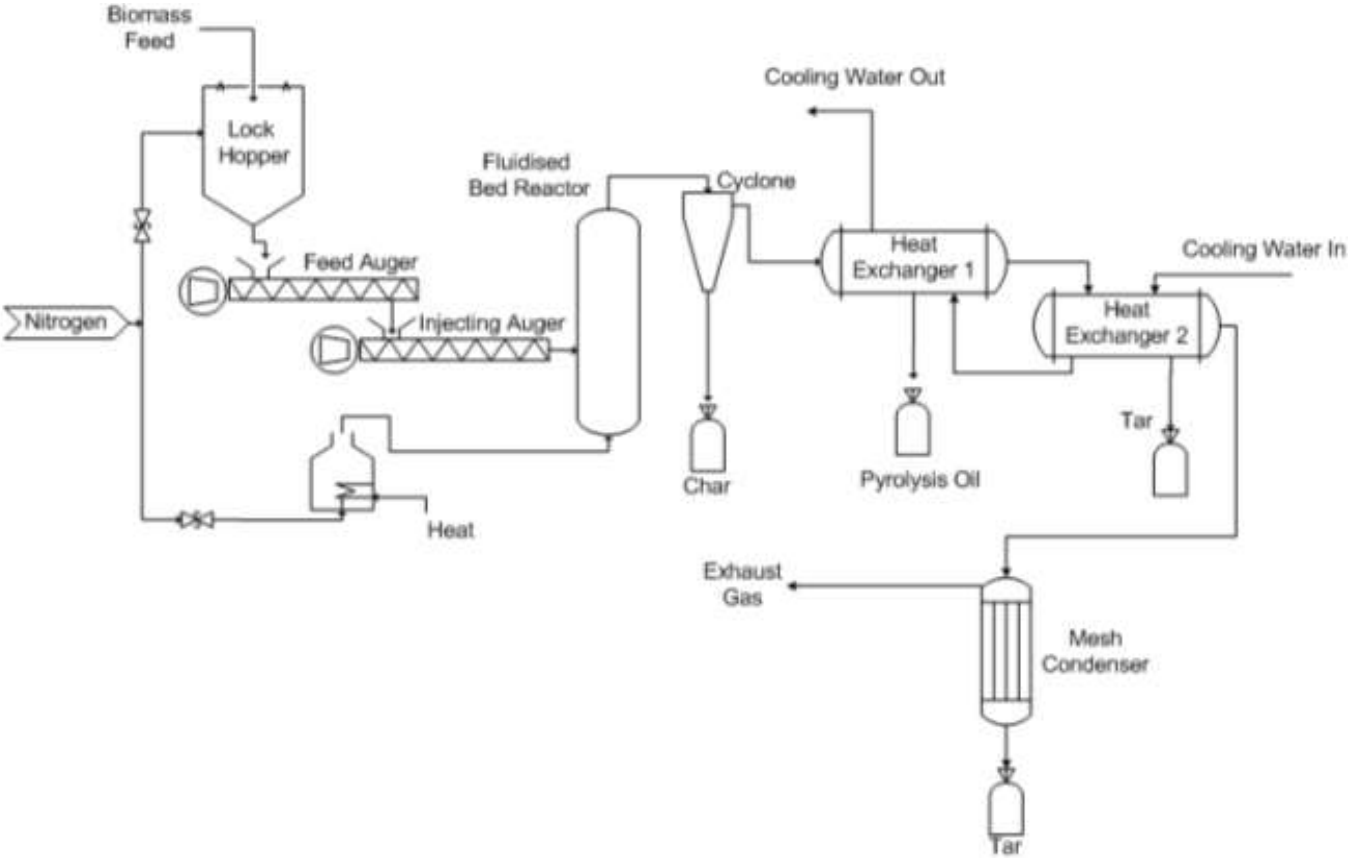

Figure 3.2: The process flow diagram of the fluidised bed pyrolysis unit used in the experiments.

Figure 3.3: Photographs of the drop tube and the second auger to feed the feedstock to the reactor.

Figure 3.4: Inside view of the hopper filled with sawdust feedstock and the internal rotary auger.

In the experiments, properties of the pyrolysis oil (bio-oil), non-condensable gas and solid chars produced under different operational conditions were sampled and analysed. In addition, viscous tars were also separated from the liquid product in some experiments and analysed. Analysis also included the pH, composition and calorific value of liquid and solid products. Overall 60 successful runs were completed during which high yields of bio-oil and tars were produced. There were several commissioning runs completed before the formal experiments were conducted. In the commissioning runs, substantial efforts were taken to identify and resolve issues with the system. Modifications for resolving these issues will be described in Section 3.5 of this chapter to highlight some important considerations in the system improvement.

3.2 Experimental Methodology and Procedures

The variables for the experiments were firstly decided with consultancy with project sponsors research collaborators which include operation temperature of the pyrolysis, sawdust feeding rate, type of biomass used (*Pinus Radiata* sawdust, *Pinus Radiata* bark, mixture of *Pinus Radiata* sawdust and bark, *Eucalyptus Nitens* sawdust). Feesctocks and pyrolysis products (bio-char, gas and liquid) were analysed at CRL Energy Ltd., Lower Hutt, Wellington. Mass and energy balances were completed on the raw data collected during the experiments and the data provided by the lab technicians. A

number of excel spread sheets was created to record all of the raw data and the calculations. The details of the raw data and calculations are presented in the Appendices of this thesis.

Below is the Safety Operating Procedure used to operate the unit.

NOTE:

Emergency Shut-down:

Turn OFF temperature controllers on control box.

Turn OFF main switch on control box.

Stop gas flow via gas flow controller.

Turn OFF nitrogen regulators and valve.

Turn OFF feed auger motor.

Prior to the equipment start up all the containers used will be weight and values will be recorded. In addition, the biomass feed will be described (type, colour, particle size) and weight.

START UP

1. *Start-up safety check:(work your way through the checklist as well as following points)*

    1. Ensure equipment is in a safe condition to operate, no open ended/broken wires.
    2. Ensure N2 supply is high (more than 1 full bottle (10 cubic meters of Nitrogen) is available).
    3. Check that the Nitrogen feed piping is connected and ready for operation
    4. Ensure the cyclone collector is in place and sealed.
    5. Ensure hopper is filled with feed material, and butterfly valve is closed
    6. Ensure condensers are in place and sealed.
    7. Ensure the cooling water into the heat exchangers is running, V03 open.
    8. Turn ON 3 phase power switch at the wall labelled 'Main wall plug'.
    9. Turn ON power switches on control box 'Control Box Main Switch' and individual switches at the back of the 4 controllers (Inlet Plenum Controller, Pyrolyser Controller, Cyclone Controller 1, Cyclone Controller 2). Controller displays should light up.
    10. Ensure the Nitrogen gas inline heaters remain turned off, until the gas is flowing.
    11. Ensure that the Nitrogen gas controller is on.
    12. Turn ON the manual switch for the elbow heaters 'Elbow Heater Switch' set at the marked set point.
2. *Set and note set-points of temperature controllers, note the starting time of the experiment, note the ambient temperature on the day of the experiment*.

Current Set Points:

Nitrogen Heater Controller	560°C (do NOT turn it on yet!!!)
Inlet Plenum Controller	520°C
Pyrolyser Controller	520°C
Cyclone Controller 1	300°C
Cyclone Controller 2	300°C

3. *Leave elements on to pre-heat system until set points are reached.*
4. *Open V03.*
5. *Ensure first Nitrogen pressure regulator near V05 is set to 800 kPa.*
6. *Ensure second Nitrogen pressure regulator is set to 300 kPa.*
7. *Use computer to set the gas flow controller is set to desired value.*
8. *Set and note set point of Nitrogen heater.*
9. *Monitor temperatures to ensure system is stable. When you are satisfied the feed can be started. Turn on V04.*
10. *The temperature controllers must be quickly turned off while the 'Feed Auger Motor Main Switch' (both of them) are started to avoid any electrical feedback which could damage the heaters. Alter 'Injection Auger Motor' to the desired value.*

a) *Turn OFF all the temperature controllers via switches at rear.*
b) *Turn ON feed auger 'Feed Auger Motor Main Switch'.*
c) *Turn ON injection auger 'Injection Auger Motor'.*
d) *Turn ON all the temperature controllers via switches at rear.*
e) *Set and record speed setting of feed auger controller.*

OPERATION

11. *Monitor temperatures, pressure drop, feed level in hopper.*
12. *Always turn OFF nitrogen heater before the nitrogen flow is stopped.*

IF A HOPPER NEEDS TO BE REFILLED:

1. Stop nitrogen flow into the hopper using the V04.
2. Fill hopper through butterfly valve and close butterfly valve.
3. Open the nitrogen flow valve allowing once again the gas flow into the hopper, V04 open.
4. Monitor the feed in the hopper, reduce bridging phenomenon via using a 'soft ends' hammer.

SHUTDOWN:

13. *Turn OFF 'Control Box Main Switch' on control box.*
14. *Manually turn OFF 'Elbow Heater Switch' and unplug the elbow heaters 'Elbow Heater wall plug'.*
15. *Stop gas flow via gas flow controller.*
16. *Turn OFF nitrogen regulators and valves V04 and V05.*
17. *Unplug the unit off the wall 'Main wall plug', thus insuring it is isolated from the electricity prior product collection and unit clean up.*
18. *Let equipment cool to near room temperature before attempting to open bio-char, bio-oil receivers.*
19. *Note any deviations from standard operating procedure.*
20. *If repairs required lock out the unit.*

3.3 Materials

3.3.1 Biomass Feedstock

For the experiments, a local sawmill provided sawdust and bark from *Pinus Radiata* and sawdust from *Eucalyptus Nitens*. All feedstocks were chemically characterised by proximate analysis (moisture, volatile fraction, ash and fixed carbon), ultimate analysis (C, H, N, O, S) and gross calorific value (GCV) using the standard chemical analytical methods described in section 4. Additionally, indicative values for the content of hemicellulose, cellulose and lignin were taken from the literature. The results of the analysis are presented in Table 3.1.

Table 3.1: Biomass feedstock characterisation (sawdust results from CRL Energy Ltd, 2012; results of *Pinus Radiata* bark from Güngöra, 2012).

	***Pinus Radiata* sawdust**	***Eucalyptus Nitens* sawdust**	***Pinus Radiata* bark**
Ash (wt%)	0.4	0.8	3.1
Volatile (wt%)	85.5	82.4	69.3
Fixed carbon (wt%)	12.8	15.4	20.8
Gross calorific value, ($MJ.kg^{-1}$ (dry mass based, or db)	24.79	24.97	18.98
C, wt% (db)	64.9	62.6	48.9
H, wt% (db)	5.22	4.87	4.95
N, wt%, (db)	1.16	0.01	0.21
S, wt% (db)	0.01	0.03	0.18
O, wt% (db)	28.71	32.49	45.76

As seen in Table 3.1, *Pinus Radiata* and *Eucalyptus Nitens* sawdust samples have similar ash and volatile content and GCV values but different results than those of *Pinus Radiata* bark. The ultimate-analysis results also show similarities between the *Pinus Radiata* and *Eucalyptus Nitens* sawdust samples, except for nitrogen content. *Pinus Radiata* bark has a low content of volatile matter, ash, oxygen

and sulphur and much higher fixed-carbon content than *Pinus Radiata* sawdust, which significantly affects the pyrolysis product.

The major constituents in woody biomass are cellulose, hemicellulose and lignin, while the minor constituents are organic and inorganic extractives. The composition of these constituents varies by species of wood (Mohan et al., 2006). In its original form, *Pinus Radiata* (softwood) has a lower density and is less durable than eucalyptus (hardwood). The following sections briefly describe the major components of *Pinus Radiata* sawdust and bark and *Eucalyptus Nitens* sawdust. Past studies have shown that biomass pyrolysis can be divided into various stages during which these components decompose, as described in chapters 1 and 2. Therefore, understanding the wood composition aids in analysing the pyrolysis process and products.

Cellulose

In its original form, wood consists of 40–45% cellulose, based on dry matter. *Pinus Radiata* stands at the lower end of the range, at 40% cellulose, while *Eucalyptus Nitens* reaches the high limit, at 45% cellulose (Dominguez, 2008; Moreno, 2004). However, in *Pinus Radiata* bark, cellulose accounts for only 17% of dry mass (Güngöra, 2011). At the wood micro-structural level, cellulose is the major structural component, forming the framework of minute strands in wood cell walls. Therefore, it directly affects wood strength and stiffness (Mohan et al., 2006). Cellulose is insoluble and has a crystalline structure which resists thermal decomposition more readily than hemicellulose. Cellulose degrades between 250°C and 350°C (Wild, 2008). Venderbosch and Prins (2010) found that cellulose was stable up to 310°C. Nearly all the cellulose was converted to condensable gas and organic vapours between 320°C and 420°C.

Hemicellulose

Hemicellulose is another major component in wood composition, accounting for 25–35**%** of the weight of dry wood, compared to a typical value of 28.5% for softwoods and 19.2% for hardwoods

(Dominguez, 2008). However, *Pinus Radiata* bark contains only 16.5% hemicellulose (Güngöra, 2011). Hemicellulose degradation occurs at 180–300°C, producing more volatile matter and less char and tars than cellulose (Mohan et al., 2006; Wild, 2008). Runkel and Wilke (1951, as cited in Mohan et al., 2006) found that the hemicellulose is lost during slow pyrolysis at 130–194°C, with the majority removed by 180°C. Venderbosch and Prins (2010) found that, under thermogravimetric analysis, hemicellulose began decomposing at 220°C and had decomposed completely at approximately 400°C.

Lignin

Lignin accounts for 28% of mass in *Pinus Radiata* wood and 31% in eucalyptus wood (Dominguez, 2008; Moreno, 2004). Lignin is characterised as an amorphous cross-linked resin without a specific structure (McCarthy & Islam, 2000). In *Pinus Radiata* bark, lignin contributes 33% of dry mass (Güngöra, 2011). Lignin pyrolysis produces greater residual char than cellulose (Mohan, 2006). Wild (2008) found that lignin decomposition in wood begins at 220°C and continues up to 480°C, with a maximum rate achieved at around 400°C. Therefore feedstock with higher lignin content, and thus lower hemicellulose content, produces more char during pyrolysis (Zhang et al., 2010). Venderbosch and Prins (2010) found that, under thermogravimetric analysis, lignin began decomposing at 160°C and had decomposed completely decomposed by 800–900°C.

3.4 Products Analysis

3.4.1 Elemental Composition, Calorific Value and Ash Composition of Solids and Calorific Value of Liquids

Solid product and feed samples was analysed to calculate their proximate, ultimate and calorific value characteristics. The proximate characteristics were determined through the standard methods. The International Organization for Standardization (ISO) 1171 was used to determine ash composition, ISO 11722 for moisture content, and ISO 562 for volatiles. The sulphur content was determined by the American Society for Testing and Materials method (ASTM) D4239, and the GCV solid and liquid samples by an LECO AC350 model calorimeter following ISO 1928.

3.4.2 Moisture Content in Solid Feedstock

Before biomass was used as a feed for the reactor, it was air dried (if weather conditions allowed), or a WatVic oven was used to dry the feed samples over 4-6 hours (dependent on the sample original moisture content) to achieve the target moisture content of less than 10% (dry basis). After drying, the biomass was kept in closed containers. Before each run, biomass samples were first analysed in accordance with ISO 1171 to measure their moisture content and ensure the consistency of the feeds between runs. A weighed sample in a capsule was placed overnight into an oven preheated to 105–110°C through which a current of air passed. The sample was then removed and weighed.

3.4.3 pH of Liquids

SOLSTAT's EMP 1500 Research Bench Mains Digital pH Meter (with automatic temperature compensation) was used to measure the pH of the condensate solutions.

3.4.4 Gas Analysis

Gas analysis was carried out using micro gas analyser Agilent 3000A MicroGC, which consists of an injector, columns, flow control valves and a thermal conductivity detector (TCD). The MicroGC quanti-

fied the composition of CO_2, CO, O_2 and N_2 gas samples collected in Tedlar® Gas Sampling Bagsbags and taken to an on-site lab.

3.5 Process Issues/Improvements Discussion

Throughout commissioning and testing the fast-pyrolysis rig, various problems were encountered and resolved. Some were solved with minor changes, but others required redesign of certain parts of the equipment or control of software development and communication with the suppliers. The following are some modifications and engineering troubleshooting performed in the present study.

During the first cycle of experiments, nitrogen gas was supplied by Manpak in 15 nitrogen bottles. The monthly rent for Manpak nitrogen was $300, plus an additional cost for the gas and delivery ($1,300 one-off payment). Due to the high cost, it was proposed to design and build a new system with 4 nitrogen bottles running at once and the bottles changed as needed. On average, 1 run uses up to 1–1.5 bottles of N_2, each containing 10 m^3 of gas at ambient pressure. This consumption includes the gas used for preheating, operation of the experiment and cool down.

In the newly designed system, nitrogen gas is supplied from bottles and fed through the flow controller to ensure that the flow rate is independent of gas pressure. Figures 3.5 and 3.6 illustrate the exterior and interior of the system. Nitrogen flow is controlled by an integrated controller, which includes a valve, sensor and controller.

In the experiments, nitrogen gas was also used to purge the hopper, which accounted for about one-tenth of total nitrogen consumption. This measure reduced bridging of the feedstock in the hopper and leakage of the air into the system. It also prevented the backflow of the gases from the reactor to the feeding system and the hopper.

Figure 3.5: Nitrogen gas supply system bottles secured outside of the building.

Figure 3.6: Nitrogen gas supply system inside pressure relief system.

The nitrogen gas flow rate is controlled through a flowmeter via a computer software. Throughout the commissioning process some difficulties were encountered in the gas flowrate control and bugs were found in the control system. An automatic safety guard was then installed which switches off the system if indicators show system overheating.

Nitrogen gas is heated by two 750kWh parallel inline electrical trace heaters as sown supplied by RS New Zealand. A safety switch is connected to the nitrogen gas inline heaters. This switch turns off the heater if the nitrogen gas is over heated.

One of the common issues in the system was hight back pressure. Multiple methods have been applied to addrss this issue. One of which was getting rid of a cyclone. In the original system, there were two cyclones to collect the solid bio-char. However, there was potential condensation in the second cyclone if it was not approppriately insulated. After initial trials and engineering analysis, it was decided to use only one cyclone in the system. Figures 3.7 (a) shows the solid char collecetd from the first cyclone and Figure 3.7(b) shows the solid char collected from the second cyclone from the initial trials. It can be seen from the figurs that the seocnd cyclone collected insignificant amount of char, less then 1 g, compared to ~300g of bio-char collected from the first cyclone.

a)  b) 

Figure 3.7: Bio-char collected from the first cyclone (a) and from the second cylone (b) in the initial commisioning trials.

'Sealrite' steel-graphite gaskets were used to seal the unit. They were perfect to prevent leakages and kept operating at high temperatures in the pyrolysis unit. New gaskets did not require to be changed as frequently.

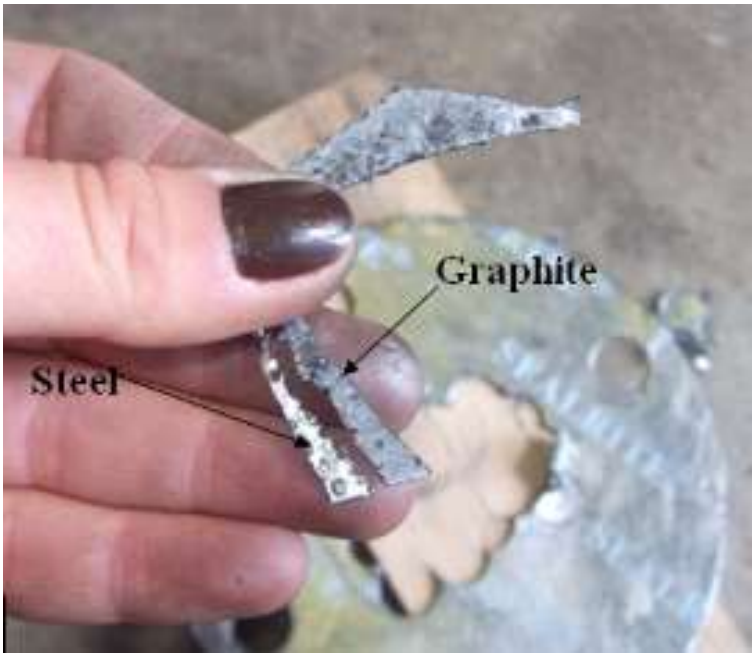

Figure 3.8: A close up of the steel-graphite sheet layers.

To ensure high temperature of the bed, the reactor was insulated with cow wool and later fiberglass. Temperature monitoring systems were additionally installed. Figures 3.9 and 10 show some of the modifications which significantly improved production and efficiency of the process.

Figure 3.9: Old Insulation 'Cow Wool'.

Figure 3.10: New Insulation 'Fiberglass'.

The fluidised bed reactor, cyclone and connections between them were reinsulated, reducing heat loss, increasing temperature of the reaction and providing higher product yields. Reinsulating was done with fiberglass, replacing the cow-wool insulation. This change was decided on as part of a H&S measure as the unit is being pulled part regularly for maintenance and Cow-wool can have negative effects wellbeing, if regular exposure occurs.

Additional heaters were installed in the system shown in Figure 3.11. These further improved the conditions inside the reactor and assisted in keeping the temperature up.

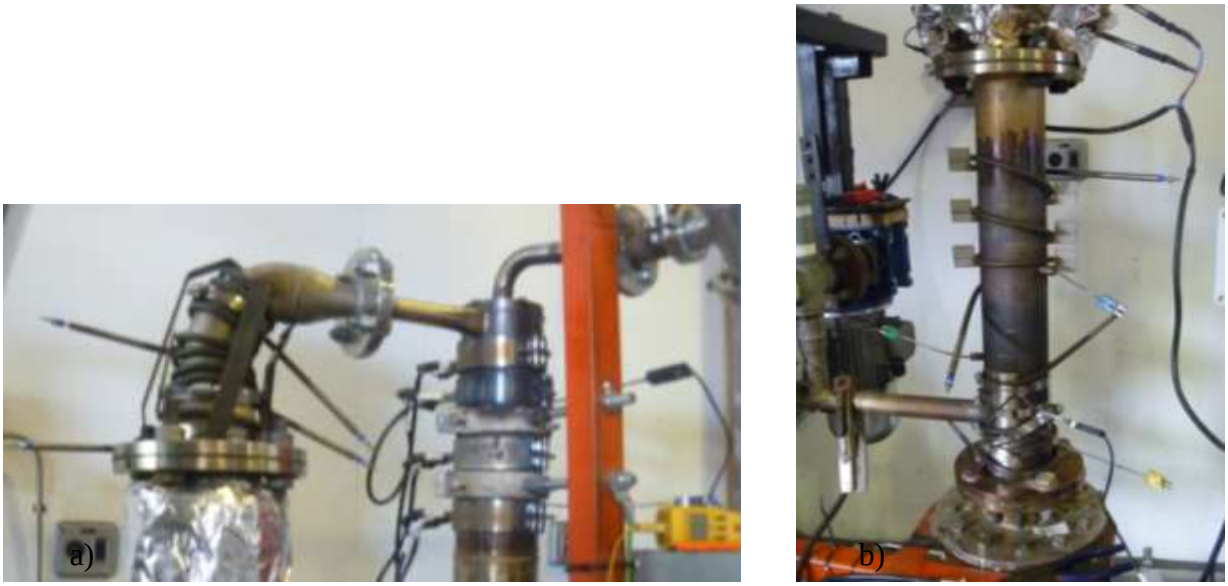

Figure 3.11: a) Additional heaters on the cyclone and exit from the reactor; b) Installed heaters through the body of the reactor.

The nitrogen gas heat transfer 'Box' is another area of significant heat loss, thus a thorough double insulation was an important step towards process efficiency improvement. The box location is shown in Figure 3.12 a. Firebricks and clay were used for the internal insulation of the 'Box'. Figures 3.12-3.13 show step by step process of Box insulation.

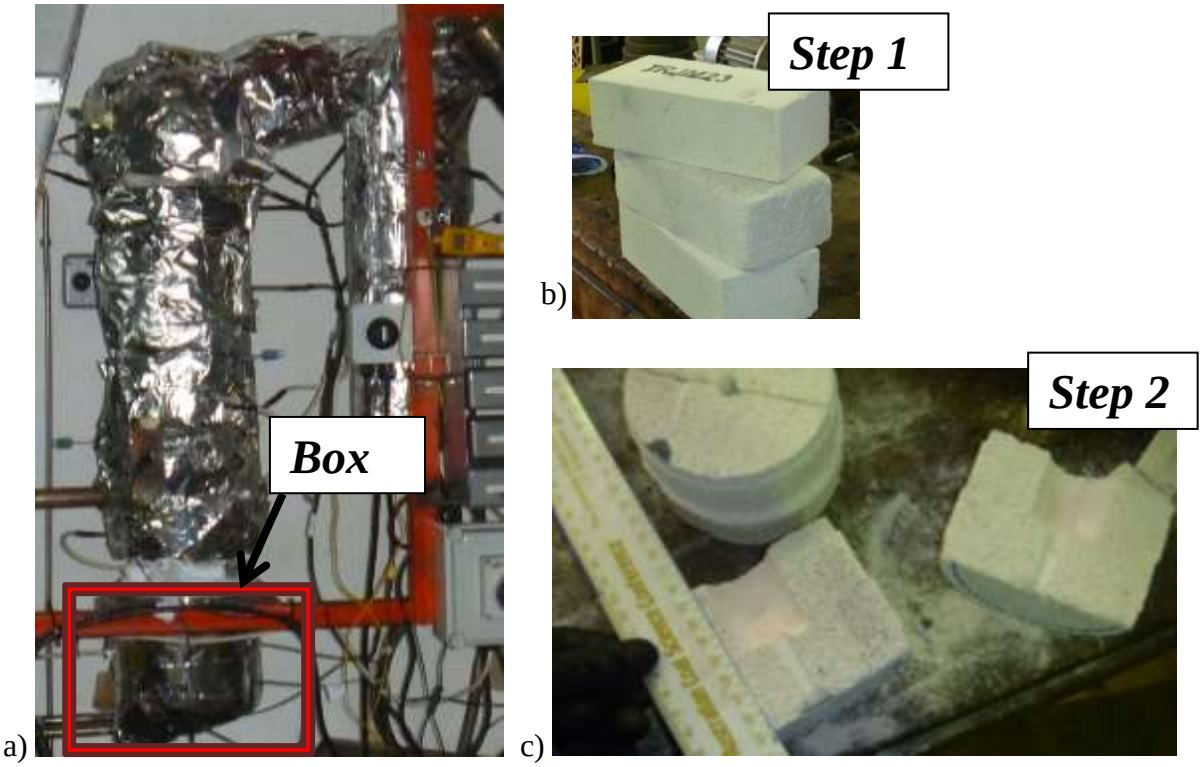

Figure 3.12: a) Location of the 'Box', b) and c) Firebricks.

a) 

b) 

c) 

Figure 3.13: a) Before the insulation, b) 'One Step' and c) After the insulation inside the 'Box'.

The addition of a mesh scrubber was another significant measure, which improved system efficiency. Figure 3.14a shows inside the scrubber, before modifications. The mesh scrubber effect on such small size plant was created with stainless steel sponges placed on top of each otheralong the length of the scrubber base. The sponges are held by a clamp made out of sheet-metal with a large mesh. At the exit, gas travels through a final layer of fine mesh, Figure 3.14 b. Figure 3.14 c shows a brand new steel sponge used and the sponge after a few runs. Using the metal sponges and fine mesh at the end of the process increased the surface area that the gas contacts, which resulted in higher liquid products collection yields.

a) 

b) 

c) 

Figure 3.14: Mesh condenser : a) Mesh condenser steel base, b) Compareson of the unused steel sponge and used process sponge, c) Clean mesh size demonstration.

When considering a scrubber design for the upscale, the accumulation of tar on the mesh should be considered. It is difficult to collect portions of the sample accumulated on the mesh. The use of an electrostatic precipitator should be considered for an upscale.

The composition of the gas exiting into the atmosphere is important before the process is commersiallised. The process is required to recieve a council concent prior construction. This concent is based on environmental and health and safety impacts the process has. Gas quality on the small scale was tested using system shown in Figure 3.15. The samples were collected using sealed

bags, which were tested with the Agilent 3000A MicroGC Gas Chromatography System analyser on site.

a)  b) 

Figures 3.15: a) Gas sampling port b) Collected gas sample.

A second heat exchanger was installed to create and additional process gas cooling step. This is shown on Figure 3.1. Having two cooling heat exchangers in the system improved cooling of the gas, and created a secondary collection port for the liquid product. Dependant on the process conditions and properties of the liquid, the collected product at this point of the process is either bio-oil or tar.

3.1.3 Blockage Issues

Blocking and continuous maintenance of the reactor has been a big issue during the two years of this project. Blockage in the reactor occurred frequently and was due to different reasons. Description of some examples follows.

Auger

a)  b) 

Figure 3.16: a) High back pressure during the process due to a jammed auger and b) Blocked injecting auger.

A temporarily installed bubbler caused blocking of the auger. The bubblers purpose was to filter the exhaust gas. The height difference between the bubbler and the hopper resulted in large back pressure. The back pressure forced the feed to block the augers (Figure 3.16). In order to solve this issue the bubbler was replaced with a scrubber. The installed scrubber was positioned at the same height level as the hopper, to avoid significant height difference and consequently back pressure. After a number of experiments, it was found that water treatment of the exhaust gas on such small scale does not have substantial effect on the products. Although the scrubber should be used in the larger scale process.

Cyclone/Connections

Another reason for high back pressures were blockages in most of the piping/connections of the equipment, examples are shown in Figures 3.17 and 3.18.

a)  b) 

Figures 3.17 a and b: Photos of the blocked fragments of the unit.

Figure 3.18: Connection 'pipe' leading towards cyclone 2

a)  b) 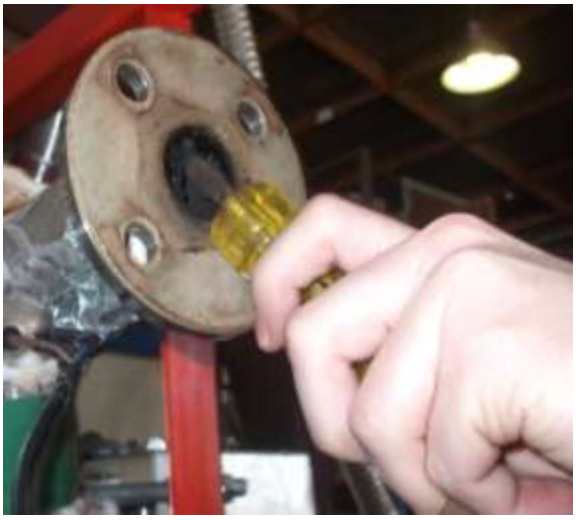

Figures 3.19: a) Heat cleaning of the blocked heat exchanger, b) Manually cleaning the blockage.

From the Figures (3.16-3.19) it can be concluded that the blockage of the connections between the major equipment units is an area which needs addressing. The connection joints of the unit got blocked because of the solids (bio-char) in the gas and reoccurring condensation in the process. When the hot mixture of process gas and solids exited the reactor, contact with cold steel connections caused solids to 'stick' to the inside walls. This build up continuously decreased the inside diameter of the connections the process gas travelled through until they completely blocked. Unfortunately there is no fast way to fix this problem. The process unit requires some redesign to reduce the repetitive blockage of this piping and potentially installation of a heating system further along the system up to the heat exchangers. Figures 3.16 a and b show methods applied to clean the blockages. The blockage cleaning in the connections was done manually using a screwdriver and other

tools at hand (Figure 3.19 b) or heat treating sections of the unit with an industrial gas torch (Figure 3.19 a).

Leaks

Leakes in the system occured due to wearing out of the gaskets (Figure 3.20 a) and a need for new bolts.

a)  b) 

Figure 3.20: a) An old gasket still on the equipment and b) a New gasket in the joint of the unit.

Flexitallic Thermiculite 715 Fiber Gaskets (Figure 3.20) were the old gaskets used for the unit. After pyrolysis unit was pulled apart. The Flexitallic gaskets were rather worn out and lost the compression ability after use. When the equipment was pulled apart for a clean up most of the old gaskets (Figure 3.20 a) were found to be broken or damaged. New gaskets (previously mentioned on Figure 3.5) were cut out of steel graphite sheets.

Figures 3.21: a) All the equipment used in the process of creating the new gaskets, b) Two of 18 gaskets cut out, c) and d) examples of the new gaskets location.

Gaskets were changed on the cyclone and the fluidised bed reactor connections. Figure 3.21 shows the process of cutting out of the new gaskets out of a graphite sheet and the equipment used to make new gaskets. The Sealrite sheet alternates layers of graphite and steel. The graphite gasket material is good for high temperature and high pressure operational conditions process.

After a number of runs the new gaskets proved to work well and no more leaks were observed. Additionally, the graphite materials showed no ageing or embrittlement problems, in comparison to

many other gasket materials. It was found that the new gaskets have long term stability of compressibility and recovery over a wide temperature range. New gaskets were found to be more durable. Figure 3.20 b shows a new gasket placed in the joint.

Heat-exchanger

After different runs the first heat exchanger blocked up. Then type of blockage was dependant on the feedstock and process operating conditions. Figure 3.22 shows an example of the blocked heat exchanger blocked by a solidified tar residue. A gas torch was used to heat treat and clean this section of the unit (Figure 3.19 a).

Figure 3.22: Blocked up heat-exchanger.

Another cleaning option is to rinse the unit through with acetone; however that process is much more time consuming compared to the heat cleaning method. Large volume of acetone is required, if this chemical is chosen for the cleaning process.

Chapter 4: Experimental Results and Discussion

4.1 Introduction

4.1.0 Specific terminologies used in Chapter 4 cited from The Free Dictionary by Farlex (2013)

Ash: The non-aqueous residue remaining after the sample is combusted.

Calorific Value (CV): The amount of heat produced when the fuel or the feed sample is combusted.

Energy Density: The amount of energy stored in a fuel or a feed sample per unit volume.

Total Organic Carbon (TOC): The amount of bound carbon in an organic solution. This is used here as a water quality indicator.

Volatiles or Volatile matter: The portion of the sample, which is released, in theory, as vapours during heat treatment, and consequently forms bio-oil after condensation.

4.1.1 Experimental Iterations and the Selected Results

In biomass pyrolysis, the yields of liquid, gas and solid char vary with the operational conditions as well as the feedstock properties. It is expected that rapid heating of the biomass (flash pyrolysis) and rapid cooling (quenching) of the hot gas, which exits the reactor after the gas-solid separation in the cyclone, would enhance the liquid product yield. On the other hand, slow heating and slow quenching would produce more solid char and non-condensable gas. Therefore, the operational conditions chosen would depend on the products desired.

In the present study, 50 productive runs with different feedstocks and operational conditions were completed on the pyrolysis rig located in the laboratory at CRL Energy Ltd., Wellington. Of the 50 runs, 15 runs were performed to examine the effects of mixing *Pinus Radiata* sawdust and barks in different proportions as the feedstock (7 runs with 50% sawdust and 50% bark and 8 runs with 70% sawdust and 30% bark). 32 runs were performed to examine the effects of varying particle sizes of the *Pinus Radiata* sawdust in the feedstock (27 runs with 0.15 to 0.4 mm particle size and 5 runs with particle size smaller than 0.15 mm). In addition 3 runs were performed to pyrolyze *Eucalyptus*

Nitens feedstock with particle sizes ranging from 0.15 mm to 0.4 mm. From these experimental runs, 100 liquid samples were collected and sent to CRL Energy Ltd., and subsequently to Opus International Consultants, for analysis and bio-bitumen production. For each run, product composition and yields were measured. The results were related to feedstock properties such as moisture content, particle size, fluidised bed operating temperature, for further analysis.

In the current set up, too many uncontrollable factors influence the temperature during each run. The best solution, for the purpose of reporting the results in this thesis, was to record the actual temperature during the experimental runs. This was considered to be a better option compared to rounding up the temperature to the closest set interval value. On an average, 23% to 34% of bio-oil was collected from different feeds. Total yield of liquid products for different feedstocks varied from 40% to 50%. Here, 'liquid' is used as the generalised term for bio-oil and tar products, i.e. liquid is the total volume of tar and bio-oil together. The bio-char yields varied between 13% and 24 % depending on the feedstock used. Based on the collected data, a large portion of the collected products was gas, which varied between 38% and 55%. Here, gas refers to all remaining gas from the rig after the condensers. As stated in Chapter 3 (Figure 3.1), condensers are the final step in the process, prior to the exhaust. Figures 4.1(a) and 4.1(b) show photos of bio-oil and tar, respectively, while Figure 4.2 shows the bio-char product compared with the feedstock of dried sawdust used in the process.

In order to produce bio-bitumen, tar and bio-oil are mixed under required conditions. This mixture will be then be mixed with normal bitumen, derived from the crude oil. The mixture thus produced has properties that are similar to the actual (petroleum based) bitumen, as determined by the Opus analysis, and is called bio-bitumen. It was concluded through Opus that better quality bio-bitumen could be produced, by increasing the proportion of bio-tar. Therefore, a higher yield of tar is the target in the present study. Tar yield varied from 3% for *Eucalyptus Nitens* sawdust, to 14% for mixture of 70% *Pinus Radiata* sawdust and 30% *Pinus Radiata* bark, with particle sizes ranging from 1.5 mm to 4 mm, for both sawdust and bark. Therefore, the 70/30 *Pinus Radiata* sawdust/bark mixture is

the most favourable feedstock option. It is believed that the high tar yield was due to high resin content of the bark feedstock. However, using pure bark was not possible in the current system due to the feeding blockage. In the runs with 50% sawdust and 50% bark, stable feeding was very difficult to manage and manipulate. Thus, the focus was trained on 70% sawdust and 30% bark. When the sawdust/bark mixture with a higher proportion of bark (e.g., 50/50) was tested, the feeding system was blocked. Thus, the results obtained by the 50/50 *Pinus Radiata* sawdust/bark mixture were not reliable. Therefore, it was decided that no more trials would be conducted for feed mixtures with a bark proportion higher than 30%.

The results with regard to the effect of operational temperature will be presented and discussed in Section 4.2, and the results with regard to the feedstocks and their properties (moisture content, particle size) will be presented in Sections 4.3, 4.4 (moisture content) and 4.5 (particle size), respectively.

Most useful products, the liquids (bio-oil and tar) and the solid (bio-char), are presented and discussed later in this thesis work. Even though gas is considered to be a useful product (Pang, 2013), the system does not have an established method of collecting or reusing it. This is another area for future in-depth research. Thus the gaseous product of the process will not be thoroughly investigated and analyzed in this thesis. Two gas samples were analyzed on the gas analyzer Agilent 3000A MicroGC. Table 4.1 lists the results. N_2 was found to be the component which took up 85-90% of the system's exiting gas. O_2 was 8-12% of the exiting gas. Other substances took up under 1% of the exhaust gas samples.

Table 4.1: Gas samples analyzed. Both were collected from the *Pinus Radiata* sawdust run with particle sizes ranging from 1.5 mm to 4 mm; 480°C operating bed temperature.

	Gas sample 1 collected 9/01/2012	**Gas sample 2 collected 9/02/2012**
CH_4	0.127%	0.015%
CO_2	0.350%	0.046%
C_2H_4	0.002%	0.003%
C_2H_6	0.032%	0.004%
H_2	0.007%	0.006%
O_2	7.957%	11.86%
N_2	90.60%	84.41%
CO	0.390%	0.011%

a)  b) 

Figure 4.1: Photographs of collected a) bio-oil and b) tar samples.

Figure 4.2: Photographic comparison of the sawdust and the bio-char products.

4.1.2 Bio-oil and Tar Products

Figure 4.1 (a) and 4.1 (b) show the photographs of two types of liquid products, bio-oil, and tar, collected during a single run. Most of the chemical tests and further experimental investigation was carried out by Philip Herrington, at Opus International Consultants Ltd. Some noticeable differences in the physical properties of the two liquids, and in their appearance, were recognized during product collection and handling. A description of some of the recognized properties follows.

Bio-oil that was collected was dark orange-brown or dark reddish-brown in color. From the literature, the appearance of the bio-oil is described differently, and it depends on the feedstock and the pyrolysis process (Mohan, 2006). The bio-oil collected in the present study was homogenous in appearance. It is reported that bio-oil typically contains 0.2-1.0 wt % bio-char (Bridgwater and Czernik, 2004), however no bio-char was observed in liquids collected in the present study.

The collected bio-oil was easy to pour and did not mix well with water. Diebold and Bridgwater (1997) state that bio-oil typically contains between 15-35 wt % water, but has an upper limit of around 30-50 wt % water (Mohan, 2006). In the present study, the collected bio-oil samples contained about 10% water after the initial separation of water from the bio-oil in the experiments (Herrington, 2012).

Generally the miscibility properties of bio-oils depend on the water content of the bio-oil (which has limited solubility with water). Bio-oil is typically miscible with polar solvents and immiscible with petroleum derived fuels, due to its high polarity and hydrophilic nature (Mohan, 2006).

The collected tar was a dark brown or black in color. The tar was mostly homogenous in appearance. However, occasional tar ‘lamps’ were found in the collected product. Tar ‘lamps’ are clusters of a thicker tar product that is solid in appearance. These were soft to touch, but stayed as a solid ‘lump’ when observed. These lamps melted when they were heated. After heating, the tar product became liquid which flowed easily, resembling the collected bio-oil. The liquid tar (after being heated) was still much denser than the bio-oil. In addition, the tar also has physical and chemical properties that

are different from the bio-oil. When cooled down after heating, tar 'lamps' disappeared and the tar liquid became harder to pour than before it was heated.

As expected, the bio-oil was found to have a much lower viscosity than the tar product. The viscosity of the bio-oil is typically between 15 and 35 cSt at 50 °C (Hasanah, 2012), while the viscosity of tar varies between 108 to 560 cSt at 50 °C (Engineering ToolBox, 2013).

When stored under room conditions in closed jars over a couple of months, the bio-oil did not show much change in appearance and physical properties. However, after being stored under the same conditions for the same period of time, the tar became much thicker and denser. When both the samples were stored in a refrigerator for a couple of months, no changes in their appearance or flowing behavior were noticed in either sample.

Literature suggests that bio-oil, if stored for a long time, polymerizes and undergoes an ageing effect. In the long run, this transforms the bio-oil into a tar-like compound. Oasmaa and Kuoppala (2003) concluded that over the first six months of storage, major physiochemical changes take place within the bio-oil, resulting in undesirable changes to its physical properties. These include an increase in water content, viscosity, density, flash point, pour point, and a decrease in the heating value.

Both bio-oil and tar have a distinctive smells. Once in contact with cloth or skin, both are very sticky and hard to get rid of. The toxicity and smell of liquid products collected in the process are influenced by the feedstock used and the operating conditions of the pyrolysis process (Diebold, 1997). Acute oral toxicity is estimated to be around 700 mg/kg of body weight (Prins, 2010).

If the pyrolysis rig is dismantled prior to stopping the nitrogen gas flow, or occasionally during dismantling of the cyclone, pyrolysis vapors and liquid airborne droplets may be inhaled or may come

in contact with the eyes. This occurred during some experimental runs on the CRL rig. Sufficient safety gear should be worn; otherwise eye and lung damage may occur. A burning sensation followed by watering of the eyes was observed, when direct contacted occurred. Diebold (1997) found bio-oil skin toxicity to be low, however some if his findings suggest that it may be carcinogenic.

In addition, the calorific values of the liquid products collected from the biomass pyrolysis experiments were also measured, and the results show that tar has high calorific values of 20-21 MJ/kg. Meanwhile, the bio-oil samples have calorific values of about 10-11 MJ/kg. Therefore, the tar has a much higher calorific value (CRL Energy Ltd, Lower Hutt lab, 2012). It was also found that samples of tar and bio-oil collected during higher nitrogen gas flow rate runs had slightly higher calorific values.

4.1.3 Bio-char Product

Figure 4.2b shows the solid bio-char products collected during the experimental runs. During the experiments performed in the present study, the feedstock type and composition significantly affected the chemical composition and GCV of the bio-char. Table 4.2a shows the GCVs of the bio-char products and the feedstocks. The properties of a Rotowaro coal sample are also presented in the table for comparison, because bio-char is a potential substitute for coal as a solid fuel. Table 4.2a shows that bio-chars collected from higher temperature pyrolysis (450°C) had higher a GVC than those collected from lower temperature pyrolysis (350°C). The GCV of the solid char from high-temperature pyrolysis is also higher than that of feedstock (*Pinus Radiata* sawdust and bark) and coal. This demonstrates bio-char's potential to be used as a solid fuel.

Table 4.2 (a): Gross Calorific Values of Bio-char samples, *Pinus Radiata* Feedstocks and Coal.

	GCV (MJ/kg)
Bio-char sample 1 - 350°C	20.45
Bio-char sample 2 - 450°C	25.85
Bio-char sample 3 - 450°C	25.19
Pinus Radiata	20.23
Pinus Radiata bark	21.33
Rotowaro coal	22.20

Table 4.2 (b): Contents of ash, volatiles and fixed carbon in the bio-char samples collected from biomass pyrolysis at different temperatures, (wt% db = weight % dry basis).

	Bed temperature	Ash	Volatile matter	Fixed carbon
	°C	wt% db	wt% db	wt% db
Bio-char sample 1	442	4.1	28.7	63.4
Bio-char sample 2	452	7.6	24.6	63.4
Bio-char sample 3	458	7.3	23.7	65.1
Bio-char sample 4	461	7.8	23.3	64.8
Bio-char sample 5	464	7.8	21.1	64.4
Bio-char sample 6	468	7.0	21.7	67.9
Bio-char sample 7	469	8.1	20.4	68.8
Bio-char sample 8	474	7.7	22.1	66.4

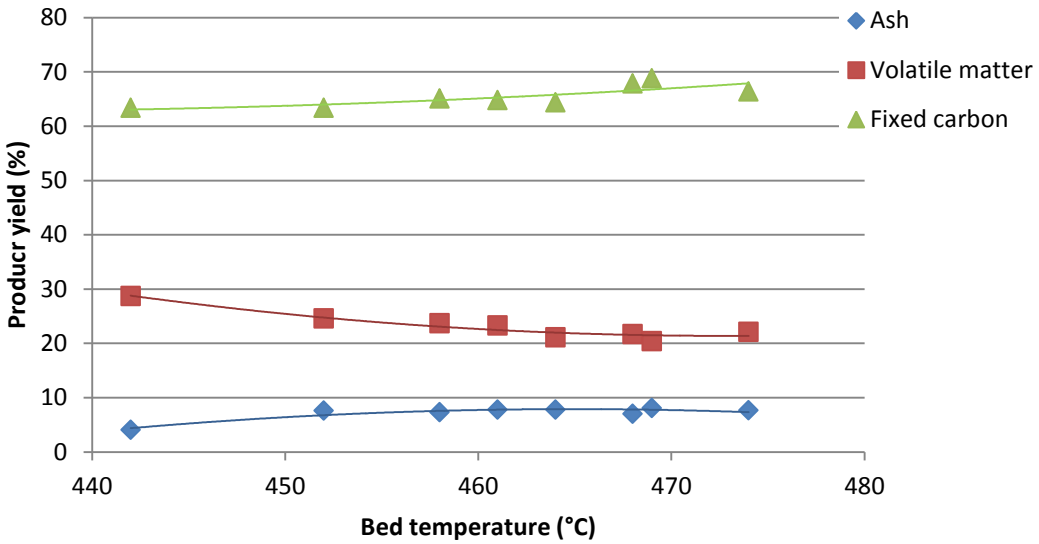

Figure 4.3: Ash, volatiles and fixed carbon composition in the bio-char product samples collected at different temperatures.

Table 4.2b and Figure 4.3 show the content of ash, volatile matter and fixed carbon in bio-char samples collected from the pyrolysis of *Pinus Radiata* sawdust at different operation temperatures (temperature inside the fluidised bed reactor) ranging from 440°C to 475°C. As seen in Table 4.2b, bio-char samples collected at higher temperatures had lower content of volatile matter. This difference indicates that higher temperatures accelerated the biomass decomposition and reactions in the pyrolysis reactor, releasing more gas products, some of which subsequently condensed into form liquid product.

Carbon, the main component of bio-char, is fixed, with its content ranging from 63.4% to 68.8%. This value is important because an application of solid bio-char might be carbon sequestration. Table 4.2 (b) and Figure 4.3 show that the carbon and ash content increased with pyrolysis temperature. The ash and fixed-carbon content in the bio-char product are important when the bio-char is used as solid fuel in a boiler.

Table 4.3: Elemental Composition of a Bio-char Sample Collected Using *Pinus Radiata* Sawdust

Bio-char sample tested	
S wt% db	<0.01
C wt% db	64.1
H wt% db	4.97
N wt% db	0.15
O wt% db	26.03

In the ultimate analysis described in Chapter 3, the *Pinus Radiata* bark samples had a higher ash composition than the *Pinus Radiata* sawdust. All samples tested had a high volatile matter composition, 85% for untreated *Pinus Radiata* sawdust and 52% for bio-char. On average, bio-char samples had a calorific value of 25 MJ/kg, slightly higher than 22 MJ/kg for coal. Table 4.3 shows the elemental composition of the bio-char sample collected from the pyrolysis of *Pinus Radiata* sawdust at a 470°C bed temperature. As expected, the analysis produced results consistent with a fixed-carbon content of 64.1% in the char. The other elements in the char analysis were 5% hydrogen, 26% oxygen, 0.15% nitrogen and 0.01% sulphur.

4.2 Effects of Feedstock on Product Yields

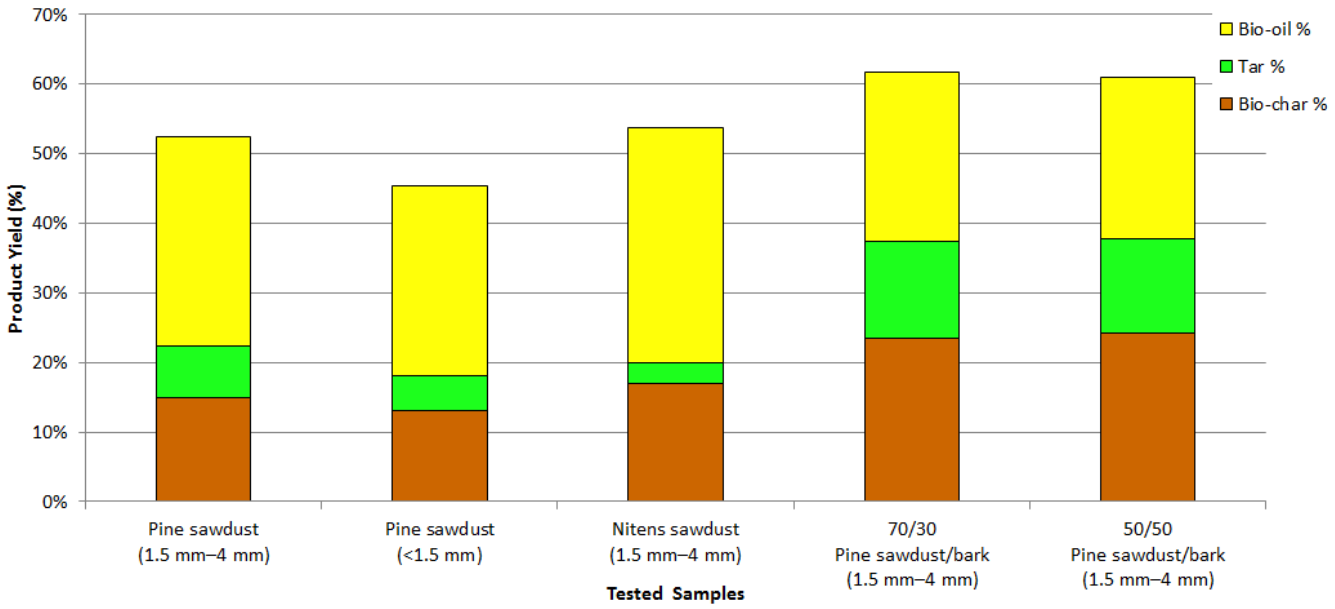

Note. The feedstock runs were *Pinus Radiata*—pine, *Pinus Radiata* bark—bark and *Eucalyptus Nitens*—nitens. Remains from the 100% total product composition were gas emitted through the exhaust outlet.

Figure 4.4: Average product yields collected from different feedstock runs.

Figure 4.4 shows the average product yields (bio-oil, tar and bio-char), while Figure 4.5 shows only the liquid products (tar and bio-oil) from the pyrolysis of different feedstocks at 465°C. As the total yield should be 100%, the remaining product is the non-condensable gas, which is not included in this figure. In Figure 4.4, it can be seen that the highest yield of tar collected was approximately 15% for feedstocks of 70/30 and 50/50 *Pinus Radiata* sawdust/*Pinus Radiata* bark mixtures. However, due to difficulty operating the current system as mentioned in section 4.1, a more practical feed of 70/30 *Pinus Radiata* sawdust/bark was tested more extensively. Average tar yields from the pyrolysis of *Pinus Radiata* sawdust were about 10%.

Bio-oil yields were observed to be highest for *Eucalyptus Nitens* feed experiments, about 35%. *Pinus Radiata* sawdust experiments produced about 30% bio-oil yields.

Bio-char yield from the pyrolysis of 100% sawdust (both wood species) was 15% ± 2%. However, in the pyrolysis of the mixed sawdust and bark, the bio-char yield was 22%. Figure 4.4 shows that mixed-feed pyrolysis clearly produced much higher yields of bio-oil, tar and bio-char. However, consistent operation of the pyrolysis of these mixture feeds was difficult to achieve with the current pyrolysis system. Therefore, *Pinus Radiata* sawdust was selected for the investigation of the effects of pyrolysis temperature, particle size and feed moisture content.

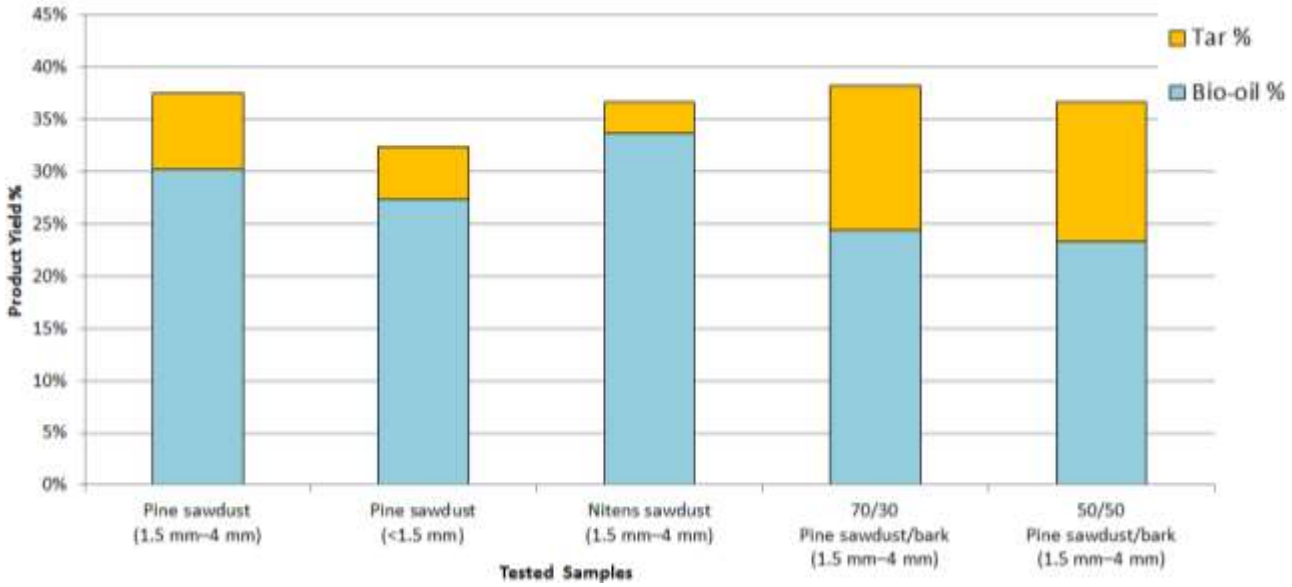

Note. The feedstock runs were *Pinus Radiata*—pine, *Pinus Radiata* bark—bark and *Eucalyptus Nitens*—nitens.

Figure 4.5: Average liquid product yields collected from different feedstocks

In a study by Oasmaa (2009), the bio-liquid yields were highest for wood biomass pyrolysis and lowest for pyrolysis of agro-biomass which contained a high amount of alkali metals. The nitrogen, sulphur and chlorine content were higher in agro-biomasses and forest residues than in bark-free wood such as sawdust. More CO_2 was formed with agro-biomasses. In this research, pyrolysis of *Pinus Radiata* sawdust produced less CO_2 emissions compared with *Eucalyptus Nitens* or bark—another reason for the selection of *Pinus Radiata* sawdust as the basic feed option, rather than *Eucalyptus Nitens* or bark mixtures.

In this thesis, tar is the most valuable substance, followed by bio-oil produced during fast pyrolysis. Therefore, it is important to show how much tar and bio-oil are produced during runs with different feeds.

4.3 Effects of Operation Temperature on the Product Yields

4.3.1 Pinus Radiata Feedstock

Figure 4.6 shows the experimental results from pyrolysis runs at operation temperatures of 442 to 474°C using *Pinus Radiata* sawdust feedstock. In Figure 4.6, the filled bars show the collected yields of bio-oil and bio-char, while the discrete solid squares and the plotted lines show the yields of tar collected during those runs. The detailed data collected during the experiments can be found in the Appendices.

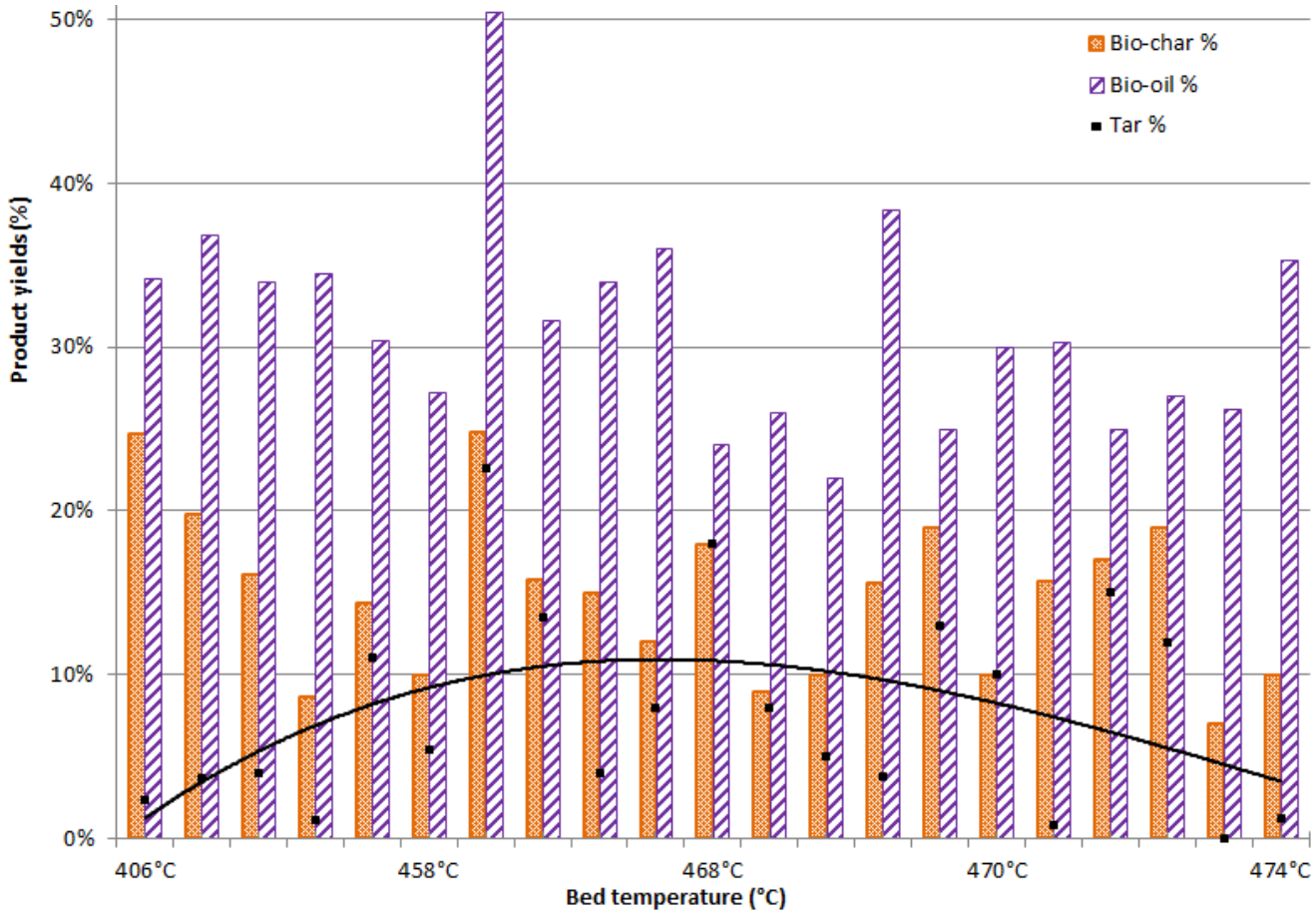

Figure 4.6: Yields of Bio-oil, Tar and Bio-char from Pyrolysis of *Pinus Radiata* Sawdust (1.5–4 mm) as a function of operation temperature

In Figure 4.6, it can be seen that no significant correlation between the product yields (bio-oil, tar and bio-char) and the operation temperature was found. However, products with less liquid tended to be produced at higher temperature pyrolysis. The total bio-char yields varied between 15% and –20%, total yields of bio-oil between 30% and 50%, and total yields of tar between 5% and 15%. As the total yield should be 100 wt%, the remainder is expected to be non-condensable gas.

The experimental results from the present study were compared with data from the literature (Salehi, 2011; Heo, 2008; Xi-Feng, 2006) as shown in Figures 4.7a, b and c. Figure 4.7a shows the results of Heo (2008) from the pyrolysis of sawdust from waste furniture, Figure 4.7b the results of Salehi (2011) from the pyrolysis of mallee woody biomass, and Figure 4.7c the results from the present study. Specifically, Figure 4.7(c) shows that higher yields of bio-oil from the pyrolysis of *Pinus Radiata* sawdust were achieved from 458°C to 465°C but decreased with higher operation temperatures.

Results obtained in this research were in agreement with the findings of Heo et al. (2008), who conducted pyrolysis experiments using sawdust from waste furniture under various reaction conditions. The various factors were temperature, particle size, feed rate and flow rate of the fluidizing medium in the fluidized-bed reactor. Similar to the completed investigations described in this thesis, Heo (2008) found that 450°C was the optimum pyrolysis temperature for increased yields of bio-oil. In his research, Heo (2008) stated that size of sawdust did not affect the production of bio-oil. He also found that the fluidisation gas flow rate and biomass feeding rates did not greatly affect the bio-oil yields within the tested ranges.

The results from the present study are also consistent with the findings of Xi-Feng (2006) that the liquid yield largely depends on the feedstock type and temperature. The maximum liquid (bio-oil and tar) yields collected by Xi-Feng (2006) were 56% at 465°C for rice husk, 61% at 490°C for pine sawdust and 60% at 475°C for mixture of rice husks and pine sawdust.

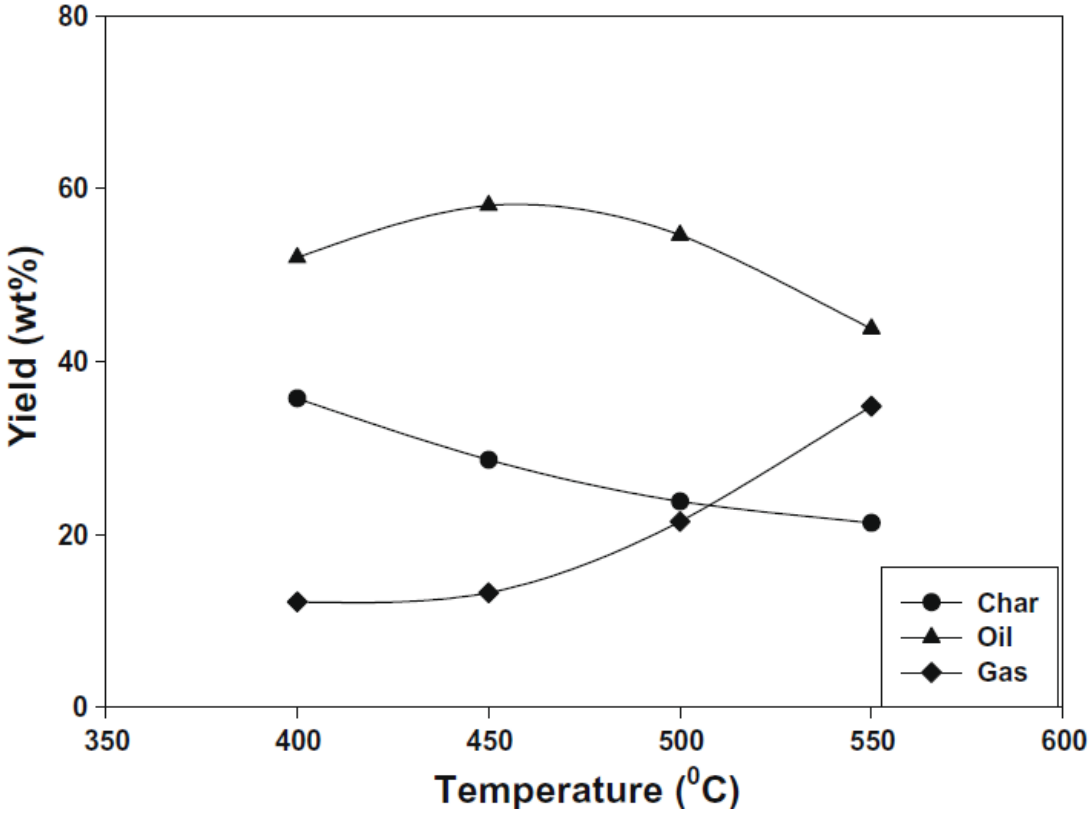

Figure 4.7 (a): Yields of products from Biomass Pyrolysis as a function of operation temperature: Results of Heo (2008)

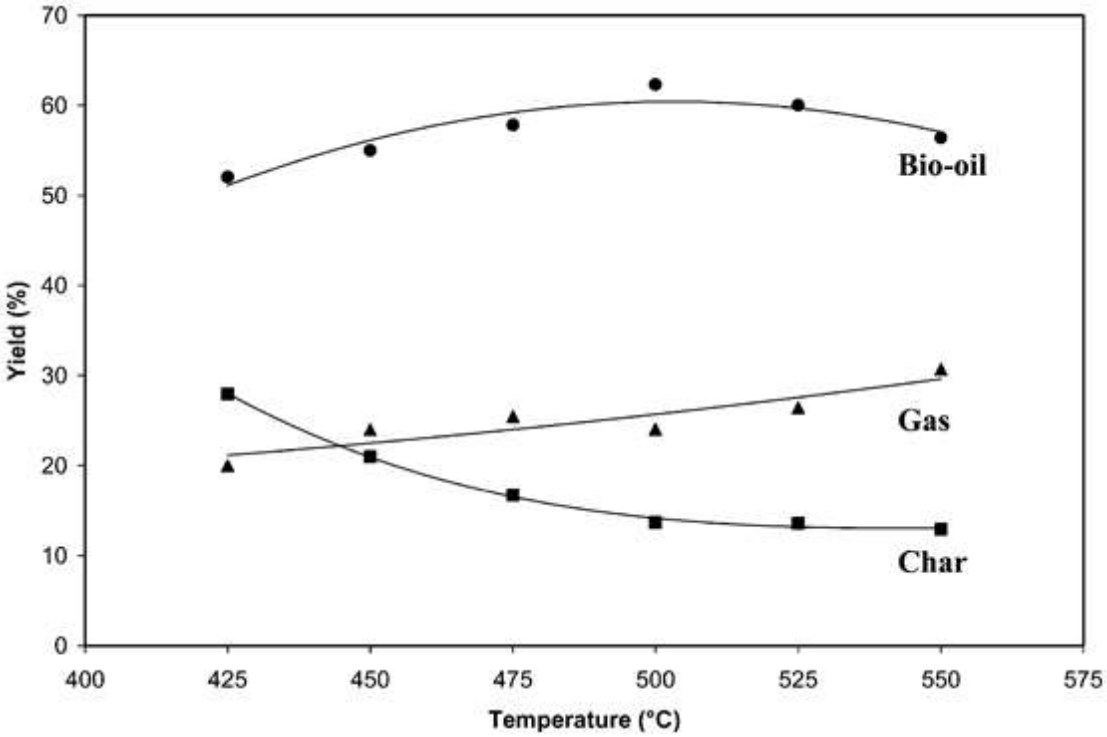

Figure 4.7 (b): Yields of products from Biomass Pyrolysis as a function of operation temperature: Results of Salehi (2011)

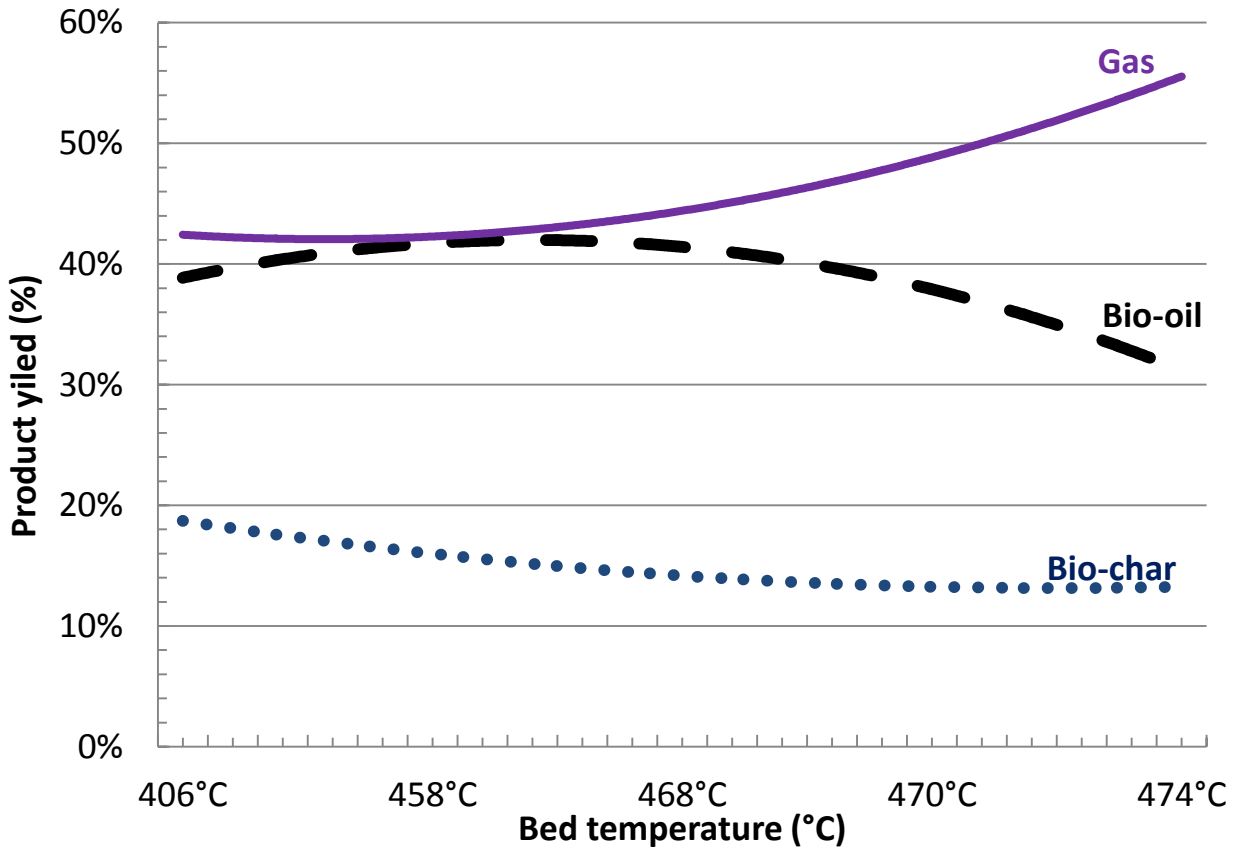

Figure 4.7 (c): Yields of products from Biomass Pyrolysis as a function of operation temperature: Data from the Present Study

The results from the present study are also consistent with the findings of Salehi (2011); however, much higher gas yields were found from the experiments conducted in the present study. It is possible that a higher fluidisation gas flow rate was used in the present study, which would discourage the formation of condensate nuclear in the condenser. In addition, the design of the condenser and filter for bio-oil/tar might not be highly effective at removing the bio-oil and tar from the non-condensable gas. This is an area for further investigation and improvement.

4.3.2 Eucalyptus Nitens Feedstock

Figure 4.8 shows the results of pyrolysis experiments using *Eucalyptus Nitens* sawdust (with particles size of 1.5–4 mm) as feedstock. The tar yield ranged from 1% to 5%, while the yields of bio-oil and bio-char were 34% and 17%, respectively. As tar is the target product in this study, the tar yields

from the pyrolysis of *Eucalyptus Nitens* was considered too low. Therefore, no further experiments involving it were planned, and the focus was placed on the *Pinus Radiata* feedstock.

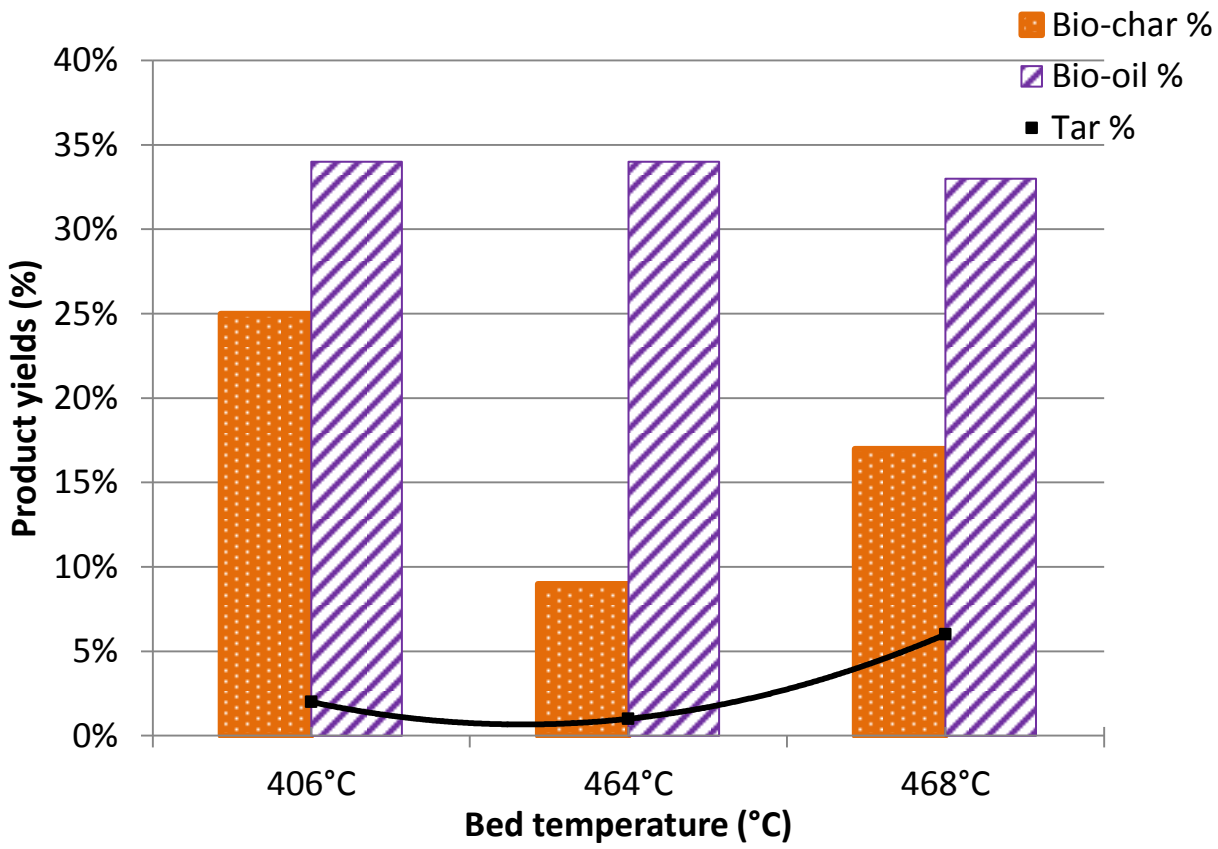

Figure 4.8: Yields of Tar, Bio-oil and Bio-char from Pyrolysis of *Eucalyptus Nitens* Sawdust (1.5–4 mm) at different operation temperatures.

Experiments on *Eucalyptus Nitens* showed that the highest yield of tar was produced at the pyrolysis temperature of 468°C. The bio-oil yield remained the same throughout all three experiments. All three experimental runs were assumed to have the exact same properties, as they were competed using the same batch of *Eucalyptus Nitens*. The optimum treatment temperature for *Eucalyptus Nitens* is 468°C as it produced the highest yield of tar product.

4.3.3 Mixed Sawdust and Barks

In OPUS Laboratory (2012) experiments, pyrolysis liquid products were a solution of organic compounds consisting of 8%–15% water. Fast pyrolysis of forestry residue yielded less liquid product com-

pared to pyrolysis using bark-free wood. Ten to 15% of this liquid separates as an extractive-rich top layer.

Bark is another waste material produced by the agricultural, pulp and paper industries. Every tree consists of at least 5% bark. The next step in this research investigation then was to consider mixtures of bark and sawdust for the pyrolysis process feedstock. Figures 4.9 and 4.10 present the results of different ratios of sawdust and bark used as feedstock. The mixtures were dried to 8%-12% moisture content and kept in a vacuum-like environment before use in the experimental runs. The selected ratios were 30% *Pinus Radiata* bark combined with 70% *Pinus Radiata* sawdust and 50% *Pinus Radiata* bark combined with 50% *Pinus Radiata* sawdust. Table 4.4 shows data collected from several completed tests.

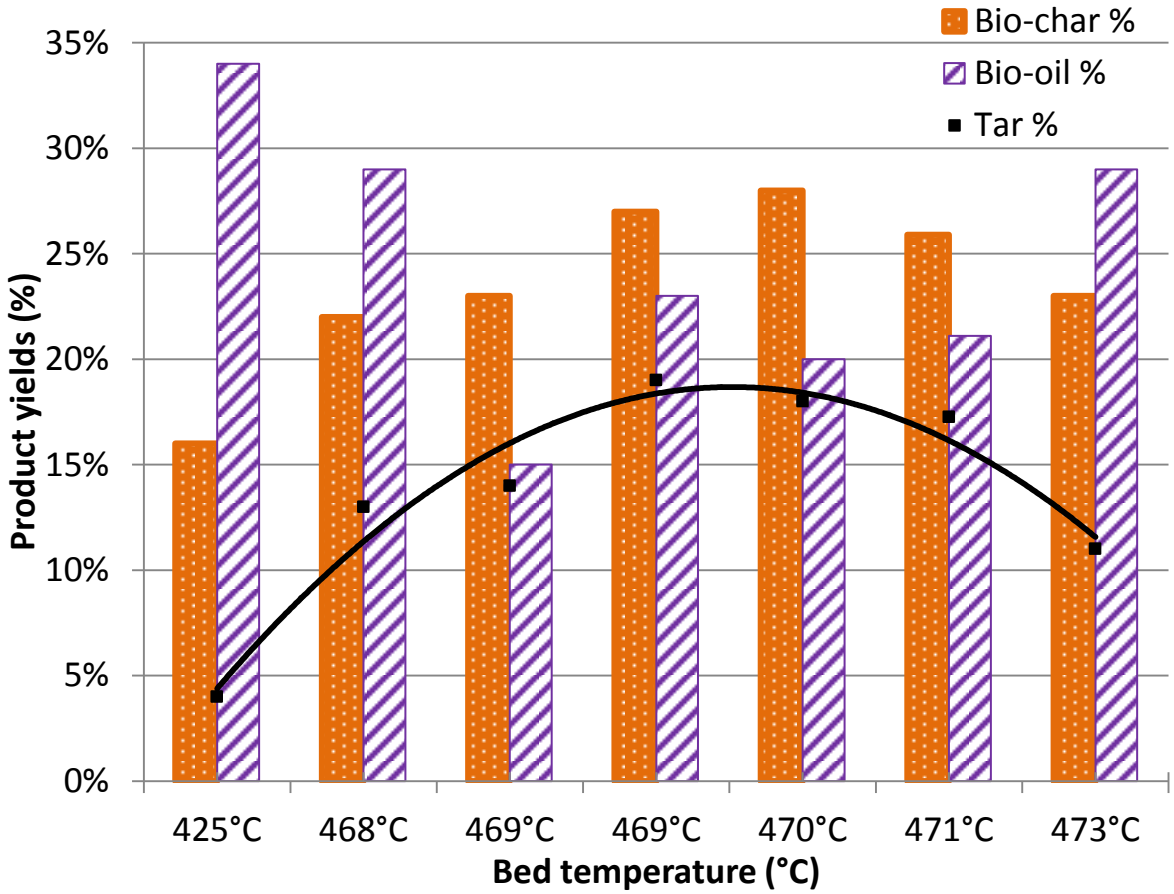

Figure 4.9: Plot of the effect of process temperature on 70/30 *Pinus Radiata* Sawdust/ *Pinus Radiata* Bark feed product yields

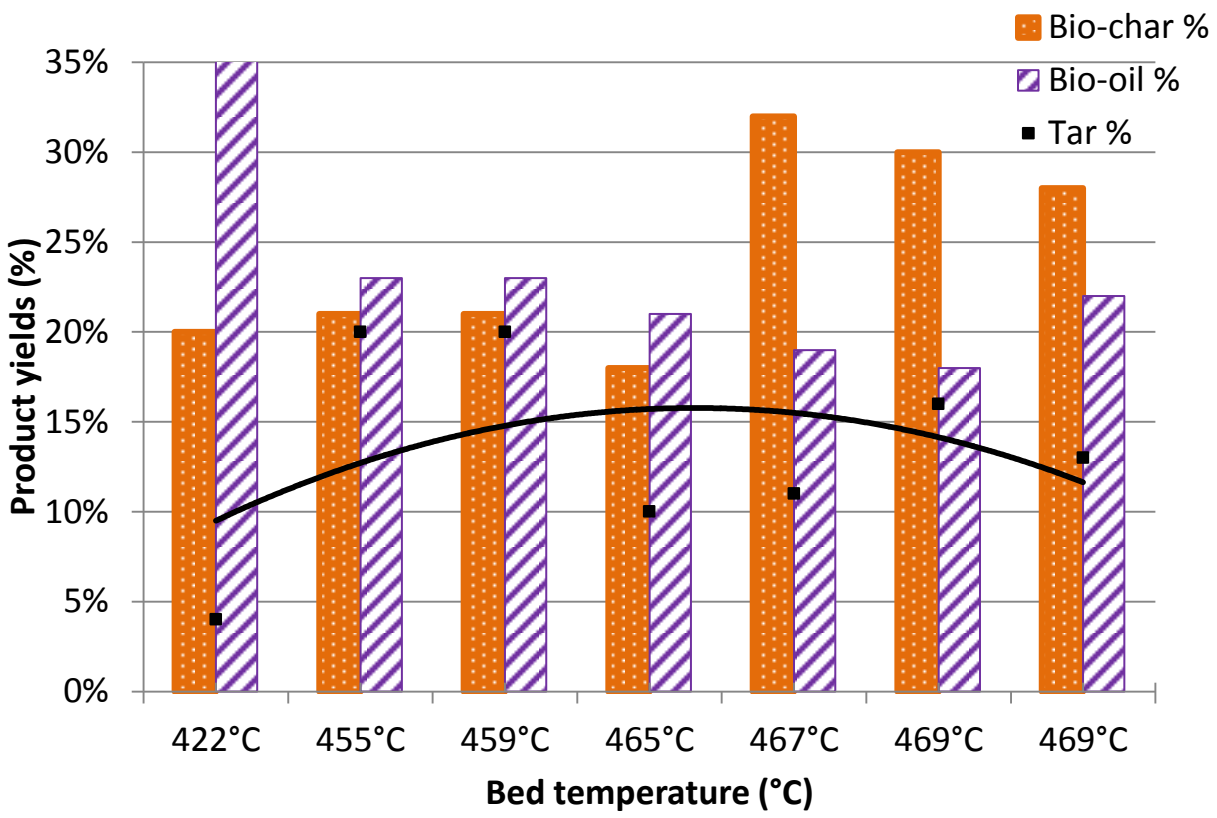

Figure 4.10: Plot of the effect of process temperature on 50/50 *Pinus Radiata* Sawdust and *Pinus Radiata* Bark feed product yields.

Table 4.4: Data Collected During Mixture Runs (Feedstock Size 1.5–4.4mm)

Run number	Avg. bed T (°C)	Moisture content feed wt%	Bio-char wt%	Tar wt%	Bio-oil wt%
70/30 Pinus Radiata sawdust/bark					
Sample 1	424.8	9.51	16 %	4 %	34 %
Sample 2	468.0	8.40	22 %	13 %	29 %
Sample 3	468.8	8.11	23 %	14 %	15 %
Sample 4	469.2	9.40	27 %	19 %	23 %
Sample 5	469.9	8.11	28 %	18 %	20 %
Sample 6	470.6	8.26	26 %	17 %	21 %
Sample 7	472.8	7.18	23 %	11 %	29 %
50/50 Pinus Radiata sawdust/bark					
Sample 1	421.6	9.83	20 %	4 %	37 %
Sample 2	469.4	11.67	30 %	16 %	18 %
Sample 3	469.4	12.31	28 %	13 %	22 %
Sample 4	466.6	8.03	32 %	11 %	19 %

The 70/30 mixture runs produced on average 14% tar, 24% bio-oil and 24% bio-char. Compared with 7% tar, 30% bio-oil and 15% bio-char collected on average from *Pinus Radiata* sawdust runs, the 70/30 mixture might seem like the most attractive option for further investigation because of its higher tar yields; however, its bio-oil yields are lower. The 50/50 *Pinus Radiata* bark/ *Pinus Radiata* sawdust runs did not show much improvement in the total average yields collected, with 13% tar, 23% bio-oil and 24% bio-char. Bark is denser than sawdust (Oasmaa, 2002); therefore, a higher portion of bark in the feed mixture caused problems in the reactor system used for investigations at the CRL Energy Laboratory in Wellington.

Surprisingly, the highest yield of bio-oil was collected at the lowest temperature run using the 70/30 mixture (see Figure 4.9). The bio-char yield collected during the 70/30 runs was mostly 10% higher than runs with only sawdust. Tar yields were highest at the 469–470°C reaction temperature. During the experimental runs with the 50/50 ratio, the average bio-char yield was 20%, with a maximum of 30% at 467°C. The average tar yield was 15% to 20%, reasonably high. Bio-oil yields varied from 20% to 25% of the feed.

Operating temperature (inside the reactor), heating rate (of the biomass feedstock) and residence time (of feed in the reactor) are key parameters that affect fast-pyrolysis products. The yield of solid product decreases and the liquid product yield increases as the operating temperature and residence time are increased. The selection of the operational conditions for the pyrolysis process depends on the target product yield and desired product composition. From the completed research, the temperature was found to have the most influence on the product yields (see Table 4.5 and Figure 4.6). Within the temperature domain of this study, the bio-char yield decreased significantly as the pyrolysis temperature was increased. The bio-oil yield declined as the sawdust particle size rose. The water content in bio-oil increased as did the sawdust particle size.

4.4 Effects of Feed Moisture Content

The feed moisture content of the collected samples was measured at the CRL Energy Laboratory in Wellington. Three to four samples were taken from each batch of feedstock before the experimental run. The data collected from tests on laboratory samples of *Pinus Radiata* sawdust is illustrated in Figure 4.11. The properties of the collected products vary with different operational conditions.

Table 4.5 summarises the results of eight runs. Feed moisture content was varied deliberately. The purpose of these tests was to analyse and follow up on any difference that the moisture content of the feedstock made in the product yields. The bed temperatures of the runs were reordered. Collected bio-oil was sampled and tested by an external laboratory. The results of the completed analysis are discussed but are not available for inclusion in this thesis.

Table 4.5: Samples from Regular *Pinus Radiata* Sawdust Runs (1.5–4 mm Particles)

Run number	Bed T (°C)	Feed moisture content (wt%)	Bio-char (wt%)	Tar (wt%)	Bio-oil (wt%)	Gas (wt%)
Sample 1	421.6	8.20	19.8%	3.6%	36.8%	39.7%
Sample 2	424.8	19.60	16 %	4 %	34 %	46 %
Sample 3	466.5	7.85	9 %	4 %	16 %	71 %
Sample 4	468.0	11.27	18 %	18 %	24 %	40 %
Sample 5	468.6	16.84	10 %	5 %	22 %	63 %
Sample 6	470.2	7.22	19 %	13 %	25 %	43 %
Sample 7	472.9	7.36	17 %	15 %	25 %	43 %
Sample 8	473.9	8.23	19 %	12 %	27 %	42 %

As seen in Table 4.5, feedstocks which originally had a high moisture content mostly produced high yields of gas (46%–63%). Samples 2, 4 and 5 had a high moisture content. However, in Sample 3, low moisture content in the feed and high gas yield production was observed (see Table 4.5). Thus, there must be other factors which influenced the yield outcomes. No direct relationships were observed between the feed moisture content and product yields in Table 4.5. However, a slightly different conclu-

sion can be drawn from Figure 4.11. After chemical analysis on the bio-oils, Harrison observed that feedstock samples which had a higher moisture content at the injection into the hopper step had higher H_2O content in their composition (Harrison, 2012). Figure 4.11 presents a clearer trend of the moisture content in feedstock analysis than Table 4.5.

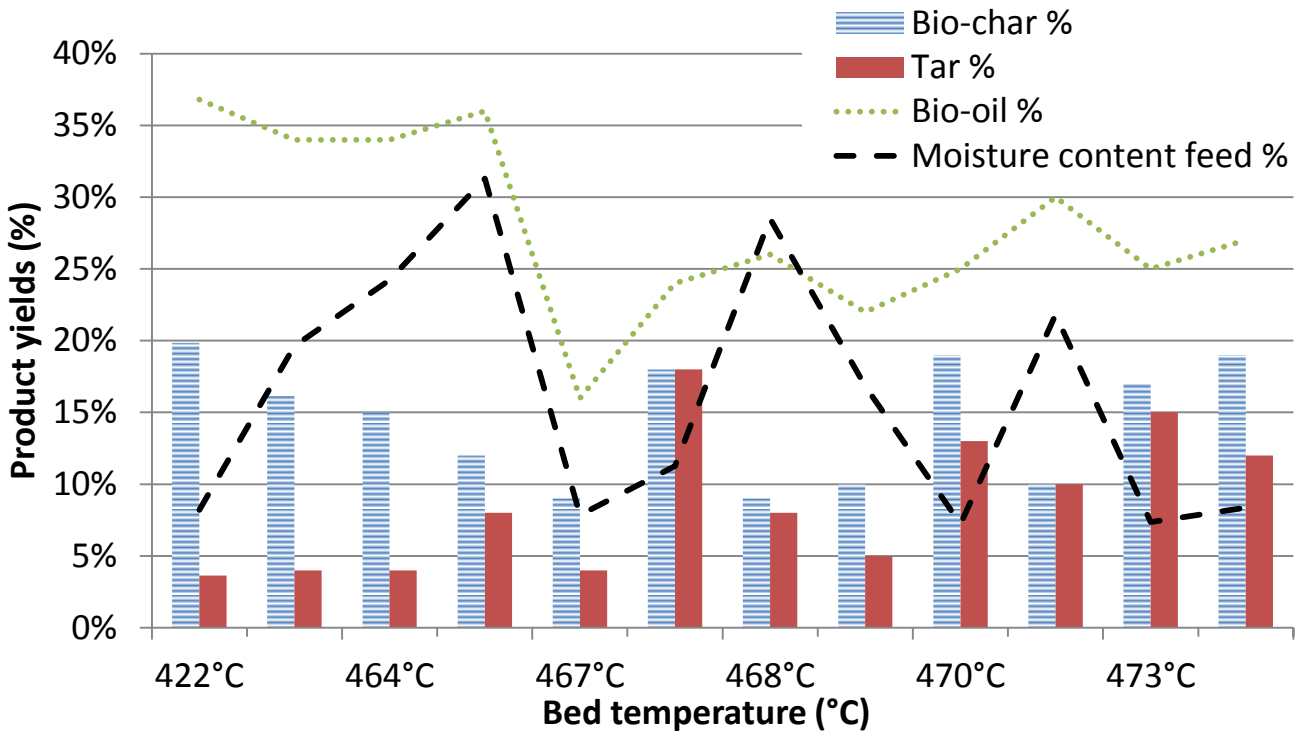

Figure 4.11: Representation of useful products yield collected during the experiment against the moisture content of *Pinus Radiata* samples (Percentage)

Figure 4.11 shows that the relationship between the bio-oil yields and moisture content of the feedstock is much greater than the correlation between the moisture content and yields of other products. Peaks in the 'moisture content feed %' line correspond with peaks in the 'bio-oil %' product yield line. Similarly, the troughs of these plots follow one another; these results are expected because bio-oil products have aqueous content (Harrison, 2012). Tar and bio-char products generally do not have water yields in their compositions. In most cases, the results in Figure 4.11 indicate that higher moisture content in the feed material generates higher bio-oil liquid product yields during pyrolysis, primarily because of the higher water content in the bio-oil (Harrison, 2012). Thus, additional moisture content in the feed does not add value to the system products. Nevertheless, some H_2O consistency in the feedstock is important

for the pyrolysis reaction (Sadaka, 2007). Based on Table 4.5, the most beneficial moisture content in the feedstock was 10% 12% of the feed because most tar and bio-oil yields were produced by the *Pinus Radiata* sawdust feedstock with moisture content in this range.

Darmstadt (1999) conducted vacuum pyrolysis of maple bark and softwood bark with 6% to 24% moisture content at 500°C. Darmstadt (1999) found that maple bark produces bio-char yields of 30%, but for softwood bark, the bio-char yield was smaller (23%–28%). Darmstadt (1999) suggested that the bio-char yield of maple bark pyrolysis depends only slightly on the bark moisture. Darmstadt (1999) studied the surface and bulk chemistry of bio-char through electron spectroscopy chemical analysis (ESCA) secondary ion mass spectroscopy (SIMS) and Raman Spectroscopy (RS), respectively. Darmstadt (1999) suggested that, by decreasing bark moisture, the charcoal surface becomes more graphite-like and that the bark moisture had only a limited influence on the bulk structure.

Table 4.6a shows the moisture content of the feedstock used and the product yields that Darmstadt (1999) collected during his pyrolysis experiments in 1999. Generally, the types of wood Darmstadt used are similar to those used in this thesis. Table 4.6b presents the product yields and the moisture of the feed used in this thesis. Darmstadt (1999) does not clarify which softwood' tree he used; 'hardwood' refers to Maple (*Acer saccharum marsh*). In Table 4.6b, 'softwood' describes *Pinus Radiata*; 'Softwood +SW Bark' *Pinus Radiata* plus *Pinus Radiata* bark runs mixed at different ratios; and 'hardwood' for *Eucalyptus Nitens* feedstock.

In Table 4.6a, Darmstadt's data shows that the products of vacuum pyrolysis of softwoods are 56%–57% liquid and 22%–28% solid. These values are higher than the 40%–44% liquid and 15–20% solid product yields from the softwood researched for this thesis. Another difference in the present work (see Table 4.6b) was the influence of the moisture content of the feed on the liquid products yield. Higher moisture in the feed created more liquid, specifically bio-oils yields, as observed and discussed in Figure 4.11. Additionally, pyrolysis of the hardwood sample resulted in much lower yields of liquid and

solid products. The pyrolysis of sawdust generated 39% liquid products and 17% solid products compared to 62% liquid and 30% solid products reported by Darmstadt's (1999) at the same moisture content in the feed. The differences between vacuum and flash pyrolysis and different feedstocks used were identified as the main reasons for the variance in the findings.

Table 4.6 (a): Product Yields Collected from Softwood and Hardwood Sample Runs by Darmstadt (1999)

		Product yields (wt%)		
	Feed moisture content (wt%)	**Solid**	**Liquid**	**Gas**
Softwood S#1	42.4	22.6%	56.7%	20.7%
Softwood S#2	6.1	28.4%	57.1%	14.5%
Hardwood S#1	42.5	30.2%	62.9%	6.9%
Hardwood S#2	12.1	30.2%	62.6%	7.2%
Hardwood S#3	7.3	31.0%	63.4%	5.6%
Hardwood S#4	6.0	31.6%	62.8%	5.6%

Table 4.6 (b): Data collected during 2012 research at CRL Energy.

		Product yields (wt%)		
	Feed moisture content (wt%)	**Solid**	**Liquid**	**Gas**
Softwood S#1	8.20	20 %	40 %	40 %
Softwood S#2	19.60	16 %	38 %	46 %
Softwood S#3	24.22	15 %	38 %	47 %
Softwood S#4	21.81	10 %	40 %	50 %
Softwood S#5	31.29	12 %	44 %	44 %
Softwood + SW Bark S#1	9.83	20 %	41 %	39 %
Softwood + SW Bark S#2	9.51	16 %	38 %	46 %
Softwood + SW Bark S#3	8.11	28 %	38 %	34 %
Softwood + SW Bark S#4	11.67	30 %	34 %	36 %
Softwood + SW Bark S#5	12.31	28 %	35 %	37 %
Hardwood S#1	11.62	17 %	39 %	44 %

According to Darmstadt (1999), bio-char produced during vacuum pyrolysis had a reasonably high surface area (200–300 m^2/g). Thus, the author concluded that the studied material was an attractive feedstock for the production of activated carbon. The surface area of bio-char collected during the original research discussed in this thesis was not measured. This could be a task for future investigation.

Some research underway is aimed at investigating bio-oil substitutes for liquid petroleum fuels. Bio-oil offers some advantages in transport, storage, combustion, retrofitting and flexibility in production. However, if this is to be a subject for further study, the water content in the liquid products of the process (bio-oil) needs to be accounted for. A high water content in the collected products was identified during runs using the wetter feedstock.

4.5 Effects of Feedstock Particle Size for *Pinus Radiata*

Particle size is an important characteristic of the feedstock. It influences the speed of the reaction and controls the temperature profile within the biomass particle during pyrolysis. The possibility of a temperature gradient existing within the particle was further explored. The time required for the centre of a particle to reach the reaction temperature was comparable to the time needed for the various pyrolysis reactions to occur; thus, the lag in heat transfer must be considered (Zhang, 2007). The surface temperature of the solid is not completely determined by the fluidized bed reactor or nitrogen gas temperature. Additionally, the energy generated or consumed (exo/endothermic) during the primary and secondary pyrolysis reactions influences the temperature (Zhang, 2007). The particle sizes researched in this study were <1.5 mm and 1.5–4 mm.

Zhang (2007) investigated the heat and energy transfer inside sawdust particles heated by hot gas during pyrolysis. Zhang (2007) assumed that the energy was transferred by convection to volatile products at the sawdust particle surface. Radiation was assumed to be negligible. Zhang's (2007) model was studied and slightly modified to match the conditions of the system in this thesis and the research variables in the pyrolysis rig used at the CRL Energy laboratory. The following model can determine the time it

takes for a particle to reach pyrolysis temperature and thus react. The particle size and temperature of pyrolysis process are required to predict the average residence time of the particle in the reactor.

To calculate the residence time of the sawdust particle in the fluidised bed reactor, the heat rate of energy transfer from the heated nitrogen gas to the particle is required. This can be expressed using equation of convection (Perry & Green, 2007):

$$q = hA_p(T_g - T_p) \qquad (1),$$

where q is the net heat rate of energy transfer from heated nitrogen gas to the sawdust particle;
h is the heat transfer coefficient corresponding to the total surface area of the hot gas (nitrogen) with a sawdust particle; T_g and T_p are the gas and particle temperatures; and A_p is the surface area of the particle.

In addition to the convection heat transfer process, sawdust and nitrogen gas heat exchange occurs due to the conduction energy exchange process (Perry & Green, 2007):

$$q = m_p C_p \frac{dT_p}{dt} = \rho_p V_p C_p \frac{dT_p}{dt} \qquad (2),$$

where m_p is the weight of the sawdust particle; ρ_p is the density of the sawdust particle; C_p is the heat capacity of the sawdust particle; and V_p is the volume of the sawdust particle.

Since radiation heat exchange was assumed to be negligible, the sum of conduction and convection represent the total energy and heat exchange process in the sawdust–nitrogen gas system. Thus, equations (1) and (2) are combined and rearranged produce equations (3), (4), (5), (5), (6), (7) and (8).

$$\frac{dT_p}{dt} = \frac{6Nuk_g}{\rho_p C_{p\,particle} d_p^2}(T_g - T_p) \qquad (3),$$

where Nu is the Nusselt number (Equation (4), Perry & Green, 2007); k_g is the thermal conductivity of the nitrogen gas (Equation (5), Perry & Green, 2007); d_p is the diameter of the sawdust particle; and $\frac{dT_p}{dt}$ is the change of the temperature of the sawdust particle with time.

$$Nu = 2 + 0.60Re^{1/2}Pr^{1/3} \qquad (4),$$

where *Re* is the Reynolds number for nitrogen gas (Equation (6), Perry & Green, 2007) and *Pr* is nitrogen's Prandtl number, (Equation (7), Perry & Green, 2007).

$$k_g = -9.2093 * 10^{-3} + 8.5836 * 10^{-5} * T_g - 1.8941 * 10^{-8} * T_g^2 \qquad (5)$$

$$Re = \frac{d_p v_g \rho_g}{\mu_g} \qquad (6)$$

$$Pr = \frac{\mu_{gas} C_{p\,gas}}{k_{gas}} \qquad (7)$$

$$t = t_{final} - t_{initial} = \frac{\rho_p C_p d_p^2}{6Nuk_g} \left(T_g * \left(T_{p\,final} - T_{p\,initial}\right) - \frac{\left(T_{p\,final} - T_{p\,initial}\right)^2}{2}\right) \qquad (8),$$

where *t* is the time it takes for the sawdust particle of the diameter d_p to reach the pyrolysis temperature, in other words, the residence time of the sawdust particle in the fluidised bed reactor.

Constants used in the model: (Equations (1)–(8))

$\rho_{particle} = 551.036 \ \frac{kg}{m^3}$, density of pine sawdust (Engineering ToolBox, 2013)

$\rho_{gas} = 0.44854 \ \frac{kg}{m^3}$, density of nitrogen at 1 bar and 480 °C (Engineering ToolBox, 2013)

$C_{p\,particle} = 1.39 \ \frac{kJ}{kg\,K}$, heat capacity of sawdust (Engineering ToolBox, 2013)

$C_{p\,gas} = 1.11 \frac{kJ}{kg\,K}$, heat capacity of nitrogen gas (Engineering ToolBox, 2013)

$\mu_{gas} = 0.018\ cPs$, absolute viscosity of nitrogen (Engineering ToolBox, 2013)

Table 4.7: Reaction Time Results Produced by the Heat Exchange Model at Decided Diameter Sawdust Particles, Equation (8) Outputs.

Pyrolysis bed temperature	Particle diameter	Time *
°C	m	s
480	0.0040	36.87
480	0.0015	5.185
480	0.0001	0.023

* Time for a sawdust particle to react

Zhang (2007) found that particles with a diameter of 0.1 mm (0.0001 m) take approximately 0.026 s to reach the surrounding gas temperature at 649°C. Model variations due to a lower temperature are considered in this0 thesis model in equation (8). Based on Zhang's (2007) model, particles with a diameter of more than 0.5 mm (0.0005 m) require more than 0.48 s to reach the gas temperature. According to equation (8), which was created specifically for the pyrolysis rig used in this research, particles with a diameter of 4 mm (0.004 m) take approximately 37 s to react (Table 4.7). Sawdust particles with a diameter of 1.5 mm (0.0015 m) take 5 s, while 0.1 mm (0.0001 m) particles take 0.023 s to reach a fluidised bed temperature of 480°C. Thus, as expected, larger particles take longer to react.

From the collected data (Figure 4.6), most liquid products were collected during the run at 464°C, with low tar yields. Using sawdust with a diameter of less than 1.5 mm is not recommended for an upgraded system. Faster reaction times were observed for smaller-sized samples of the feedstock. This result was expected because, when in contact with hot gas, smaller particles react faster.

Gaston (2011) stated that, with an increase in particle size, the formation of light gasses decreases and the formation of bio-char increases and that yields of gas product increase with temperature. For large particles, the power-law dependence of particle devolatilisation time on sphere diameter holds true (Gaston, 2011). With an increase in the size of the spheres, the formation of tars and polycyclic aromatic hydrocarbons grows (Gaston, 2011). Gaston (2011) indicates that higher yields of liquid products and bio-char are expected in pyrolysis experiments with larger particles of sawdust. Figure 4.12 and Table 4.8 show yields collected from runs with small-particle size sawdust (<1.5 mm). These experiments were aimed to determine the difference in product yields if the size of the feed was changed. Thus, Figure 4.12 (small feedstock) was compared with Figure 4.6 (ordinary feedstock), which shows the maximum yields of bio-oil and tar collected at 460°C. Some high collected yields have also been observed at the bed temperatures of 465°C and 470°C. As seen in Figure 4.12, the highest bio-oil yield from *Pinus Radiata* sawdust with particles of less than 1.5 mm was observed at 464°C, while tar yields

were highest at 435°C. Further tests are needed to make more concrete evaluations of the optimum operation conditions for this particular feed size. Nevertheless, from these tests, it can be concluded that no major improvements in product yields were obtained after decreasing the size of the feedstock particles.

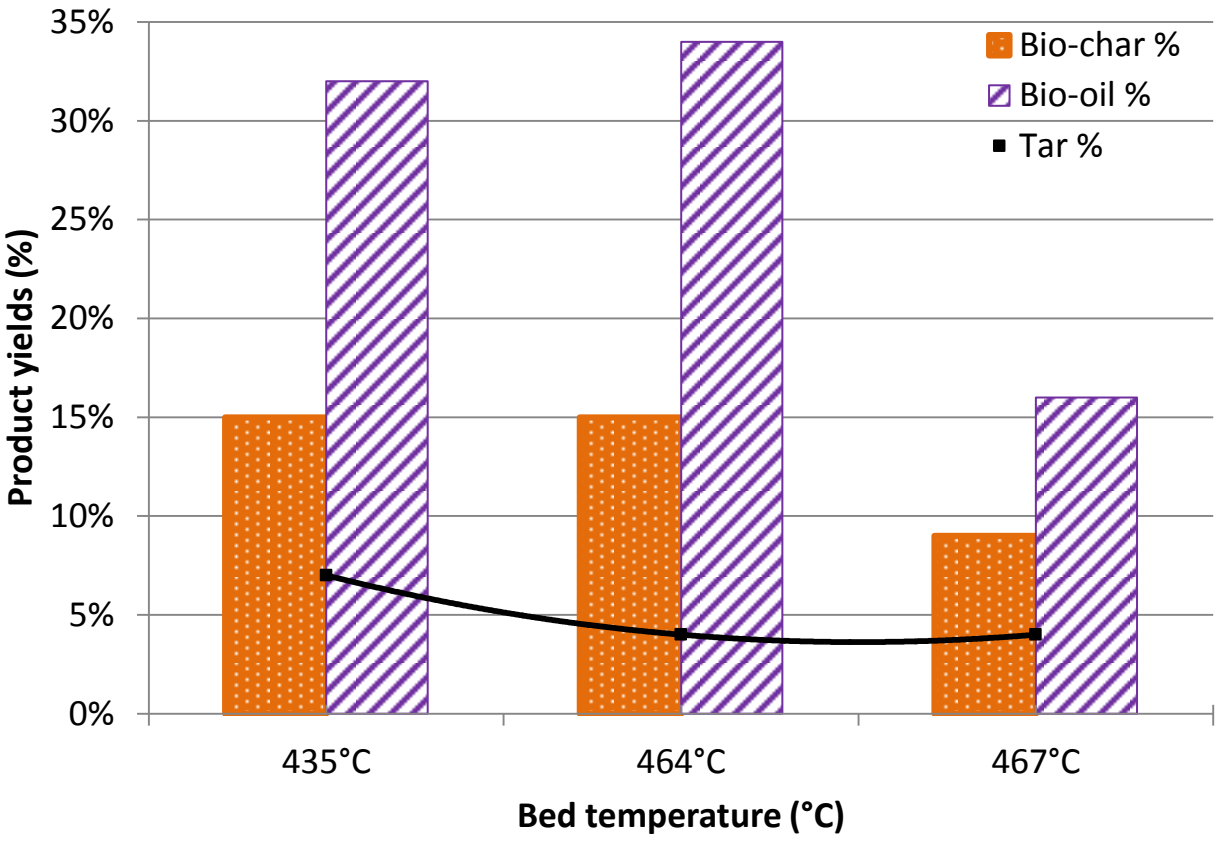

Figure 4.12: Effect of process temperature on *Pinus Radiata* Sawdust (< 1.5 mm) feed product yields

Table 4.8: Collected Yield during Runs with *Pinus Radiata* Sawdust (< 1.5 mm)

Run number	Avg. bed Tempera-ture (°C)	Moisture content feed (wt%)	Bio-char (wt%)	Tar (wt%)	Bio-oil (wt%)
Pinus Radiata sawdust (<1.5 mm)					
Sample 1	435.0	12.55	15 %	7 %	32 %
Sample 2	463.7	5.27	15 %	4 %	34 %
Sample 3	466.5	7.85	9 %	4 %	16 %

The collected data indicate that smaller sawdust does not improve the average yield of useful products. On average, the products from <1.5 mm-sized *Pinus Radiata* samples were 5% tar, 27% bio-oil and 13% bio-char, compared to 7% tar, 30% bio-oil and 15% bio-char from the *Pinus Radiata* runs with 1.5–4 mm samples. These results prove Gaston's theory (2011) and agree with his finding: Higher liq-uid and solid yields are produced from larger-sized sawdust particles.

Chapter 5: Upgrade Scale Plant for Bio-bitumen Production via Pyrolysis of Woody Biomass

5.1 Bio-Bitumen Production Plant from Biomass Pyrolysis

Utilisation of 'green' and sustainable resources for production of highly demanded bitumen in the New Zealand roading industry will offer benefits for New Zealand's economy and environment. The estimated production capacity of the proposed plant upgrade (Figures 5.1 to 5.9 show proposed plant process flow diagrams) is 4000 tonnes per year of bio-bitumen production, to be used in the roading industry. The expected plant conversion efficiency is about 53% which is the key parameter for estimating the raw material supply and economic analysis for the plant. Conversion efficiency estimates how efficiently inputs are converted to outputs. In this part of study, a through economic analysis has been performed and the results will be presented in Chapter 6.

From the economic analysis, the total annual income expected from the preliminary proposed plant is about $5.5 million per year; with the capital investment of $8 million and raw material costs of $3.6 million per year. In the economic analysis, the design, constriction and commissioning period is assumed to be one year while the plant operational lifetime is 20 years. Based on the above assumptions, the predicted payback period is around 6 years. Furthermore, a sensitivity analysis was completed to determine the effect of product and feedstock pricing on the economic feasibility of the process.

The above economic analysis is based on a green field plant, however, a more profitable option for further development may be constructing a bio-bitumen plant on site an existing wood processing plant (pulp and paper plant) or a bio-oil production plant (if there was one to be built in New Zealand).This will reduce initial investment and raw materials costs.

Tar and bio-oil are the target products of the proposed process, however, for economic analysis, bio-char and non-condensable gas are also considered as products which will have some values. The raw material is *Pinus Radiata,* a popular plantation species in New Zealand. Bio-char collected during the pyrolysis of *Pinus Radiata* can be transformed into fuel via briquetting, pelletizing or combined with biomass or coal. Chemical and physical properties of the bio-char are unaffected by wetting and long term water contact. This unique property allows bio-char to be a good fuel choice for storage in humid climate locations. Additionally recent research has found that bio-remediation of agricultural soil with bio-char reduces fertilizer application requirement by more than 50% and increases the land productivity by over 50% (Krishnaratne, 2008).

Pinus Radiata sawdust is pyrolyzed in a bubbling fluidized-bed reactor at operation temperatures between 450 and 550 °C. The fluidised bed reactor volume, nitrogen flow rate through the distributor plate as well as the gas fluidisation rate are optimized to maximize the liquid yield. This is followed by the separation of the liquid, gas and solid products while the liquid is used for production of bio-bitumen. There are three main products collected in this system. Solid product (bio-char) is collected from the bottom of cyclones. Liquid product (bio-oil) is collected from condensers – quenchers in which the pyrolysis gas is cooled down and heavy molecular compounds are condensed to form liquid product. Mesh condenser and an electrostatic precipitator (ESP) are used to collect the other heavier and viscous liquid product (tar). Process gas collected from the system is mostly recycled. Process gas refers to the non-condensable gas, which was found to mostly consist of N_2. Collected analysis of non-condensable gas is shown in Table 4.1. Non-condensable gas is also referred to as ‘exhaust’ gas in this thesis.

Following are details of a pilot scale bio-bitumen plant from biomass pyrolysis process. This will be followed by the PFDs and P&IDs.

5.2 Biomass Pre-treatment and Pyrolysis

The process flow diagram (PFD) for the biomass pre-treatment and pyrolysis is shown in Figure 5.1, and the corresponding piping and instrument diagram (P&ID) in Figure 5.2. Before pyrolysis, the woody biomass of *Pinus Radiata* needs pre-treatment, including sizing and drying. From among the various suppliers throughout New Zealand, a price quote of $50 per tonne of *Pinus Radiata* sawdust delivered to Wellington from Levin was obtained from JB's Environmental Ltd. Biomass can be sourced from residue from wood-processing plants, as well as low-quality logs. The original form of biomass includes sawdust, barks, chips and off-cuts. Depending on the source, the moisture content of biomass varies from 10% for wood residues from wood-remanufacturing plants to 150% for wood residues from sawmills. Therefore, a pre-treatment process is needed to prepare a uniform process-feed mixture with the target particle size and required moisture content. The optimised moisture content for the feed material in the designed process was determined to be 10% before the gasification process. Pulverizing, drying and sieving the delivered feedstock will improve biomass and produce material with more uniform properties. The biomass feeding rate for the pilot-scale plant is 544 kg/h at a dry basis.

The fast-pyrolysis process is expected to have a solid retention time of 2 s in the reactor. High heating rates are needed in the fluidized bed reactor to maximise bio-oil production. Finely ground biomass feed is fed to the reactor bed through the feeding augers. Inside the fluidised bed reactor, the fluidisation gas provides heat to the biomass particles. Heat is also supplied by the bubbling bed material (silica sand) from the pyrolysis reactor walls. More detailed calculations on the sawdust-particle pyrolysis reaction time and residence time in the fluidised bed reactor can be performed based on Zhang et al. (2007). The fluidised bed material is silica sand with particles of 0.5–0.7 mm.

The bubbling fluidised-bed reactor is made of stainless steel. The temperature in the reactor will be monitored using 5 K-type thermocouples on the vertical axis at 5 locations spread equally throughout the reactor body. Nitrogen, which is the fluidisation gas, is fed into the reactor through two channels:

through the biomass feeding at 8 kg/hr and from the reactor bottom at 90 kg/hr. The small stream of nitrogen gas through the feeding augers is first injected into the feeding locked hopper. The continuous supply of nitrogen prevents gas backflow from the pyrolysis reactor and also helps reduce the risk of blockages in the feeding system. Nitrogen will be produced on-site to reduce input raw materials costs and to supply a sufficient amount rapidly and immediately.

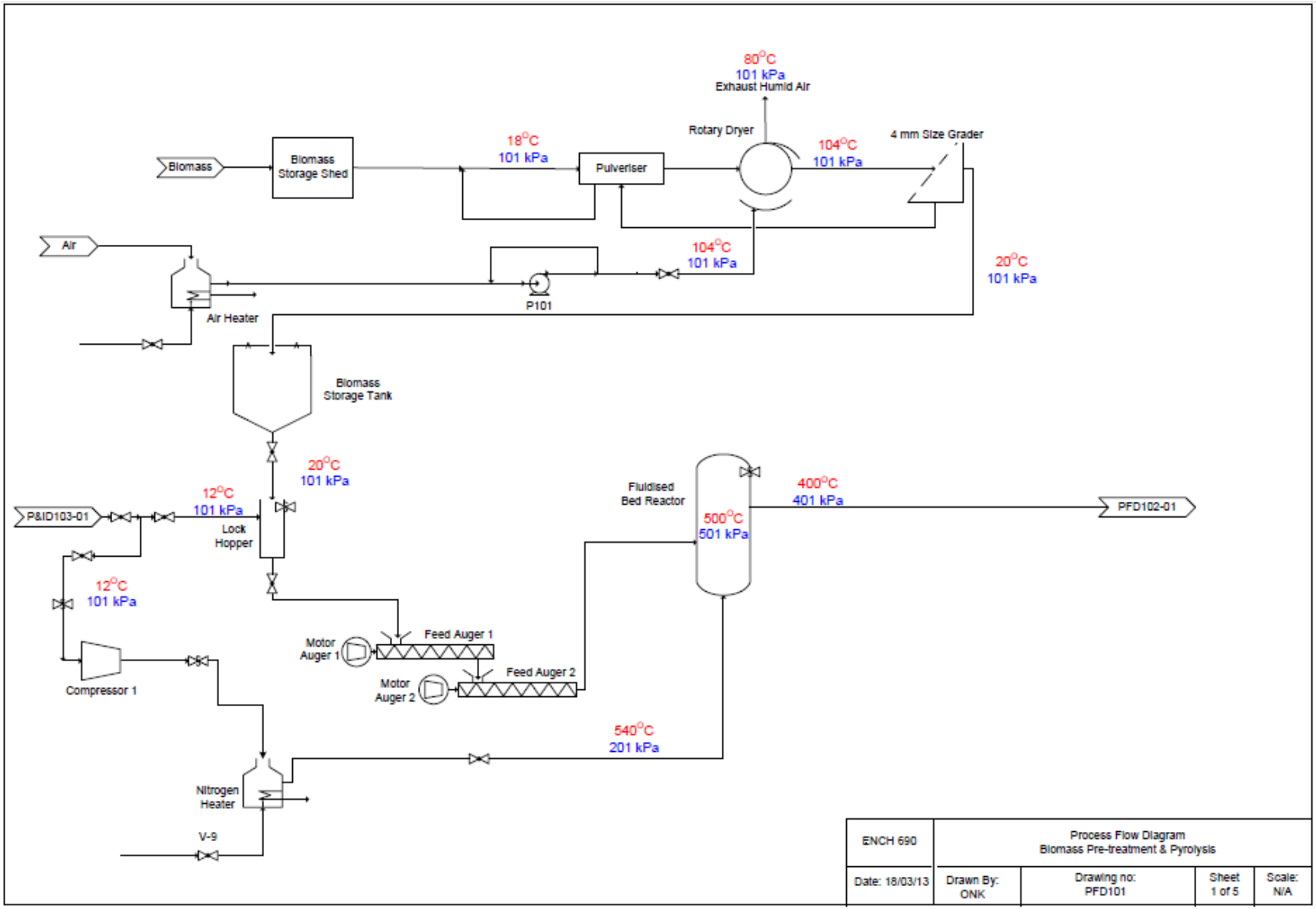

Figure 5.1: The PFD of the biomass pretreatment and pyrolysis process for production of bio-bitumen from woody biomass.

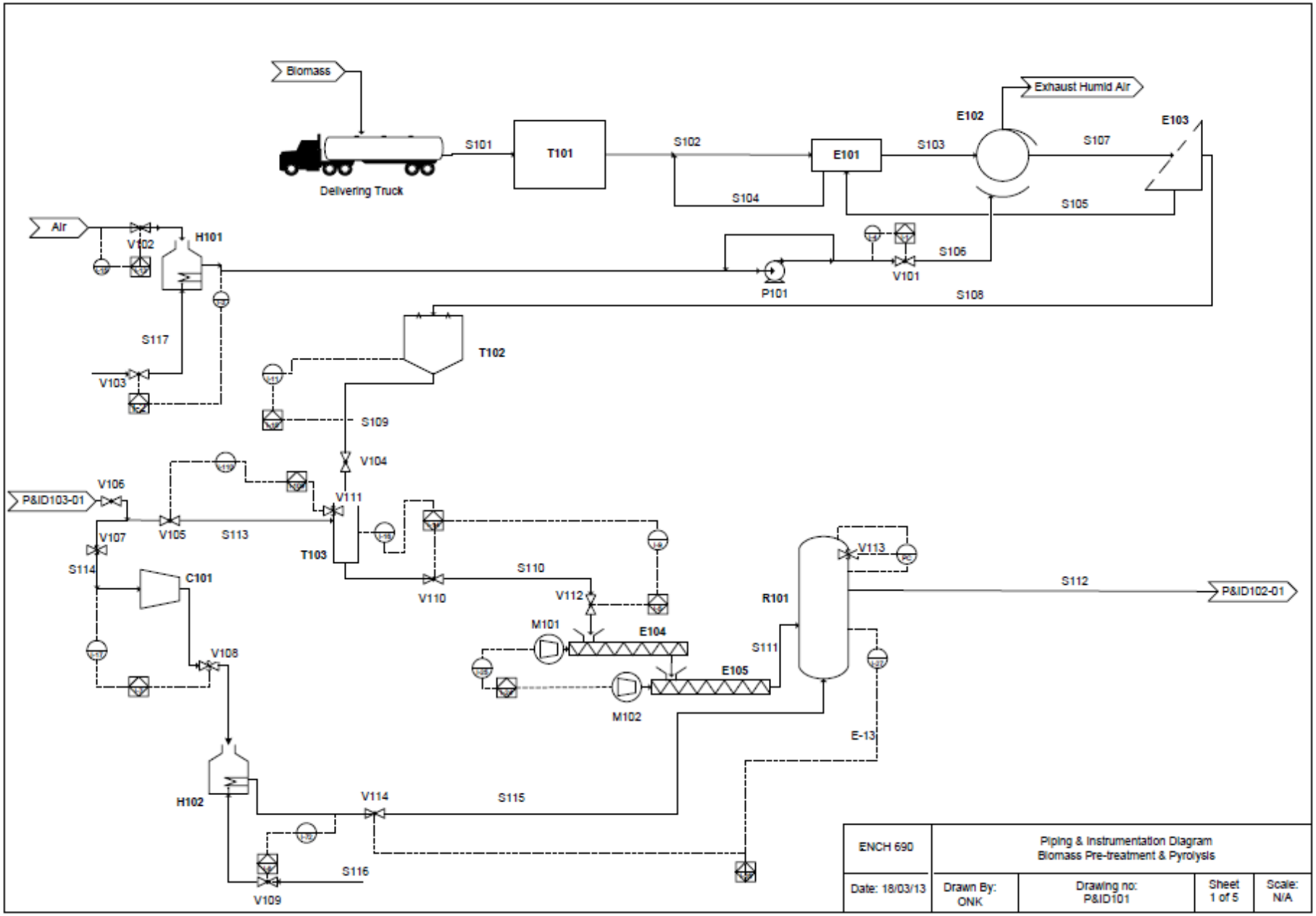

Figure 5.2: P&ID of biomass pre-treatment and pyrolysis for production of bio-bitumen.

5.3 Phase Separation Process

Figure 5.3 shows the PFD for the phase separation section of the plant, including vapour-char separation in 2 cyclones and gas condensation in the condensers. The corresponding P&ID is shown in Figure 5.4. First, 2 stage cyclones perform gas–solid separation. The transfer lines from the pyrolysis reactor to the bio-char separators (cyclones) and from the cyclones to the condensers will be maintained at 300–350°C to prevent the pyrolysis vapour from condensing.

The bio-char, which is the solid product, separates and is collected from the bottom of the cyclones. After solids separation, quenchers rapidly cool the pyrolysis vapours, producing a light-coloured liquid product—pyrolysis oil (bio-oil). Following current design, quenchers cool the gas stream from 300°C to 18°C. At 18°C, the vapour flows into the stainless steel mesh condenser for further phase separation. The mesh acts as a filter, and due to the high surface area and temperature difference of the metal and the gas, the first dose of tar liquid product is collected at this step. Tar also results from the heavy liquid fraction of the process. The vapour flows from the steel condenser for further processing.

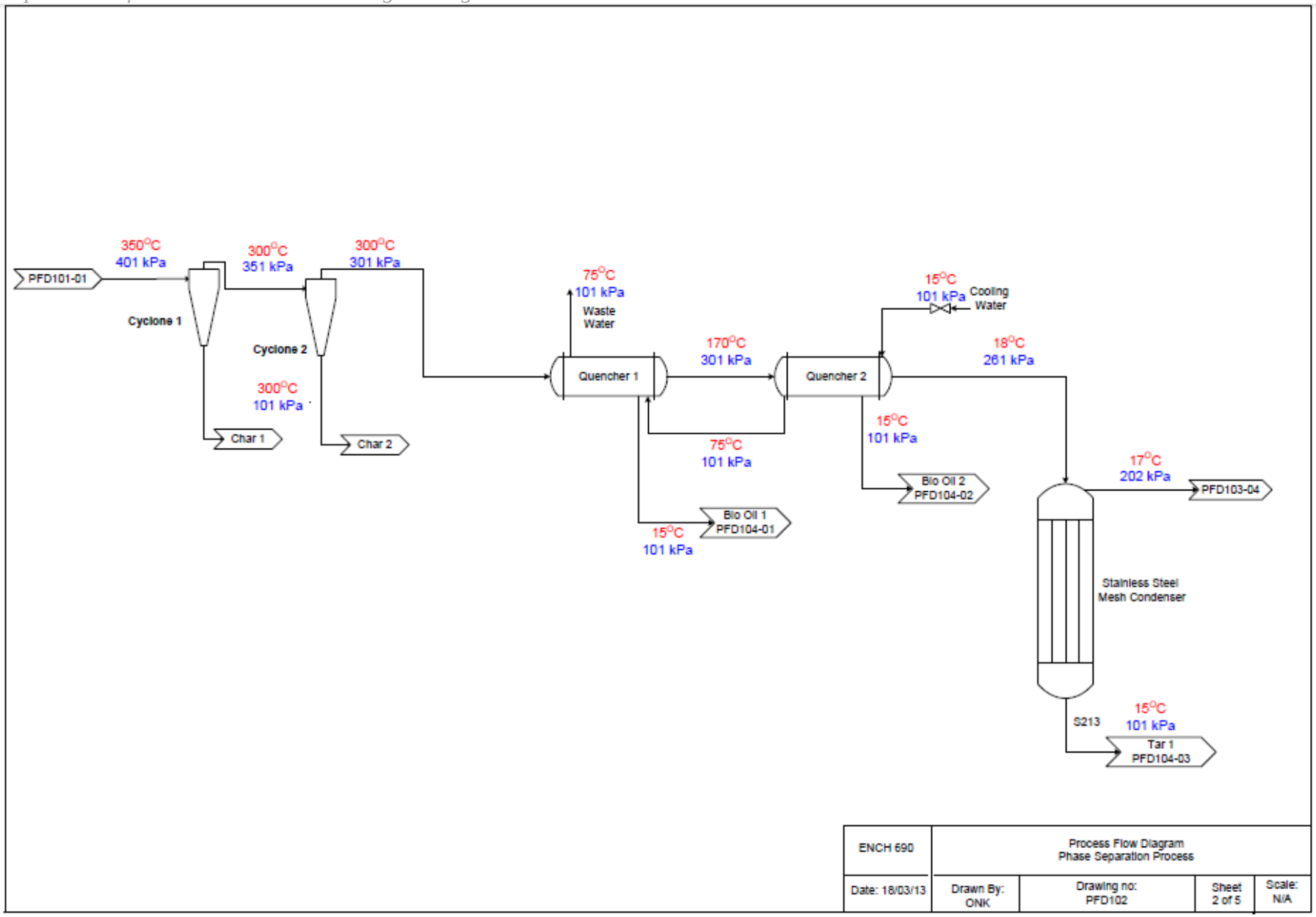

Figure 5.3: The PFD of the phase separation section including vapour-char separation and bio-oil-gas separation in the biomass pyrolysis for production of bio-bitumen.

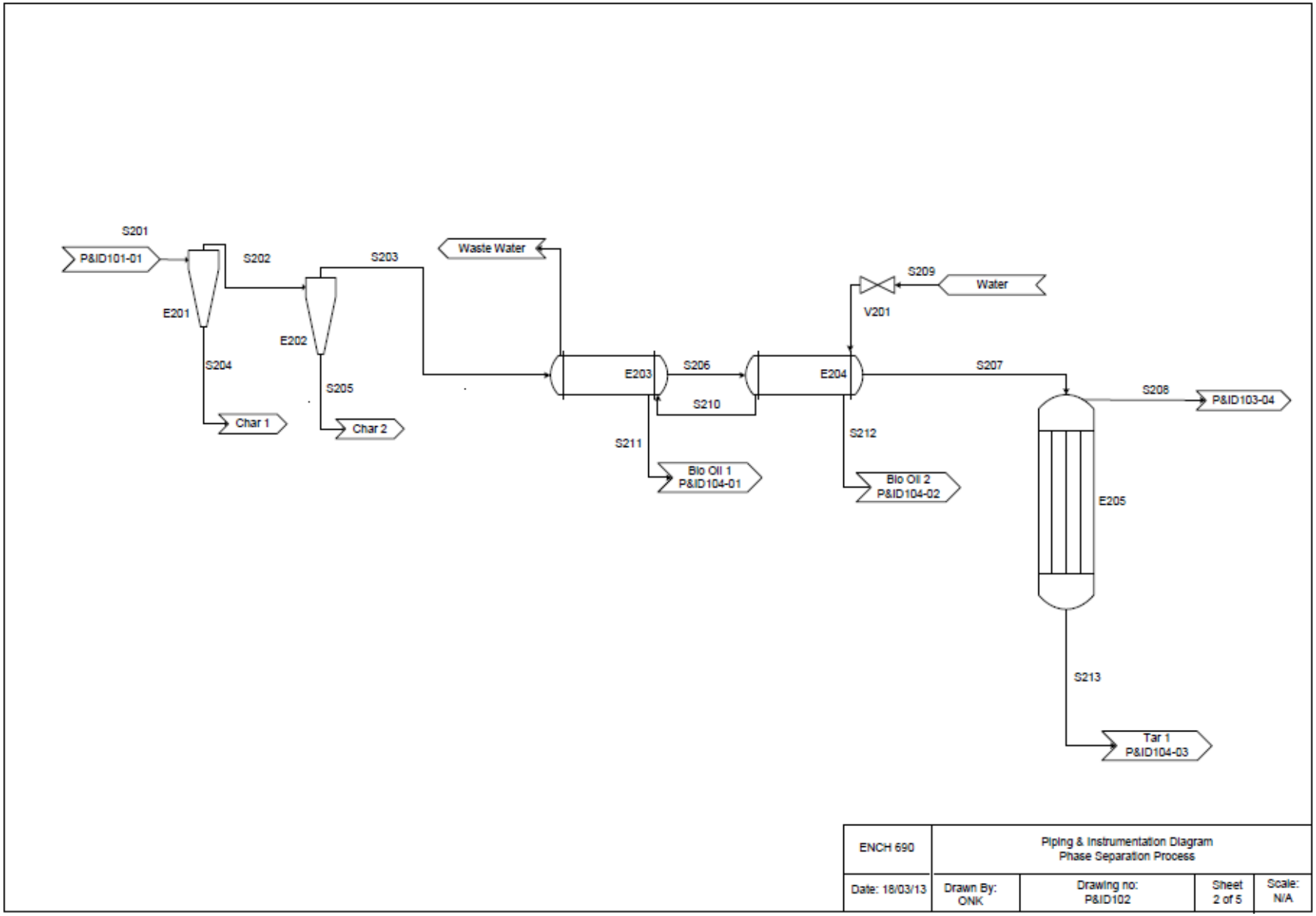

Figure 5.4: The P&ID of the phase separation section including vapour-char separation and bio-oil-gas separation in the biomass pyrolysis for production of bio-bitumen.

5.4 Condensation of Light Molecular Compounds and Nitrogen Production

Figure 5.5 shows the PFD for final stage of liquid-product collection and nitrogen-gas production. The corresponding P&ID is displayed in Figure 5.6. As seen in these figures, the vapour travels from the second-stage condenser to an electrostatic precipitator (ESP), which acts as an electrostatic air cleaner. The technique of ESP has been effectively applied by the chemical and process engineering industry. Potential suppliers are listed in the Appendix.

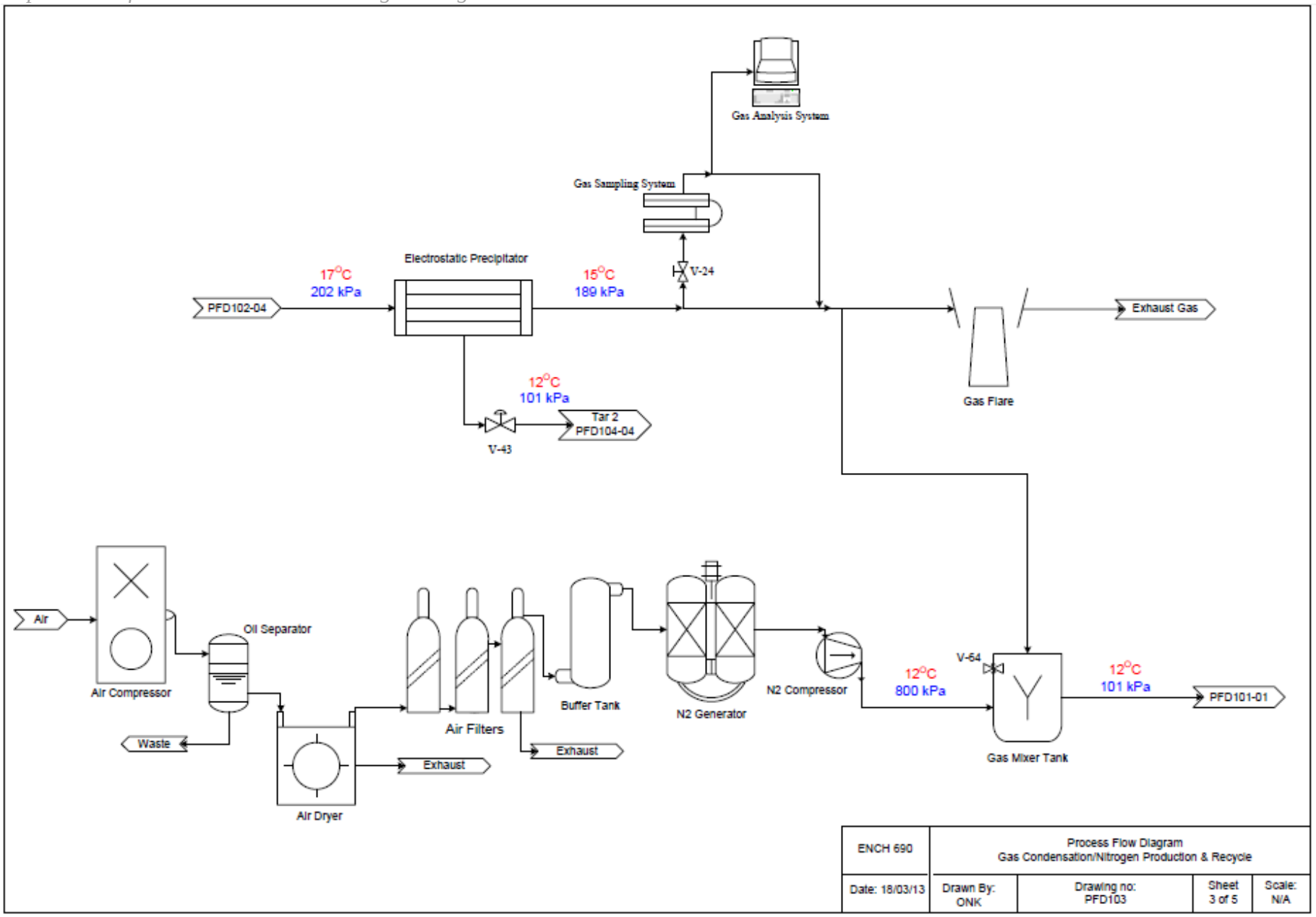

Figure 5.5: PFD of final stage of liquid product collection and process nitrogen gas production.

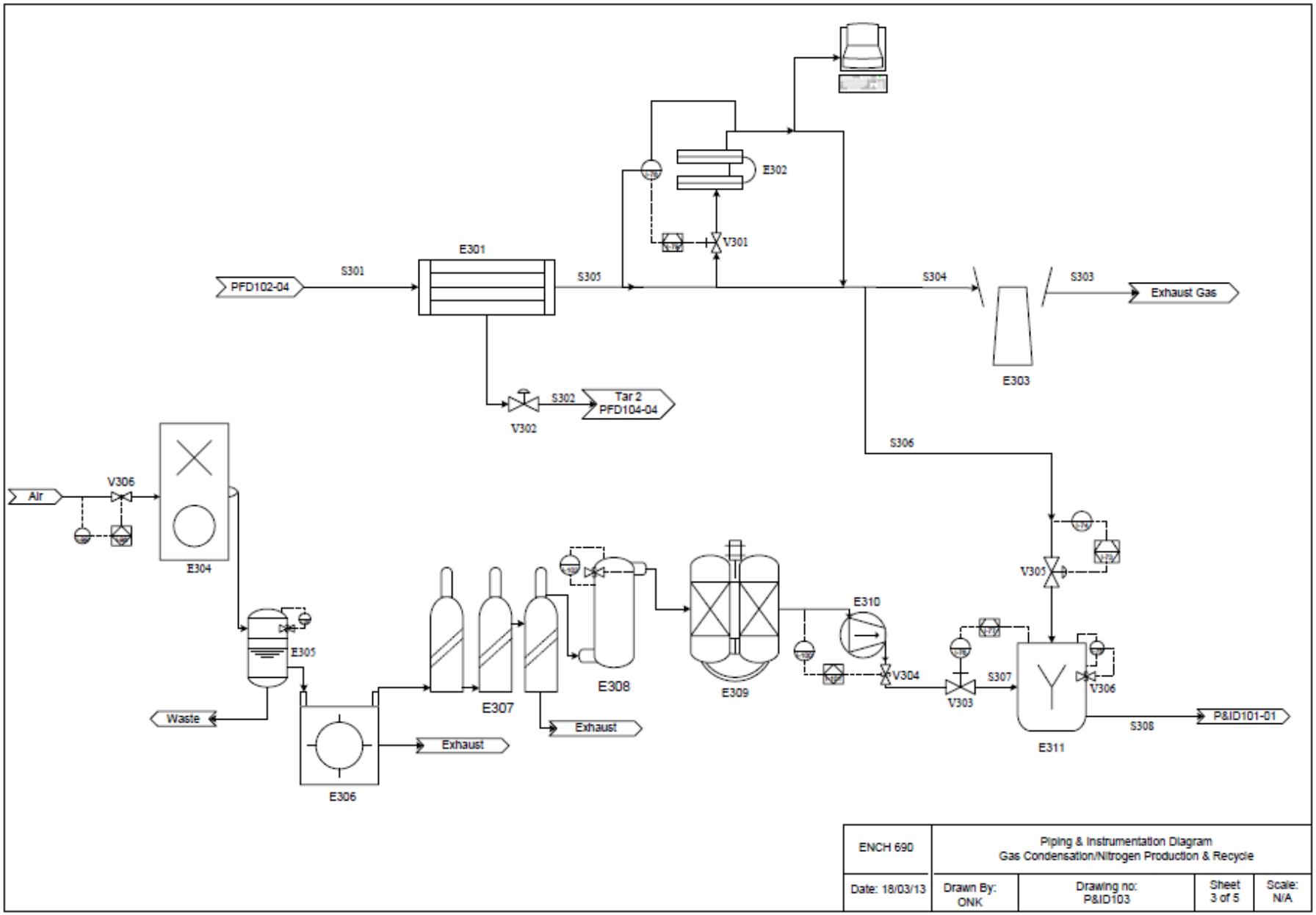

Figure 5.6: P&ID of final stage of liquid product collection and process nitrogen gas production.

ESP efficiently separates the oil droplets from the process vapour. Induced electrostatic charge acts as separation force. ESP is known to be a highly efficient filtration device which is frequently used for large-scale vapour/gas separation. In addition, ESP applies energy only to the vapour matter collected, resulting in low consumption of electricity (Van Paasen, 2004). The ESP consists of a row of thin vertical wires, followed by a stack of large vertical flat metal plates. Gas stream flows horizontally through the spaces between the wires and then passes through the stack of plates. Negative voltage acts between wires and plates. High enough voltage ionises the gas around the electrodes. Negative ions flow to the plates and charge the gas-flow oil vapour particles (Wikipedia, 2013).

The ionised oil droplets follow the negative electric field created by the power supply and move to the grounded plates. The ionised oil droplets are long hydrocarbon chains (a percent of the heavy oil fraction of the process). Newly separated tar from the device accumulates on the collection plates, forming a layer. The final load of liquid product (tar) is collected at this step.

The gas-sampling system is connected to the exhaust gas stream and the personal computer (PC). It logs and ensures that the exhaust gas emitted is within limits and regulations for gaseous air pollutants. Carbon monoxide gas is burnt off in a gas flare. An adjusted portion of the cold processed gas is recycled. The exiting gas mainly consists of 85% N_2 (which can be recycled back into the process), 10% O_2 and small amounts of CO, CO_2, CH_4 and other gases, based on CRL Gracefield Lab (2012) research conducted in Wellington. Pang (2013) pointed out that it might be more useful to recover the combustible gases from the non-condensable gas mixture when the plant is upgraded. This option was not explored further in this thesis and can be investigated in follow-up research.

Nitrogen gas is important for the proposed production process and will be generated on site from atmospheric air. The air will be compressed, dried and filtered before entering the buffer tank and nitrogen generator. Produced nitrogen will be stored on site and pumped by the nitrogen compressor into the

mixing tank. Excess nitrogen can be sold to research labs which do not require 100% nitrogen, while the rest will be used and recycled in the process.

The proposed plant's nitrogen-gas production equipment is based on the TCN series nitrogen generator, which is available in the industry and can be readily bought and installed at competitive prices. Although purchasing a nitrogen generator increases capital costs, it will save a large sum on operation input costs in the long term.

5.5 Bio-Bitumen Production

The bio-oil and tar produced by biomass pyrolysis are collected in 4 operation units throughout the process plant. The streams are mixed with chemical A at a 1:1 ratio to the bio-mixture (bio-oil + tar). Chemical A reduces the oxygen level and improves the stability of the solution. It thus neutralises acidic activity in the bio-oil and tar mixture, lessens the reactivity of certain compounds in the mixture and lowers the water content. No heating is required in the CSTR mixer tank 1. The mixture is next pumped to the bio-hydrocarbons tank, where chemical A and hydrocarbons are separated. Chemical A is then filtered and recycled, while the treated hydrocarbons mixtures travel to the distillation column. The distillation column then separates the liquid mixture into useful product and wastes, with a product yield of 85%. Pure bitumen derived from crude oil is mixed with the useful product in the heated, CSTR mixer tank 2. The pure bitumen will be supplied locally from Z Energy stations (previously called Shell), manufactured originally at Marsden Point Oil Refinery in Whangarei, New Zealand. Bitumen and the organic mixture are stirred in mixer tank 2 for 8 hours at 60 °C, which generates the bio-bitumen product ready for roading use.

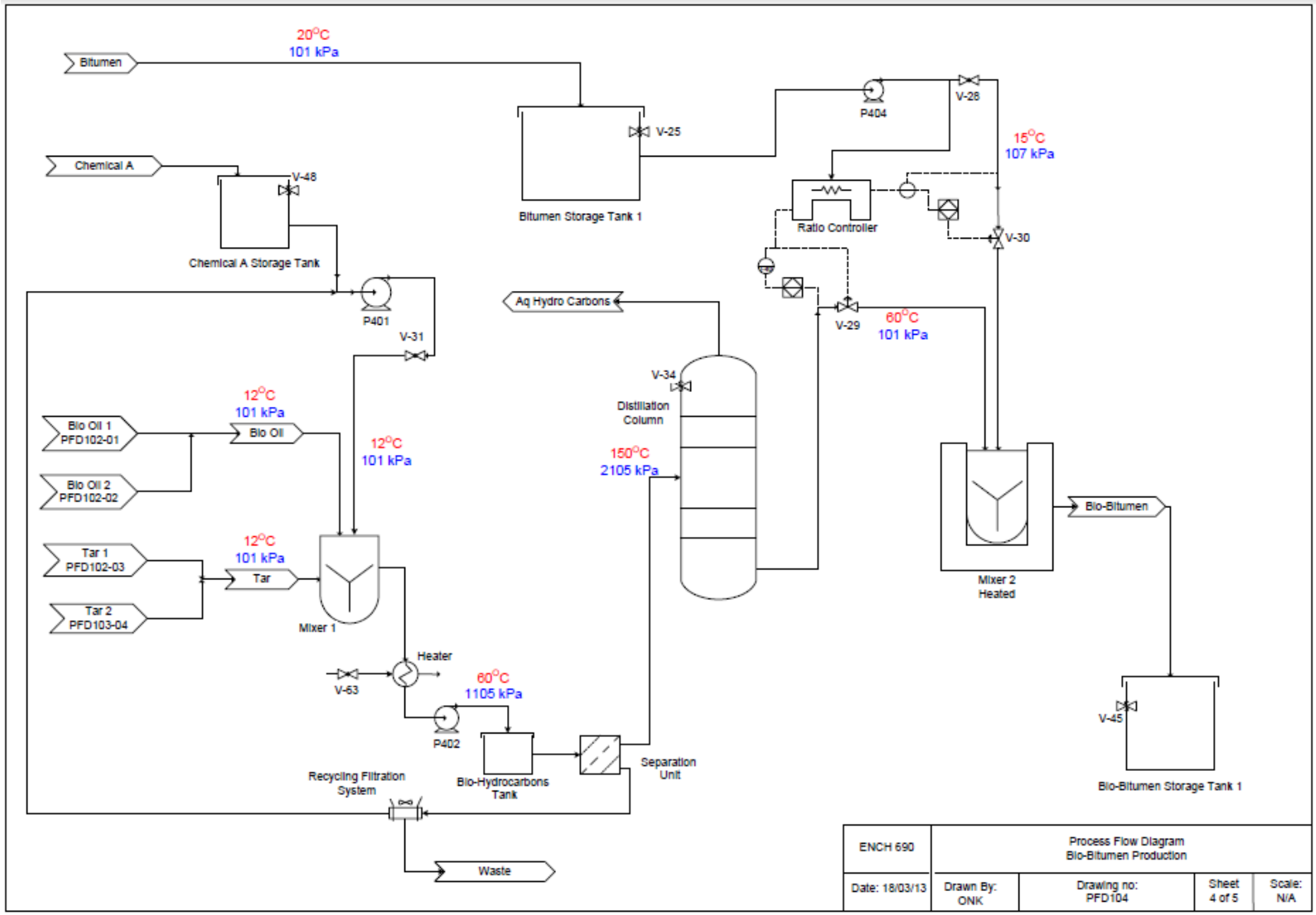

Figure 5.7: PFD of bio-bitumen production using biomass pyrolysis tars.

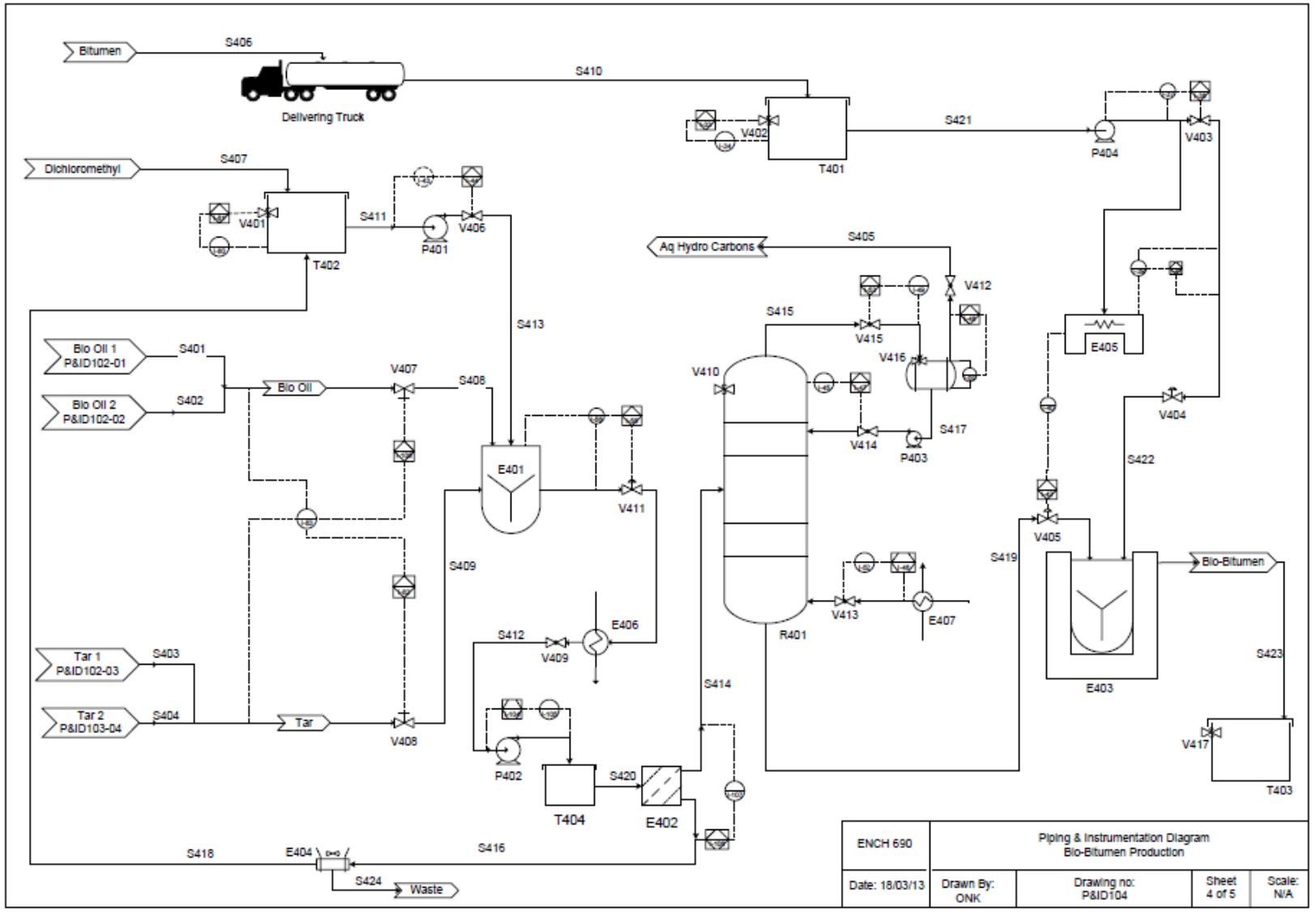

Figure 5.8: P&ID of bio-bitumen production using biomass pyrolysis tars.

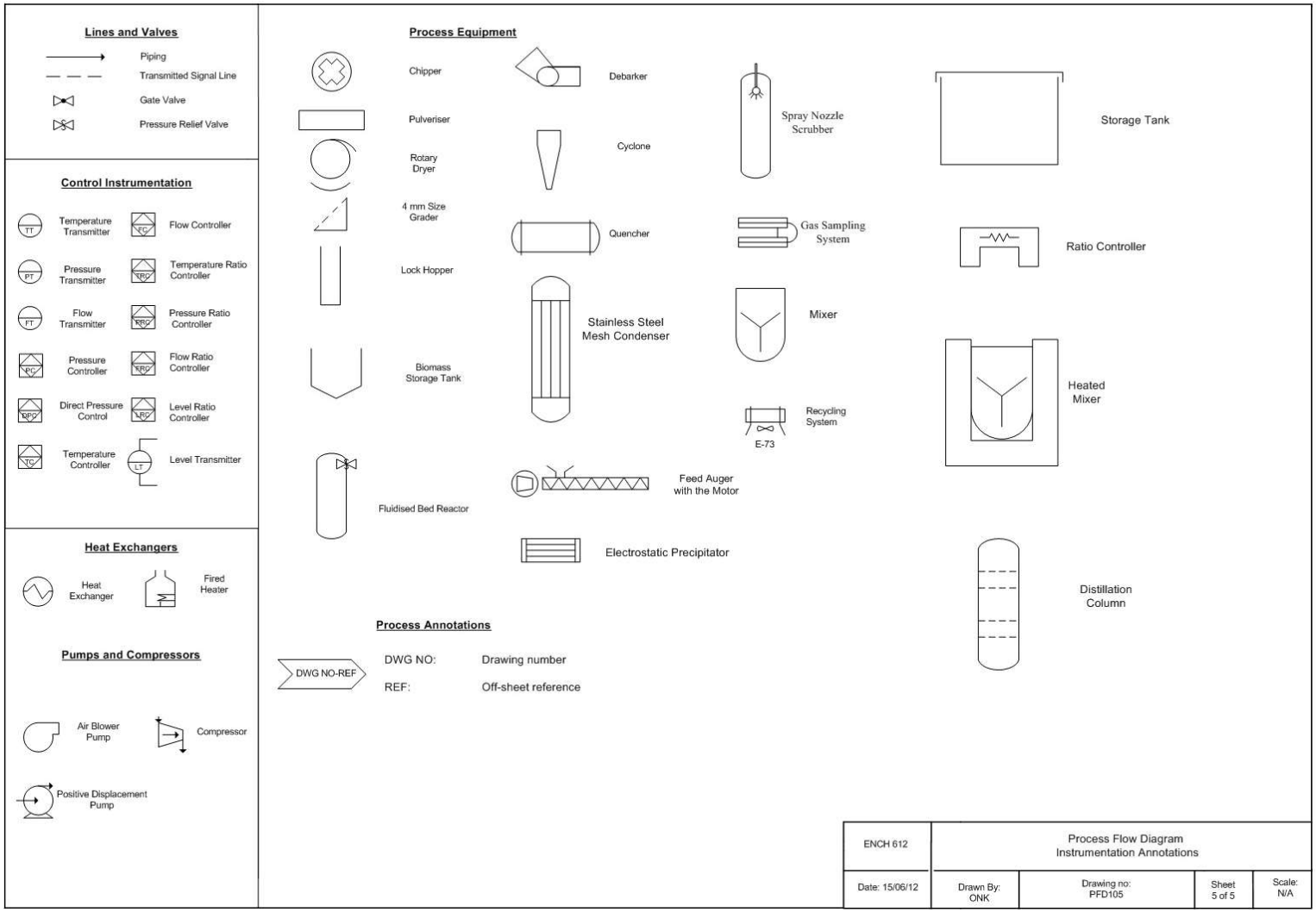

Figure 5.9: PFD of instrumentation annotations used in bio-bitumen production through biomass pyrolysis.

Chapter 6: Economic Analysis, Costs, Production Prediction

6.1 Costs

Techno-economic analysis (TEA) is used to analyse new technology for commercial applications. The proposed process will be an attractive investment on a large scale if the commercial plant can generate a profit. Chapter 5 presents the process flow diagrams (PFDs) which show how biomass would be converted into bio-bitumen, combustible gas and bio-char. Process and instrumentation diagrams (P&ID) illustrate the process in greater detail. These diagrams were designed based on the small-scale fluidised bed reactor. The scale-up design was constructed using *Plant Design and Economics for Chemical Engineers* (Peters & Timmerhaus, 2003) and the third edition of *Products and Process Design Principles: Synthesis, Analysis and Design* (Seider, Lewin, Widagdo, 2008). Equipment costs were calculated based on *Process Capital Cost Estimation for New Zealand* (Society of Chemical Engineers New Zealand, 2007).

Economic analysis was performed to determine the feasibility of the design proposed in Chapter 5 for current quoted prices and possible market prices for the newly developed products. The main feedstock for the plant process is woody biomass (*Pinus Radiata* sawdust). Other inputs are nitrogen gas (produced on site), bitumen (used in the bio-bitumen mixture) and chemical A. The process products are bio-bitumen (a newly developed liquid product for the New Zealand roading industry) and bio-char (a solid product entering a partially developed market thoroughly described in Section 2.4). A cost index for 1991 to 2013 and US currency conversion factor were used in the values from these books which were not in 2013 New Zealand currency. The cost indices from Marshall and Swift (2013) were used.

The first step in TEA is to compare the costs of the overall consumed materials to the revenue gained from the sale of all products. Direct consumed-materials costs for the process are woody biomass, bitumen and chemical A. The revenue-generating process products are bio-bitumen and biochar. The total annual material consumption and products are listed in Table 6.1, along with the cost and revenue gained. Average prices for wood sawdust were sourced from JB's Environmental LTD through direct email communication. The 2008 bitumen prices were sourced from Olsen (2008), and the 2012 quotes from the Z-Energy and Mobile petroleum and bitumen suppliers. Bio-char prices were based on McHenry (2009), while the suppliers Air Liquide and BOC confirmed nitrogen gas prices in personal communications.

Table 6.1: Mass Flow and Prices of Consumer Materials and Products from a Commercial Biomass to Bio-bitumen Plant

Inputs/ Product	Flow (kg/hr)	Flow (tonne/yr)	$/tonne	$/yr
Wood	530	4,300	$ 50	$ 212,400
Bitumen	430	3,400	$ 1,000	$ 3,427,200
Chemical A	15	120	$ 100	$ 11,500
Bio-bitumen	490	4,000	$ 1,200	$ 4,478,700
Nitrogen	90	700	$ 1,500	$ 1,050,000
Bio-char	70	550	$ 1,000	$ 545,460

Note. Raw materials include wood, bitumen and chemical A. Products are bio-bitumen, nitrogen and bio-char.

Table 6.2: Simple Price of Bio-bitumen Production

Cost	$ 3,651,000		
Gain	$ 6,400,000		
Total Bio-bitumen	4,000	Tonnes	
Cost/tonne	$ 910	$/tonne of bitumen	($3,651,000/4,000 tonne)
Net Cost/tonne	$ 687	$/tonne of bitumen (without revenue from N_2)	(($6,400,000-$3,651,000)/4,000tonne)

Note. The first set of assumptions for the production cost of bio-bitumen had a liquid production yield of 38% (bio-oil and tar combined), 15% bio-char yield of 15%, and bio-bitumen mix ratio of 20% bio-mix and 80% bitumen.

Tables 6.1 and 6.2 show that the cost for a unit tonne of bio-bitumen is $910, without considering the capital investment depreciation. The net cost for a unit tonne of bio-bitumen, based on the annual profit gained from bio-bitumen and bio-char sales, is $687, without considering the capital investment depreciation and potential revenue gain from N_2 sales. This cost analysis was based on an annual bio-bitumen production of 4,000 tonnes and a bio-bitumen of 20% water free tar and bio-oil from biomass pyrolysis and 80% bitumen. This price is lower than the $1,000 to produce a tonne of bitumen from crude fossil oil. However, this bio-bitumen price does not include the initial capital investment costs.

The next step in TEA is to estimate the total capital costs for construction of the bio-bitumen plant, including equipment and installation costs. Additionally, the annual expenses for labour and utilities need to be included in the overall calculations to determine the current net present value of the proposed investment project.

It was recognised that biomass pyrolysis can generate different yields of bio-oil and tar and that bio-oil/tar might be mixed with bitumen at different ratios, which would affect bio-bitumen costs and total annual plant-production capability. Therefore, 3 mixture ratios were analysed: 1:4 (20% bio-mixture, 80% bitumen), 1:1 (50% bio-mixture, 50% bitumen) and 1:9 (10% bio-mixture, 90% bitumen). Three cases of product yields for the collected liquid and bio-char from the biomass pyrolysis were also considered. First, in the maximum-liquids case, the products consisted of 65% liquid (bio-oil and tar) and 20% solid (bio-char). Second, in the medium-yield case, it was assumed that the liquid yield was 52% and the bio-char yield 17% from the pyrolysis of woody biomass. Third, in the minimum-yield case, the liquid yield was 38%, and the bio-char yield 14%. It is expected that, in each case, the price of the bitumen will affect the costs of the bio-bitumen, as presented in Figure 6.1.

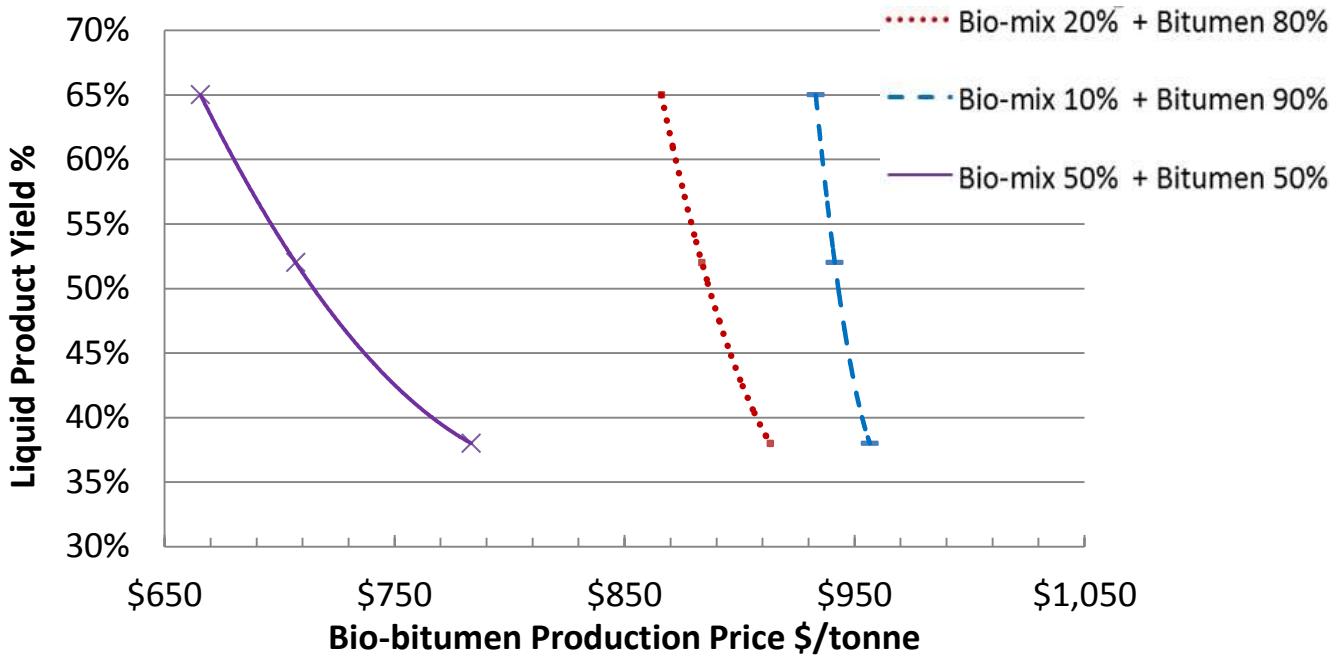

Figure 6.1: Bio-bitumen production price expected at different liquid product yields collected

The detailed calculation procedures and results for Figure 6.1 can be found in the Appendix. Using the available data and Excel Solver two models were developed:

$$C_1 = 8.5 \times Y_{bio\text{-}char} + 93.5 \times (Y_{(bio\text{-}oil+tar)}) + 413.9 \times R_{bio\text{-}mix} + 944.7 \times R_{bitumen} \quad (9),$$

where C_1 is the bio-bitumen production price ($/tonne of bio-bitumen); $Y_{bio\text{-}char}$ is the bio-char yield collected during biomass pyrolysis (wt%);$Y_{(bio\text{-}oil+tar)}$ is the total yield of liquid products during biomass pyrolysis (wt%); $R_{bio\text{-}mix}$ is the ratio of bio-mix in the bio-bitumen production (0.20 in the 20% Bio-Mix+80% Bitumen mixture); and $R_{bitumen}$ is the ratio of bitumen in the bio-bitumen production (0.80 in the 20% Bio-Mix+80% Bitumen mixture).

$$C_2 = 10.1 \times Y_{bio\text{-}char} + 209.2 \times (Y_{(bio\text{-}oil+tar)}) + 1010 \times R_{bitumen} \quad (10),$$

where C_2 is the bio-bitumen production price ($/tonne of bio-bitumen) calculated when only the ratio of bitumen is considered to influence the price; $Y_{bio\text{-}char}$ is the bio-char yield collected during biomass pyrolysis (wt%); $Y_{(bio\text{-}oil+tar)}$ is the total yield of liquid products during biomass pyrolysis (wt%); and $R_{bitumen}$ is the ratio of bitumen in the bio-bitumen production (0.80 in the 20% Bio-Mix+80% Bitumen mixture).

Equations (9) and (10) were developed to calculate the price of the bitumen production if the bio-bitumen mixture ratio and the liquid and solid yields from biomass pyrolysis are known. Table 6.3 shows the results of these two scenarios. In Table 6.2, 100% wood feed is the biomass feedstock mass used as a reference. Wood pyrolysis generates 20% solid products (referred to as bio-char) and 65% liquid products (including bio-oil and tar).

In bio-bitumen production, the useful product is extracted from the bio-oil and tar mixture. The useful product for the production of the bio-bitumen is 27%, based on the initial woody biomass feed. The extracted product then undergoes distillation, from which 86% of the previously extracted useful product volume is available for the following bio-bitumen production step. In this step, the distilled useful product is combined with the petroleum-derived bitumen at the pre-set ratio (Case 1: 20% distilled bio-mix and 80% bitumen; Case 2: 10% distilled bio-mixture, 90% bitumen). Finally, the bio-bitumen is produced.

Table 6.3: Costs Analysis Results for Two Cases Based on the Feeding Materials Only

	Process flow case 1	Case 1 tonne/yr	Process flow case 2	Case 2 tonne/yr
Wood feed	100%	4247	100%	4247
Bio-char	**20%**	849	**14%**	595
Bio-oil+tar	**65%**	2761	**38%**	1614
After DCM* Extraction	27%	745	27%	436
Distillation	86%	641	86%	375
Bio-mix	**20%**	641	**10%**	375
Bitumen	**80%**	2564	**90%**	3373
Bio-bitumen	100%	3205	100%	3747

Inputs/ Product	$/tonne	$/yr	$/yr
Wood	$ 50	$ 212,350	$ 212,350
Bitumen	$ 1,000	$ 2,563,999	$ 3,372,645
Bio-bitumen	$ 1,200	$ 3,845,998	$ 4,496,860
Bio-char	$ 1,000	$ 849,400	$ 594,580

Cost		$ 2,776,349	$ 3,584,995
Revenue		$ 4,535,148	$ 4,904,070
Total Bio-bitumen	tonnes	3205	3747
Cost /tonne	$/tonne of bitumen	$ 866	$ 957

* DCM is a special chemical used during the extraction process.

6.1.2 Estimation by Listing and Costing Main Plant Items

Plant capital and operational costs are presented for a case with an annual production of bio-bitumen of 4,000 tonnes, bio-bitumen mixture of 20% bio-mix and 80% bitumen and pyrolysis yields of 38% bio-liquids (bio-oil and tar combined) and 14% bio-char. Completed analysis is based on the techniques suggested in *Economics for Chemical Engineers* (Peters & Timmerhaus, 2003) and the second edition of

Products and Process Design Principles: Synthesis, Analysis and Design (Seider, Lewin, Widagdo, 2008).

Fixed Capital Costs:

	Details	Cost (NZD$)
Equipment selection	Process equipment cost of Freight on Board (f.o.b)	$ 989,100
Piping	Instrumentation and controls	$ 135,000
Instrumentation	Piping	$ 259,650
Electrical	Electrical	$ 103,860
Buildings	Auxiliaries	$ 519,300
Storage provided in Performance and Cost Evaluation (PCE)	Working capital	$ 632,500
Site development not applicable	Engineering and supervision	$ 405,050
Ancillary buildings none required	Total direct plant costs	$ 789,300
Total physical plant cost	Delivered process equipment costs	$ 1,038,600
Design and engineering	Installation	$ 425,800
	Battery limits and service	$ 301,200
	Evacuation and site preparation	$ 103,860
	Total	$ 5,703,300

Variable Operational Costs:

Raw materials, solvent make-up			
	Wood	$ 212,370	
	Bitumen	$ 3,427,200	
	Chemical A	$ 11,450	
Total Annual Raw Materials		$ 3,651,000	
Miscellaneous materials, 10% of maintenance cost			$ 21,100
Total annual utilities			$ 768,060
Shipping and packaging			$ -
	Administrative costs		$ 521,000
	Distribution and selling costs		$ 347,300
	Total		$ 5,308,400

Fixed Operational Costs:

Maintenance, as 5% of fixed capital	$ 210,800
Plant overheads, as 50% of operating labour	$ 305,000
Laboratory, as 30% of operating labour—total annual labour	$ 610,000
Capital charges, 6% of fixed capital (bank rate 4%)	$ 42,200
Land and local tax and insurance rates	$ 42,200
Research and development	$ 434,100
Depreciation	$ 578,800
Total	$ 1,187,000

According to this cost analysis, the total capital costs are $5.703 million, while the annual operational costs are $6.495 million, including $5.308 million for materials and $1.187 for fixed operational costs. The fixed operational costs include manual labour, maintenance, overhead, laboratory and research and development. Costs calculation indicates that the proposed project is highly maintenance and labour intensive, as also recognised on a smaller scale. This is among the issues which can be addressed to decrease the total annual operational costs. Further investigation into reducing equipment costs should be conducted before any large investments.

6.1.3 a Pricing estimation – assumptions set 1

To calculate a more realistic product price of the bio-bitumen from the proposed plant, additional factors have been considered.

The first set of assumptions for production cost of bio-bitumen were pyrolysis production liquid yields of 38% (bio-oil and tar combined), 15% bio-char yields, a bio-bitumen mixing ratio of 20% bio-mix and 80% bitumen, and 10,000 tonnes of wood processed daily in the pyrolysis reactor.

Variable Costs

Raw materials, solvent make-up	$	3,651,000		
Miscellaneous materials, 10% of maintenance cost	$	21,000		
Utilities	$	768,000		
Administrative costs	$	536,800		
Distribution and selling costs	$	347,300		
	Subtotal		***$***	***5,308,200***
Annual production rate of bio-bitumen	4,000		tonne/year	
Price of Raw Materials	$	940	$/tonne produced	Bio-Bitum

Fixed Costs:

Maintenance, as 5% of fixed capital	$	210,800		
Plant overheads, as 50% of operating labour	$	305,000		
Total annual labour	$	450,000		
Capital charges, 6% of fixed capital (bank rate 4%)	$	342,200		
Insurance, 1% of fixed capital	$	42,200		
Depreciation	$	578,800		
Land and local tax and insurance rates	$	121,500		
Direct Product Costs	Subtotal		***$***	***1,263,600***

Sales expenses	$	353,800		
Research and development	$	434,100		
	Subtotal		***$***	***788,000***

Annual Production Costs	***$***	***6,795,400***	$/yr
Annual production rate of bio-bitumen	4,000		tonne/yr
Production costs	***$***	***1,700***	$/tonne bio-bitumen produced

Based on the costs analysis in Section 6.1.2, the total cost of bio-bitumen production and distribution is $1,700/tonne without considering the internal rate of return (IRR) for the investment. This value is much higher than the current market bitumen price of $1,000/tonne. Therefore, if bio-bitumen is the sole product from the plant and the mixture ratio was 20% bio-mix and 80% bitumen, the investment would produce a loss.

However, two factors could improve the outlook of the commercial plant. First is the environmental benefit of using the renewable feedstock of wood and agricultural waste. Throughout New Zealand, there are 1.7 million hectares of *Pinus Radiata* plantation forests, and forest harvesting, wood-processing plants and pulp and paper mills produce a total annual residue of 4–6 million cubic metres (New Zealand Ministry of Agriculture and Forestry, 2008). Utilization of these resources is the target of both New Zealand government and industry in order to achieve the goals of the Kyoto and Montreal Protocols (Casswell-Laird, 2008).

Secondly, bio-char and non-condensable gas are also generated by the design and could be sold in the existing market. If these two co-products are included, total annual revenue is expected to be $6.6 million. In this case, the sale price of the bio-bitumen is $1,200/tonne.

6.1.3 b Pricing Estimation - Assumptions Set 2

Another set of assumptions for calculating the production cost of a bio-bitumen tonne had a pyrolysis production liquid yield of 65% (bio-oil and tar combined), 20% bio-char yield, bio-bitumen mixture ratio of 50% bio-mix and 50% bitumen, and 10,000 tonnes of wood processed daily in the pyrolysis reactor.

Summary of Production Costs:

Variable Costs

Raw materials, solvent make-up	$	727,826	
Miscellaneous materials, 10% of maintenance costs	$	21,083	
Utilities	$	768,058	
Administrative costs	$	520,954	
Distribution and selling costs	$	347,303	
	Subtotal		***$ 2,385,224***
Annual production rate of bio-bitumen	916		tonne/yr
Price of Raw Materials	$	794	$/tonne Bio-Bitumen produced

Fixed Costs:

Maintenance, as 5% of fixed capital	$	210,833	
Plant overheads, as 50% of operating labour	$	305,000	
Total annual labour	$	610,000	
Capital charges, 6% of fixed capital (bank rate 4%)	$	252,999	
Insurance, 1% of fixed capital	$	42,167	
Depreciation	$	578,838	
Land and local tax and insurance rates	$	121,556	
Direct Product Costs	Subtotal		***$ 1,397,845***

Sales expenses	$	189,153	
Research and development	$	434,129	
	Subtotal		***$ 623,282***
Annual Production Costs	***$***	***3,783,069***	$/yr
Annual production rate of bio-bitumen	4,000		tonne/yr
Production Costs	***$***	***946***	$/tonne Bio-Bitumen produced

Based on the costs analysis in Section 6.1.2, the total cost of the bio-bitumen production and distribution is $946/tonne, without considering the IRR for the investment. This value is slightly lower than the current market bitumen price of $1,000/tonne. Therefore, if bio-bitumen were the sole product from the plant, the investment would barely make a profit. The properties of a bio-bitumen

mixture ratio of 50% bio-mix and 50% bitumen were analysed by Harrington (2013), who found them to be similar to that considered acceptable for roading industry requirements.

6.1.4 Break-down of Capital Cost Summary

The capital costs of the plant were determined by estimating the major plant item costs (MPIC). This estimation and the Lang Factors were used to calculate the total capital investment (TCI). The difference between the two production cases discussed in Sections 6.1.4a and b was found to be negligible; therefore, only one set of MPIC is presented. Figure 6.2 shows the breakdown of plant equipment items in the MPIC.

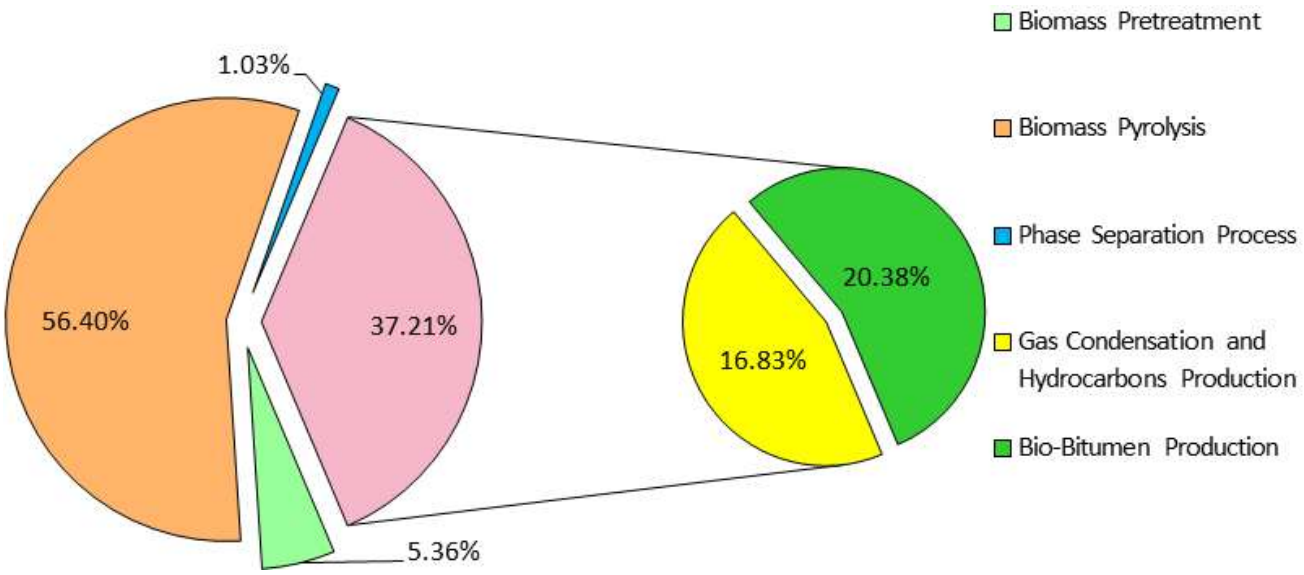

Figure 6.2: Main Plant Items Costs.

A breakdown of all the processes and machinery is shown in Figure 6.2 and Table 6.4. The biomass pre-treatment equipment and facilities include a pulveriser, rotary dryer, size grater for sawdust and biomass storage tanks. The biomass pyrolysis system includes the augers, hopper feed system and fluidised bed reactor. The biomass pre-treatment and biomass pyrolysis equipment and facilities can be found in Figure 5.1 (PFD101) and Figure 5.6 (P&ID101).

The processes and equipment for after pyrolysis include cyclones for solid and gas separation and heat exchangers for bio-oil and gas initial separation (see Figures 5.2 (PFD102) and 5.7 (P&ID102)). Next are the gas condenser and filter for bio-oil collection and tar collector, as shown in Figures 5.3 (PFD103) and 5.8 (P&ID103). The bio-bitumen production phase of the proposed plant design is the key step for the bio-bitumen new product production. This stage involves various mixers and continuously stirred tank reactors (CSTRs), some of which are heated. The bio-bitumen production process also includes a distillation column and recycling system, shown in Figures 5.4 (PFD104) and 5.9 (P&ID104).

Table 6.4: Proportions of the Major Plant Item Costs (MPIC) for the Bio-bitumen Production Plant

%MPIC	Stage
5.36	**Biomass pre-treatment**
56.40	**Biomass pyrolysis**
1.03	**Phase separation process**
16.83	**Gas condensation and hydrocarbons production**
20.38	**Bio-bitumen production**

Figure 6.2 and Table 6.4 show that a large proportion of the equipment costs occur in biomass pyrolysis (56%), followed by bio-bitumen production (20%) and gas condensation and tar production (17%). The main reason for this price difference is the fluidised bed pyrolysis reactor used early in the process. Condensers and distillation column are the next most-expensive components in the system. The total estimated capital investment is $5.703 million, which includes the physical plant costs and total direct installation costs described in Section 6.1.2.

The cost for locally installed equipment was calculated at $0.99 million, including engineering supervision, materials and construction expenses. This is divided into various components as shown in Table 6.5.

Table 6.5: Locally Installed Equipment and Costs

Details	***Cost (NZ$)***
Biomass Pre-treatment	$ 53,000
Biomass pyrolysis	$ 558,000
Phase separation process	$ 10,200
Gas condensation and hydrocarbons production	$ 166,500
Bio-bitumen production	$ 201,600
Pumps	$ 21,000
Heaters	$ 24,000
Compressors	$ 10,000
Heat exchangers	$ 11,016
Total Capital Expenditure (CAPEX) for locally installed equipment	$ 990,000

6.2 Economic Analysis

The current wholesale prices of the feedstock materials and products were quoted from a number of sources listed in the Appendix. Based on Williamson (2011), a drop in pulp wood prices in New Zealand is expected in the near future because of less demand for pulp and paper and a lack of reinvestment in the pulp and paper mill infrastructure. The wood price thus will be relatively stable or fall. On the other hand, the price of bitumen has increased by 500% over the past 30 years. A rise in the price of bitumen and consequently bio-bitumen can be almost guaranteed. As well, labour and other costs might also increase with time. In the following discussion, an economic sensitivity analysis is presented in which wood prices drop by up to 50%, bitumen prices rise by up to 30%, and the bio-bitumen selling price rises by up to 10%. With an increase in bitumen prices, the price of so-called environmentally sustainable bitumen will also rise. As discussed, some industries charge more for eco-products. As well, the bang-for-your-buck mind-set dominates the roading industry. Both approaches can be found in today's economic market. A company's decisions might be based on its values and ethics code, the amount of financial investment available and the country's economic environment (i.e., an expansion or regression phase of the economy and business cycles). Thus, at some point in the future, the bio-bitumen price per tonne might be higher than the price of regular bitumen.

6.3 Cash Flow Analysis

The cash flows in a manufacturing company are linked to the material flows in a process plant. The net cash flow at any time is the difference between earnings and expenditures. It has been assumed that it will take 1.5 years to construct the plant. Figure 6.3 shows the annual operating costs in the current economic model. Thus, the largest feedstock cost for the plant is bitumen, with significant costs also associated with utilities usage.

Note: Figure 6.3a. In the first set of assumptions, the pyrolysis production liquid yield is 38% (bio-oil and tar combined) the bio-char yield 15%, the bio-bitumen mixing ratio 20% bio-mix and 80% bitumen, and 10,000 tonnes of wood are processed daily in the pyrolysis reactor.

Figure 6.3 (a): Breakdown of Annual Operating Costs, Assumptions Set 1

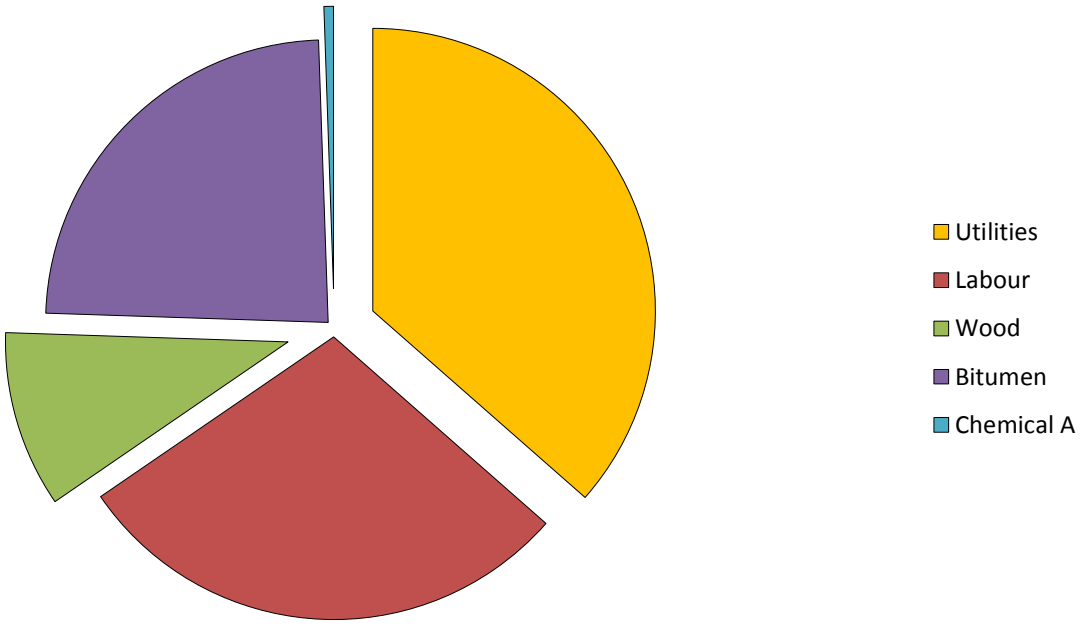

Note: Figure 6.3b. In the second set of assumptions, the pyrolysis production liquid yield is 65% (bio-oil and tar combined), bio-char yield 20%, the bio-bitumen mixing ratio 50% bio-mix and 50% bitumen, and 10,000 tonnes of wood are processed daily in the pyrolysis reactor

Figure 6.3 (b): Breakdown of Annual Operating Costs, Assumptions Set 2

The makeup of the annual inputs costs streams based on current prices is shown in Figure 6.4. The majority of costs for the plant will come from the bitumen raw material supply. The following average prices were estimated from collected information. For assumptions set 1 (Figure 6.4a), annual utilities, including water and electricity, were estimated to be $768,000 per year. Annual labour was estimated at $610,000. The estimated price of wood needed annually was $212,000. Total price of the bitumen required annually was estimated at $ 3,400,000, while chemical A costs were estimated at $11,500 per year.

For assumptions set 2 (Figure 6.4b), annual utilities, including water and electricity, and annual labour costs were similar for those of set 1. The estimated price of wood needed annually remained $212,000. Chemical A was still estimated to cost $11,500 per year. The total price of the bitumen required annually decreased to $1,054,000 due to the new bio-bitumen ratio of 50% bio-mix and 50% bitumen.

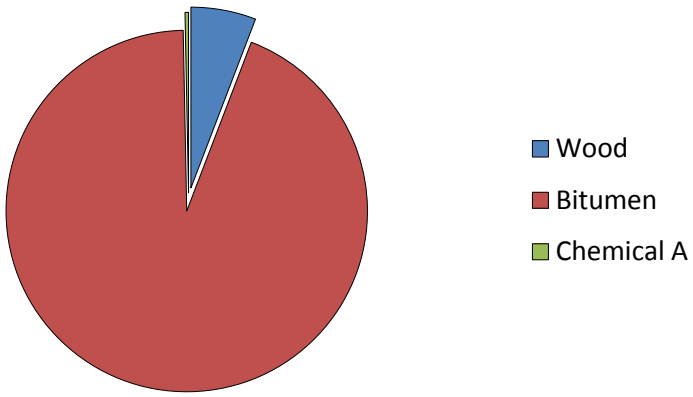

Note: Figure 6.4a. In the first set of assumptions, the pyrolysis production liquid yield is 38% (bio-oil and tar combined) the bio-char yield 15%, the bio-bitumen mixing ratio 20% bio-mix and 80% bitumen, and 10,000 tonnes of wood are processed daily in the pyrolysis reactor.

Figure 6.4 (a): Breakdown of Annual Raw Materials Input Costs Streams, Assumptions Set 1

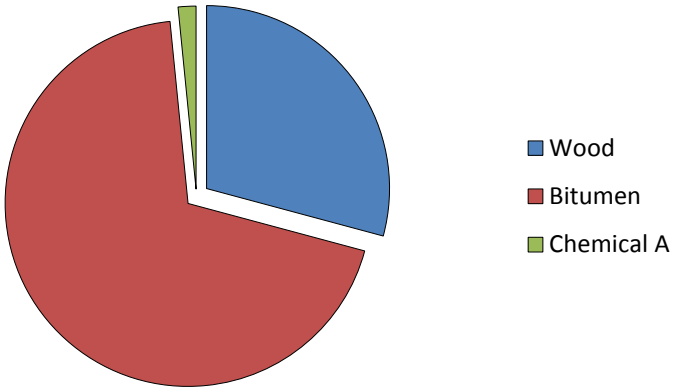

Note: Figure 6.4b. In the second set of assumptions, the pyrolysis production liquid yield is 65% (bio-oil and tar combined), bio-char yield 20%, the bio-bitumen mixing ratio 50% bio-mix and 50% bitumen, and 10,000 tonnes of wood are processed daily in the pyrolysis reactor.

Figure 6.4 (b): Breakdown of Annual Raw Materials Input Costs Streams, Assumptions Set 2

The cash flow diagram in Figure 6.5 shows the projected cumulative cash flows for a pyrolysis production liquid yield of 65% (bio-oil and tar combined), bio-char yield of 20% and a bio-bitumen mixture ratio of 50% bio-mix and 50% bitumen. The lifetime of the plant is 15 years.

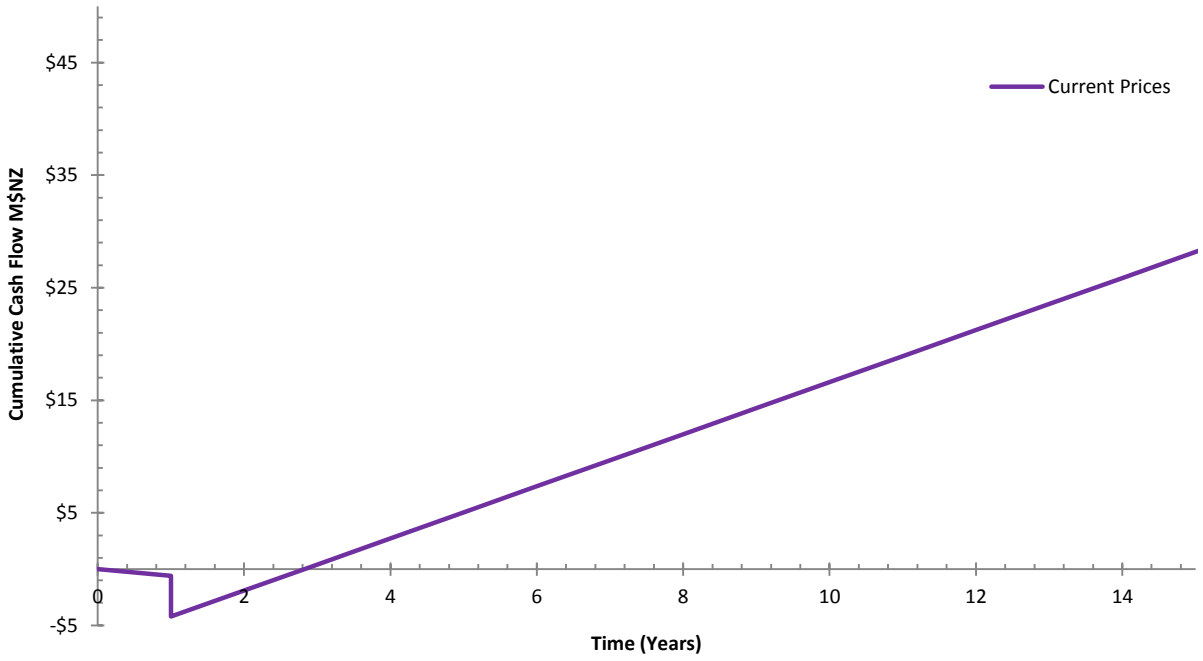

Note: Figure 6.5. In the second set of assumptions, the pyrolysis production liquid yield is 65% (bio-oil and tar combined), bio-char yield 20%, the bio-bitumen mixing ratio 50% bio-mix and 50% bitumen, and 10,000 tonnes of wood are processed daily in the pyrolysis reactor.

Figure 6.5: Cash Flow Diagram for Current and Predicted Pricing, Assumptions Set 2

As shown in Figure 6.5, at current pricing, the plant has a payback period of 3 years. Dependent on the shareholders' required return on investment period and IRR on the portfolio compared with the market risk rates, shares should be priced and offered to potential investors. Overall, if moved forward, the process would benefit the environment and economy of New Zealand. However, given the current economic conditions and recession, it might not be the best time to start construction of this project. Another option is to heavily involve government funds, which would provide the project with sufficient resources for the next step.

6.4 Sensitivity Analysis

A sensitivity analysis was conducted to determine the effect of product and feedstock pricing on the economic feasibility of the process. Each parameter was changed, and the difference in annual revenue from the base pricing model was recorded. This enabled demonstrating the effect on annual revenue from a significant change in each variable.

The horizontal axes in Figures 6.6 and 6.7 show the percent change in the sensitivity parameter, and the vertical axis the change in annual revenue in millions of NZ$. For example, if the price of bitumen falls by 20% (i.e., -20% on x axis), the change (increase) in annual revenue will be NZ$0.5 million (i.e., change on the y axis) in Figure 6.6. A vertical line for the specified variable indicates a greater effect on the revenue from a given variation.

In Figure 6.5, it can also be observed that the costs of bitumen and bio-bitumen most influence annual revenue. Wood and chemical A purchase prices have minimal influence on annual revenue, shown by the horizontal representing those variables costs. The more horizontal the line, the less the influence of the variable cost on annual revenue.

The pricing sensitivity analysis in Figure 6.6 shows that the biomass–to–bio-bitumen process is the least influential factor. Among the least influential factors for annual revenue in Figure 6.6, wood prices are more influential than the price of chemical A because the process requirement for wood is much higher. Base case prices assumed in the complete sensitivity analysis are presented in Table 6.6. Based on Figures 6.5 and 6.6, income revenue is most sensitive to bitumen and wood prices.

Table 6.6: Base Case Prices Used for Sensitivity Analysis

Product	Base case prices	Units
Wood	50	NZ$/tonne
Bio-char	1,000	NZ$/tonne
Bitumen	1,000	NZ$/tonne
Chemical A	100	NZ$/tonne
Bio-bitumen	1,200	NZ$/tonne

Note. Base case assumes a bio-bitumen ratio of 20% bio-mix and 80% bitumen, pyrolysis yield of 38% bio-liquids (bio-oil and tar) and bio-char yield of 15%.

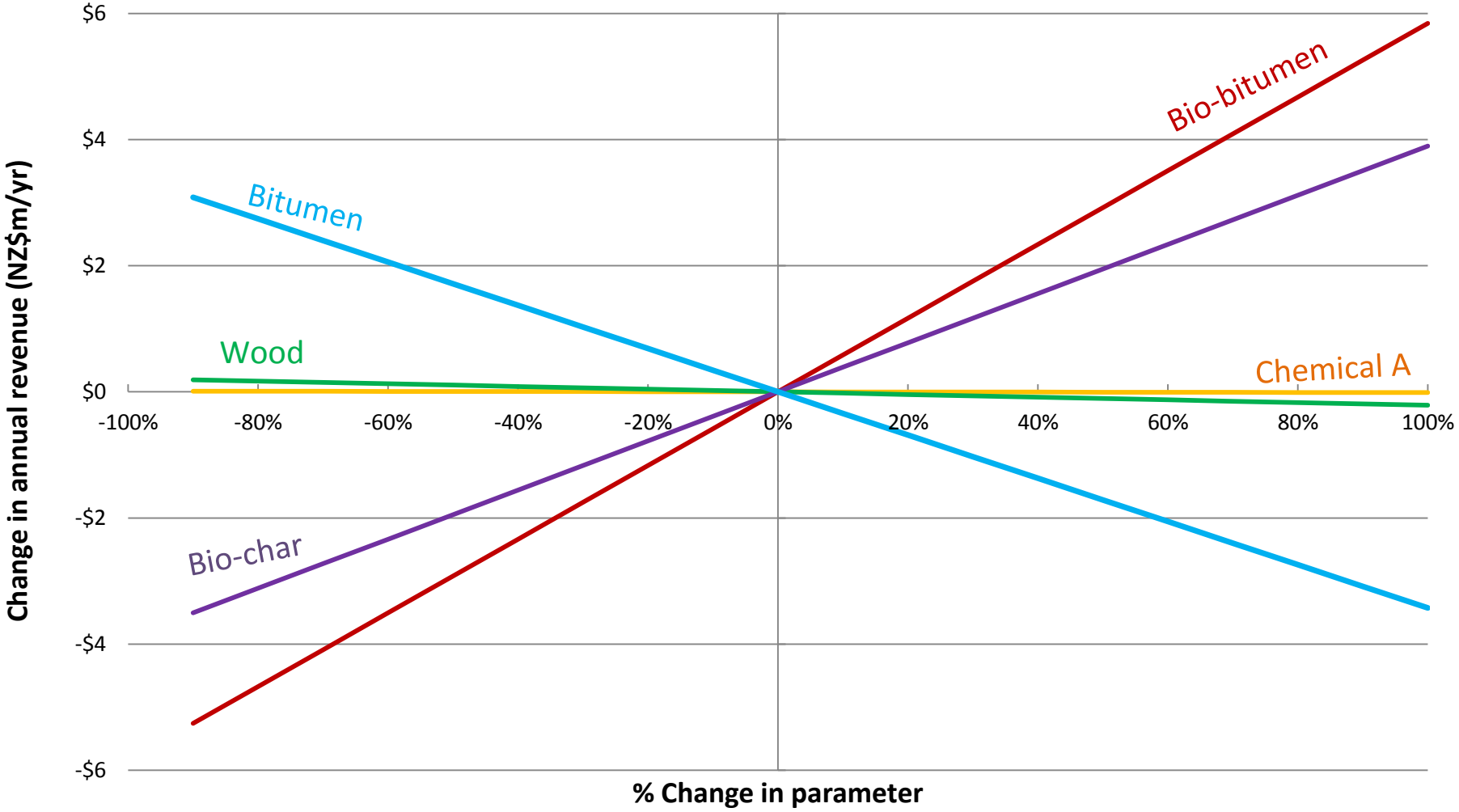

Figure 6.6: Pricing sensitivity analysis for production of bio-bitumen.

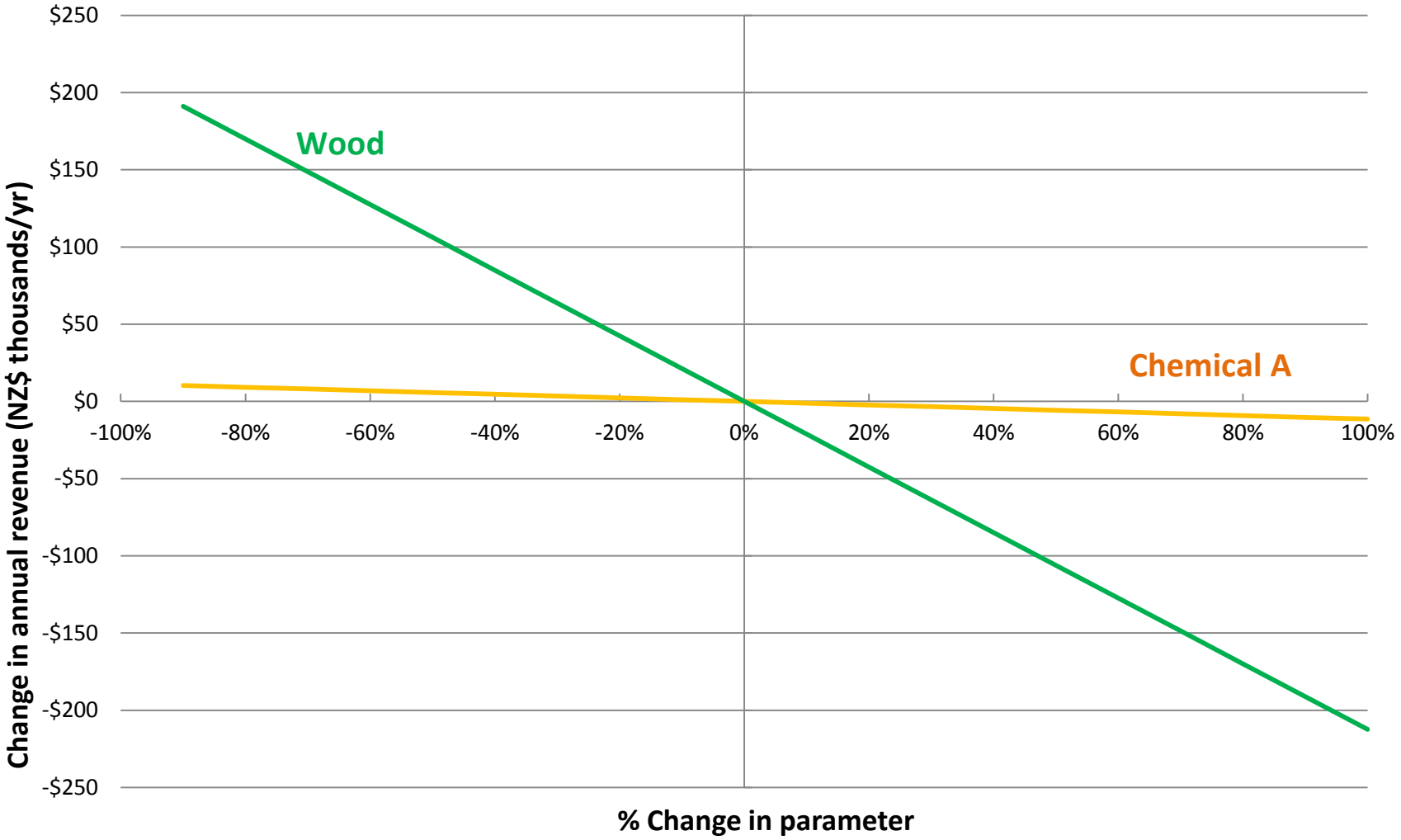

Figure 6.7: Pricing sensitivity analysis for the least influential factors in production of bio-bitumen.

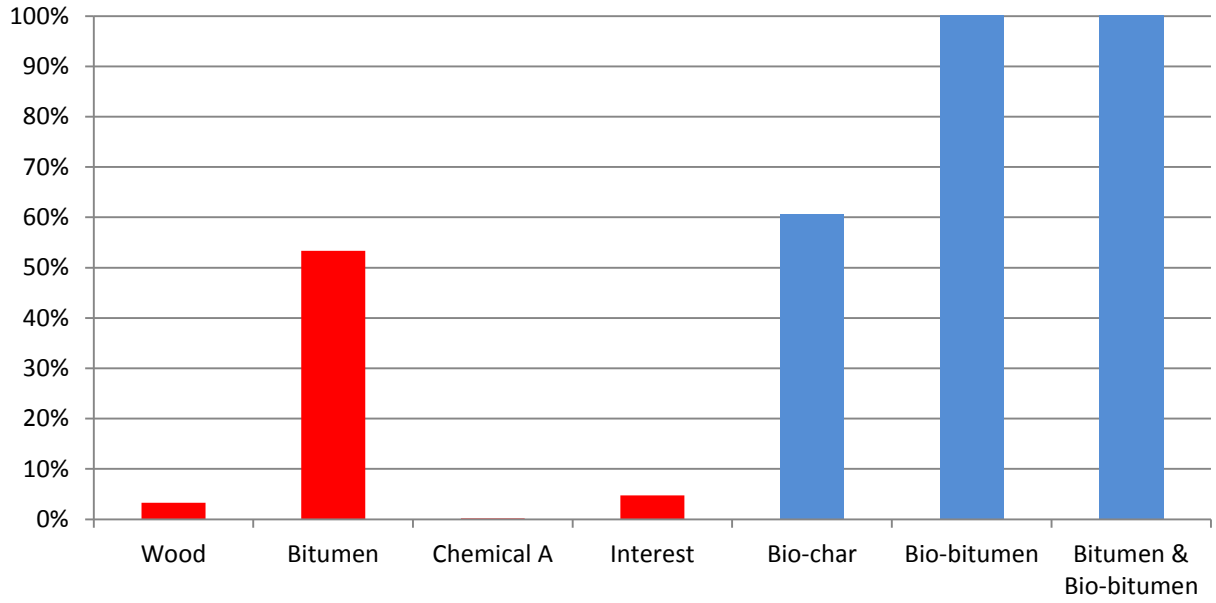

Figure 6.8: Influences of changes in each feed material on total feeding material cost, and influence of prices of products on revenue change.

A comparison of the sensitivity of the annual revenue to each price parameter is shown above in Figure 6.8, where the vertical axis is the percent change in annual revenue for a 1% change in the parameter. These numbers represent the slope of the parameter line in Figure 6.6, with a higher number indicating higher influence of the variable on the revenue.

Chapter 7: Conclusions and Recommendations

7.1 Conclusions

7.1.1 Research Conclusions

- *Pinus Radiata* liquid product (bio-oil) is more acidic then *Eucalyptus Nitens* condensate.
- 47% average yield of liquid products collected from the *Pinus Radiata* sawdust makes continuous fast pyrolysis process an attractive investment for further processing and upscale of the process.
- Dependant on the products and their properties desired, pyrolysis feedstock material and operating conditions may be determined.
- Total yield of liquid products produced vary from 40-50%. Some experiments completed on *Pinus Radiata* sawdust produced much higher liquid yields at higher temperatures, which emphasizes the importance of pyrolysis process research into determination of the optimum plant operation conditions.
- During the experimental runs it was found that organic tar collected by all condensers in total varies from 5-30%, dependant on the operational conditions and system modifications.
- From yields collected from *Pinus Radiata* sawdust no direct correlation was made between the bed temperature and the tar yields collected. However at higher temperatures more total liquid products were produced.
- From the completed research, it was established that pyrolysis of *Pinus Radiata* sawdust produces less CO_2 emissions, compared with *Eucalyptus Nitens* or bark. This is one of the reasons to use *Pinus Radiata* sawdust as feed for the process instead of *Eucalyptus Nitens* or bark mixtures.
- Collected experimental results indicate that the higher the moisture content of the feed material, the higher total liquid product yields from the process. Mostly these yields are higher because of the higher water content in the bio-oil, thus additional moisture content in the feed does not add value to the products.
- Pyrolysis of the hardwood sample produced much lower yields of liquid and solid products compared with that of the softwood samples. Hardwood: 39% liquid and 17% solid and Softwoods: 40-44% liquid yields and 15-20% solid product yields.

- Pyrolysis runs completed using *Eucalyptus Nitens* feed samples produced on average 3% tar, 34% bio-oil and 17% bio-char yields from 1.5 mm - 4 mm size particles in bulk. *Eucalyptus Nitens* runs produced very small tar yields to consider this feedstock for the upgrade process.
- 70/30 mixture runs produced on average 14% tar, 24% bio-oil and 24% bio-char during the experimental run. This compared with 7% tar, 30% bio-oil and 15% bio-char may seem like a more attractive option for further investigation with higher tar yields, however lower bio-oil yield should be noted as included in future calculations. 50/50 *Pinus Radiata* sawdust/ *Pinus Radiata* bark runs have not shown much of an improvement on the total average yields collected, with 13% tar, 23% bio-oil and 24% bio-char.
- Most tar yields were produced during 70/30 *Pinus Radiata* sawdust/*Pinus Radiata* bark mixture run, followed by 50/50 *Pinus Radiata* sawdust/*Pinus Radiata* bark runs. However the sawdust/bark mixture runs blocked the system, making operation harder. The current equipment design does not allow completing numerous runs with these feedstocks.
- The total bio-char yields collected vary between 15-20% of the feed, 30-50% yield of the light pyrolysis oil (bio-oil product) is expected from the process, 5-30% of heavy oil – tar product, and 15-30% exhaust gas.
- Bio-char samples collected at higher pyrolysis temperatures had lower volatile matter.
- Increase in pyrolysis process temperature mostly increases ash content in the solid product.
- From completed analysis *Pinus Radiata* bark samples had higher ash composition than *Pinus Radiata* sawdust. All samples tested had a high volatile matter composition, with 85% for untreated *Pinus Radiata* sawdust and 52% for bio-char.
- On average, fast pyrolysis bio-char samples had 25 MJ/kg CV, which was slightly higher than coal value of 22 MJ/kg.
- Analysed pyrolysis bio-char samples collected in this research consisted of 65% carbon, 5% hydrogen and 26% oxygen.

- Trials completed by Milne on a smaller scale demonstrated that soil organic carbon levels shape agro-ecosystem function and influence soil fertility and physical properties, such as aggregate stability, water holding capacity and cation exchange capacity (CEC).
- Bio-char use in agriculture was additionally observed to decrease greenhouse gas emissions associated with agricultural development; reduce phosphate, nitrate and agrochemicals pollution of streams and groundwater; reduce the need for fertilizer and compost; reduce soil acidity (raise pH); increase soil microbial biomass and support earthworms. Bio-char improves soil moisture retention.
- Table 7.1 shows a summary of the yields of liquids and solid products for various feedstocks.

Table 7.1: Experimental results summarising table

Feed type	**Bio-char (wt%)**	**Tar (wt%)**	**Bio-oil (wt%)**
Radiata Pine sawdust (1.5 mm–4 mm)	15%	7%	30%
Radiata Pine sawdust (<1.5 mm)	13%	5%	27%
Eucalyptus Nitens sawdust (1.5 mm–4 mm)	17%	3%	34%
70/30 Radiata Pine sawdust/Radiata Pine bark (1.5 mm–4 mm)	24%	14%	24%
50/50 Radiata Pine sawdust/Radiata Pine bark (1.5 mm–4 mm)	24%	13%	23%

7.1.2 Upgrade Design Conclusions

- The proposed in Chapter 5 plant design provides an idea of what a commercial bio-bitumen production plant would require for an upgrade. The total estimated capital investment is $5.703 million. This includes the physical plant costs and total direct installation costs.
- Fluidised bed pyrolysis reactor was the most expensive component in the proposed design. Condensers and distillation column are the next most expensive components of the system.
- Completed techno-economics analysis indicates that a large proportion of the equipment costs of the proposed plant design was the biomass pyrolysis part of the plant, 56%. This was followed by a bio-bitumen production part of the plant, 20%. And subsequently gas condensation and bio-liquids (bio-oil and tar) production was 17% of the total main plant equipment cost.
- It was found that the input materials (wood, chemical A and bitumen) were the largest part of the on-going bio-bitumen plant operations costs. The sum of input materials expenses took up more than 50% of the total bio-bitumen production cost, during the most likely production case calculations. The assumptions for the most likely case were pyrolysis production liquid yields 38% (bio-oil and tar combined), 15% bio-char yields, bio-bitumen mixing ratio was 20% bio-mix and 80% bitumen, given 10 000 tonne of wood processed in the pyrolysis reactor daily. The production cost for one tonne of bio-bitumen was $1700 in this case.
- The assumptions for another case analysed, assumed pyrolysis production liquid yields 65% (bio-oil and tar combined), 20% bio-char yields, bio-bitumen mixing ratio was 50% bio-mix and 50% bitumen, given 10 000 tonne of wood processed in the pyrolysis reactor daily. The production cost for one tonne of bio-bitumen when these assumptions held true was $ 946. Input materials costs were still 50% of the total production expense. However the change in the bio-bitumen mixing ratio decreased the total amount of raw material (bitumen) required, consequently decreasing the production cost.
- Input materials accounted for large percentage of the total output cost, therefore effectively by reducing the input materials costs the production cost of bio-bitumen will substantially reduce. Total

input materials required may be reduced via changing the bio-bitumen mixture ratio or by improving pyrolysis process production yields (bio-oil and tar production yields).

- Bio-char is another product generated in the Chapter 5 design, which can be sold into existing market.
- Sensitivity analysis demonstrated that the bitumen purchase price was the most influential factor on the annual revenue of the plant.
- At current pricing the proposed plant design has a payback period of 3 years.
- To develop and construct a profitable factory a lot of improvements need to be considered. On a smaller scale the developed process has shown progress over the past two years of research, which suggests potential future for this project. However just a simple increase in size is not sufficient when developing a similar process which processes 1000 times more feed. If bio-bitumen is further developed and correctly introduced to the market, New Zealand may be the leading country in roading industry for many years ahead. Therefore even though this particular design may not provide the highest return on investment at this stage, the project itself shows potential. Following are recommendations which may be considered for further research and re-design.

7.2 Recommendations

Problems encountered during the two-year operation of the fast pyrolysis rig at CRL Energy included issues with heating, blockages, bridging, maintenance, and fouling. The fast pyrolysis process highly depends on temperature and thus requires an extremely well insulated system. One frequent issue was continuous blockages in the pipes and equipment connections caused by prior product build up. As a result, the normally continuous production was interrupted, and time was required to perform maintenance and repairs. A thorough redesign of the system to increase connection diameter size or extend connection heating would reduce product advanced condensation and avoid this problem in the future. Sawdust bridging in the hopper was another reoccurring problem. On a small scale, this can be easily alleviated using a soft ended hammer, but repairs on a larger scale require additional effort. Additional information on the problems encountered and purposed solutions are discussed in Section 3.5.

7.2.1 Research

Bio-char collected during fast pyrolysis is a valuable product and serves as an additional revenue source in the agricultural industry. Studies completed prior 2013 report promising results, but additional investigation on the collected solid samples (bio-char) is needed to determine the best application in New Zealand.

There is also a need for further research into the safety of bio-char application in the soil environment, particularly concerning hazardous metal contaminants present in the original biomass. Small-scale trials are needed to determine optimal bio-char ratio application practices specifically for New Zealand soils. Recommended concentration may begin from as little as 38 t of bio-char per hectare (Bridle 2004).

In addition, the potential effects of the manufacturing process on human health has yet to be thoroughly investigated. Gases and smoke emitted during fast pyrolysis are flammable and toxic. Greater attention to plant operation is warranted, particularly as the process is commercialised on a larger scale. Additional fire and safety equipment precautions must be reinforced during plant construction and operation.

7.2.2 Design

An overhaul of the current bio-bitumen production process to promote optimal efficiency must focus on equipment design. There are several industry-developed techniques that may prove useful in improving bio-bitumen production. Bedmuthaa (2009) proposed designs for single-stage and two-stage tubular electrostatic precipitators. In the proposal, a nitrogen stream containing very fine droplets of fogging oil was forced through an electrostatic precipitator chamber. Bedmuthaa found that 98.6 wt% of the oil droplets present in the turbulent jet mechanically collected onto the ESP test chamber inner walls. This two-stage tubular ESP was expanded for use in a fluidized bed pilot plant used for biomass pyrolysis and resulted in a droplet collection efficiency of 95 wt%. Such demisters will extend the process intensification gains of short residence time processes, such as fast pyrolysis, to the product recovery train. The outer cylinder of the tubular ESP was made of Teflon®, which is resistant to corrosion and has exceptional dielectric properties, including a high dielectric strength over a wide range of frequencies and a low dissipation (Bedmuthaa, 2009).

Economic analysis of the redesign, detailed in Chapter 6, showed that the plant was only viable under very specific ideal conditions and would not be viable under current financial conditions in New Zealand. Increased plant efficiency combined with reductions in operating costs, equipment, and wood could improve the current financial climate and make the process economically sustainable.

A mobile pyrolysis plant design, proposed by Alternative Energy Solutions (2007), is a potentially less expensive alternative to plant refurbishment. The plant design theoretically decreases operational expenses by constructing a small plant at a remote location. This small-scale plant uses forest residues as the biomass source and produces a high yield of liquid used for fuel or road construction (Alternative Energy Solutions, 2007).

In an economic evaluation conducted by Alternative Energy Solutions, a mobile fast pyrolysis plant in NZ at an initial $4.5-5 million investment yields an ROI in approximately 5 years and may save 20% of

petroleum fuel cost (Alternative Energy Solutions, 2007). The proposed plant would process 100 tonne per day of dry residue, primarily waste wood collected at a projected $20/tonne. However, data in the present study appears to contradict this projection. Waste wood cost in 2012-2013 was $50/tonne, far higher than the operational expenses estimated by the Alternative Energy Solutions proposal, and encompassing approximately half of the initial investment cost. Additional evaluation of the mobile plant design to determine its economic viability is recommended.

Another alternative is construction of the bio-bitumen plant at the site of an existing pyrolysis or pulp and paper plant. Although there is not any pyrolysis plant currently under construction, this may change in the future. A number of petroleum oil industry companies, such as Z Energy and Mobile, have discussed construction of a pyrolysis plant in New Zealand (Herrington, 2013) with the intention of manufacturing bio-fuel to replace petroleum fuel (McGuiness, 2012). Pyrolysis primarily produces bio-oil, highly desired as a petroleum replacement, and tar, an undesired waste material. A potential follow up of the present study, which was performed in conjunction with CRL Energy (Wellington, 2012), could focus on construction of a smaller, on site side plant to the main factory owned by Z Energy and Mobile. This smaller plant would utilize the tar waste product using technology discussed in the present study.

The recommended design is to use two lock hoppers in parallel; this setup allows bio-fuel production to continue even during an auger blockage, bridging phenomenon, or necessary maintenance. One tank can be pressurized while the other is used to feed the gasifier (Haiming, 2009; Konemann, 2009).

List of References

1. 'Air Liquid' and 'BOC' (2012); phone quotes from gas suppliers, nitrogen gas prices
2. 'Z-Energy' and 'Mobile' (2012); suppliers quotes for petroleum and bitumen prices
3. Agilent 3000 Micro Gas Chromatograph Agilent Technologies (2001); "GC User Guide"; 2002 Agilent Technologies, Inc.; 2850 Centerville Road Wilmington, DE 19808-1610
4. Alternative Energy Solutions (2007); "Bio-oil Option" Report, FIDA Engineering Solutions: Remote Bio energy; retrieved from http://www.bioenergy.org.nz/documents/liquidbiofuels/AESBiooilOptionsPaper.pdf
5. Amonette J.E., Camps-Arbestain M., Chia C. H., Cowie A., Foidl N., Hook J. (2010); "An investigation into the reactions of bio-char in soil"; Australian Journal of Soil Research, Vol 48(6-7):501.
6. ANZ, (2013); "Foreign Exchange Calculator", ANZ Bank New Zealand Limited http://www.anz.co.nz/common/calculators/foreignexchange/examplenz.asp
7. Arias M., Polvillo O., Rodríguez J., Hernández M., González-Pérez J., González-Vila F. (2006); "Thermal transformations of pine wood components under pyrolysis/gas chromatography/mass spectrometry conditions"; Journal of Analytical and Applied Pyrolysis, Vol 77(1): 63-67
8. Atutxa A., Gayubo A., Olazar M. and Bilbao J. (2005). "Kinetic Description of the Catalytic Pyrolysis of Biomass in a Conical Spouted Bed Reactor.", Energy and Fuels, Vol 19(3): 765-774.
9. Azeez D., Akeem M., Odermatt J. and Willner T. (2010); "Fast Pyrolysis of African and European Lignocellulosic Biomasses Using Py-GC/MS and Fluidized Bed Reactor."; Energy and Fuels, Vol 24 (3): 2078-2085.
10. Barrow C., (2012); "Bio-char: Potential for countering land degradation and for improving agriculture"; Geography Department, College of Science, Swansea University; Applied Geography Vol 34:21-28
11. Bedmuthaa R., Ferrantea L., Briensa C., Berrutia F., Inculet I. (2009); "Single and two-stage electrostatic demisters for biomass pyrolysis application"; Chemical Engineering and Processing: Process Intensification, Vol 48(6):1112-1120

12. Biochar Farms (2013); “Biochar” ; BIOCHAR Farms.org, (assessed June 2012)

13. Boateng D., Akwasi A., Goldberg N. and Hicks K. (2007); "Bench-Scale Fluidized-Bed Pyrolysis of Switchgrass for Bio-Oil Production."; Ind. Eng. Chem. Res., Vol 46(7): 1891-1897.

14. Branca C. and Elefante R. (2006), "Devolatilization of Conventional Pyrolysis Oils Generated from Biomass and Cellulose."; Energy and Fuels, Vol 20(5): 2253-2261

15. Bridgwater A. and Czernik S., (2004); ”Overview of application of biomass fast pyrolysis oil”; Energy and Fuels, Vol (18):590-598

16. Bridgwater T. (2010); “Biomass Pyrolysis” presentation, Bioenergy Research Group Aston University, Birmingham B4 7ET, UK, IEA Bioenergy, York, 12 October 2010, http://www.ieabioenergy.com/DownLoad.aspx?DocId=6737

17. Bridle T.R. (2004); “Use of pyrolysis to recover energy and nutrients from biosolids.”, http://www.wef.org/NR/rdonlyres/7DA581D9-C0D3-4E5C-B127-AC68B7ABA6DD/0/Bridle_Paper.pdf (accessed August 2012).

18. Bruun S., Jensen E. S., Jensen L. S. (2008), “Microbial mineralization and assimilation of black carbon: dependency on degree of thermal alteration”; Organic Geochemistry Vol 39: 839-845.

19. Casswell-Laird O., (2008); “International Environmental Agreements: Does Montreal Have Lessons for Kyoto?”; Oscar Casswell-Laird Research Assistant Institute of Policy Studies, IPS Working Paper 3/2008

20. Chan K. Y., Zwieten L. V., Meszaros I., Downie A., Joseph S. (2008); “Using poultry litter biochar as soil amendments.”; Australian J. Soil Res. Vol 46: 437-444.

21. Chia C., Munroe P., Joseph S. and Lin Y. (2010); ”Microscopic characterisation of synthetic Terra Preta”; Australian Journal of Soil Research, Vol 48(6/7): 593-605

22. Corbett L. W. (1965); "Manufacture of Petroleum Asphalt," Bituminous Materials: Asphalts, Tars, and Pitches, 2(I); editor: Hoiberg A. J., New York: Interscience Publishers, 1965; p. 81–122. Vol. 2, Part 1.

23. CRL Energy Ltd, (2012); ‘An elemental composition of a char sample collected using pine sawdust.’, Lower Hutt lab.

24. CRL Energy ltd, (2012); Biomass Feedstock Analysis (CRL Energy ltd, 2012).

25. Darmstadt H., Pantea D., Summchen L., Roland U., Kaliaguine S., Roy C. (2000); "Surface and bulk chemistry of charcoal obtained by vacuum pyrolysis of bark: influence of feedstock moisture content."; Journal of Analytical and Applied Pyrolysis, Vol 53(1):1-17

26. De Wild P.J., Den Uil H., Reith J.H., Kiel J.H.A., Heeres H.J. (2009); "Biomass valorisation by staged degasification: A new pyrolysis-based thermochemical conversion option to produce value-added chemicals from lignocellulosic biomass"; Journal of Analytical and Applied Pyrolysis, Vol 85(1–2):124-133

27. Demirbas A., (2004) "Effects of temperature and particle size on bio-char yield from pyrolysis of agricultural residues."; J. Anal. Appl. Pyrol. Vol 72: 243–248.

28. Demirbas A. (2010); "Biorefineries: For Biomass Upgrading Facilities (Green Energy and Technology)", Publisher Springer 2010, ISBN: 1848827202.

29. Department of Environmental Protection (2002); "Western Australian Guidelines for Direct Land Application of Biosolids and Biosolid Products."; Waters and Rivers Commission, Department of Health, Perth, Western Australia.
http://www.agric.wa.gov.au/content/SUST/GREENHOUSE.PDF (accessed 25 July, 2012).

30. Diebold J. and Bridgwater A. (1997); "Overview of Fast Pyrolysis of Biomass for the Production of Liquid Fuels," in Developments in Thermal Biomass Conversion, The IEA Bioenergy Handbook on Biomass Pyrolysis

31. Dominguez J., Oliet M., Alonso V., Gilarranz M. and Rodriguez F. (2008); "Thermal stability and pyrolysis kinetics of organosolvlignins obtained from Eucalyptus globulus."; Industrial Crops and Products, Vol 27(2): 150-156

32. Downie A., Crosky A., Munroe P. (2009); "Physical properties of biochar. In 'Biochar for environmental management. Science and technology."; Editors J Lehmann, S Joseph, pp. 13-32; Earthscan: London; Antal and Gronli 2003

33. Dynamotive, 2009; Dynamotive CQuest BioChar Information Booklet, The Evolution of Energy, By Dynamotive Energy Systems Corporation, TerraChoice Environmental Marketing Inc., 1280 Old Innes Road, Suite 801, Ottawa, Ontario, K1B 5M7

34. Eckmeier E., Gerlach R., Skjemstad J., Ehrmann O., Schmidt M. (2007); "Minor changes in soil organic carbon and charcoal concentrations detected in a temperate deciduous forest a year after an experimental slash-and-burn."; Biogeosciences Vol 4(3):377-383.

35. Enecon, 2001; "Integrated tree processing of mallee eucalypts. Oil Mallees – Profitable Land-care" http://www.rirdc.gov.au/reports/AFT/01-160.pdf (accessed 25 July, 2012).

36. Engineering ToolBox, (2013); Values looked up: Density of pine sawdust, Density of nitrogen at 1 bar and 480 °C, Heat capacity of sawdust, Heat capacity of nitrogen gas, Absolute viscosity of nitrogen; Engineering ToolBox; http://www.engineeringtoolbox.com/

37. Gaston K., Cheah S., Parent Y., Jarvis M., Vinzant T., Smith K., Thornburg N., Nimlos M., Magrini-Bair K. (2012); "Nickel cerium olivine catalyst for catalytic gasification of biomass"; Applied Catalysis B: Environmental, Vol (134–135):34-45

38. Graetz R. D. and Skjemstad J.O., (2003); "The charcoal sink of biomass burning on the Australian continent." CSIRO Atmospheric Research Technical paper No. 64 http://www.cmar.csiro.au/e-print/open/graetz_2003a.pdf (accessed 25 July, 2012).

39. Gungora A., Onenc S., 2012; "Comparison between the "one-step" and "two-step" catalytic pyrolysis of pine bark"; Journal of Analytical and Applied Pyrolysis Vol 97:39–48

40. Hasanah U., Setiaji B., Anwar C. (2012); "The Chemical Composition and Physical Properties of the Light and Heavy Tar Resulted from Coconut Shell Pyrolysis"; J. Pure App. Chem. Res., Vol 1(1):26-32

41. Heo H. S., Park H. J., Park Y. K., Ryu C., Suh J., Suh Y. W., Yim J. H., Kim S. S. (2010); "Bio-oil production from fast pyrolysis of waste furniture sawdust in a fluidized bed"; Bioresource Technology, Vol 101(1):S91-S96

42. Herrington P. (2012) ; Personal discussion with Phil Herrington- Principal scientist, Opus International Consultants, 24 January 2012

43. Herrington P. (2012) ; Personal discussion with Phil Herrington- Principal scientist, Opus International Consultants, 30 May 2012

44. Herrington P. (2012); Herrington referred to his communication with Mr John Vercoe, Technical manager, Bitumen Supply, Works Infrastructure Ltd (Importer of bitumen to New Zealand).

45. Herrington P. (2012); Bio-oil samples analysis results.

46. Herrington P. (2013); In person discussion March 2013

47. Hills A. (2013); Personal discussion and site visit with Anthony Hills - plant control operator at Marsden Point refinery, Whangarei, New Zealand, February 2013

48. International Bio-Char Initiative, (2012); "Biochar"; http://www.biochar-international.org/ (assessed June 2012)

49. International Standards: ISO 1928, ASTM D4239, ISO 562, ISO 1171, ISO 11722

50. JB's Environmental (2013), personal email [jbatjbs@xtra.co.nz] communication on 19 March 2013 with JB's Environmental Ltd, Price quote for ***Pinus Radiata*** from JB's Environmental Ltd.

51. Jin H., Larson F. (2009); "Performance and cost analysis of future, commercially mature gasification-based electric power generation from switchgrass."; Biofuels, Bioproducts and Biorefining, Vol 3(2):142–173

52. Keiluweit M., Nico P., Johnson M., Kleber M. (2010); "Dynamic molecular structure of plant biomass-derived black carbon (biochar)."; Environmental Science & Technology Vol 44: 1247-1253.

53. Keiluweit M., Sun K., Kleber M., Pan Z., Xing B. (2010);"Sorption of fluorinated herbicides to plant biomass-derived biochars as a function of molecular structure"; Bioresource Technology, Vol 102(21): 9897-9903

54. Krishnaratne J. (2008); "Using biochar to improve soil health and leaf production in Sri Lankan tea plantations"; Dilmah Conservation; http://www.dilmahconservation.org/news-and-articles/using-biochar-to-improve-soil-health-and-leaf-production-at-tea-plantations-in-sri-lanka/ (assessed March 2012)

55. Krishnaratne J. (2008); "Using biochar to improve soil health and leaf production in Sri Lankan tea plantations"; IUCN Sri Lanka in 2008 in partnership with the Tea Research Institute of Sri Lanka (TRI); Dilmah Conservation; http://www.bio-char-international.org/ (assessed June 2012)

56. Krishnaratne J. (2008); "Using biochar to improve soil health and leaf production in Sri Lankan tea plantations"; IUCN Sri Lanka in 2008 in partnership with the Tea Research Institute of Sri Lanka (TRI); Dilmah Conservation; http://www.bio-char-international.org/ (assessed June 2012)

57. Kuzyakov Y., Subbotina I., Chen H., Bogomolova I., Xu X. (2009); "Black carbon decomposition and incorporation into soil microbial biomass estimated by 14C labeling."; Soil Biology & Biochemistry Vol 41(2):210-219

58. Lehmann J. (2007); "Bio-energy in the black.", Front. Ecol. Environ. Vol 5: 381–387.

59. Lehmann J., Pereira da Silva J., Steiner C., Nehls T., Zech W., Glaser B. (2003); "Nutrient availability and leaching in an archaeological Anthrosol and a Ferralsol of the Central Amazon basin: fertiliser, manure and charcoal amendments."; Plant Soil Vol 249:343–357.

60. Lesueur D. (2008); "The colloidal structure of bitumen: Consequences on the rheology and on the mechanisms of bitumen modification", Advances in Colloid and Interface Science, Vol 145(1–2):42-82

61. Marshall and Swift (2013); "Marshall and Swift equipment cost indexes" published each month in Chemical Engineering; For a complete description of these indexes, see R. W. Stevens, Chetn. Eng., Vol 54(11):124

62. Massey University, (2013); "Why Biochar?", New Zealand Biochar Research Center;.http://www.bio-char.co.nz/why.html (assessed June 2012)

63. McBeath A. V., Smernik R. J. (2009); "Variation in the degree of aromatic condensation of chars."; Organic Geochemistry, Vol 40: 1161-1168.

64. McCarthy J. L. and Islam A. (2000); "Chapter 1, Lignin: Historical, Biological, and Materials Perspectives"; American Chemical Society Symposium Series 742: Washington, DC, 2000.

65. McGuinness M. (2012); Personal communication with Mike McGuinness, Managing director, BP Oil NZ; In person discussion on 12 July 2012 at Energy Federation of New Zealand, Annual General Meeting, 'Wheels to wheel – a journey through the New Zealand supply chain'

66. McHenry M. (2009); "Agricultural bio-char production, renewable energy generation and farm carbon sequestration in Western Australia: Certainty, uncertainty and risk"; Agriculture, Ecosystems & Environment, Vol 129(1–3):1-7

67. McHenry M.P., (2008); "Agricultural bio-char production, renew able energy generation and farm carbon sequestration in Western Australia: Certainty, uncertainty and risk"; Agriculture, Ecosystems & Environment, Vol 129(1–3): 1–7

68. Milne E., Powlson, D.S., Cerri, C.E. (2007); "Soil carbon stocks at regional scales (preface)."; Agric. Ecosyst. Environ. Vol 122(1–2)

69. Mohan D., Pittman C.U. and Steele P.H. (2006); "Pyrolysis of wood/biomass for bio-oil: A critical review."; Energy Fuel, Vol 20:848-889

70. Mohan D., Pittman C.U. and Steele P.H. (2006); "Pyrolysis of wood/biomass for bio-oil: A critical review."; Energy Fuel, Vol 20:848-889

71. Moreno R., Antolin G., Reyes A. and Alvarez P. (2004); "Drying characteristics of forest biomass particles of *Pinus Radiata*."; Biosystems Engineering, Vol 88(1): 105-115.

72. New Zealand Ministry of Agriculture and Forestry, (2008); "New Zealand Forest Industry Facts & Figures 2008/2009"; retrieved from http://www.mpi.govt.nz/portals/0/documents/forestry/statistics/forestry-stats/facts-figures-08-09.pdf

73. NZTA (New Zealand Transport Agency) (2005); The National Land Transport Programme-NLTP; Land Transport New Zealand; Posted 28 June 2005, http://www.transfund.govt.nz/funding/nltp/2006/speech.html.

74. NZTA FAQ 2009; NZTA (New Zealand Transport Agency) (2009), Land Transport New Zealand; Posted 28 June 2005, http://www.nzta.govt.nz/resources/urban-design/

75. Oasmaa A., (2002); “Fast Pyrolysis of Forestry Residue. 1. Effect of Extractives on Phase Separation of Pyrolysis Liquids”; Energy and Fuels, Vol 17 (1):1–12

76. Oasmaa A., Arpiainen V., Kuoppala E. and Sipila K. (2010); "Fast Pyrolysis Bio-Oils from Wood and Agricultural Residues"; Energy and Fuels, Vol 24(9): 6548-6554.

77. Oasmaa A. and Kuoppala E. (2011); "An Approach for Stability Measurement of Wood-Based Fast Pyrolysis Bio-Oils."; Energy and Fuels, Vol 25(7): 3307-3313.

78. Oasmaa A., Kuoppala E. (2003); “Fast Pyrolysis of Forestry Residue. 3. Storage Stability of Liquid Fuel”; Energy Fuels, Vol 17 (4):1075–1084

79. Oasmaa A., Kuoppala E., Yrjö S. (2003); “Fast Pyrolysis of Forestry Residue. 2. Physicochemical Composition of Product Liquid.”; Energy and Fuels, Vol 17(2):433 - 443.

80. Olsen C. (2012), “Bitumen price soars”; Chris Olsen - CEO Roading NZ, Contractor Magazine Article, Contrafed Publishing Co. Ltd; September 2012, http://www.contrafedpublishing.co.nz/Technical/Bitumen+price+soars.html; Posted September 2012

81. OPUS laboratory results, (2012); Personal communication with Harrington P. June 2012.

82. Orfao J., Antunes F. and Figueiredo J. (1999); "Pyrolysis kinetics of lignocellulosic materials – three independent reactions model."; Fuel, Vol 78: 349-358.

83. Pang S. (2013); Constructive discussion and direct communication.

84. Perry R. and Green D. (2007); “Perry's Chemical Engineers' Handbook”; Chemical engineering; McGraw-Hill Publication date; 8th Edition; Pages 2640; ISBN 0-07-142294-3

85. Peters and Timmerhaus (2003); “Plant Design and Economics for Chemical Engineers”; 5th edition (Max S. Peters, Klaus D. Timmerhaus and Ronald E. West, McGraw-Hill, NY

86. Peters M. and Timmerhaus K. (2003); “Plant Design and Economics for Chemical Engineers”; 5th edition Max S. Peters, Klaus D. Timmerhaus and Ronald E. West, McGraw-Hill, NY

87. Prins M. (2006), “Torrefaction of wood: Part 2. Analysis of products”; Journal of Analytical and Applied Pyrolysis, Vol 77(1): 35-40

88. Qiang L., Xi-Feng Z. (2009); "Overview of fuel properties of biomass fast pyrolysis oils."; Energy Conversion and Management, Vol 50: 1376-1383.

89. Rcchar.inc, (2013); "Profile: Rechar—Creating Affordable Opportunities for Bio-char Production and use in Western Kenya"; 2013 International Bio-char Initiative; http://www.biochar-international.org/rechar (accessed 21 August, 2012).

90. Read J. and Whiteoak D. (2003), "The Shell Bitumen Handbook", Fifth Edition. Thomas Telford Publishing, Thomas Telford Ltd, 1 Heron Quay, London E14 4JD,UK

91. Rodríguez-Valverde M.A., Ramón-Torregrosa P., Páez-Dueñas A., Cabrerizo-Vílchez M.A., Hidalgo-Álvarez R. (2007); "Imaging techniques applied to characterize bitumen and bituminous emulsions"; Advances in Colloid and Interface Science, Vol 136(1–2):93-108

92. Sadaka S. and Boateng A. (2009); "Pyrolysis and Bio-oil", University of Arkansas publication - FSA1052, Agriculture and Natural Resources 2009; http://www.uaex.edu/Other_Areas/publications/PDF/FSA-1052.pdf

93. Sadaka S. and Boateng A. (2009); "Pyrolysis and Bio-oil", University of Arkansas publication - FSA1052, Agriculture and Natural Resources 2009; http://www.uaex.edu/Other_Areas/publications/PDF/FSA-1052.pdf

94. Saddawi J., Williams A. and Wojtowicz M. (2010); "Kinetics of the Thermal Decomposition of Biomass."; Energy and Fuels, Vol 24: 1274-1282.

95. Salehi E. and Harding T. (2009); "Bio-oil from Sawdust: Pyrolysis of Sawdust in a Fixed-Bed System."; Energy and Fuels, Vol 23(7): 3767-3772.

96. Salehi E. and Harding T. (2011); "Bio-oil from Sawdust: Effect of Operating Parameters on the Yield and Quality of Pyrolysis Products."; Energy and Fuels, Vol 25(9): 4145-4154.

97. Salehi E. and Harding T. (2011); "Bio-oil from Sawdust: Effect of Operating Parameters on the Yield and Quality of Pyrolysis Products."; Energy and Fuels, Vol 25(9): 4145-4154

98. Sascha R., Kersten A., Prins W. and Wim Van Swaaij M. (2005); "Biomass Pyrolysis in a Fluidized Bed Reactor. Part 1: Literature Review and Model Simulations."; Industrial Engineering Chemistry Research, Vol 44(14): 5079-5089.

99. SCENZ (Society of Chemical Engineers NZ), (2007); Bouman R, Jesen S, Wake M, Earl W; "Process Capital Cost Estimation for New Zealand 2007; ISBN 0-473-10257-9

100. Seider W., Seader J., Lewin D., Widagdo S. (2008); "Product and Process Design Principles: Synthesis, Analysis and Design", 3rd Edition, 736 pages, ISBN 978-0-470-04895-5

101. Singh B., Singh B.P., Cowie A.L. (2010); "Characterisation and evaluation of biochars for their application as a soil amendment."; Australian Journal of Soil Research Vol 48:516-525

102. Solantausta Y., Sipilä K., Lindfors C., Lehto J., Autio J., Jokela P., Alin J. and Heiskanen J. (2011); "Bio-oil production from biomass – Steps towards demonstration."; Energy and Fuels, Vol 26(1):233-240

103. Steinbeiss S., Gleixner G. and Antonietti M. (2009); "Effect of biochar amendment on soil carbon balance and soil microbial activity"; Soil Biol. Biochem. Vol 41:1301–1310.

104. Steiner C., Teixeira W., Lehmann J., Nehls T., Vasconcelos de Macedo J., Blum W., Zech W. (2007); "Long term effects of manure, charcoal and mineral fertilization on crop production and fertility on a highly weathered Central Amazonian upland soil."; Plant and Soil Vol 291:275-290.

105. Strausz O., Morales-Izquierdo A., Kazmi N., Montgomery D., Payzant J., Safarik I., Murgich J. (2010); "Chemical Composition of Athabasca Bitumen: The Saturate Fraction"; Energy Fuels, Vol 24 (9):5053–5072

106. The Free Dictionary by Farlex (2013); terms looked up 'Newtonian fluids', 'The flash point', 'Pour point', 'Lubricity'; Farlex Inc; http://www.thefreedictionary.com/

107. Tuck A. (2010); "Bitumen Supply and Performance"; Downer ltd, Higgins 'Green Team' presentation; Presented November 2010, Reaa.co.nz (assessed April 28, 2012)

108. Uslu A., Faaij A., Bergman P. (2008); "Pre-treatment technologies, and their effect on international Bioenergy supply chain logistics. Techno-economic evaluation of torrefaction, fast pyrolysis and pelletisation."; Energy, Vol 33: 1206-1223.

109. Van Paasen S., (2004); "Tar removal with a wet electrostatic precipitator"; Presented at "The 2nd World Conference and Technology Exhibition on Biomass for Energy, Industry and Climate Protection" in Rome, Italy, 10-14 May 2004

110. Venderbosch and Prins (2010); "Fast pyrolysis technology development"; Biofuels, Bioproducts and Biorefining, Vol 4(2):178–208

111. Wang X., Kersten A., Sascha R., Prins W. and Wim Van Swaaij M. (2005); "Biomass Pyrolysis in a Fluidized Bed Reactor. Part 1: Literature Review and Model Simulations."; Industrial Engineering Chemistry Research, Vol 44(14): 5079-5089.

112. Wikipedia (2013); 'CEC', June 2013, Wikipedia, Wikimedia Foundation, Inc.; http://en.wikipedia.org/wiki/Cation_exchange_capacity (accessed August 2012).

113. Wikipedia (2013); 'Road surface', June 2013, Wikipedia, Wikimedia Foundation, Inc.; http://en.wikipedia.org/wiki/Road_surface (accessed August 2012).

114. Wikipedia, (2013); "Electrostatic precipitator"; June 2013, Wikipedia, Wikimedia Foundation, Inc.; http://en.wikipedia.org/wiki/Electrostatic_precipitator (accessed August 2012).

115. World Asphalt to 2009; Freedonia Group 2005; Reported in Performance, summer 2006, Nynas bitumen, Belgium; Posted 28 Dec 2005, http://www.freedoniagroup.com/DocumentDetails.aspx?DocumentID=46747

116. Xi-Feng Z., Ji-Lu Z., Qing-Xiang G., Qing-Shi Z. (2006); "Pyrolysis of rice husk and sawdust for liquid fuel" ; Journal of Environmental Sciences, Vol 18(2): 392-396

117. Zanzi R., Bai Z., Capdevila P., Bjornbom E. (2001); "Pyrolysis of biomass in presence of steam for preparation of activated carbon, liquid and gaseous products; In: 6th World Congress of Chemical Engineering. Melbourne. http://hemfristorg.com/zanzi/paper/paper6.pdf (accessed August 2012).

118. Zhang J., Toghiani H., Mohan D., Pittman C. U., Toghiani R. K. (2007); "Product Analysis and Thermodynamic Simulations from the Pyrolysis of Several Biomass Feedstocks"; Energy Fuels, Vol 21 (4): 2373–2385

119. Zhang J., Toghiani H., Mohan D., Pittman C.H., Toghiani R. K. (2007); "Product Analysis and Thermodynamic Simulations from the Pyrolysis of Several Biomass Feedstocks"; Energy Fuels, Vol 21(4): 2373–2385

Appendix

8.1 Experimental Runs Matrix

CRL Energy

Bio-bitumen

Created on 26-Nov-12

by Olga Kolokolova

							T at __ height within the reactor from the sand bed										
Run Date	**N2 main flow (l/min)**	**N2 hop-per flow (l/min)**	**Total Feed (g)**	**Set T N2 in (°C)**	**T Cy-clone (°C)**	**Avg Bed T (°C)**	**5 cm up**	**10 cm up**	**25 cm up**	**Motor Setting**	**Feed Moisture Content**	**Char %**	**Tar %**	**Oil %**	**Air %**	**Sample Name Given (Char example)**	
3/27/2012	35	3	1000	560	300.0	474.0	475.2	486.0	305.7	8.0	-	7.0%	0.0%	26.2%	66.8%	12-27/03-PS474-SLD	pine sawdust
4/5/2012	35	3	1000	560	300.0	457.9	457.1	467.3	522.9	11.9	-	10.0%	5.4%	27.2%	57.4%	12-05/04-PS458-SLD	pine sawdust
4/10/2012	40	3	1000	560	300.0	451.5	450.2	457.3	367.2	11.9	-	14.4%	11.0%	30.4%	44.2%	12-10/04-PS452-SLD	pine sawdust
4/11/2012	40	3	2000	560	300.0	458.4	455.0	462.2	485.4	11.9	-	24.8%	22.6%	50.4%	2.2%	12-11/04-PS458-SLD	pine sawdust
4/16/2012	40	3	2890	560	300.0	460.6	459.0	464.2	451.1	10.1	-	15.8%	13.5%	31.6%	39.1%	12-16/04-PS461-SLD	pine sawdust
4/18/2012	40	3	2266	560	300.0	468.7	467.4	472.2	470.2	11.9	-	15.6%	3.8%	38.4%	42.2%	12-18/04-PS469-SLD	pine sawdust
5/1/2012	40	3	3256	560	300.0	470.9	468.3	473.4	487.1	10.5	-	15.7%	0.8%	30.3%	53.3%	12-01/05-PS468-SLD	pine sawdust
5/7/2012	40	3	2410	561	300.0	474.3	472.3	487.3	478.4	10.5	-	10.0%	1.2%	35.3%	53.5%	12-07/05-PS474-SLD	pine sawdust
5/10/2012	60	3	1000	520	300.0	463.8	461.8	467.4	486.2	9.1	-	24.8%	1.0%	20.0%	54.2%	12-10/05-PS464-SLD#1	pine sawdust
5/10/2012	30	3	906	520	300.0	441.6	439.6	459.0	406.3	9.1	-	8.6%	1.1%	34.4%	55.8%	12-10/05-PS442-SLD#2	pine sawdust
5/16/2012	40	3	1929	560	300.0	406.4	404.2	412.0	357.6	11.8	-	24.7%	2.3%	34.2%	38.8%	12-16/05-PS406-SLD	pine sawdust
5/22/2012	40	3	2479	560	300.0	421.6	417.7	406.5	349.7	11.8	8.20	19.8%	3.6%	36.8%	39.7%	12-22/05-PS422-SLD	pine sawdust
5/28/2012	40	3	2006	560	322.0	424.8	419.0	409.0	349.2	11.4	19.60	16.1%	4.0%	34.0%	46.0%	12-28/05-PS425-SLD	pine sawdust
6/11/2012	40	4	2292	560	241.0	435.0	428.2	420.9	352.8	11.4	12.55	15.0%	7.0%	32.0%	46.0%	12-11/06-OPS435-SLD	old mans pine
6/18/2012	65	4	1300	560	277.0	466.5	454.7	432.0	338.0	10.4	7.85	9.0%	4.0%	16.0%	71.0%	12-18/06-PS466-SLD	pine sawdust
6/21/2012	65	4	1812	560	360.8	463.7	457.1	454.3	360.0	8.5	24.22	15.0%	4.0%	34.0%	47.0%	12-21/06-PS464-SLD	pine sawdust
6/25/2012	65	4	1500	560	340.7	468.6	463.7	462.2	340.0	8.5	16.84	10.0%	5.0%	22.0%	63.0%	12-25/06-PS469-SLD	pine sawdust
6/27/2012	65	4	1720	560	358.2	470.4	466.2	464.6	358.0	8.5	21.81	10.0%	10.0%	30.0%	50.0%	12-27/06-PS470-SLD	pine sawdust
6/29/2012	65	4	1400	560	340.7	468.2	464.6	462.5	399.0	8.5	28.51	9.0%	8.0%	26.0%	57.0%	12-29/06-PS468-SLD	pine sawdust
7/3/2012	65	4	1760	560	329.6	465.8	461.4	460.2	372.8	8.5	31.29	12.0%	8.0%	36.0%	44.0%	12-03/07-PS466-SLD	pine sawdust
7/5/2012	65	4	1374	560	309.8	478.4	473.7	460.6	333.6	8.5	6.93	16.0%	18.0%	13.0%	53.0%	12-05/07-SPS478-SLD	small pine sawdust
8/13/2012	65	3	1000	560	300.0	463.8	461.8	467.4	486.2	9.1	11.62	9.0%	1.0%	34.0%	56.0%	12-13/08-NS463.8-SLD	nitens
8/15/2012	65	3	1929	560	300.0	406.4	404.2	412.0	357.6	11.8	11.62	25.0%	2.0%	34.0%	39.0%	12-15/08-NS406.4-SLD	nitens

8/24/2012	65	3	2479	560	300.0	421.6	417.7	406.5	349.7	11.8	9.83	20.0%	4.0%	37.0%	39.0%	12-24/08-5P/5B-421.6-SLD	50/50 pine sawdust/bark
8/29/2012	65	3	2006	560	322.0	424.8	419.0	409.0	349.2	11.4	9.51	16.0%	4.0%	34.0%	46.0%	12-29/08-7P/3B-424.8-SLD	70/30 pine sawdust/bark
8/31/2012	65	3	2292	560	241.0	435.0	428.2	420.9	352.8	11.4	12.55	15.0%	7.0%	32.0%	46.0%	12-31/08-SPS435-SLD	<1590 microns pine sawdust
9/4/2012	65	3	1300	560	277.0	466.5	454.7	432.0	338.0	10.4	7.85	9.0%	4.0%	16.0%	71.0%	12-04/09-SPS466.5-SLD	<1590 microns pine sawdust
9/7/2012	65	3	1812	560	360.8	463.7	457.1	454.3	360.0	8.5	5.27	15.0%	4.0%	34.0%	47.0%	12-07/09-SPS463.7-SLD	<1590 microns pine sawdust
9/14/2012	65	3	1816	560	304.2	467.6	463.6	464.2	345.1	8.4	11.62	17.0%	6.0%	33.0%	44.0%	12-14/09-NS467.6-SLD	nitens
9/19/2012	65	3	1310	560	332.5	472.8	470.1	469.1	353.6	8.4	7.18	23.0%	11.0%	29.0%	37.0%	12-19/09-7P/3B-472.8-SLD	70/30 pine sawdust/bark
9/21/2012	65	3	1314	560	313.6	468.0	464.1	462.8	320.8	8.4	8.40	22.0%	13.0%	29.0%	35.0%	12-21/09-7P/3B-468.0-SLD	70/30 pine sawdust/bark
10/1/2012	65	3	1252	560	326.4	468.8	463.4	463.6	365.8	8.4	8.11	23.0%	14.0%	15.0%	49.0%	12-01/10-7P/3B-468.8-SLD	70/30 pine sawdust/bark
10/3/2012	65	3	1406	560	312.9	469.9	462.0	460.9	312.4	8.4	8.11	28.0%	18.0%	20.0%	34.0%	12-03/10-7P/3B-469.9-SLD	70/30 pine sawdust/bark
10/8/2012	65	3	1456	560	299.0	469.4	464.7	464.1	339.6	8.4	11.67	30.0%	16.0%	18.0%	36.0%	12-08/10-5P/5B-469.4-SLD	50/50 pine sawdust/bark
10/10/2012	65	3	1286	560	298.2	469.4	464.7	464.1	339.6	8.4	12.31	28.0%	13.0%	22.0%	37.0%	12-10/10-5P/5B-469.4-SLD	50/50 pine sawdust/bark
10/15/2012	65	3	1588	560	298.8	469.2	464.5	463.8	345.2	8.4	9.40	27.0%	19.0%	23.0%	31.0%	12-15/10-7P/3B-469.2-SLD	70/30 pine sawdust/bark
10/18/2012	65	3	2008	560	297.0	466.6	462.3	459.6	356.3	8.4	8.03	32.0%	11.0%	19.0%	38.0%	12-18/10-5P/5B-466.6-SLD	50/50 pine sawdust/bark
10/24/2012	65	3	1564	560	297.0	470.6	462.3	459.6	356.3	8.4	8.26	25.9%	17.3%	21.1%	35.7%	12-24/10-7P/3B-470.6-SLD	70/30 pine sawdust/bark
11/29/2012	65	3	1626	560	297.0	473.9	463.4	461.1	347.8	8.4	8.23	19.0%	12.0%	27.0%	42.0%	12-10/05-PS464-SLD	pine sawdust
12/3/2012	65	3	1888	560	310.0	472.9	463.0	460.0	333.9	8.4	7.36	17.0%	15.0%	25.0%	43.0%	12-24/10-PS470.6-SLD	pine sawdust
12/5/2012	65	3	1850	560	314.0	470.2	464.7	462.8	343.4	8.4	7.22	19.0%	13.0%	25.0%	43.0%	12-10/05-PS464-SLD	pine sawdust
12/12/2012	65	3	1866	560	306.0	468.0	463.4	461.4	360.1	8.4	11.27	18.0%	18.0%	24.0%	40.0%	12-24/10-PS470.6-SLD	pine sawdust
12/20/2012	65	5	747	560	306.0	454.6	464.4	462.5	343.4	8.1		21%	20%	23%	36%	12-20/12-5P/5B-455-SLD	
2/1/2013	65	5	1184	560	350.0	464.9	463.0	460.0	350.0	7.1		18%	10%	21%	51%	13-01/02-5P/5B-465-SLD	
2/5/2013	65	5	1150	560	294.0	459.4	461.7	453.8	335.7	7.1		21%	20%	23%	37%	13-05/02-5P/5B-460-SLD	
2/12/2013	65	5	834	560	289.4	447.2	467.4	464.9	452.4	10.1		13%	35%	18%	34%		

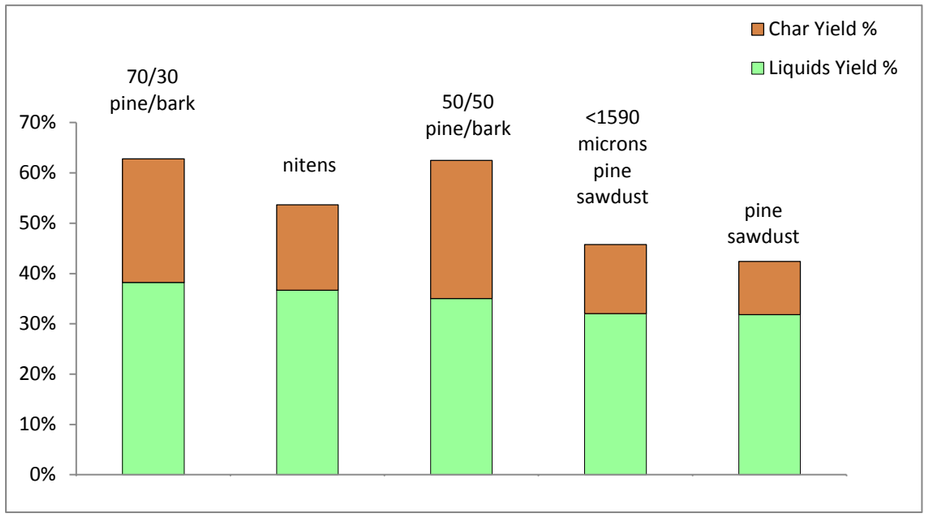

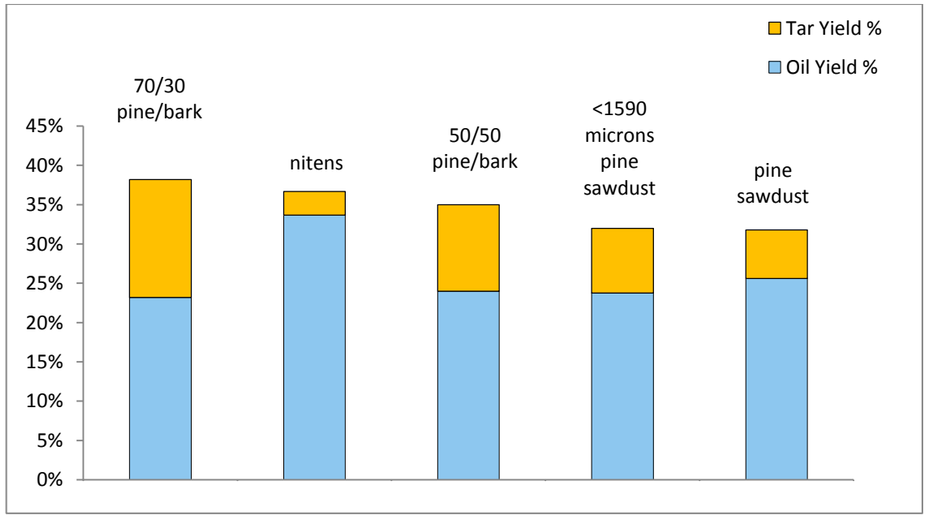

University of Canterbury (CRL Energy)

Bio-bitumen

Created on 17-Jan-13

by Olga Kolokolova

Run Date	Avg Bed T (°C)	MC feed %	Bio-char %	Tar %	Bio-oil %	Air %	Liquid %
pine sawdust (1500 microns - 4 mm)							
5/16/2012	406.4	-	24.7%	2.3%	34.2%	38.8%	36.5%
5/22/2012	421.6	8.20	19.8%	3.6%	36.8%	39.7%	40.4%
5/28/2012	424.8	19.60	16.1%	4.0%	34.0%	45.9%	38.0%
5/10/2012	441.6	-	8.6%	1.1%	34.4%	55.8%	35.5%
4/10/2012	451.5	-	14.4%	11.0%	30.4%	44.2%	41.4%
4/5/2012	457.9	-	10.0%	5.4%	27.2%	57.4%	32.6%
4/11/2012	458.4	-	24.8%	22.6%	50.4%	2.2%	73.0%
4/16/2012	460.6	-	15.8%	13.5%	31.6%	39.1%	45.1%
6/21/2012	463.7	24.22	15.0%	4.0%	34.0%	47.0%	38.0%
7/3/2012	465.8	31.29	12.0%	8.0%	36.0%	44.0%	44.0%
12/12/2012	468.0	11.27	18.0%	18.0%	24.0%	40.0%	42.0%
6/29/2012	468.2	28.51	9.0%	8.0%	26.0%	57.0%	34.0%
6/25/2012	468.6	16.84	10.0%	5.0%	22.0%	63.0%	27.0%
4/18/2012	468.7	-	15.6%	3.8%	38.4%	42.2%	42.2%
12/5/2012	470.2	7.22	19.0%	13.0%	25.0%	43.0%	38.0%
6/27/2012	470.4	21.81	10.0%	10.0%	30.0%	50.0%	40.0%
5/1/2012	470.9	-	15.7%	0.8%	30.3%	53.3%	31.0%
12/3/2012	472.9	7.36	17.0%	15.0%	25.0%	43.0%	40.0%
11/29/2012	473.9	8.23	19.0%	12.0%	27.0%	42.0%	39.0%
3/27/2012	474.0	-	7.0%	0.0%	26.2%	66.8%	26.2%
5/7/2012	474.3	-	10.0%	1.2%	35.3%	53.5%	36.5%
pine sawdust (<1500 microns)							0.0%
8/31/2012	435.0	12.55	15.0%	7.0%	32.0%	<1500 microns pine sawdust	39.0%
9/7/2012	463.7	5.27	15.0%	4.0%	34.0%	<1500 microns pine sawdust	38.0%
9/4/2012	466.5	7.85	9.0%	4.0%	16.0%	<1500 microns pine sawdust	20.0%
nitens sawdust (1500 microns - 4 mm)							0.0%
8/15/2012	406.4	11.62	25.0%	2.0%	34.0%	nitens	36.0%
8/13/2012	463.8	11.62	9.0%	1.0%	34.0%	nitens	35.0%
9/14/2012	467.6	11.62	17.0%	6.0%	33.0%	nitens	39.0%
70/30 pine sawdust/bark							0.0%
8/29/2012	424.8	9.51	16.0%	4.0%	34.0%	70/30 pine sawdust/bark	38.0%
9/21/2012	468.0	8.40	22.0%	13.0%	29.0%	70/30 pine sawdust/bark	42.0%
10/1/2012	468.8	8.11	23.0%	14.0%	15.0%	70/30 pine sawdust/bark	29.0%
10/15/2012	469.2	9.40	27.0%	19.0%	23.0%	70/30 pine sawdust/bark	42.0%
10/3/2012	469.9	8.11	28.0%	18.0%	20.0%	70/30 pine sawdust/bark	38.0%
10/24/2012	470.6	8.26	25.9%	17.3%	21.1%	70/30 pine sawdust/bark	38.4%
9/19/2012	472.8	7.18	23.0%	11.0%	29.0%	70/30 pine sawdust/bark	40.0%
50/50 pine sawdust/bark							0.0%
8/24/2012	421.6	9.83	20.0%	4.0%	37.0%	50/50 pine sawdust/bark	41.0%

12/20/2012	454.6		21.0%	20.0%	23.0%	50/50 pine sawdust/bark	43.0%
2/5/2013	459.4		21.0%	20.0%	23.0%	50/50 pine sawdust/bark	43.0%
2/1/2013	464.9		18.0%	10.0%	21.0%	50/50 pine sawdust/bark	31.0%
10/18/2012	466.6	8.03	32.0%	11.0%	19.0%	50/50 pine sawdust/bark	30.0%
10/8/2012	469.4	11.67	30.0%	16.0%	18.0%	50/50 pine sawdust/bark	34.0%
10/10/2012	469.4	12.31	28.0%	13.0%	22.0%	50/50 pine sawdust/bark	35.0%

pines						
7/5/2012	478.4	6.93	16.0%	18.0%	13.0%	workshop pine sawdust
6/11/2012	435.0	12.55	15.0%	7.0%	32.0%	old mans pine
2/12/2013	447.2		12.6%	35.4%	18.2%	soabean oil/sawdust

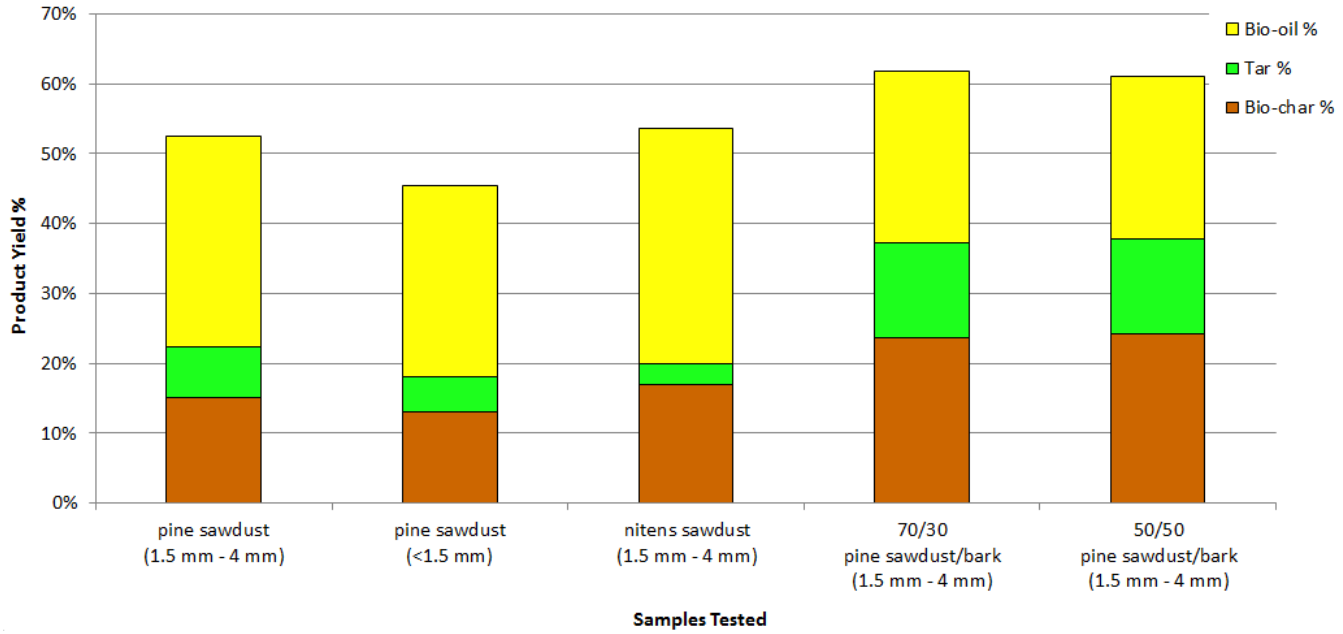
70%
60%
50%
40%
30%
20%
10%
0%
Product Yield %
Bio-oil %
Tar %
Bio-char %
pine sawdust (1.5 mm - 4 mm)
pine sawdust (<1.5 mm)
nitens sawdust (1.5 mm - 4 mm)
70/30 pine sawdust/bark (1.5 mm - 4 mm)
50/50 pine sawdust/bark (1.5 mm - 4 mm)
Samples Tested

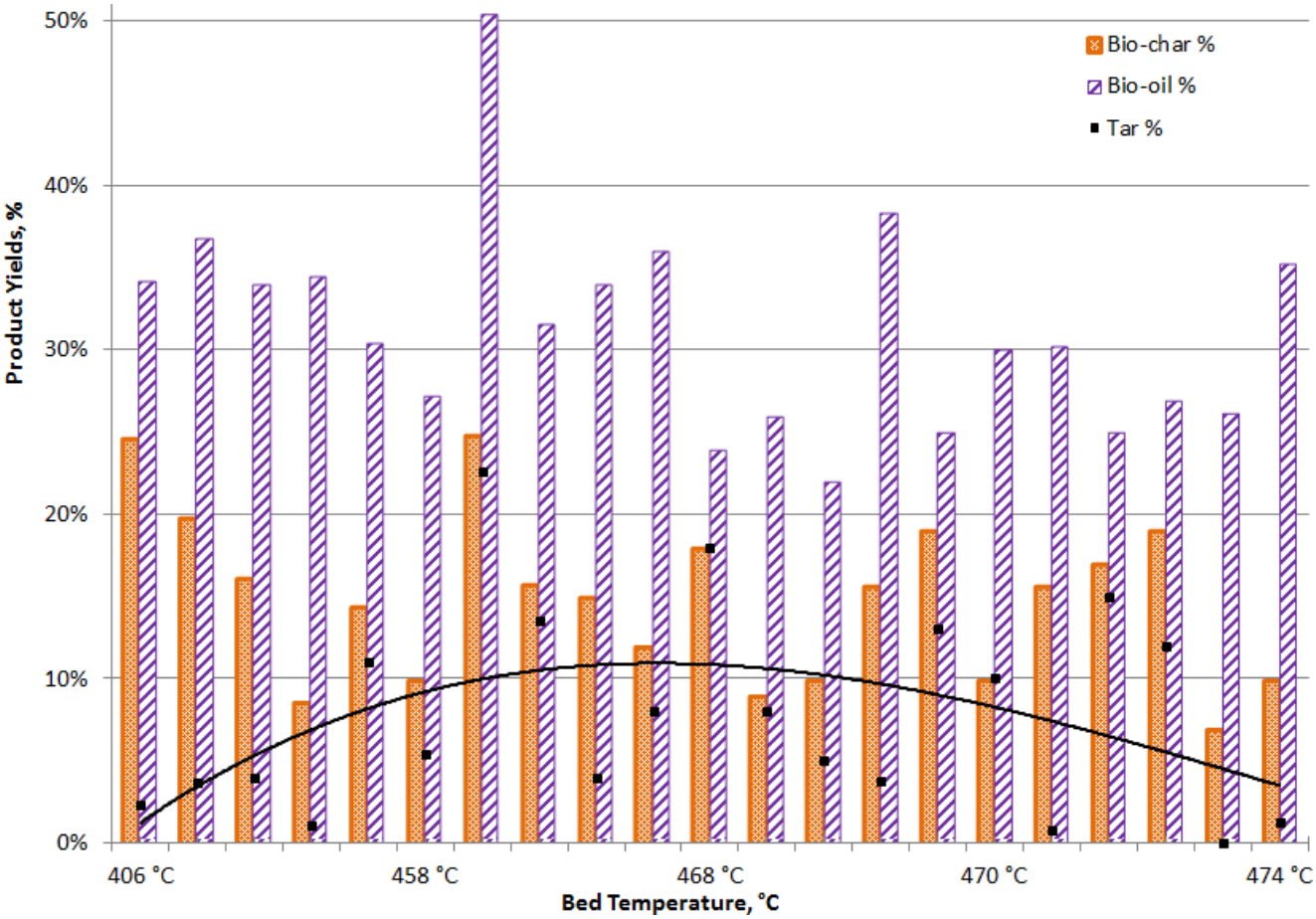
50%
40%
30%
20%
10%
0%
Product Yields, %
Bio-char %
Bio-oil %
Tar %
406 °C
458 °C
468 °C
470 °C
474 °C
Bed Temperature, °C

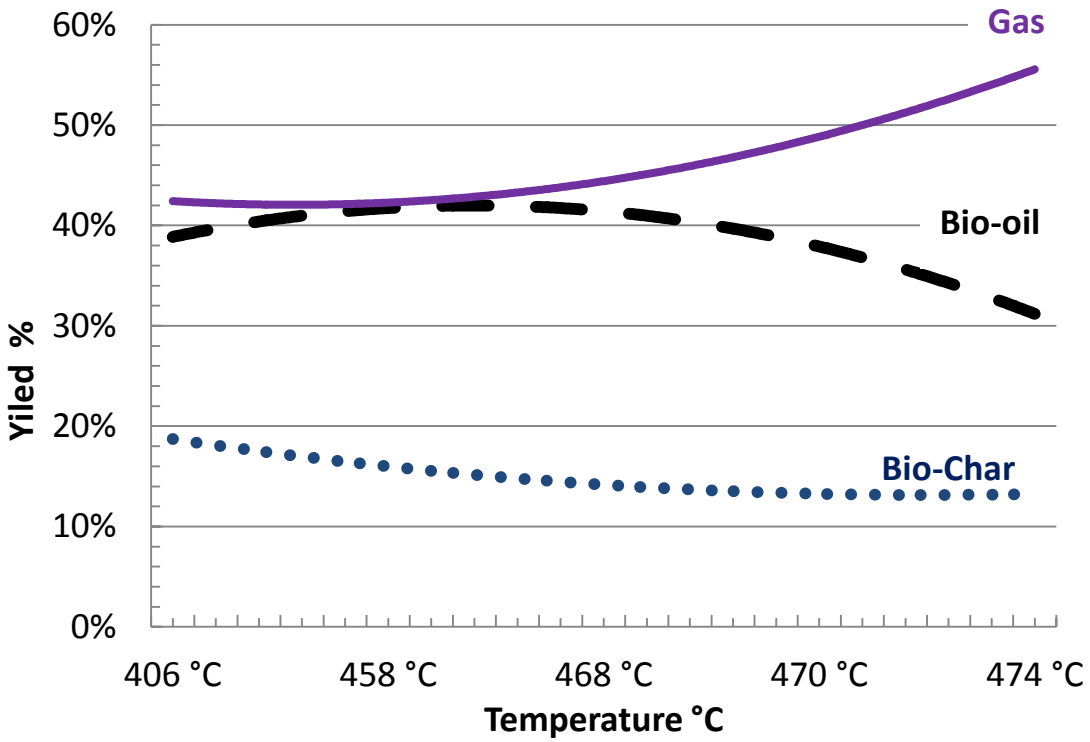
60%
50%
40%
30%
20%
10%
0%
Yiled %
Gas
Bio-oil
Bio-Char
406 °C
458 °C
468 °C
470 °C
474 °C
Temperature °C

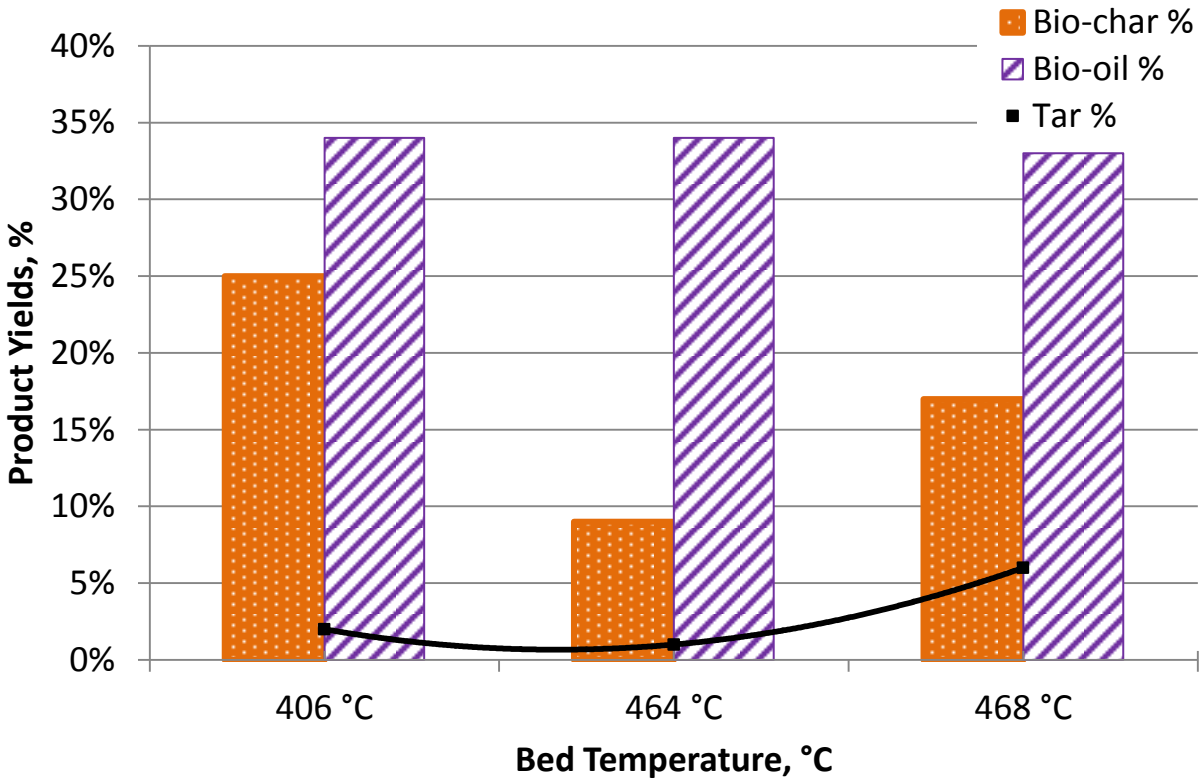
Bio-char %
Bio-oil %
Tar %
40%
35%
30%
25%
20%
15%
10%
5%
0%
Product Yields, %
406 °C
464 °C
468 °C
Bed Temperature, °C

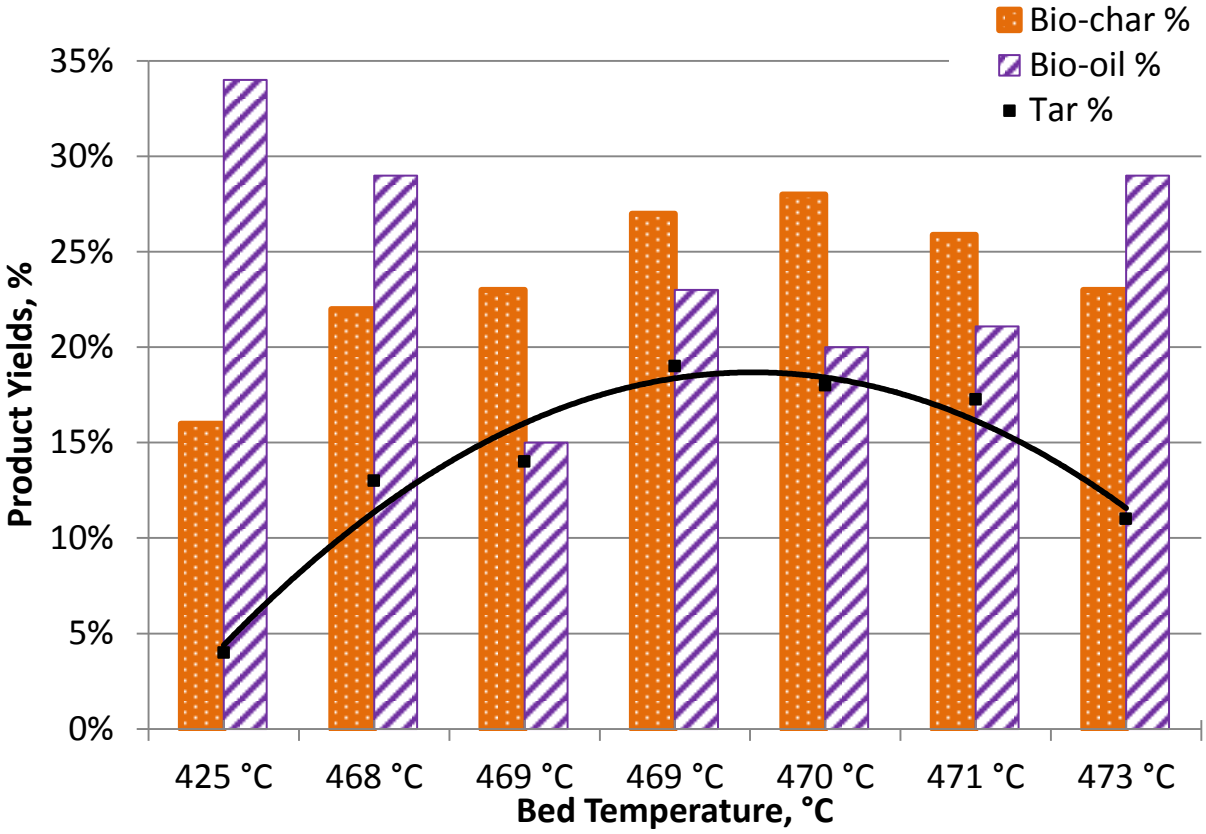
Bio-char %
Bio-oil %
Tar %
35%
30%
25%
20%
15%
10%
5%
0%
Product Yields, %
425 °C
468 °C
469 °C
469 °C
470 °C
471 °C
473 °C
Bed Temperature, °C

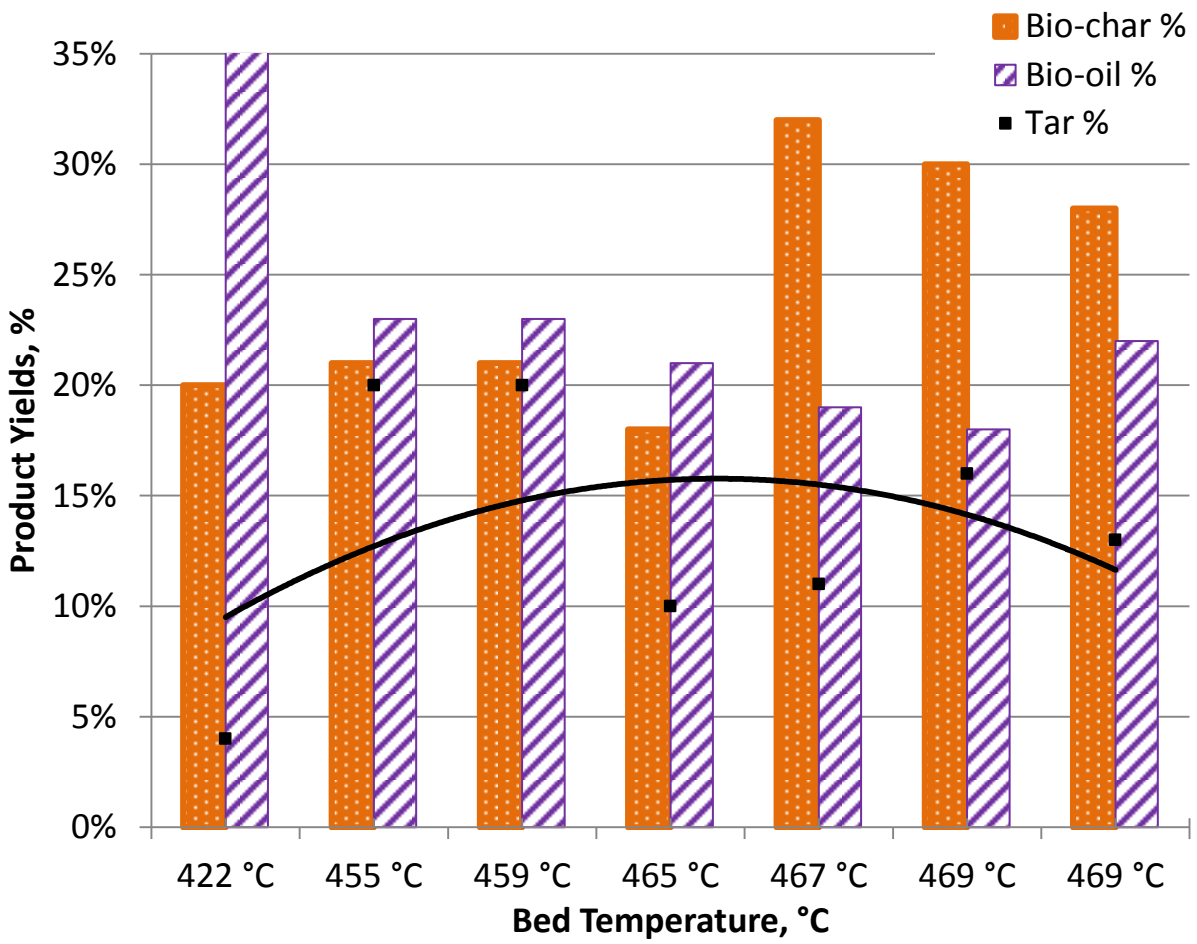
Bio-char %
Bio-oil %
Tar %
35%
30%
25%
20%
15%
10%
5%
0%
Product Yields, %
422 °C
455 °C
459 °C
465 °C
467 °C
469 °C
469 °C
Bed Temperature, °C

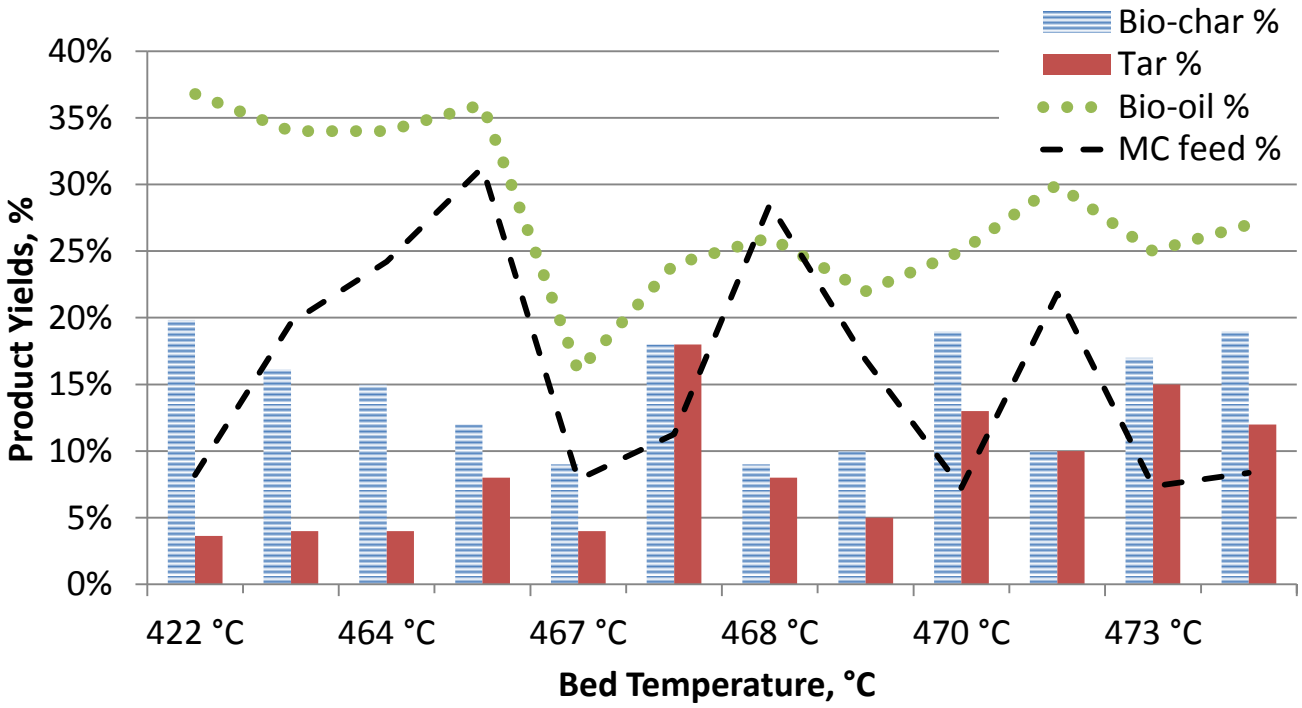
Bio-char %
Tar %
Bio-oil %
MC feed %
40%
35%
30%
25%
20%
15%
10%
5%
0%
Product Yields, %
422 °C
464 °C
467 °C
468 °C
470 °C
473 °C
Bed Temperature, °C

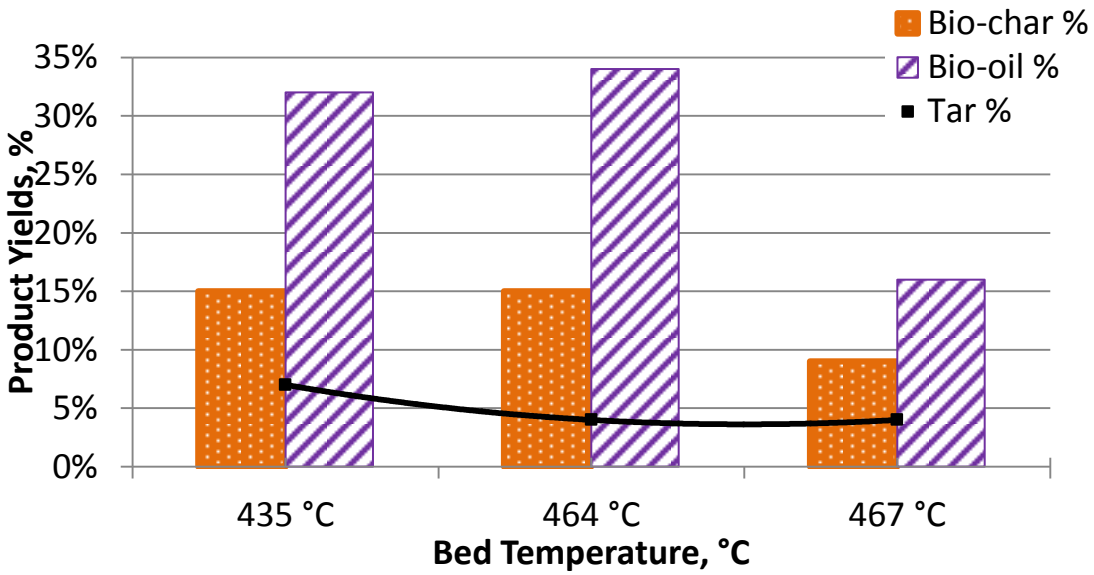
Bio-char %
Bio-oil %
Tar %
35%
30%
25%
20%
15%
10%
5%
0%
Product Yields, %
435 °C
464 °C
467 °C
Bed Temperature, °C

8.2 Toxicity

Gases and smoke emitted during the process are flammable and toxic for human. A great deal of attention should be drawn to the issue, if the process was to be commercialised. A fire safety should be reinforced in then reactor location of the plant. Additionally, breathing masks are important for the employees working around or participate in the process during operational hours. Furthermore, a good ventilation system is essential.

Pyrolysis bio-oil is flammable, toxic and carcinogenic, thus required specific handling during operation and maintenance. Air Pollutants like Sulfur Oxides (SOx) (root acid rains), Nitrogen Oxides (NOx) (root ozone, smog and respiratory problems), Carbon Monoxide (CO) and Carbon Dioxide (CO2) can be potentially emitted during the process and need to be thoroughly monitored and taken care of.

Volatile Organic Compounds (VOCs) toxic and carcinogenic. Furthermore, VOCs elevate ozone and smog levels in the lower atmosphere, causing respiratory problems.

8.2.1 CRL Energy safety procedure:

Pysolyser Operating Procedure ***CRL Fast Pyrolyser***

…… ……

Operator Name Date

Emergency Shutdown:

Turn OFF temperature controllers on control box. ☐

Turn OFF main switch on control box with ‘Control Box Main Switch‘. ☐

Stop gas flow via gas flow controller, ‘Get Red-y’ software. ☐

Turn OFF nitrogen regulators and valves (on the bottles and the inlet valve V04). ☐

Turn OFF feed auger motor ‘Feed Auger Motor Main Switch‘. ☐

Turn OFF the elbow heater manually ‘Elbow Heater Switch’. ☐

Turn OFF the air pump and the air compressor, which it runs of. ☐

Follow the Safety Check List to Ensure equipment is in a safe condition to operate.

Start-up:

Ensure equipment is in a safe condition to operate. No open ended/broken wires ☐

Ensure N2 supply is high ☐
(more than 1 full bottle (~10 cubic meters of Nitrogen) is available)

Check that the Nitrogen feed piping is connected and ready for operation ☐

Ensure the cyclone collector is in place and sealed. ☐

Ensure hopper is filled with feed material, and butterfly valve is closed ☐

Ensure condensers are in place and sealed. ☐

Ensure the cooling water into the heat exchanger is running, V03 open. ☐

Turn on the air compressor for the air-pump. Turn on the air pump. ☐

Ensure the air compressor and the pump are running. ☐

Ensure the water drop bucket valve into the bucket is in open position, ☐
but the valve out of the bucket is in shut position. Bucket should be empty.

Turn ON 3 phase power switch at the wall, labelled ‘Main wall plug’. ☐

Ensure the Nitrogen gas inline heaters remain turned off, until the gas is flowing. ☐

Turn ON the manual switch for the elbow heaters ☐
‘Elbow Heater Switch’, set at the marked set point.
Plug in at the supply, if required ‘Elbow Heater wall plug’.

Set and note set-points of temperature controllers.

Nitrogen Heater Controller	560°C
Inlet Plenum Controller	520°C
Pyrolyser Controller	520°C
Cyclone Controller 1	300°C
Cyclone Controller 2	300°C

Leave elements on to pre-heat system (2-3 hours). ☐

Note all the temperatures, ensure they are stable, ensure they are at the required set point. ☐

Turn ON power switches on control box. Controller displays should light up. ☐

Ensure the Nitrogen gas inline heaters remain turned off, until the gas is flowing. ☐

Ensure V03 is open. ☐

Ensure first Nitrogen Pressure regulator near V05 is set to 800 kPa. ☐

Ensure second Nitrogen Pressure regulator is set to 300 kPa. ☐

Use computer to set the gas flow controller is set to desired value: 65 l/min ☐

The Nitrogen flow through the hopper set to 4 l/min, V04 is open ☐

Set and note set point of Nitrogen heater 560°C ☐

Monitor temperatures to ensure system is stable. When you are satisfied the feed can be started. However, the temperature controllers must be quickly turned off while the three-phase motors are started to avoid any electrical feedback which could damage the heaters.

Turn OFF all the temperature controllers via switches at rear. ☐

Turn ON feed auger ‘Feed Auger Motor Main Switch’. ☐

Turn ON injection auger ‘Injection Auger Motor’. ☐

Turn ON all the temperature controllers via switches at rear. ☐

Set and record speed setting of feed auger controller 8.4 or other desired value ☐

Operation:

Monitor temperatures, pressure drop, feed level in hopper etc. ☐

Always turn OFF nitrogen heater before the nitrogen flow is stopped. ☐

If hopper needs to be refilled:

Turn OFF all the temperature controllers via switches at rear. ☐

Switch OFF feed augers 'Feed Auger Motor Main Switch'. ☐

Stop nitrogen flow using gas flow controller and close V04. ☐

Fill hopper through butterfly valve and close butterfly valve. ☐

Re-start nitrogen flow via gas flow controller and open V04. ☐

Switch ON feed augers 'Feed Auger Motor Main Switch' and 'Injection Auger Motor'. ☐

Turn ON all the temperature controllers via switches at rear. ☐

Shutdown:

Turn OFF main switch on control box ‘Control Box Main Switch’. ☐

Manually turn OFF ‘Elbow Heater Switch’ ☐

Unplug the elbow heaters ‘Elbow Heater wall plug’ ☐

Stop gas flow via gas flow controller, shut V04. ☐

Turn OFF nitrogen regulators and valve V05. ☐

Unplug the unit off the wall ’Main wall plug’, thus insuring it is isolated ☐

from the electricity prior product collection and unit clean up.

Let equipment cool to near room temp before ☐

attempting to open char, bio-oil, tar receivers.

p

Note any deviations from standard operating procedure:

……..

……..

……..

Further notes:

……..

……..

……..

If repairs required lock out the unit ☐

8.3 Summary of the Environmental Concerns:

Table 8.1: Source/ Pollutant/ Technology Table.

Source	Pollutant	Technology
Rotary Drier	Air, surface water	Reduce entrainment, set lower particle size limit
Fluidised Bed Reactor	Ground water, soil (sand from bed material)	Melted ash disposal/treatment Disposed of in an appropriate landfill site.
Char	Land/soil pollution	Use for agricaltural or fuel purposes.
Spray Nozzel Wet Scrubber	Waste Water with Organic compounds	Required to be disposed of accordingly to health and safety regulations of the region in environmentally healthy manner
Product transport	Wild-life, nearby residents	Reduce traffic volume where possible Restrict delivery hours, concentrate where pratical
Plant noise	Wild-life, nearby residents	Increase production throughput during the day and reduce at night

8.4 Operation Hazards Summary

Table 8.2: Hazard/Consequence/Safeguard/Action Table.

Hazard	Consequence	Safeguard	Action
High temperature of parts of equipment	May burn if touched	Hot parts are covered with insulation; Wear thermal insulating gloves if touching hot parts	Run cold water over burnt area for 10 minutes
Gas leak	Suffocation, CO poisoning	Low O_2 alarm, CO alarm	Emergency shutdown, evacuation of area, ventilation
'Bio-oil': skin contact, eye contact, ingestion	May cause skin irritation, burns, corneal injury	Wear gloves, lab coat & safety glasses	Follow procedure on MSDS
Char inhalation	May irritate mucous membranes and the respiratory tract	If dusting is a problem, a NIOSH/MSHA approved dust respirator must be worn.	Follow procedure on MSDS

Freshly produced Char may be subject to auto ignition and spontaneous heating, when exposed to air	Fire, dust explosion	Do not open char receiver until it has cooled to near room temperature	Follow procedure on MSDS
Leakage or water supply failure (no flow) in the cold line	Steam generation, condensables clogging gas discharge	Monitor operation, bubbler on gas outlet to indicate flow	Turn feed OFF, turn elements OFF, restore cooling water supply
Nitrogen- low/no flow	No fluidisation, build-up of feed material in reactor	Bubbler on gas outlet to indicate flow	Initiate shutdown

8.5 CRL Solids Analysis Report.

CRL Energy Ltd

CRL INTERNAL REPORT OF ANALYSIS

Description: Solid and liquid biomass samples received from Olga Kolokolova for analysis.

Attention: Olga Kolokolava

Customer Reference:			11/25/11PS5 40/SLD	11/30/11PS5 40/SLD	11/08/12PS5 40/SLD	Untreated sawdust	Untreated bark	11/25/11PS5 40/LQD	11/30/11PS5 40/LQD	11/02/12PS5 40/LQD	11/02/12PS5 40/ORG	11/08/12PS5 40/LQD	11/08/12PS5 40/ORG
CRL Energy Ltd Reference:			98/832	98/833	98/835	98/836	98/837	98/838	98/839	98/840	98/841	98/842	98/842B
Analysis - As Received Basis													
Moisture	(ISO 5068)	%	1.9	1.7	1.1	9.5	26.5	Liquid	Liquid	Liquid	Liquid	Liquid	Liquid
Analysis - Dry Basis ('as received' basis for liquids)													
Ash	(ASTM D 1102)	%	29.2	11.2	4.8	0.4	3.0						
Volatile Matter	(ISO 562)	%	30.2	37.0	52.2	85.0	63.0						
Fixed Carbon	(by difference)	%	40.7	51.8	43.1	14.6	34.0						
Gross Calorific Value	(ISO 1928)	MJ/kg	20.45	25.85	25.19	20.23	21.33	10.95	10.61	11.41	21.95	9.30	20.83
Total Sulphur	(ASTM D4239)	%			<0.01							<0.01	<0.01
Total Carbon	(ISO / TN 12902)	%			64.1								
Total Hydrogen	(ISO / TN 12902)	%			4.97								
Total Nitrogen	(ISO / TN 12902)	%			0.15								
Total Oxygen	(by difference)	%			26.0								

Date of Issue: 16/01/12

Ben Rumsey
Research Officer

THIS REPORT MUST NOT BE QUOTED EXCEPT IN FULL

8.6 Material Safety Data Sheet for pyrolysis bio-oil

CIRAD	Material Safety Data Sheet		
	Date of issue: May 31, 2006	MSDS Creation Date according to regulation 91/155/EU: May 31, 2006	1/7
	UPR 42 Biomasse - Energie CIRAD - FORET		

SECTION 1: PRODUCT NAME AND COMPANY IDENTIFICATION

Common name: Bio-oil
Trade name: Wood, Hydropyrolyzed
Other names: pyrolysis oil, bio-crude-oil, bio-fuel-oil, wood liquids.
Packaging sizes: 25 kg drums, 200 kg drums and 1 tone containers.
Use: Value-added liquid fuel for heat electricity, transport fuels, chemicals (renewable energy / CO2 neutral)
Manufacturer: Joël BLIN - CIRAD-Forêt UPR Biomasse Energie / TA 10/16 - 73, Rue Jean-François Breton - 34398 MONTPELLIER, CEDEX 5
Supplier: Contact the distributor in your country.
Emergency: (33) 04 67 61 65 21

SECTION 2: COMPOSITION, INFORMATION ON INGREDIENTS

Technological processes used in production of the substance: Fast pyrolysis / Fluidized bed reactor / Circulating fluidized bed / Ablative Pyrolysis reactor / Vacuum pyrolysis.

Official name	% w/w	CAS#	EINECS#	EU Symbol/Risk phrases*
Wood, hydropyrolyzed	100	94114-43-9	302-678-6	C; Xi; R34-43

*Text of Symbol and R-phrases: see section 15

List of some chemicals that have been identified in the literature in biomass derived pyrolysis liquids. The yield given is the largest reported yield on a wet liquid basis. Only those chemicals that have been repeatedly reported are included.
Chemicals *in italic* are classified as hazardous substances; some of them have an occupational threshold value (see section 8).
Concentrations lower than 1% is neglected and chemicals are listed without comments.

Acids : *Formic acid < 10% / Acetic acid 10%*
Esters : *Methyl formate* < 1.9%
Alcohols: *Methanol < 1.4% / Ethanol < 3.6% / Ethylene glycol < 1.1%*
Aldehydes : *Formaldehyde < 2.4% / Acetaldehyde < 8.5% / Glyoxal / Acroleine / Methylglyoxal < 4%*
Ketones : Acetone < 2% / 2-Butanone
Phenols : *Phenol < 2.1%* / Methyl phenols / 2-Ethylphenol / *Hydroquinone* / Catechol < 5%
Guaiacols : 2-Methoxyphenol / 4-Methylguaiacol
Syringols : 2,6-Dimethoxyphenol
Sugars : Fructose / 1,6-anhydroglucofuranose
Furans : *Fururyl alcohol* < 5.2% / *2-Furanone*
Misc. Oxygenates: Hydroxyacetaldehyde < 15.4% / Hydroxyacetone / Acetal
Alkenes : Dimethylcyclopentene
***Aromatics** : ppm range
Nitrogen compounds: none
Soluble Lignin

*As expected some polyaromatic hydrocarbons that represent a potential health and safety concern, have also been detected in some hydropyrolysed wood samples.

For example, two carcinogenic hydrocarbons have been identified by GC/MS:
Benz(a)anthracen (CAS# 56-55-3) : 0.25 ppm (range 0 to 1.68 ppm for 19 different samples)
Benz(a)pyrene (CAS# 50-32-8) : 0.38 ppm (range 0.03 to 1.88 ppm for 19 different samples)

These values are fare below the official limit that requires an H&S labeling.

CIRAD	Material Safety Data Sheet		
	Date of issue: May 31, 2006	MSDS Creation Date according to regulation 91/155/EU: May 31, 2006	2/7
	UPR 42 Biomasse - Energie CIRAD - FORET		

SECTION 3: HAZARD IDENTIFICATION

Fire and explosion hazard:

- Flammable liquid at extremely high temperatures.
- Slow evaporation rate.
- Not an explosive when subjected to heat or shock.

Health hazard:

Primary routes of exposure: skin contact, eye contact, ingestion.

- **Eyes:** Corrosive, causes burns, severe corneal injury.
- **Skin:** Corrosive, causes burns or strong irritation.
- **Ingestion:** Causes burns to mouth, oesophagus and gastrointestinal tract if swallowed.
- **Inhalation:** Causes irritation to the respiratory tract.

SECTION 4: FIRST AID MEASURES

Eyes:

Immediately flush eyes with plenty of tepid water for at least 15 minutes, occasionally lifting the upper and lower lids.
Any contact lens must be removed. Get medical attention even if the injury appears to be mild.

Skin contact:

Remove all contaminated clothing immediately and wash affected skin area with soap and water.

Ingestion:

First immediately rinse your mouth several times with water. Should the product be swallowed administer 2-3 glasses of water for dilution.
Do not induce vomiting. Stay calm and seek medical advice.

Inhalation:

If eye, nose or throat irritation from dust or mists develops, move to fresh air until symptoms disappear.

Generalities:

Give nothing by mouth to an unconscious person.
If breathing is irregular or has stopped, give artificial respiration.
In all cases of doubt or if symptoms persists, seek medical attention and show this sheet to the doctor.

Antidote:

No specific antidote exists. The product is acidic (pH 2 -3) and is partly soluble in water. Treat symptomatically.

SECTION 5: FIRE FIGHTING MEASURES

Extinguishing media:

Water, carbon dioxide, foam, dry powder.
Use water spray to cool product containers and tanks near the fire.

Special exposure hazards in a fire:

Do not inhale smoke from the fire. Wear self-contained breathing apparatus and full protective clothing.
Explosion risk due to pressure increase into containers placed near a fire.
The heat may melt the containers allowing the content to mix with extinguishing water.

SECTION 6: ACCIDENTAL RELEASE MEASURES

Personal precautions: evacuate people upwind from the spill area.
Environmental precautions: do not allow the product to enter drains or surface water.

Methods for cleaning up:
To handle spills, the following preliminary advices are given.

- **Small quantities (< 1000 ml)**
  The suggested actions for such spillage are:
  Wear rubber gloves and suitable eye and face protection. If there is an inadequate ventilation, a suitable organic vapours filter mask or NIOSH approved respirator must be worn. Cover contaminated area with an inert adsorbent e.g. vermiculite, sawdust. Take up the used adsorbent and place it in a container for disposal or incineration.

- **Large quantities (> 1000 ml)**
  For spillage of significant quantities first evacuate rapidly workers present in the area and then take the same actions as described above.

SECTION 7: HANDLING AND STORAGE

Handling
Combustible.
Keep away from sources of ignition. Take precautionary measures (e.g. earthing) against electrostatic discharges.
When transferring the product and opening containers, avoid inhalation of vapours or gases. Ensure good ventilation when handling the product.
During tank cleaning operations follow special instructions provided by the manufacturer.

Storage
The product must be stored in containers suitable for combustible liquids and resistant to acids. Keep containers tightly closed at temperatures below 25°C in a well ventilated area. The product contains compounds that may either consume oxygen creating an under-pressure in the container; or may emit vapours that create an overpressure in the container.

Recommended storage materials: acid-proof steel, plastics (PETE, PP, HDPE). Filled containers may be gently heated to not more than 50°C before use for transfer of contents.

SECTION 8: EXPOSURE CONTROLS, PERSONAL PROTECTION

Engineering controls

Provide local and general exhaust ventilation to effectively remove and prevent vapors and mists generated from the handling of this product. Ensure that eyewash station and safety showers are proximal to the workplace location.

Personal protective equipment:

Eyes/Face
Wear safety glasses, chemical goggles if splashing is possible, or to prevent eye irritation from heated vapours or mists.

Skin/Hands/Feet
Wear chemically resistant gloves (nitrile gloves or thermally insulated gloves when handling hot products) and footwear with good traction to avoid slipping.
If splashing or contact with hot material is possible, consider the need for use of an impervious overcoat.
Remove contaminated clothing and clean before reuse.

Fire resistant or natural fibre clothing is recommended.

Respiratory
If ventilation is not sufficient to effectively prevent aerosols or vapours, or if airborne concentrations are above the applicable exposure limits, use a NIOSH approved organic vapour cartridge respirator. Air supplied breathing apparatus must be used when airborne concentration may exceed the limits of the air purifying respirator used.

General
Personal protective equipment (PPE) should not be considered a long-term solution to exposure control. Consult a competent industrial hygiene resource, the PPE manufacturer's recommendation, and/or applicable regulations to determine hazard potential and ensure adequate protection.
Threshold Limit Values (MAK-values) of some chemicals listed in section 1.

Chemical name	CAS#	MAK-values in ppm or ml/m3
Acetaldehyde	75-07-0	50.0
Acetone	67-64-1	500.0
Formic acid	64-18-6	5.0
Acetic acid	64-19-7	10.0
Methanol	67-56-1	200.0
Formaldehyde	50-00-0	0.3
Furfuryl alcohol	98-00-0	10.0

SECTION 9: PHYSICAL AND CHEMICAL PROPERTIES

The physical and chemical properties of the product may vary according to the used raw material, the manufacturing technology and the delivered batch.
The data below is representative of a typical bio-oil made from wood.

Colour	Dark brown viscous liquid
Odour	Strong characteristic, smoky
Density	Close to 1.2 kg/l
Water content	25 %
Water insoluble	20 % (pyrolytic lignin)
Log Pow	No data available
Viscosity-kinematics, cSt	225 at 20°C; 30 at 50°C
Surface tension, mN/m	29.2
pH	2.5
Flash point	Data is unreliable ranging from 40°C to over 110°C
Initial boiling point	< 100°C (beginning of the distillation)
Explosive properties	Not heat or shock explosive
Vapour pressure	Approximately 5 kPa at 38°C
Pour point	-20°C
Auto ignition temperature	About 500°C
Miscible with:	Acetone, methanol, ethanol
Not miscible with:	Hydrocarbons; water above 50% weight concentration

SECTION 10: STABILITY AND REACTIVITY

Chemical stability: stable under normal conditions of use and storage.

Chemical stability: conditions to avoid
Heating above 100°C: polymerization may occur with release of harmful or toxic fumes (carbon monoxide, carbon dioxide, formic acid, formaldehyde, methanol, acetaldehyde, acroleine and other organic compounds).

Corrosivity: reacts with mild steel and impure copper due to high acidity.

SECTION 11: TOXICOLOGICAL INFORMATION

The test results given below are based on one selected representative sample.

This sample has been obtained under well known operating conditions: temperature of 500°C; fluidized bed system; softwood.

- LD50 (oral, rat): >2000 mg/kg/body weight
- 7-days oral, gavage, rats: At 150 mg/kg/body weight, there were no clinical signs of toxicity, a slight reduction in the body weight gain of the females and no effect on food consumption. No macroscopic abnormalities were observed.
- Acute dermal toxicity: Test not performed as the product is corrosive.
- Dermal Irritation (rabbit): Corrosive
- Eye Irritation (not done for ethical reason): Corrosive
- Inhalation: Avoid inhalation as the product may contain hazardous substances depending on the manufacture process and temperature.
- Skin sensitization (LLNA, mice): Moderate sensitizer
- Mutagenic tests:
  1. *Ames test (Salmonella typhimurium):* Positive, the product is mutagenic in this test.
  2. *Bone marrow micronucleus test by oral route gavage in mice*: Negative
  3. *Micronucleus test in L5178 TK mouse lymphoma cells*: Light mutagenic activity
- Teratogenicity: No known or listed teratogenic effects.
- Reproductive effects: No information available.
- Neurotoxicity: No information available.
- The product contains traces of substances classified as carcinogenic (e.g. formaldehyde, acetaldehyde, and furfural).

SECTION 12: ECOLOGICAL INFORMATION

- Biodegradation (Modified Sturm Test): The product biodegrades rapidly at percentages between 32 and 50%. Low biodegradation under anaerobic conditions.
- Algal growth test: At low concentration the product has a small fertilizing effect. At higher concentration, algal growth is slightly inhibited. From 0 to 72 hours the NOEL was > 100 mg/l.
- EC50 (Acute toxicity to Daphnia Magna): > 100 mg/l

The potential to contribute to eutrophisation should be small due to the very low nitrogen, and very low minerals content of the product.
The product is not likely to bioaccumulation as most of components are highly soluble in water and/or biodegrade rapidly.

Waste treatment organisms: Large quantities may increase the pH value.

CIRAD	Material Safety Data Sheet		
	Date of issue: May 31, 2006	MSDS Creation Date according to regulation 91/155/EU: May 31, 2006	6/7
	UPR 42 Biomasse - Energie CIRAD - FORET		

SECTION 13: DISPOSAL CONSIDERATIONS

Product waste is classified as **hazardous waste.**

European waste catalogue number: 13 07 03* Other Fuels (including mixture)
Do not allow this product to reach drains or ground water.
Follow national and municipal regulations obtained from local authorities.

SECTION 14: TRANSPORT INFORMATION

The information given below is provided to assist in documentation. See also *Section 16, 1)*

ADR/RID:	UN Number: Labels: Proper shipping name: Risk Code Packaging group:	UN 2924 6 + 8 + 11 FLAMMABLE LIQUID, CORROSIVE, N.O.S. Wood distillate 30 III
IMDG:	UN Number: Labels: Proper shipping name: EmS: Packaging group:	UN 2924 6 + 8 + 11 FLAMMABLE LIQUID, CORROSIVE, N.O.S Wood distillate 3-07 III
IATA:	UN Number: Labels: Proper shipping name: Class: Packaging group:	UN 2924 6 + 8 + 11 FLAMMABLE LIQUID, CORROSIVE, N.O.S. Wood distillate 3 III

SECTION 15: REGULATORY INFORMATION

European labeling: Wood, hydropyrolysed.

Symbol C: Corrosive

R 34: Causes burns.
R 43: May cause sensitization by skin contact.
S 26: In case of contact with eyes, rinse immediately with plenty of water and seek medical advice.
S 23: Do not breathes vapours.
S 37/39: Wear suitable gloves and eye protection.
S 45: In case of accident or if you feel unwell, seek medical advice immediately and show the product label or MSDS.

CIRAD	Material Safety Data Sheet		
	Date of issue: May 31, 2006	MSDS Creation Date according to regulation 91/155/EU: May 31, 2006	7/7
	UPR 42 Biomasse - Energie CIRAD - FORET		

SECTION 16: OTHER INFORMATION

1) Transport Report
Transport, storage and handling of biomass derived fast pyrolysis liquid. Compliance with all international modes of transport.
EU Contract Nr NNE5 - 2001 - 00744 - Biotox
Web site: www.pyne.co.uk

2) Technical Report
A guide to physical property characterization of biomass derived fast pyrolysis liquids.
VTT Publications, Author: Anja Oasmaa & Cordner Peacocke.
Web site: www.vtt.fi

3) Technical Report
An assessment of bio-oil toxicity for safe handling and transportation.
Project Co-ordinator: Centre de Coopération Internationale en Recherche Agronomique pour le Développement (Cirad)
Web site:

- europa.eu.int/comm./energy/res/sector/doc/bioenergy/biotox_publishable_repport.pdf
- www.pyne.co.uk

The information contained herein is accurate to the best of our knowledge. We do not suggest or guarantee that any hazards listed herein are the only ones that exist.

CIRAD-Forêt, Aston University and the Institute for Wood Chemistry make no warranty of any kind, express or implied, concerning the safe use of this material in your process or in combination with other substances.

Users must meet all applicable safety and health standards to ensure proper use and disposal of these materials.

8.7 TEMPCO In Line Heater Manual (Page 1)

Industrial Process

Air Process Heaters

LDA In-Line Forced Air Process Heaters

Typical Applications of LDA Series In-Line Air or Gas Heaters

- *Laminating*
- *Drying*
- *Baking*
- *Shrink Fitting*
- *Plastic Welding*
- *Soldering*
- *Preheating and Metalworking*
- *Packaging*

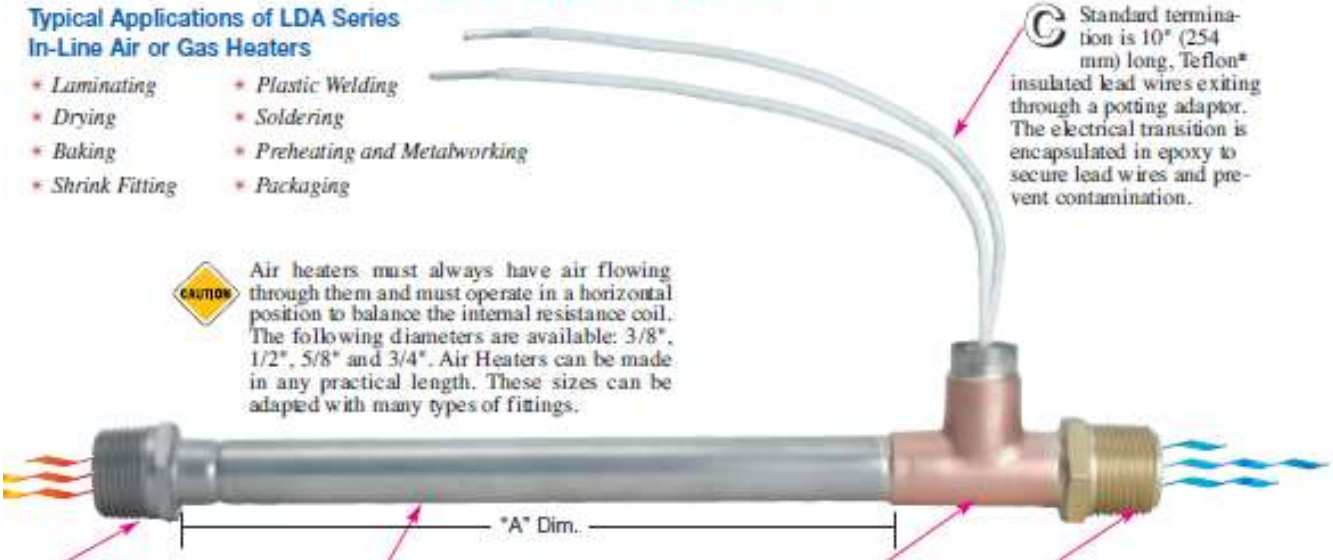

C Standard termination is 10" (254 mm) long, Teflon® insulated lead wires exiting through a potting adaptor. The electrical transition is encapsulated in epoxy to secure lead wires and prevent contamination.

CAUTION Air heaters must always have air flowing through them and must operate in a horizontal position to balance the internal resistance coil. The following diameters are available: 3/8", 1/2", 5/8" and 3/4". Air Heaters can be made in any practical length. These sizes can be adapted with many types of fittings.

A Stainless Steel NPT fitting is heli-arc welded at the air outlet.

B Alloy 304 stainless steel tubing is used to provide high temperature strength and resistance to oxidation up to outlet temperature of 1000°F (538°C). Inlet air or gas temperature up to 250°F (121°C).

D Copper "T" fitting.

E NPT Brass fitting is silver-brazed at air inlet.

LDA In-Line Air Process Heater Specifications

Heater Diameter (in)	Maximum Amperage	Cross Sectional Flow Area (in²)	Maximum CFM (ft³)	Max. Wattage/Linear Inch Of Heated Length
3/8	6	.03	8	200
1/2	10	.04	10	250
5/8	15	.070	15	375
3/4	20	.120	20	500

Note: LDA In-Line Air Process Heaters can be made in any practical length within the standard diameters.

Heater Selection

To ensure maximum heater life, heater wattage must be calculated so that it is suitable for the desired air flow. To calculate wattage, determine the air flow and temperature rise required. The following relationship can be used to determine the wattage.

$$\text{Wattage} = \frac{\text{CFM} \times \text{Temperature rise (°F)}}{3}$$

Table 1 Shows the relationship between cubic feet per minute versus maximum watts per linear inch of heated length on different heater diameters.

Maximum Watts per Linear Inch of Heated Length				
CFM	3/8" Dia.	1/2" Dia.	5/8" Dia.	3/4" Dia.
2	80	80	100	120
4	100	100	100	120
6	150	150	150	150
8	200	200	200	200
10	—	250	250	250
15	—	—	375	375
20	—	—	—	500

Note: It is recommended that the wattage not exceed the maximum watts per linear inch indicated in the above reference table.

8.8 Hazards

8.8.1 GENERAL HAZARDS

1. Hot surfaces in most of the major parts and equipment of the pyrolysis unit during operation.
2. Noise in the work area during operation.
3. The work area can be dangerous to unauthorized and not properly trained personnel.
4. Possible gas leak may also be a problem in the work area.
5. Water and other liquids and electrical equipment in close proximity with the pyrolysis unit and its equipment/parts can also pose hazards during operation

8.8.2 GENERAL AREAS FOR CONSIDERATION

1. Ensure at all times that no unauthorised personnel are present during runs. Ensure working area is clear.
2. Work personnel should always wear safety glasses and lab coat/overalls.
3. Ear protection should be worn if necessary.
4. Ensure no leakage of water and other liquids onto electrical equipment.
5. Wires and other materials should not touch the hot surfaces of the pyrolysis unit. Switch off equipment at the wall if it becomes dangerous.

8.8.3 HAZARDS ON SYSTEMS/EQUIPMENT/PARTS

Pyrolysis reactor

1. Possibility of gas leakages from joints/flanges/gaskets. – Check seals/gaskets before operation.
2. Ensure gas detector is turned on and operational while the unit is running.

Hopper

1. Gas leakages from the top: – Ensure that the top butterfly valve is closed before operation.
2. Rotating parts on motors and augers present a possible entanglement hazard. Ensure cover is over injection motor and auger while the unit is running.

Condensers

1. Blockage of the condensers with bio-oil/tar. Monitor the bubbler to ensure gas is flowing through the unit.

8.8.4 Specific hazards and hazardous situations:

Hazard	Consequence	Safeguard	Action
High temperature of parts of equipment	May burn if touched	Hot parts are covered with insulation; Wear thermal insulating gloves if touching hot parts	Run cold water over burnt area for 10 minutes
Gas leak	Suffocation, CO poisoning	Low O_2 alarm, CO alarm	Emergency shut-down, evacuation of area, ventilation
'Bio-oil': skin contact, eye contact, ingestion	May cause skin irritation, burns, corneal injury	Wear gloves, lab coat & safety glasses	Follow procedure on MSDS
Char inhalation	May irritate mucous membranes and the respiratory tract	If dusting is a problem, a NIOSH/MSHA approved dust respirator must be worn.	Follow procedure on MSDS
Freshly produced Char may be subject to auto ignition and spontaneous heating, when exposed to air	Fire, dust explosion	Do not open char receiver until it has cooled to near room temperature	Follow procedure on MSDS
Leakage or water supply failure (no flow) in the cold line	Steam generation, condensables clogging gas discharge	Monitor operation, bubbler on gas outlet to indicate flow	Turn feed OFF, turn elements OFF, restore cooling water supply
Nitrogen- low/no flow	No fluidisation, build-up of feed material in reactor	Bubbler on gas outlet to indicate flow	Initiate shutdown

8.8.5 Emergency Shutdown Procedure

1. All electrical apparatus can all be switched off from the main power switch on the unit, or the three-phase switch on the wall. Shutting down the equipment during operation presents no hazard.
2. Stop nitrogen flow by closing main valve.

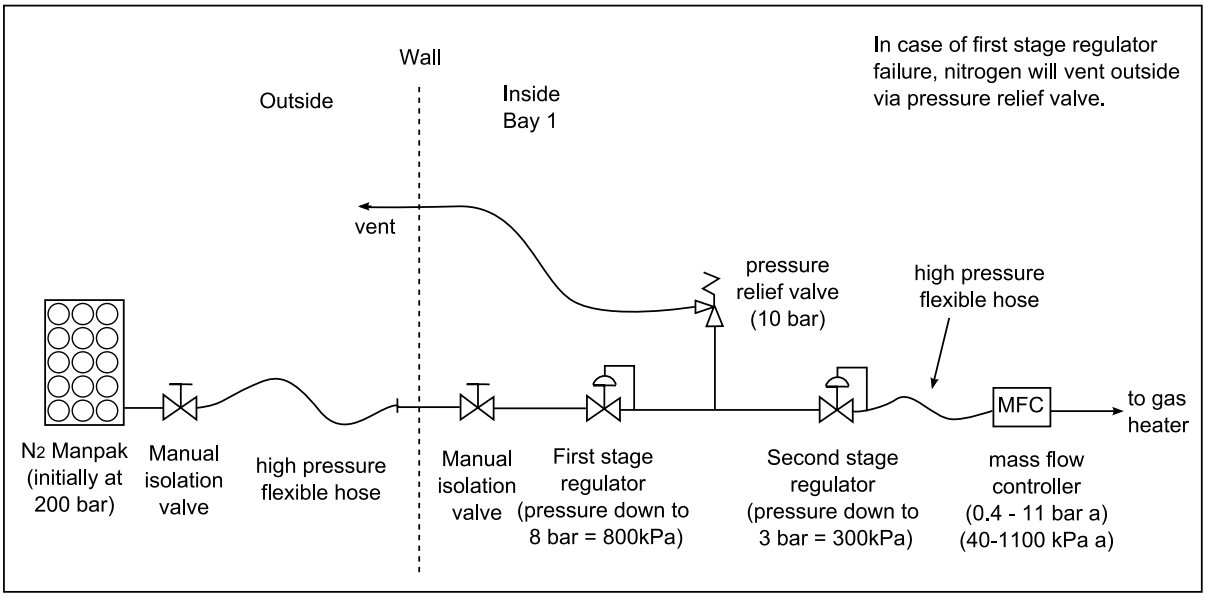

8.9 PFDs and P&IDs

Following section presents the process flow diagrams of the proposed plant.

8.9.1 Process Flow Diagrams of the Proposed Plant (PFDs)

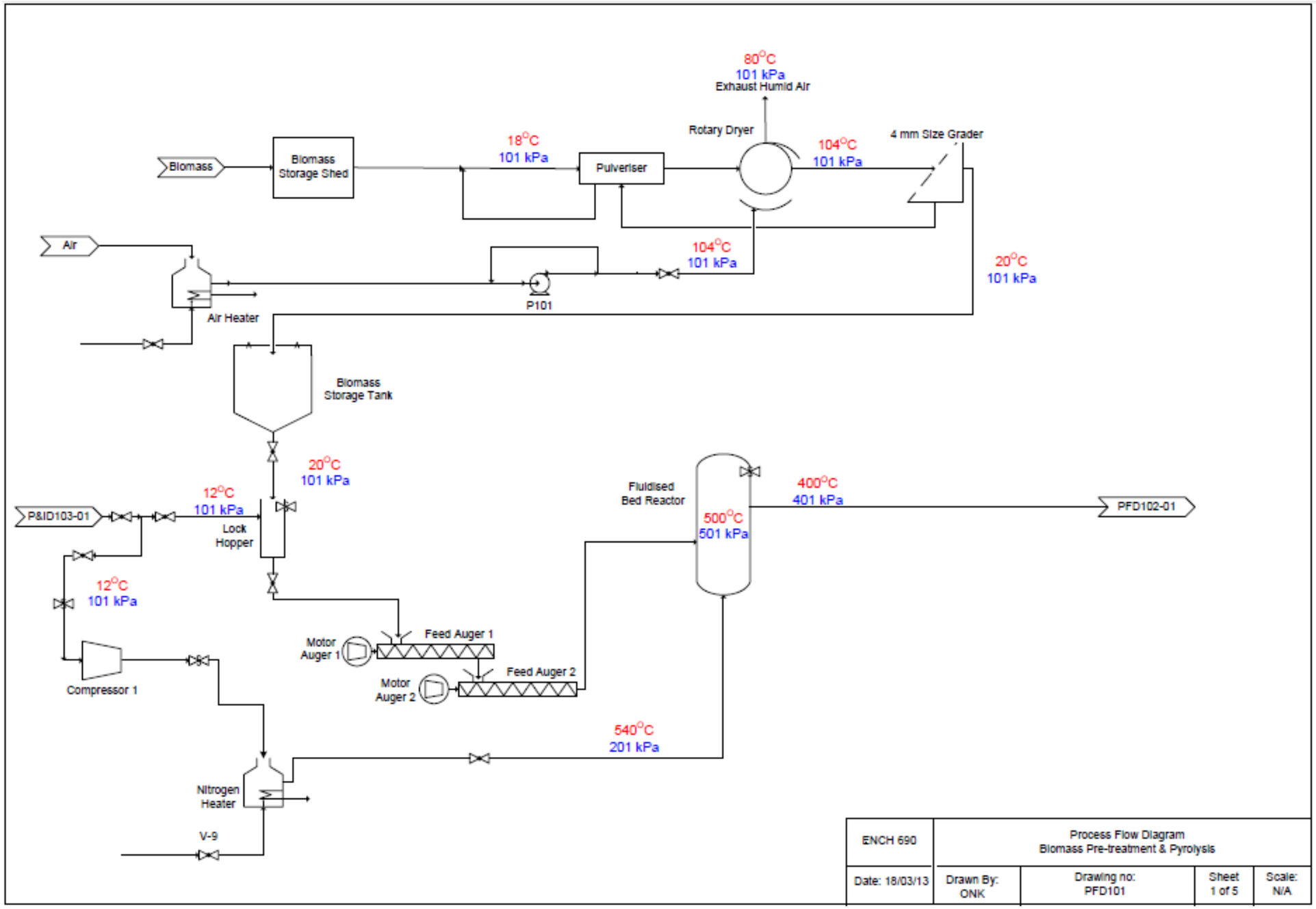

Figure 8.9.1: PFD101 - Biomass Pre-treatment & Pyrolysis.

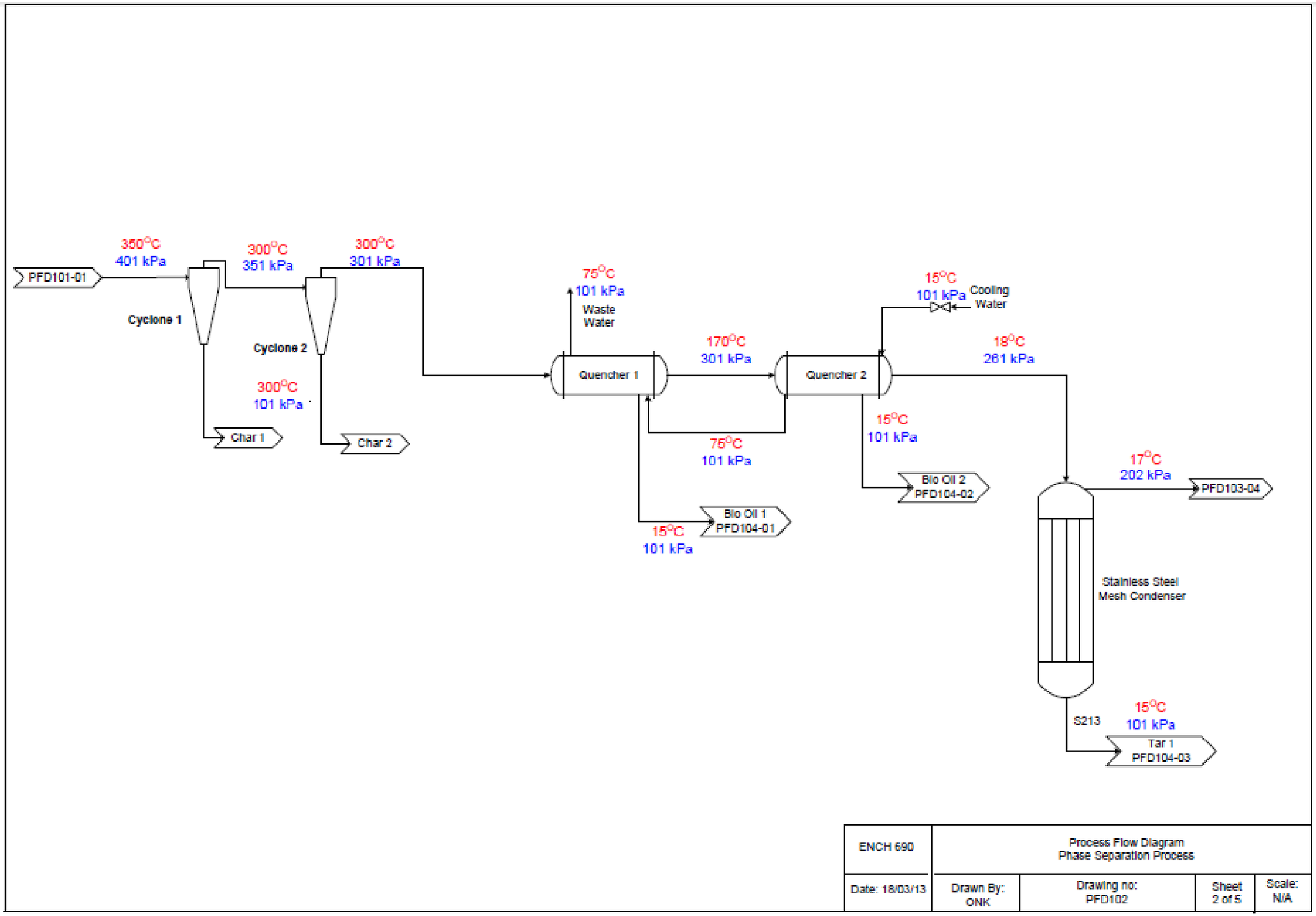

Figure 8.9.2: PFD102 - Phase Separation Process.

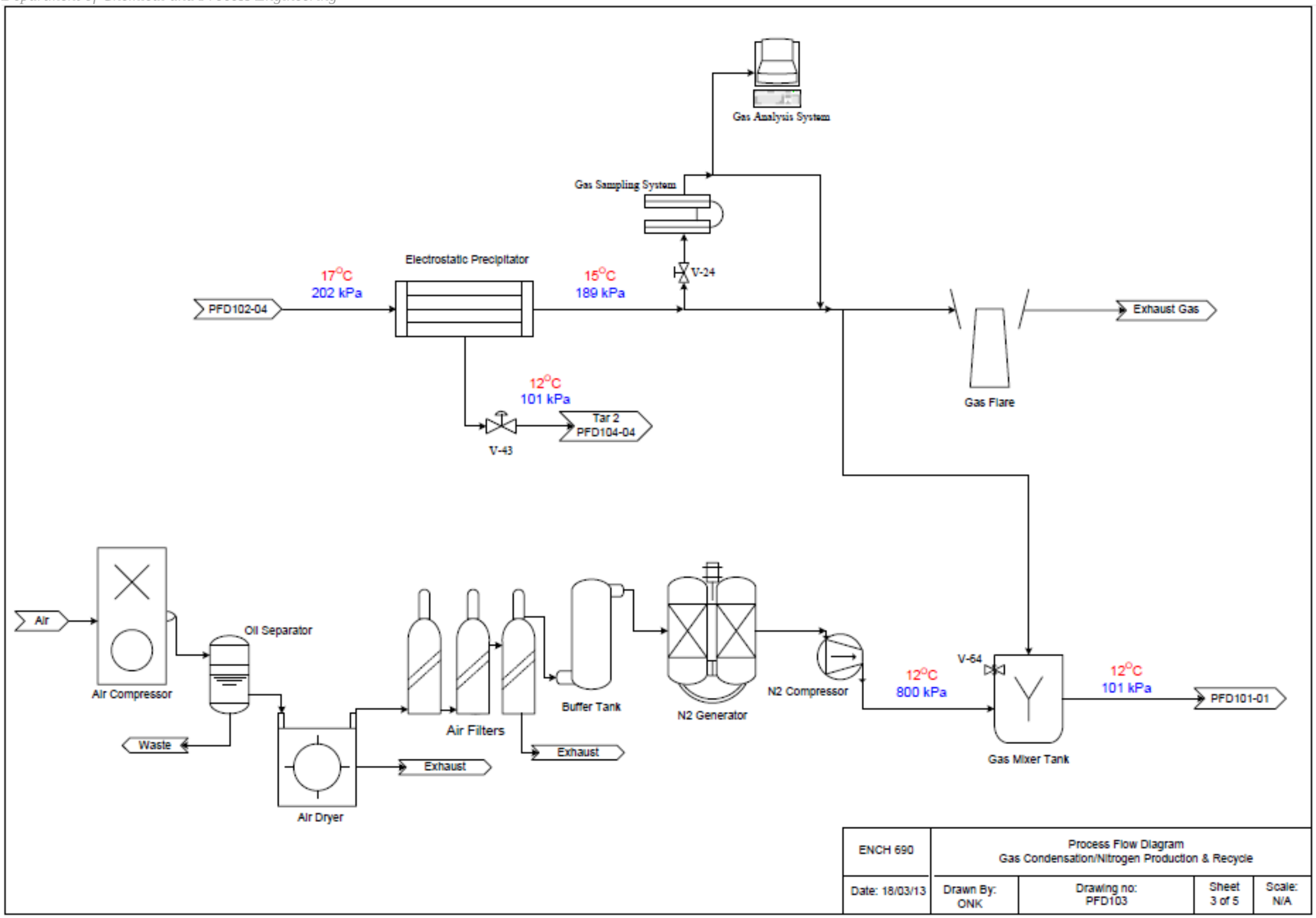

Figure 8.9.3: PFD103 - Gas Condensation/Nitrogen Production & Recycle.

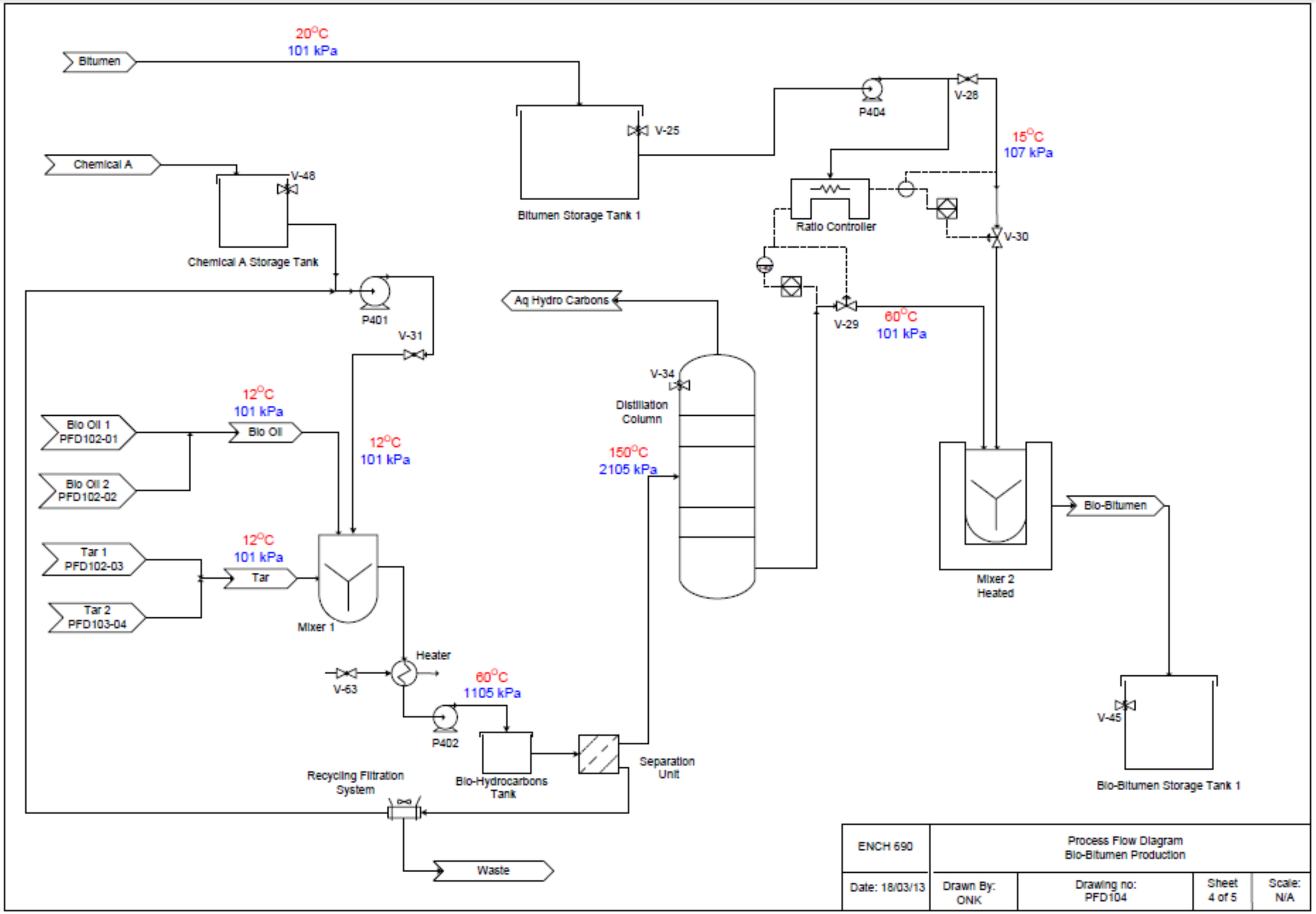

Figure 8.9.4: PFD104 - Bio-Bitumen Production.

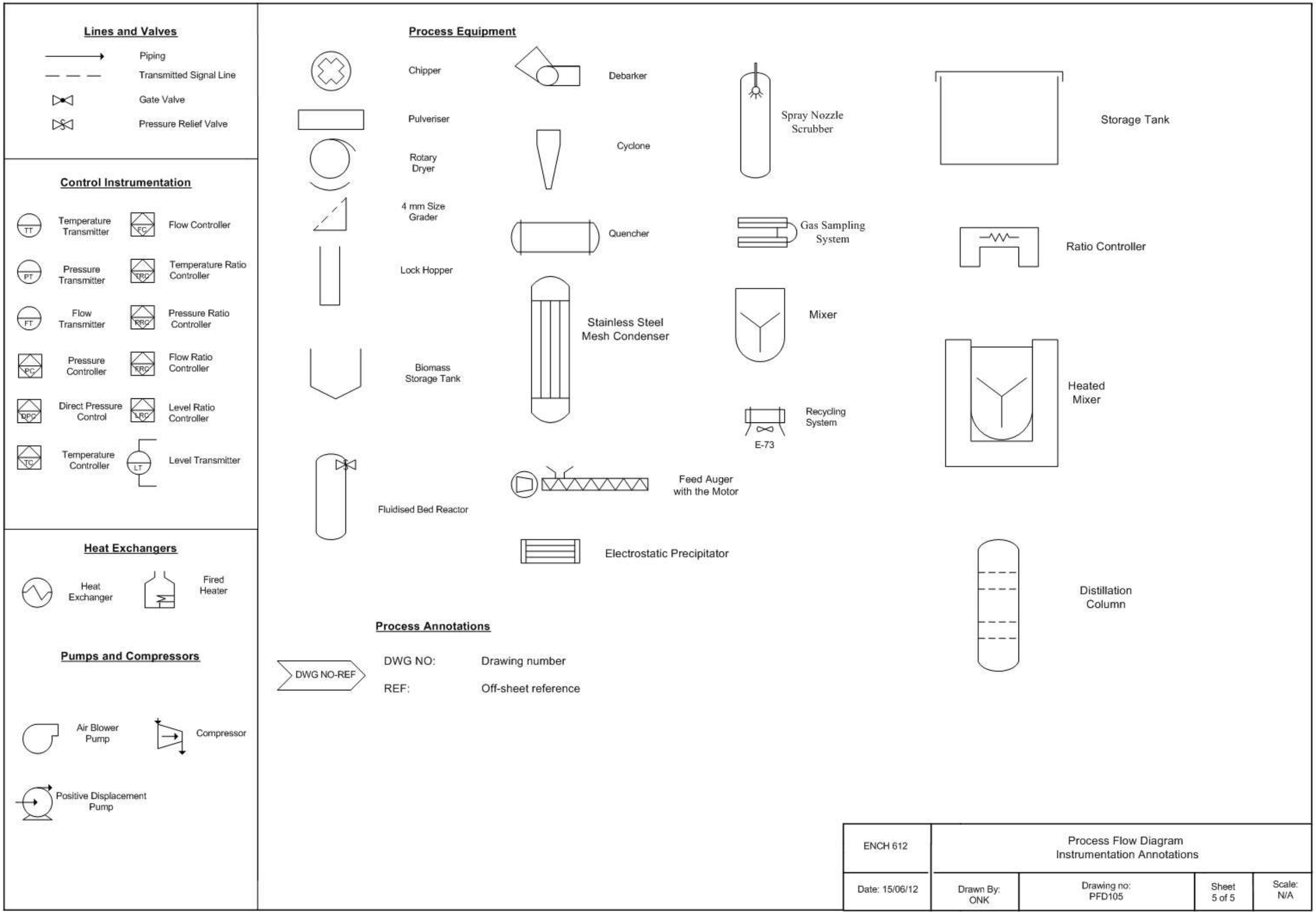

Figure 8.9.5: PFD105 - Biomass to Bio-Bitumen Production Instrumentation Annotations.

8.9.2 Piping and Instrumentation Diagrams the Proposed Plant

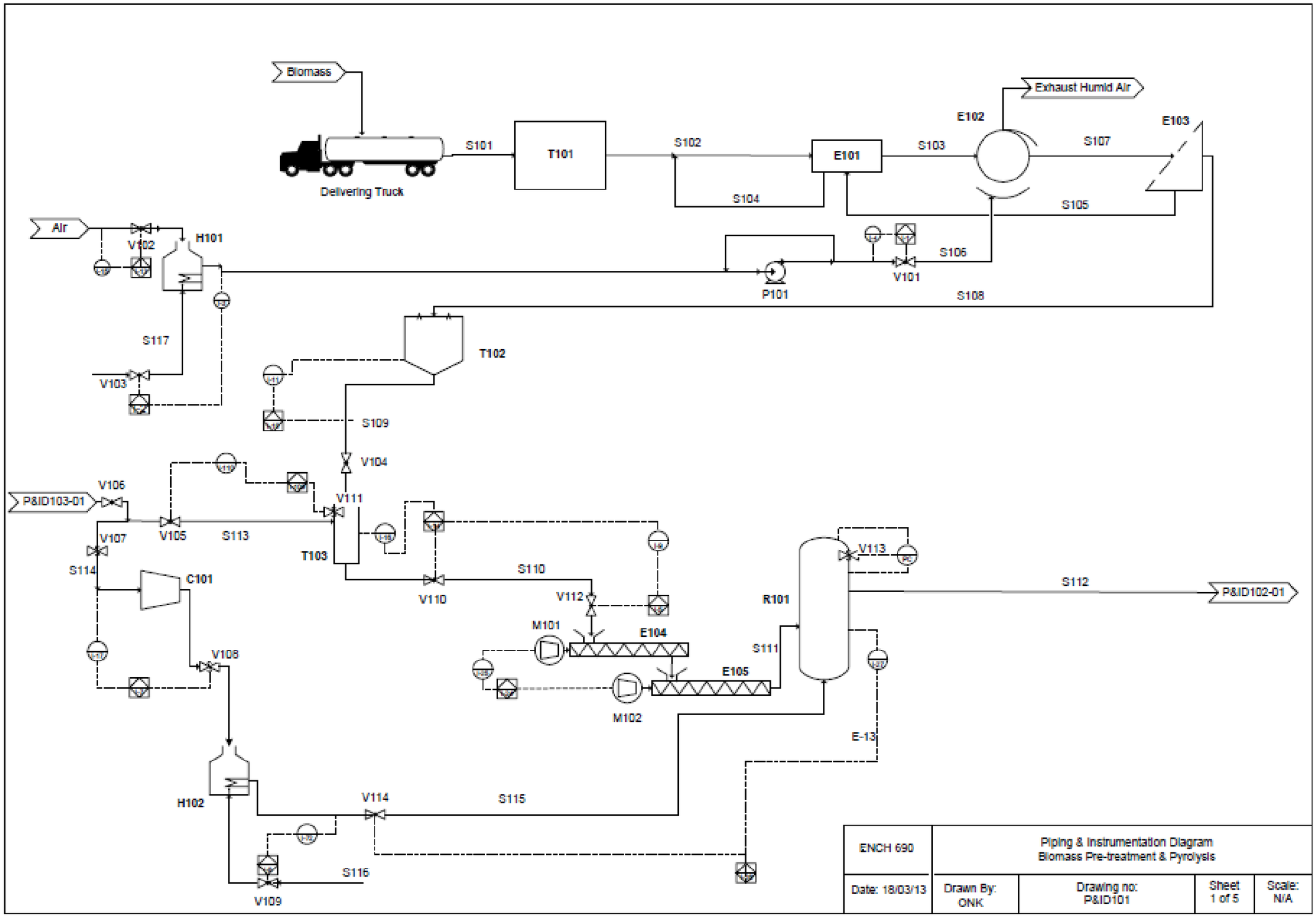

Figure 8.9.6: P&ID101 - Biomass Pre-treatment & Pyrolysis.

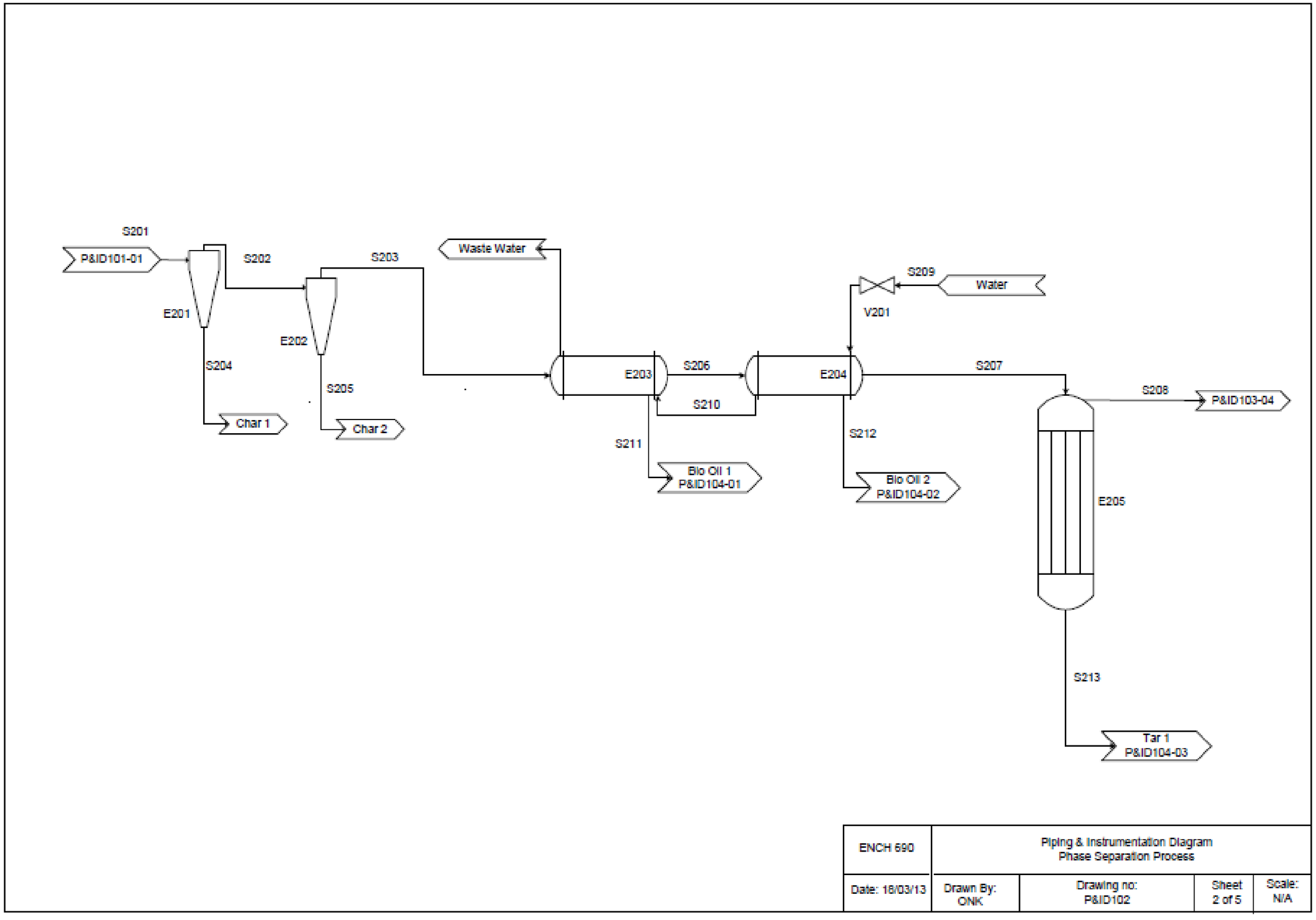

Figure 8.9.7: P&ID102 - Phase Separation Process.

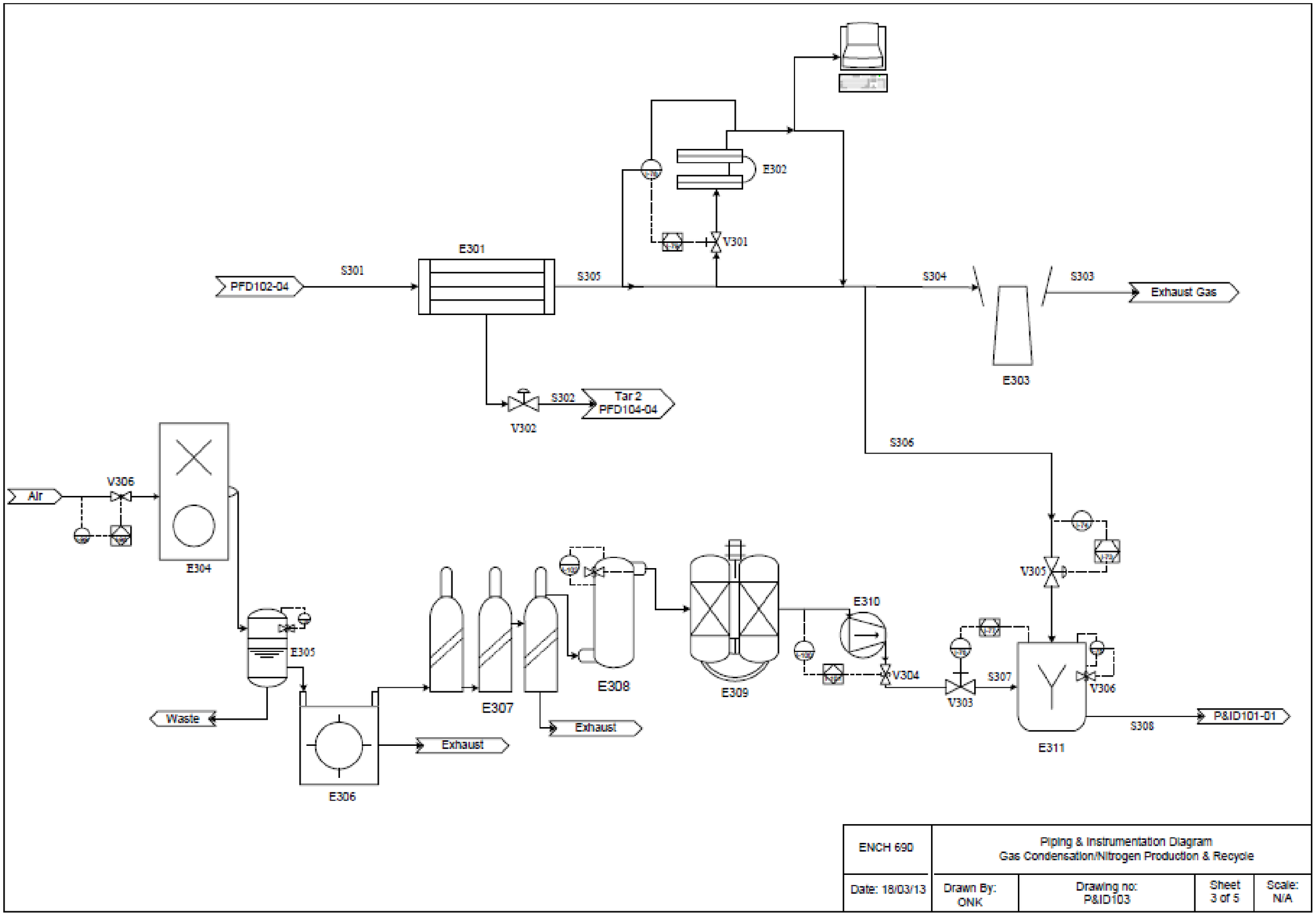

Figure 8.9.8: P&ID103 - Gas Condensation/Nitrogen Production & Recycle.

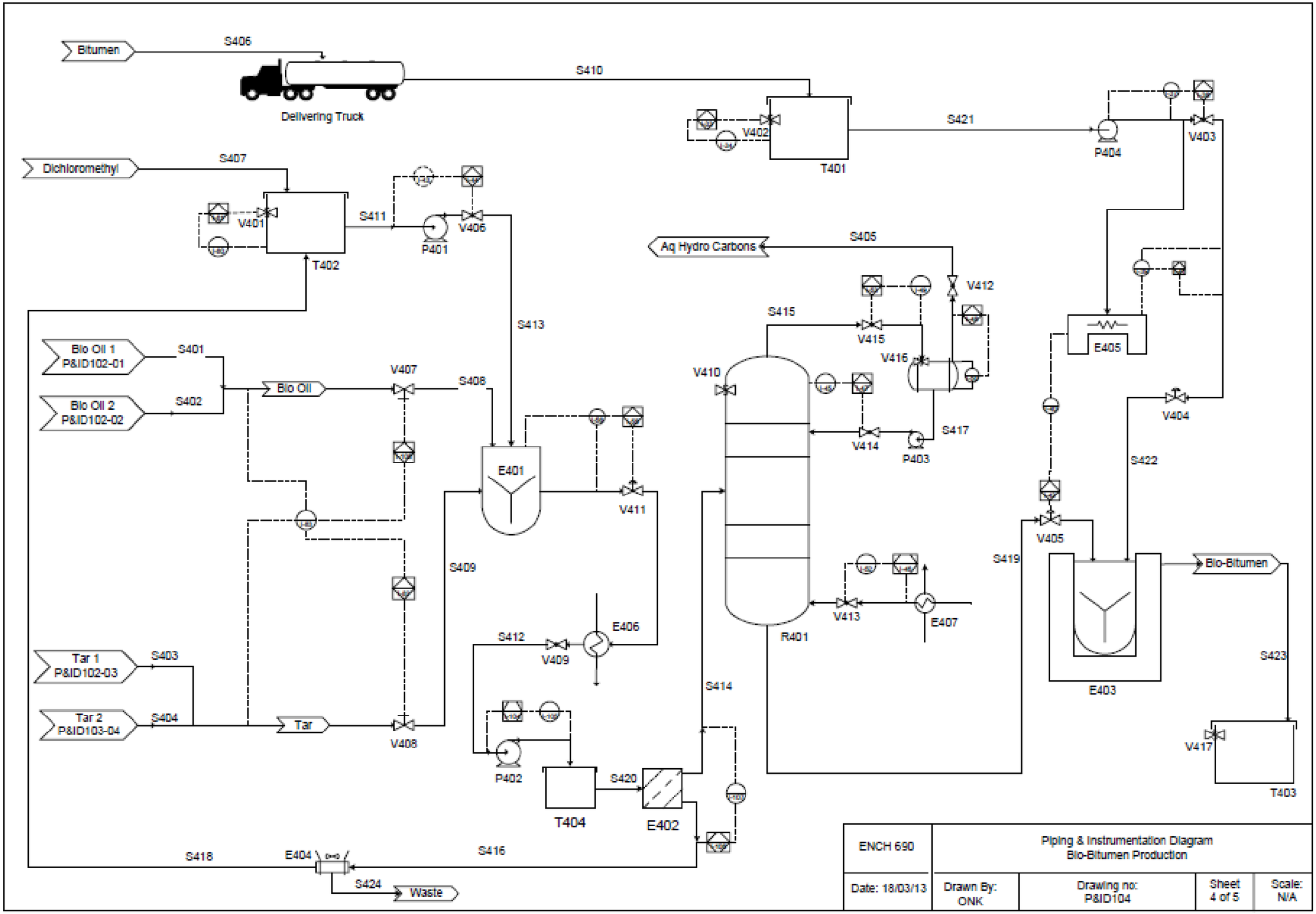

Figure 8.9.9: P&ID104 - Bio-Bitumen Production.

8.10 Stream Tables for the proposed upgrade

COMPONENT	UNITS	STREAM																	
		S101	S102	S103	S104	S105	S106	S107	S108	S109	S110	S111	S112	S113	S114	S115	S116	S117	S118
Total Flow	kg/hr	530.9	530.9	515.5	15.5	14.1	92.8	468.6	454.5	454.5	454.5	454.5	544.4	7.2	89.9	89.9	-	-	139.6
	m3/hr	1.9	1.9	1.8	0.1	0.1	73.1	1.7	1.6	1.6	1.6	1.6	777.8	5.7	70.8	70.8			
	l/min	31.6	31.6	30.7	0.9	0.8	1217.6	27.9	27.1	27.1	27.1	27.1	12962.7	94.4	1179.6	1179.6			
	kW																3.7	3.7	
Temperature	°C	18	18	18	18	18	12	104	100	20	15	15	400	12	12	540	-	-	
Pressure	kPa	101.3	101.3	101.3	101.3	101.3	101.3	101.3	101.3	101.3	101.3	501.3	401.3	101.3	101.3	201.3	-	-	
Density	kg/m3	280	280	280	280	280	1.27	280	280	280	280	280	0.7	1.27	1.27	1.27	-	-	
Vapour Fraction		0	0	0	0	0	1	0	0	0	0	0	0.8	1	1	1	0	0	

COMPONENT	UNITS	STREAM												
		S201	S202	S203	S204	S205	S206	S207	S208	S209	S210	S211	S212	S213
Total Flow	kg/hr	544.4	499.0	476.3	45.5	22.7	271.7	294.4	258.1	345.9	345.2	204.5	22.7	36.4
	m3/hr	777.8	712.8	680.4	0.1	0.1	388.2	420.6	368.7	0.3	0.3	0.2	0.0	0.0
	l/min	12962.7	11880.4	11339.3	2.4	1.2	6469.2	7010.3	6144.5	5.8	5.8	2.8	0.3	0.6
Temperature	°C	350	300	300	300	300	170	18	17	15	15	15	15	15
Pressure	kPa	401.3	351.3	301.3	101.3	101.3	301.3	261.3	202.3	101.3	101.3	101.3	101.3	101.3
Density	kg/m3	0.7	0.7	0.7	320	320	0.7	0.7	0.7	999.9	999.9	1232	1232	940
Vapour Fraction		0.7	0.7	0.7	0.1	0.1	0.75	0.75	0.85	0	0	0	0	0

energy stream
N2 flow
air

Process Case:
65% bio-oil and tar
15% bio-char
80% bitumen
20% bio-mix

Assumed
S109 22 hrs operating/day
8000 operating a year
processing 10 tonne/day of biomass
S107 initial MC of Sawdust is 20%

COMPONENT	UNITS	STREAM										
		S301	S302	S303	S304	S305	S306	S307	S308	S309	S310	S311
Total Flow	kg/hr	258.1	22.7	85.3	85.3	235.3	150.1	53.0	150.1	106.0		
	m3/hr	368.7	28.4	106.6	67.1	185.3	118.2	41.7	118.2	83.5		
	l/min	6144.5	473.5	1776.3	1118.9	3088.5	1969.5	695.5	1969.5	1391.1		
Temperature	°C	17	17	15	12	12	12	12	12	12		
Pressure	kPa	202.3	189.3	189.3	101.3	101.3	101.3	101.3	101.3	101.3		
Density	kg/m3	0.7	0.8	0.8	1.27	1.27	1.27	1.27	1.27	1.27		
Vapour Fraction		0.85	0.89	1	0.001	0	0	0	0			

COMPONENT	UNITS	STREAM																						
		S401	S402	S403	S404	S405	S406	S407	S408	S409	S410	S411	S412	S413	S414	S415	S416	S417	S418	S419	S420	S421	S422	S423	S424
Total Flow	kg/hr	204.5	22.7	36.4	22.7	28.6	428.4	14.3	227.3	59.1	428.4	286.4	572.7	286.4	114.5	31.5	458.2	2.9	435.3	97.4	572.7	389.5	389.5	486.8	22.9

	m3/hr	0.17	0.02	0.04	0.02	0.03	0.44	0.01	0.18	0.06	0.45	0.22	0.49	-	0.11	0.03	-	0.00	0.54	0.09	0.59	0.40	0.40	0.45	0.03
	l/min	2.77	0.31	0.64	0.40	0.51	7.36	0.18	3.07	1.05	7.52	3.59	8.18	-	1.91	0.49	-	0.04	9.07	1.52	9.84	6.69	6.69	7.58	0.48
Temperature	°C	12	12	12	12	12	20	12	12	12	12	12	12	200	200	200		180	180	15	15	15	15	60	60
Pressure	kPa	101.3	101.3	101.3	101.3	101.3	101.3	101.3												105.0	101.0	107.0	105.0	101.3	101.3
Density	kg/m3	1232	1232	940	940	940	970	1330	1232	940	950	1330	1167	1330	1000	1070	1167	1350	800	1070	970	970	970	1070	800
Vapour Fraction		0	0	0	0	0	1E-04	0	0	0	0	0	0		0	0.5		0.02	0	0	1E-04	1E-05	1E-04	1E-04	1E-04

8.11 Sizing and design calculations

Cyclones	**E201**	**E202**
Cyclone 1:	will design High Efficiency Cyclones	
Inlet Flow(S112/S201)	544.432899	kg/hr
	0.151231361	kg/s
	0.7	kg/m3
	15	m/s
Gas velocity	0.216044801	m3/s
Area of the Inlect Duct	0.014402987	m2
Dc	0.943958792	m
Duct area	0.08910582	m2
Δ^2	0.005580513	
**standard design diameter is 0.203 m*		
**Try Cyclones in Parallel*		
*Dc**	*0.471979396*	
Flow rate per cyclone	*0.108022401*	*m3/s*
T in the Cyclone	300	°C
	573.15	K
Viscosity of N2, μ	2.82415E-05	*Power-Law Viscosity Law use T [K]
Top	0.849562913	Dc
	0.566866734	
Dc	0.943958792	
Flow rate Q_2	777.7612842	m3/hr
Feed Inlet length	0.188791758	m
Feed Inlet opening	0.471979396	m
Gas Out	0.471979396	m
Solids Out	0.353984547	m
1	0.353984547	m
2	1.415938188	m
3	2.35989698	m
Height	3.775835168	m

**using Coulson & Richardson
d1 : mean diameter of particle separated at the standard conditions, at the chosen separating efficiency, Figures 10.45a or 10.45b,
d2 : mean diameter of the particle separated in the proposed design, at the same separating efficiency,
Dc1 : diameter of the standard cyclone D 8 inches (203 mm),
Dc2 : diameter of proposed cyclone, mm,
T_p: Particle residence time
T_g: Gas residence time,

$$d_2 = d_1\left[\left(\frac{D_{c2}}{D_{c1}}\right)^3 \times \frac{Q_1}{Q_2} \times \frac{\Delta\rho_1}{\Delta\rho_2} \times \frac{\mu_2}{\mu_1}\right]^{1/2}$$

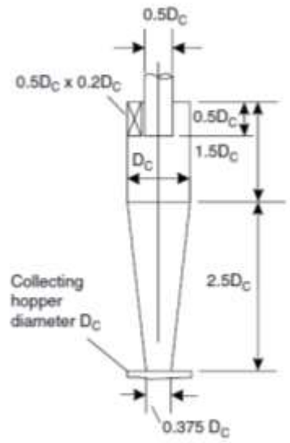

the flow when designing the real thing

1

.=0.5Dc*0.2Dc

2

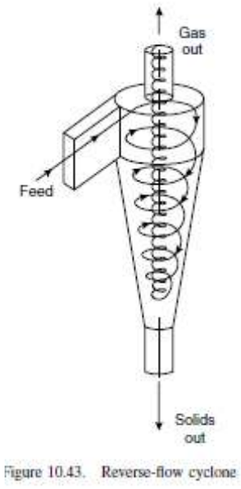

Figure 10.43. Reverse-flow cyclone

$$u_p = \left(\frac{2u^2}{D_c}\right) d_p \frac{(\rho_s - \rho_f)}{18\mu}$$

Q1 : standard flow rate:
for high efficiency design D 223 m3/h,
for high throughput design D 669 m3/h,
Q2 : proposed flow rate, m3/h,
Δρ1 : solid-fluid density difference in standard conditions D 2000 kg/m3,
Δρ2 :density difference, proposed design,
μ1 : test fluid viscosity (air at 1 atm, 20°C)

$$T_p = \frac{L}{u_p}$$

into cyclone	Q_1	223	m3/h
	$\Delta\rho_1$	2000	kg/m3
	$\Delta\rho_2$	1.311	kg/m3
	SF	209.7145	

3

D 0.018 mN s/m2,
μ2 : viscosity, proposed fluid.

$$T_g = \frac{\pi D_c N_s}{u_p}$$

Area of inlet	0.08910582	m2
Cyclone SA	11.19736759	m2
fc	0.005	for gases
ψ	0.628318531	
rt/re	1.8	
ϕ	0.95	from graph
u1	2.424586867	m/s
A of exit pipe	0.174958869	m2
u2	1.234831951	m/s
	0.331912606	millibar

3.32E-05 MPa

From Graph

Particle size (μm)	% by wt less than	% in range	Mean size/SF	eff	collected	grading	% at exit
>50	97	5	0.238419	98	4.9	0.1	1.96%
50-40	85	12	0.214577	97	11.64	0.36	7.07%
40-30	76	9	0.166894	96	8.64	0.36	7.07%
30-20	20	56	0.11921	95	53.2	2.8	55.01%
20-10	5	15	0.071526	93	13.95	1.05	20.63%
10 - 0.0	2	3	0.023842	86	2.58	0.42	8.25%
	Assumptions			OVR η	94.91	5.09	100.00%

$$\Delta P = \frac{\rho_f}{203}\left\{u_1^2\left[1+2\phi^2\left(\frac{2r_t}{r_e}-1\right)\right]+2u_2^2\right\}$$

ΔP : cyclone pressure drop, millibars

ρ : gas density, kg/m3

u1 : inlet duct velocity, m/s,

u2 : exit duct velocity, m/s,

rt : radius of circle to which the centre line of the inlet is tangential, m,

re : radius of exit pipe, m,

ϕ : factor from Figure 10.47,

ψ : parameter in Figure 10.47, given by:

$$\psi = f_c\frac{A_s}{A_1}$$

fc : friction factor, taken as 0.005 for gases,

As :D surface area of cyclone exposed to the spinning fluid, m2.

For design purposes this can be taken as equal to the surface area of a cylinder with the same diameter as the cylone and length equal to the total height of the cyclone (barrel plus cone).

A1 : area of inlet duct, m2.

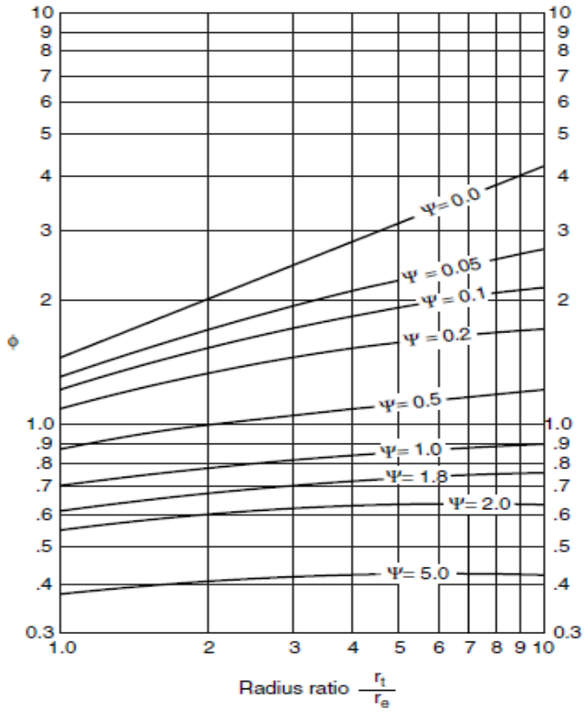

Figure 10.47. Cyclone pressure drop factor

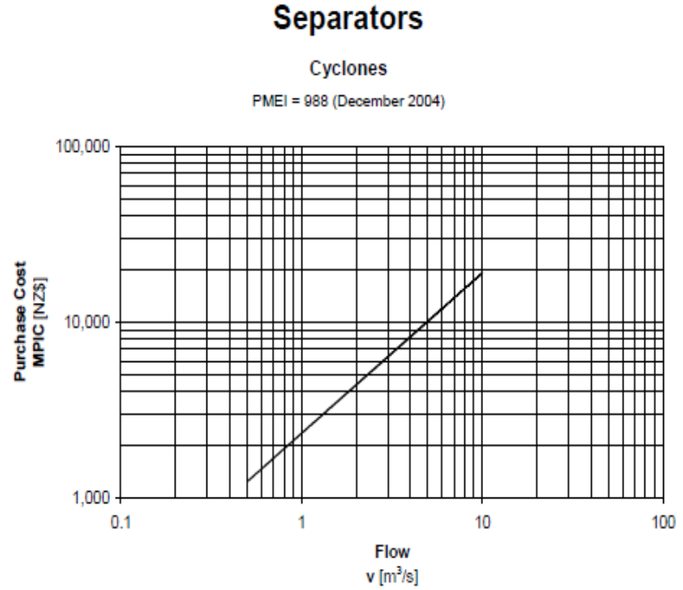

Figure 8.32 Purchased equipment costs for cyclones.

The regression equation for cyclones is:

Separator Type	Equation	R^2	df
Cyclone	**MPIC** = 2.33 x 10^3 **v** $^{0.912}$	0.990	9

For Pyrolysis (from my own research) :

Solids/Char/	8%	of the feed			
Feed (S112)	544.43	kg/hr	*544.43*		544.43 kg/hr
Char from Cyclone 1	45.8	kg/hr	S204	*45.45455*	45.79 kg/hr
Gas Out of Cyclone 1	498.6	kg/hr	S202	*498.9784*	498.65 kg/hr

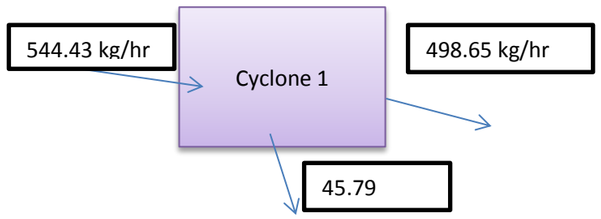

MPIC = 2.33e3*v^0.912			v [m3/s]
MPIC	576.05	$	
		Cost Scaling factor as above 4bar	
Scaling	1.1	just	
Total Cost	633.65	$	

<u>Cyclone 2:</u>	will design High Efficiency Cyclones		
Inlet Flow(S202)	498.9783535	kg/hr	
	0.138605098	kg/s	
	0.7	kg/m3	** PV=nRT with density represented as mass/volume AND take into account Moisture and major chemicals in the flow when designing the real thing
	15	m/s	
Gas velocity	0.198007283	m3/s	
Area of the Inlect Duct	0.013200486	m2	
Dc	0.943958792	m	
Duct area	0.08910582	m2	.=0.5Dc*0.2Dc
Δ^2	0.00576162		
**standard design diameter is 0.203 m*			
**Try Cyclones in Parallel*		*2*	
*Dc**	*0.471979396*		
Flow rate per cyclone	*0.099003642*	*m3/s*	
T in the Cyclone	300	°C	
	573.15	K	
Viscosity of N2, μ	2.82415E-05	*Power-Law Viscosity Law use T [K]	

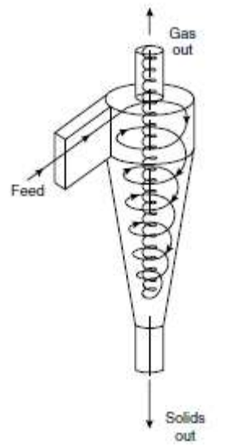

Figure 10.43. Reverse-flow cyclone

$$d_2 = d_1\left[\left(\frac{D_{c_2}}{D_{c_1}}\right)^3 \times \frac{Q_1}{Q_2} \times \frac{\Delta\rho_1}{\Delta\rho_2} \times \frac{\mu_2}{\mu_1}\right]^{1/2}$$

Top		0.849562913	Dc				
		0.566866734					
Dc		0.943958792					
Flow rate Q_2		498.9783535	m3/hr	into cyclone	Q_1	223	m3/h
Feed Inlet length		0.188791758	m		$\Delta\rho_1$	2000	kg/m3
Feed Inlet opening		0.471979396	m		$\Delta\rho_2$	1.311	kg/m3
Gas Out		0.471979396	m				
Solids Out		0.353984547	m		SF	261.8248	
	1	0.353984547	m				
			m				
	2	1.415938188					
	3	2.35989698	m				
Height		3.775835168	m				
Area of inlet		0.08910582	m2				
Cyclone SA		11.19736759	m2				
fc		0.005	for gases				
ψ		0.628318531					
rt/re		1.8					
ϕ		0.95	from graph				
u1		1.555511167	m/s				
A of exit pipe		0.174958869	m2				

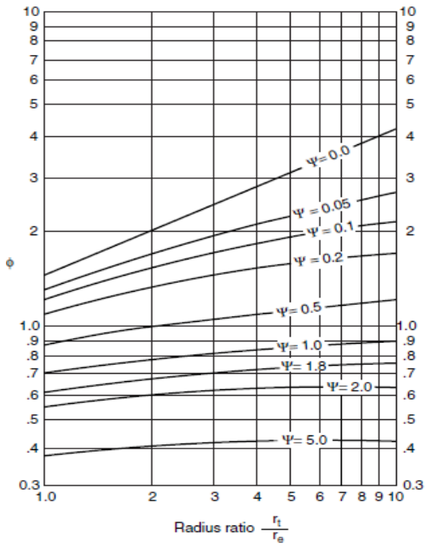

Figure 10.47. Cyclone pressure drop factor

$$\Delta P = \frac{\rho_f}{203}\left\{u_1^2\left[1+2\phi^2\left(\frac{2r_t}{r_e}-1\right)\right]+2u_2^2\right\}$$

ΔP : cyclone pressure drop, millibars

ρ : gas density, kg/m3

u1 /s,

u2 /s,

rt : radius of circle to which the centre line of the inlet is tangential, m,

1.09E-05 MPa

1

$$u_p = \left(\frac{2u^2}{D_c}\right) d_p \frac{(\rho_s - \rho_f)}{18\,\mu}$$

$$T_p = \frac{L}{u_p}$$

Particle residence time, T_p:

$$T_g = \frac{\pi D_c N_s}{u_p}$$

Gas residence time, T_g:

2

3

$$\psi = f_c \frac{A_s}{A_1}$$

**using Coulson & Richardson

d1 : mean diameter of particle separated at the standard conditions, at the
chosen separating efficiency, Figures 10.45a or 10.45b,

d2 : mean diameter of the particle separated in the proposed design, at the
same separating efficiency,

Dc1 : diameter of the standard cyclone D 8 inches (203 mm),

Dc2 : diameter of proposed cyclone, mm,

Velocity component towards wall, u_p:

Q1 : standard flow rate:
for high efficiency design D 223 m3/h,
for high throughput design D 669 m3/h,

Q2 : proposed flow rate, m3/h,

Δρ1 : solid-fluid density difference in standard conditions D 2000 kg/m3,

Δρ2 :density difference, proposed design,

μ1 : test fluid viscosity (air at 1 atm, 20°C)
D 0.018 mN s/m2,

μ2 : viscosity, proposed fluid.

re : radius of exit pipe, m,

ϕ : factor from Figure 10.47,

ψ : parameter in Figure 10.47, given by:

fc : friction factor, taken as 0.005 for gases,

As :D surface area of cyclone exposed to the spinning fluid, m2.

For design purposes this can be taken as equal to the surface area of a

cylinder with the same diameter as the cylone and length equal to the total

height of the cyclone (barrel plus cone).

A1 : area of inlet duct, m2.

For Pyrolysis (from my own research) :

*assume the next Cyclone takes out 5% of the left over Char; This make Char the total 20% of the process

Solids/Char/	5%	of the feed			
Feed (S202)	498.6	kg/hr		*498.9784*	498.98 kg/hr
Char from Cyclone 2	22.93772024	kg/hr	S205	*22.72727*	22.73 kg/hr
Gas Out of Cyclone 2	476.0406333	kg/hr	S203	*476.2511*	476.25 kg/hr

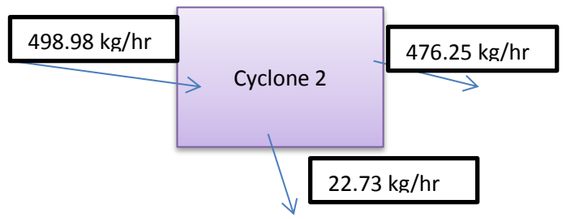

MPIC = 2.33e3*v^0.912		
MPIC	384.2895332	$
		Cost Scaling factor as above 4bar
Scaling	1.1	just
Total Cost	422.72	$

Quenchers: http://www.knm-group.com/knm_products-quench-1.htm

Feed (S109) 454.5 kg/hr 454.5455

Total Bio Oil produced

50% of feed 227.25 kg/hr

Streams divided into:

S211/S401

S212/S402

Assume E203 produces 90% of total bio oil

Assume E204 produces 10% of total bio oil

100%

Thus stream flows:

S211/S401	204.54518	kg/hr	*204.5455*
S212/S402	22.704818	kg/hr	*22.72727*
S209	345.9	kg/hr	
S210	345.2	kg/hr	

Above streams add up into stream:

S408 227.25 kg/hr

E203

S209 345.9 kg/hr

Heat Exchanger Design

Shell and Tube Heat Exchanger

hot streams are light oils

cooling water available at 15°C

Rate Equation

$Q=mC_p\Delta T$

Total Tar Produced

13% of feed 59.085 kg/hr

Streams divided into:

S213/S403

S305/S404

S306/S405

Assume E205 produces 53% of t

Assume E302 produces 47% of t

100%

Thus stream flows:

S213/S403	31.51509	kg/hr	36.36364
S302/S404	27.56991	kg/hr	22.72727

Before equation 12.1 can be used to determine the heat transfer area required for a given duty, an estimate of the mean temperature difference ΔT_m must be made. This will normally be calculated from the terminal temperature differences: the difference in the fluid temperatures at the inlet and outlet of the exchanger. The well-known "logarithmic mean" temperature difference (see Volume 1, Chapter 9) is only applicable to sensible heat transfer in true co-current or counter-current flow (linear temperature-enthalpy curves). For counter-current flow, Figure 12.18*a*, the logarithmic mean temperature is given by: 91

$$\Delta T_{lm} = \frac{(T_1 - t_2) - (T_2 - t_1)}{\ln \dfrac{(T_1 - t_2)}{(T_2 - t_1)}} \qquad (12.4)$$

where ΔT_{lm} = log mean temperature difference,
T_1 = hot fluid temperature, inlet,
T_2 = hot fluid temperature, outlet,
t_1 = cold fluid temperature, inlet,
t_2 = cold fluid temperature, outlet.

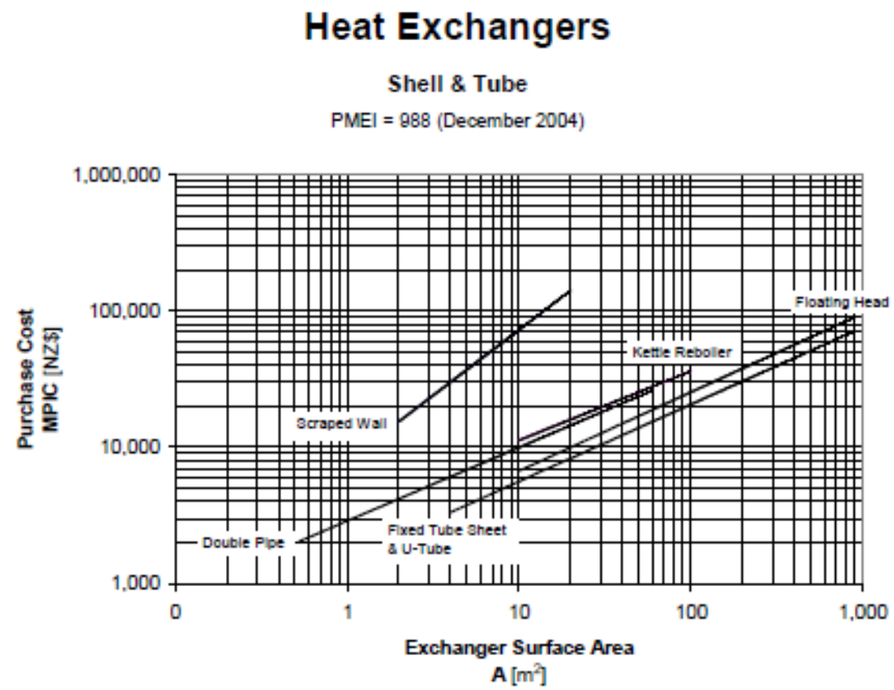

Figure 8.17 Purchased equipment costs for shell and tube and double-pipe heat exchangers.

Material factors for exotic materials can be found in Ulrich (2004, Figures 5.36, p 443). Pressure factors specific to shell and tube heat exchangers can be found in Ulrich (2004, Figure 5.37, p 444).

The regression equations for shell and tube heat exchangers are:

Heat Exchanger Type	Shell & Tube Type	Equation
Shell & Tube	Double Pipe	$MPIC = 2.88 \times 10^3 A^{0.539}$
Shell & Tube	Fixed Tube Sheet & U-Tube	$MPIC = 1.53 \times 10^3 A^{0.566}$
Shell & Tube	Floating Head	$MPIC = 1.77 \times 10^3 A^{0.578}$
Shell & Tube	Kettle Reboiler	$MPIC = 3.47 \times 10^3 A^{0.508}$
Shell & Tube	Scraped Wall	$MPIC = 7.90 \times 10^3 A^{0.964}$

Table 12.3. Standard dimensions for steel tubes

Outside diameter (mm)	Wall thickness (mm)				
16	1.2	1.6	2.0	—	—
20	—	1.6	2.0	2.6	—
25	—	1.6	2.0	2.6	3.2
30	—	1.6	2.0	2.6	3.2
38	—	—	2.0	2.6	3.2
50	—	—	2.0	2.6	3.2

Q cold 27.775 kW

27775 W

Properties	Water	Oil+Gas	
m (kg/hr)	-345.93708	227.25	
m (kg/s)	-0.0960936	0.063125	
Q (W)	27775	27775	
Tin (°C)	33	300	
Tout (°C)	102	80	
Cp (kg/J*°C)	4189	2000	
ρ (kg/m^3)	999.9	800	density
μ (Pa.s)	0.001	0.000048	viscosity
k (W/°C.m)	0.6	0.15	thermal conductivity
U (W/m^2*K)	300		

ΔT 1 198

ΔT 2 47

ΔTlm 104.99823

R 3.1884058 counter-current flow

S 0.3

Ft 0.85 temperature correction factor from the grph using R and S

ΔTm 89.248499

A 0.8068935 m^2 Q=U*A*ΔTm

MPIC=2.88*10^3*A^0.539

MPIC 2565 $

E204

S210 345.2 kg/hr

Heat Exchanger Design

Shell and Tube Heat Exchanger

hot streams are light oils

cooling water available at 15°C

Rate Equation

The general equation for heat transfer across a surface is:

$$Q = UA\Delta T_m$$

where Q = heat transferred per unit time, W,
U = the overall heat transfer coefficient, W/m^2°C,
A = heat-transfer area, m^2,
ΔT_m = the mean temperature difference, the temperature driving force, °C.

An estimate of the bundle diameter D_b can be obtained from equation 12.3b, which is an empirical equation based on standard tube layouts. The constants for use in this equation, for triangular and square patterns, are given in Table 12.4.

$$N_t = K_1 \left(\frac{D_b}{d_o}\right)^{n_1}, \qquad (12.3a)$$

$$D_b = d_o \left(\frac{N_t}{K_1}\right)^{1/n_1}, \qquad (12.3b)$$

where N_t = number of tubes,
D_b = bundle diameter, mm,
d_o = tube outside diameter, mm.

If U-tubes are used the number of tubes will be slightly less than that given by equation 12.3a, as the spacing between the two centre rows will be determined by the minimum allowable radius for the U-bend. The minimum bend radius will depend on the tube diameter and wall thickness. It will range from 1.5 to 3.0 times the tube outside diameter. The tighter bend radius will lead to some thinning of the tube wall.

Q=mCpΔT

Q cold	9.238	kW
	9238	W

Properties	Water	Oil+Gas	
m (kg/hr)	-345.17733	268.2	
m (kg/s)	-0.0958826	0.0745	
Q (W)	9238	9238	
Tin (°C)	10	80	
Tout (°C)	33	18	
Cp (kg/J*°C)	4189	2000	
ρ (kg/m^3)	999.9	800	density
μ (Pa.s)	0.001	0.000048	viscosity
k (W/°C.m)	0.6	0.15	thermal conductivity

U (W/m^2*K)	300		
ΔT 1	47		
ΔT 2	8		
ΔTlm	22.025112		
R	2.6956522		counter-current flow
S	0.3		
Ft	0.85		temperature correction facto
ΔTm	18.721346		
A	1.3981011	m^2	Q=U*A*ΔTm
MPIC=2.88*10^3*A^0.539			
MPIC	3450	$	

Stainless Steel Mesh Condenser: **E205**

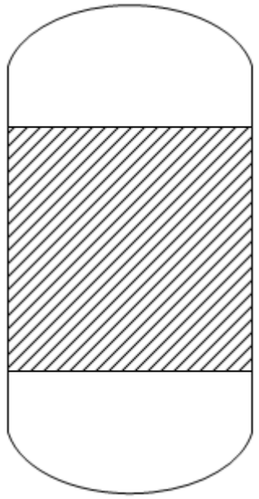

Chemical A needs to be added at 1:4 ratio to the (Bio Oil + Tar)

Chemical A is added to reduce Oxygen and improve stability of the compound

In			
S207	294.4329	kg/hr	*294.4329*
Out			
S208	258.0693	kg/hr	*258.0693*
S213	36.36364	kg/hr	*36.36364*

ρ Mixed Gas	0.8	kg/m3
Mixed Gas	294.4	kg/hr
	368.0	m3/hr

22.5	hrs operating in a day (8000/356)	To simplify for design and costing
1.5	hrs 'clean up & maintenace' daily	Condenser=Vessel + 95%of the Vessel Stainless Steel Mesh
817.16	kg 'filtered' on daily basis	
8270.6	m3 of 'filtered' on daily basis	

+ add 20% for safety reasons& vapour accumulation/pressure drop

* condenser will be a vertical cylinder

0.7 m3 Volume of the Condenser

$$e_s = \frac{\rho_L H_L g}{2 f_t} \cdot \frac{D_t}{10^3}$$

			*avg of the mix-
ρ_Liquid	0.8	kg/m3	tures
H_Liquid	325.4	m	
f_tank	145	N/mm2	$V_{one\ tank} = \frac{\pi}{4} D^2 H_L$
g	9.81	m/s2	
D_tank	1.2	m	
e_s	0.010568	mm	Tank Thickness

Volume taken up by the mesh 60%

V mesh 0.4 m3

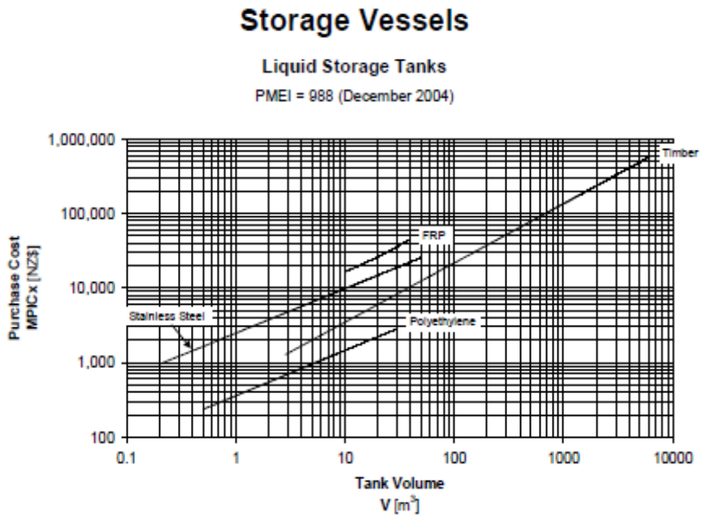

Figure 8.38 Purchased equipment costs for liquid storage tanks.

Further cost data on storage vessels can be found in Ulrich (2004, Figure 5.61 – pg 457)

The regression equations for liquid storage tanks are:

Tank Type	Equation	R^2	df
Stainless Steel	$MPIC_x = 2.48 \times 10^3 V^{0.597}$	0.995	5
Polyethylene	$MPIC_x = 358 V^{0.609}$	0.969	8

MPICx = 2.48 x 10^3 * V^0.597

MPIC	2065	$

T = 0°C	273.15	K
Cpw	4.19	KJ/kgK heat capacity of water
		for T in
b1	-0.06191	K
		for T in
b2	0.000236	K
		for T in
b3	-0.00013	K
T oven	104	°C temperature in the oven
T	12	°C the sample is at
M	15%	moisture content of the sample originaly
Ac	0.000805	additional energy factor
Cp0	1.205775	KJ/kgK heat capacity of dry wood
Cp	1.21105	KJ/kgK heat capacity of wood containing water
m	4	kg mass of the sample initially

Wood	S103		S107	*468.6036*	kg/hr
m	515.4639	kg/hr	469.1	kg/hr	
			desired		
original MC	19%		MC	10%	
T	12	°C the sample is at	T oven	104	°C temperature in the oven
Cpw	4.19	KJ/kgK heat capacity of water			
Q	17883.09	KW energy required to evaporate water to achieve the desired MC of wood			
	17.88309	MW			

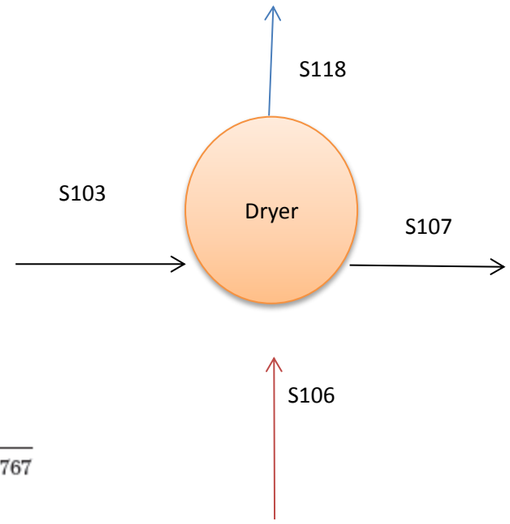

TABLE 12-18 Warm-Air Direct-Heat Cocurrent Rotary Dryers: Typical Performance Data*

Dryer size, m × m	1.219 × 7.62	1.372 × 7.621	1.524 × 9.144	1.839 × 10.668	2.134 × 12.192	2.438 × 13.716	3.048 × 16.767
Evaporation, kg/h	136.1	181.4	226.8	317.5	408.2	544.3	861.8
Work, 10^8 J/h	3.61	4.60	5.70	8.23	1.12	1.46	2.28
Steam, kg/h at kg/m² gauge	317.5	408.2	521.6	725.7	997.9	131.5	2041
Discharge, kg/h	408	522	685	953	1270	1633	2586
Exhaust velocity, m/min	70	70	70	70	70	70	70
Exhaust volume, m³/min	63.7	80.7	100.5	144.4	196.8	257.7	399.3
Exhaust fan, kW	3.7	3.7	5.6	7.5	11.2	18.6	22.4
Dryer drive, kW	2.2	5.6	5.6	7.5	14.9	18.6	37.3
Shipping weight, kg	7700	10,900	14,500	19,100	35,800	39,900	59,900
Price, FOB Chicago	$158,000	$168,466	$173,066	$204,400	$241,066	$298,933	$393,333

*Courtesy of Swenson Process Equipment Inc.
NOTE:

Required Evaporation is		Air	
46.4	kg/hr	92.78351	kg/hr

Thus a Dryer options are '1.839 m x 10.668 m' OR '2.134 m x 12.192 m'

Assume 1.839 m x 10.668 m will do the job

Thus:

S106	725.7	kg/hr	92.78351	Cp air	1.0005	KJ/kgK
S118	772.1	kg/hr	139.6439			
S117	3.7	kW	3.7			
MPIC	24106	$				

E401

Chemical A needs to be added at 1:1 ratio to the (Bio Oil + Tar)

Chemical A is added to reduce Oxygen and improve stability of the compound

In

S411	Chemical A	286.3636	kg/hr	*286.3636*
S408	Bio Oil	227.2727	kg/hr	*227.2727*
S409	Tar	59.09091	kg/hr	*59.09091*

Out

S412/S420		572.7273	kg/hr	*572.7273*
				572.7273

Mixture of the above

ρ bio oil	1232	kg/m3
Bio Oil	227	kg/hr
ρ tar	940	kg/m3
Tar	59.1	kg/hr

Chemical A	286.363636	kg/hr	
Total Mixing	0.552	m3/hr	* taking into account all the different substances mixing and their different densities
22.47	hrs operating in a day (8000/356)		
1.53	hrs 'clean up & maintenace' daily		
12870.28	kg of 'mixing' on daily basis		
12.40	m3 of 'mixing' on daily basis		

+ add 20% for safety reasons& vapour accumulation/pressure drop

14.88 m3

$$e_s = \frac{\rho_L H_L g}{2 f_t} \cdot \frac{D_t}{10^3}$$

Liquid	Mixture of Bio OIl+Tar+Chemical A		
ρ_Liquid	1086	kg/m3	*avg of the mixtures
H_Liquid	1.75	m	
f_tank	145	N/mm2	$V_{one\ tank} = \frac{\pi}{4} D^2 H_L$
g	9.81	m/s2	
D_tank	3	m	

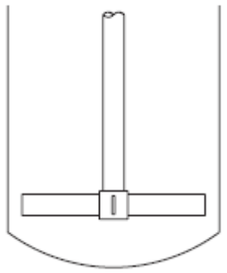

Vertical cylindrical tanks, with flat bases and conical roofs, are universally used for the bulk storage of liquids at atmospheric pressure. Tank sizes vary from a few hundred gallons (tens of cubic metres) to several thousand gallons (several hundred cubic metres).

The main load to be considered in the design of these tanks is the hydrostatic pressure of the liquid, but the tanks must also be designed to withstand wind loading and, for some locations, the weight of snow on the tank roof.

The minimum wall thickness required to resist the hydrostatic pressure can be calculated from the equations for the membrane stresses in thin cylinders (Section 13.3.4):

$$e_s = \frac{\rho_L H_{Lg}}{2 f_t J} \frac{D_t}{10^3} \qquad (13.130)$$

where e_s = tank thickness required at depth H_L, mm,
H_L = liquid depth, m,
ρ_L = liquid density, kg/m^3,
J = joint factor (if applicable),
g = gravitational acceleration, 9.81 m/s^2,
f_t = design stress for tank material, N/mm^2,
D_t = tank diameter, m.

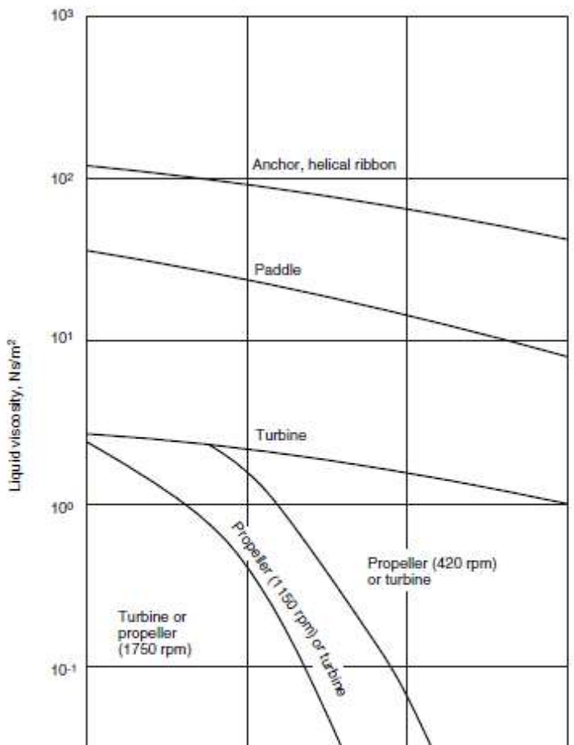

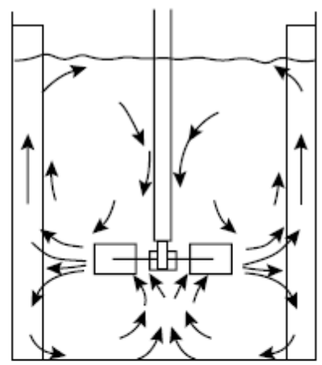

Agitator arrangements and flow patterns

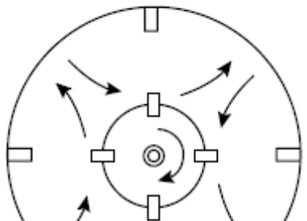

e_s	0.19	mm	Tank Thickness
Required Heating	0	MW	

Turbine Impeller

Hub-Mounted Flat-Blade Turbine

*impeller to tank diameter ratios of up to about 0.6

D agitator	1.2	m		
N	2	rps agitator speed		
K	1.4223E-08	const		
ρ_fluid	1086	kg/m3		Pa s=kg/(m s)
μ_fluid	0.00003263	Ns/m2	32.63	mPa s
		* based on T Tzanetakis, 2007		

$$v = \frac{\mu}{\rho}$$

g	9.81	m/s2
Re	95852896	
Fr	0.48929664	
b	1	
c	0	
Np	4	* from graph

$v - kinematic\ viscosiy$

$\mu - absolute\ or\ dynamic\ viscosity$

$\rho - density$

$1\,St = 100\,cSt$

$1\,St = 10^{-4}\frac{m^2}{s}$

Np	1.36331361	* from the equation
P	86474.0966	W
	0.086	MW

MPIC = 2.20 x 10^3 P + 21.5 x 10^3

MPIC	21690.243	$

E403

Agitator power consumption

The shaft power required to drive an agitator can be estimated using the following generalised dimensionless equation, the derivation of which is given in Volume 2, Chapter 13.

$$N_p = KRe^b Fr^c \qquad (10.11)$$

where N_p = power number = $\frac{P}{D^5 N^3 \rho}$,

Re = Reynolds number = $\frac{D^2 N \rho}{\mu}$,

Fr = Froude number = $\frac{DN^2}{g}$,

P = shaft power, W,

K = a constant, dependent on the agitator type, size, and the agitator-tank geometry,

ρ = fluid density, kg/m^3,

μ = fluid viscosity, Ns/m^2,

N = agitator speed, s^{-1} (revolutions per second) (rps),

D = agitator diameter, m,

g = gravitational acceleration, 9.81 m/s^2.

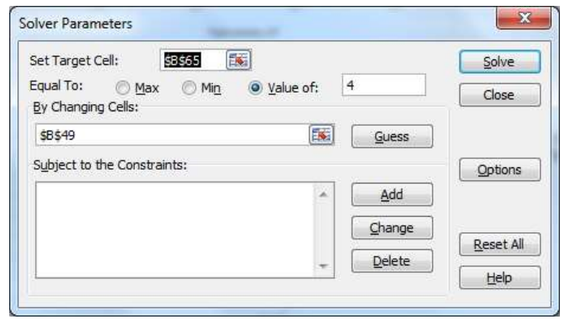

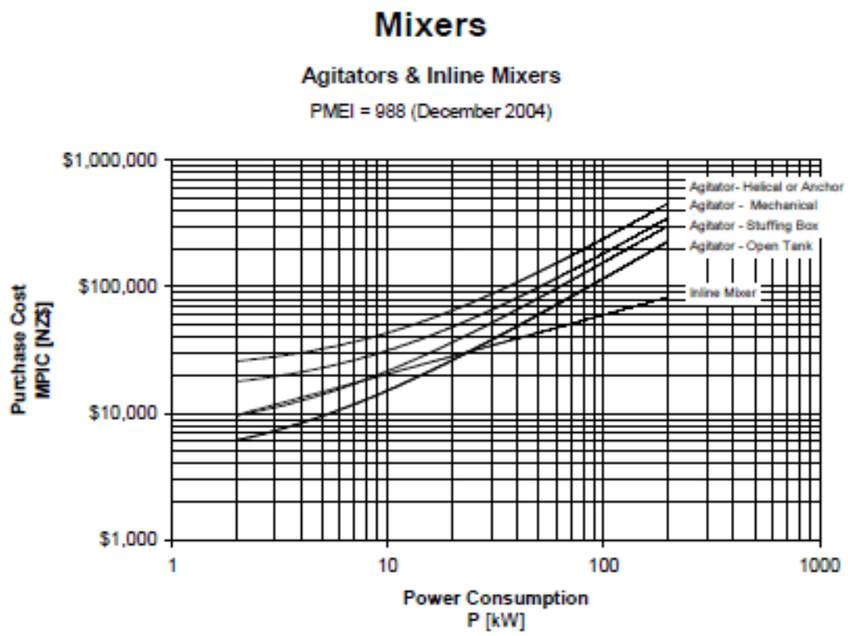

Figure 8.21 Purchased equipment costs for agitators and inline mixers. Cost of agitators includes motor, speed reducer and impeller ready for installation in a vessel. Stuffing box seals are suitable at pressure up to 10 bar (gauge). Mechanical seals are suitable for toxic or critical fluids at pressure up to 80 bar (gauge).

From research completed, known that 'Bitumen : Bio-Mix' ratio is '80% : 20%'

S419	97.3636364	kg/hr	20%	*97.36364*
S422	389.454545	kg/hr	80%	*389.4545*

Assume stored on site 10% extra of Bitumen most of the time

S410	428.4	kg/hr	*428.4*
S421	389.45	kg/hr	*389.5*
S406	428.4	kg/hr	*428.4*
S423	486.818182	kg/hr	*486.8182*
	0.45497026	m3/hr	
Assume	973.636364	kg/hr	**formula; 200%
	0.90994053	m3/hr	

*200% because Assume tanks pick up the Bio-Bitumen once a day,

thus need to be able to store at least 1.5-2 days worth of product

22.472	hrs operating in a day (8000/356)
1.528	hrs 'clean up & maintenace' daily
10939.73442	kg of Bio-Bitumen produced daily
10.22405086	m3 of Bio-Bitumen produced daily
20.44810173	m3 of Bio-Bitumen produced in two days

assume have more then one tank

~ storing 380 m3 in one tank

+ add 20% for safety reasons& vapour accumulation/pressure drop

12.26886104 m3

$$e_s = \frac{\rho_L H_L g}{2 f_t} \cdot \frac{D_t}{10^3}$$

Liquid	Mixture of Bitumen and Bio OIl+Tar		
ρ_L	1070	kg/m3	*www.wolframalpha.com
H_L	0.52070663	m	
f_t	145	N/mm2	$V_{one\,tank} = \frac{\pi}{4} D^2 H_L$
g	9.81	m/s2	
D_t	5	m	

Np 0.4 * from the equation
P 52246 W
0.055 MW

MPIC = 2.20 x 10^3 P + 21.5 x10^3

MPIC 21620 $

E311 Biomass Storage Tank

0.00	kg/hr	plant feed	kg/hr
22.472	hrs operating in a day (8000/356)		kg/hr
1.528	hrs 'clean up & maintenace' daily		
1.27	kg/m3	density	
0.000	m3/hr		

+ add 20% for safety reasons& vapour accumulation/pressure drop
0.000 m3 total volume of the storage tank

MPICs = 2.48 x 10^3 * V^0.597

MPIC 0 $

E401

Chemical A needs to be added at 1:1 ratio to the (Bio Oil + Tar)
Chemical A is added to reduce Oxygen and improve stability of the compound

In

S307	N2	53	kg/hr
S306	N2	150.1	kg/hr

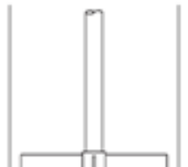

+ add 20% for safety reasons& vapour accumulation/pressure drop

5476.27 m3

$$e_s = \frac{\rho_L H_L g}{2 f_t} \cdot \frac{D_t}{10^3}$$

Liquid	Mixture of Bio Oil+Tar+Chemical A		
ρ_Liquid	1.27	kg/m3	*avg of the mixtures
H_Liquid	645.61	m	$V_{one\,tank} = \frac{\pi}{4} D^2 H_L$
f_tank	145	N/mm2	
g	9.81	m/s2	
D_tank	3	m	
e_s	0.08	mm	Tank Thickness

Required Heating 0 MW

Turbine Impeller
Hub-Mounted Flat-Blade Turbine
*impeller to tank diameter ratios of up to about 0.6

D agitator	1.2	m
N	2	rps agitator speed

K	1.4223E-08	const		
ρ_fluid	1.27	kg/m3		Pa s=kg/(m s)
μ_fluid	0.00003263	Ns/m2	32.63	mPa s
			* based on T Tzanetakis 2007	
g	9.81	m/s2		

e_s	0.09423623	mm	Tank Thickness	
Tin	15	°C		
Tout	60	°C		
Cp	215	KJ/kgK	*www.eng-tips.com/viewthread.cfm?qid=125441	
Required Heating		2.445465	KW	Q=mCpΔT
		0.002445	MW	

Turbine Impeller

Hub-Mounted Flat-Blade Turbine

*impeller to tank diameter ratios of up to about 0.6

D agitator	2.5	m		
N	0.5	rps agitator speed		
K	3.9034E-09	const		
ρ_fluid	1070	kg/m3		Pa s=kg/(m s)
μ_fluid	0.00003263	Ns/m2	32.63	mPa s
			* based on T Tzanetakis, 2007	
g	9.81	m/s2		
Re	102474717			
Fr	0.0637105			
b	1			
c	0			
Np	4	* from graph		

$v = \frac{\mu}{\rho}$

$v - kinematic\ viscosiy$

$\mu - absolute\ or\ dynamic\ viscosity$

$\rho - density$

$1\,St = 100\,cSt$

$1\,St = 10^{-4}\frac{m^2}{s}$

0

Tanks:

T101 Biomass Storage Tank

530.93	kg/hr	plant feed	S101	530.928
22.472	hrs operating in a day (8000/356)			
1.528	hrs 'clean up & maintenace' daily			
280	kg/m3	density		
1.896	m3/hr			

+ add 20% for safety reasons& vapour accumulation/pressure drop

2.275	m3 total volume of the storage tank			

MPICx = 2.48 x 10^3 * V^0.597

MPIC	4051	$

T103+E104+M101+E105+M102 Lock Hopper+2x Augers +2x Motors

*CRL Energy Ltd Data				
1000	kg/hr		feed at CRL	
MPIC		10500	$	
			assume 8000hrs/yr opera-	
12.5	m3/hr		tional	
280	kg/m3		density feed	
454.55	kg/hr		new plant feed flow	S109
a		1/2		
MPIC		7079	$	

T401 Bitumen

428.4	kg/hr	plant feed S410	428.4	
22.472	hrs operating in a day (8000/356)			
1.528	hrs 'clean up & maintenace' daily			
970	kg/m3			
0.442	m3/hr			

+ add 20% for safety reasons& vapour accumulation/pressure drop

0.530	m3/hr 120%			

11.9096 m3 total volume of the storage tank

MPICx = 2.48 x 10^3 * V^0.597

MPIC	10883	$

T402 Chemical A

286.364	kg/hr	plant feed S411	286.3636
22.472	hrs operating in a day (8000/356)		
1.528	hrs 'clean up & maintenace' daily		
970	kg/m3		
0.2952	m3/hr		

+ add 20% for safety reasons& vapour accumulation/pressure drop

0.3543	m3/hr 120%
7.9610	m3 total volume of the storage tank

MPICx = 2.48 x 10^3 * V^0.597

MPIC	8557	$

T403 Bio-Bitumen

486.818	kg/hr	plant feed S423	486.8182
22.472	hrs operating in a day (8000/356)		
1.528	hrs 'clean up & maintenace' daily		
1070	kg/m3		
0.455	m3/hr		

+ add 20% for safety reasons& vapour accumulation/pressure drop

0.546	m3/hr 120%
12.269	m3 total volume of the storage tank

MPICx = 2.48 x 10^3 * V^0.597

MPIC	11078	$

T404 Separation Tank

572.7	kg/hr	plant feed S412	572.7273
22.472	hrs operating in a day (8000/356)		
1.528	hrs 'clean up & maintenace' daily		
1167.333333	kg/m3		
0.4906	m3/hr		

+ add 20% for safety reasons& vapour accumulation/pressure drop

0.5888	m3/hr 120%
13.2304	m3 total volume of the storage tank

MPICx = 2.48 x 10^3 * V^0.597

MPIC	11589	$

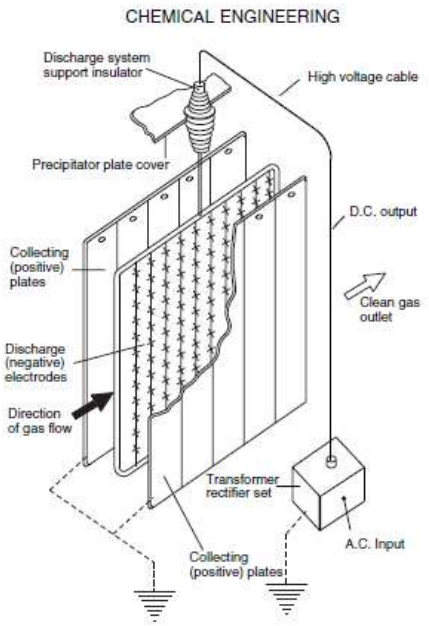

Figure 10.50. Electrostatic precipitator

Electrostatic Precipitator:
E302

MPIC	$55,000

Some suppliers:
http://windsor.co.nz/wesps.shtml
http://www.fowlerex.com.au/
http://www.turbosonic.com/products/wesp/wesp
http://www.mcgillairclean.com/index.htm
http://www.tapc.com.au/electrostatic/replacementparts.html
http://www.solution.com.my/

Electrostatic precipitator

An **electrostatic precipitator** (**ESP**), or **electrostatic air cleaner** is a particulate collection device that removes particles from a flowing gas (such as air) using the force of an induced electrostatic charge. Electrostatic precipitators are highly efficient filtration devices that minimally impede the flow of gases through the device, and can easily remove fine particulate matter such as dust and smoke from the air stream.[1] In contrast to wet scrubbers which apply energy directly to the flowing fluid medium, an ESP applies energy only to the particulate matter being collected and therefore is very efficient in its consumption of energy (in the form of electricity).

The most basic precipitator contains a row of thin vertical wires, and followed by a stack of large flat metal plates oriented vertically, with the plates typically spaced about 1 cm to 18 cm apart, depending on the application. The air or gas stream flows horizontally through the spaces between the wires, and then passes through the stack of plates.

A negative voltage of several thousand volts is applied between wire and plate. If the applied voltage is high enough an electric (corona) discharge ionizes the gas around the electrodes. Negative ions flow to the plates and charge the gas-flow particles.

The ionized particles, following the negative electric field created by the power supply, move to the grounded plates.

Particles build up on the collection plates and form a layer. The layer does not collapse, thanks to electrostatic pressure (given from layer resistivity, electric field, and current flowing in the collected layer).

Precipitator performance is very sensitive due to two particulate properties: 1) Resistivity; and 2) Particle size distribution. These properties can be determined economically and accurately in the laboratory. A widely taught concept to calculate the collection efficiency is the Deutsch model, which assumes infinite remixing of the particles perpendicular to the gas stream.

Resistivity can be determined as a function of temperature in accordance with IEEE Standard 548.

Modern industrial electrostatic precipitators

ESPs continue to be excellent devices for control of many industrial particulate emissions, including smoke from electricity-geqerating utilities (coal and oil fired), salt cake collection from black liquor boilers in pulp mills, and catalyst collection from fluidized bed catalytic cracker units in oil refineries to name a few. These devices treat gas volumes from several hundred thousand ACFM to 2.5 million ACFM (1,180 m^3/s) in the largest coal-fired boiler applications. For a coal-fired boiler the collection is usually performed downstream of the air preheater at about 160 °C (320 F) which provides optimal resistivity of the coal-ash particles. For some difficult applications with low-sulfur fuel hot-end units have been built operating above 371 °C (700 F).

The original parallel plate–weighted wire design (described above) has evolved as more efficient (and robust) discharge electrode designs were developed, today focusing on rigid (pipe-frame) discharge electrodes to which many sharpened spikes are attached (barbed wire), maximizing corona production. Transformer-rectifier systems apply voltages of 50 – 100 kV at relatively high current densities. Modern controls, such as an automatic voltage control, minimize electric sparking and prevent arcing (sparks are quenched within 1/2 cycle of the TR set), avoiding damage to the components. Automatic plate-rapping systems and hopper-evacuation systems remove the collected particulate matter while on line, theoretically allowing ESPs to stay in operation for years at a time.

Wet electrostatic precipitator

A wet electrostatic precipitator (WESP or wet ESP) operates with saturated air streams (100% relative humidity). WESPs are commonly used to remove liquid droplets such as sulfuric acid mist from industrial process gas streams. The WESP is also commonly used where the gases are high in moisture content, contain combustible particulate, have particles that are sticky in nature.

The preferred and most modern type of WESP is a downflow tubular design. This design allows the collected moisture and particulate to form a slurry that helps to keep the collection surfaces clean.

Plate style and upflow design WESPs are very unreliable and should not be used in applications where particulate is sticky in nature.

A study by the Canada Mortgage and Housing Corporation testing a variety of forced-air furnace filters found that ESP filters provided the best, and most cost-effective means of cleaning air using a forced-air system

Reactions During the Process:

Biomass→Char + Bio Oil + Tar + H2O + Gas

Secondary Reactions:

C+H2O→CO+H2

C+CO2→2CO

CH4+H2O→CO+3H2

CO+H2O→CO2+H2

Tar→CH4+H2O+CnHm+H2

Out of Quencher

* based on T Tzanetakis, 2007

C	54.59	%dry
H	6.74	%dry
O	38.57	%dry
N	0.1	%dry
ρ	1232	kg/m3
μ	32.63	mPa s
H2O	32	wt%
solids	<3	wt%
LHV	14.34	MJ/kg

Tar

* based on T Tzanetakis, 2007

C	85	%dry
H	11	%dry

Chemical Composition of the Products:

Exhaust Gas:

*from study completed by A. Phan 2008

CO	35	%dry
CO2	40	%dry
H2	6	%dry
CH4	13	%dry
CxHy(C2-C3)	2.5	%dry

Tar:

*collected at 400°C; research done by D. Lopez, 2009

C	53.4	%dry
H	6.5	%dry
N	0.2	%dry
O	40	%dry
H:O	1.46	
O:C	0.56	

Radiata Pine Biomass used:

* completed by CRL Energy laboratory, R Bell 2011

C	64.9	%dry
H	5.22	%dry
N	1.16	%dry
S	0.01	%dry
O	28.71	%dry

Char

*from E Salehi, 2011

O	1	%dry			
N	0.3	%dry	MC	1.77	wt%
ρ	940	kg/m3	Ash	12	wt%
	100-				
μ	1000	mPa s			
H2O	<3	wt%	C	75.09	%dry
solids	1	wt%	H	3.12	%dry
LHV	40	MJ/kg	N	1.18	%dry
			O	6.84	%dry
			HV	26.24	MJ/kg

Fuel cost	10	$/GJ
Electricity cost	100	$/MWh

Pulversier: **E101**

MPIC	12000	$

Size Grader: **E103**

*CRL Energy Ltd Data

1000	kg/hr	feed at CRL
MPIC	3500	$
12.5	m3/hr	assume 8000 hrs/yr operational
280	kg/m3	density feed
468.6036	kg/hr	new plant feed flow
a	2/3	
MPIC	2112	$

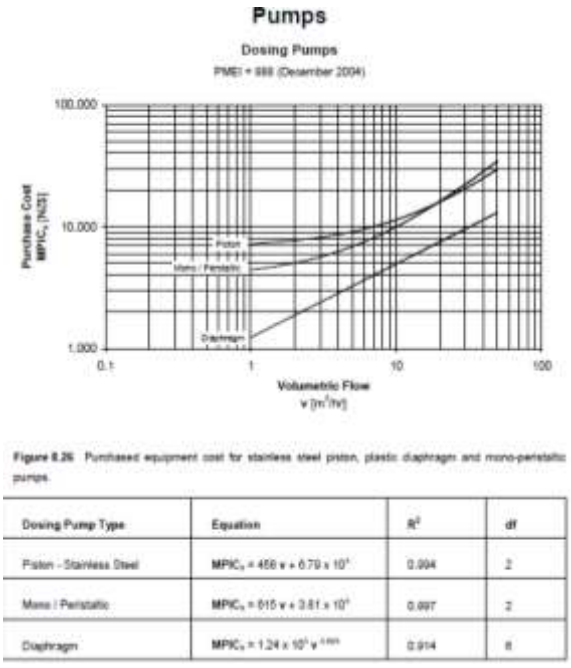

Figure 8.26 Purchased equipment cost for stainless steel piston, plastic diaphragm and mono-peristaltic pumps.

Dosing Pump Type	Equation	R^2	df
Piston - Stainless Steel	$MPIC_p = 456 v + 6.79 \times 10^3$	0.994	2
Mono / Peristaltic	$MPIC_p = 615 v + 3.81 \times 10^3$	0.997	2
Diaphragm	$MPIC_p = 1.24 \times 10^3 v^{0.855}$	0.914	8

P101

S106	92.78351	kg/hr	92.78351
ρ Air	1.27	kg/m3	
v	73.05788	m3/hr	

Price is included in the Price of the Rotary Drier

C101

n	3	* was 2 on the smaller research scale

$$W_s = \frac{n\gamma RT_1}{(0.8)(\gamma - 1)} \cdot \left[\left(\frac{P_2}{P_1}\right)^{(\gamma-1)/n\gamma} - 1\right]$$

ϒ	1.4					
T1	285.15	K	12	°C		
P2	150	kPa			Ws	Shaft Work W
P1	1000	kPa			n	number of stages
R	8.314	J/mol.K			ϒ	ratio of heat capacities
(ϒ-1)/nϒ	0.095238					
P2/P1	0.15					
	-0.1653	$\left[\left(\frac{P_2}{P_1}\right)^{(\gamma-1)/n\gamma} - 1\right]$				
nϒRT1	9957.096					
(0.8)(ϒ-1)	0.32					
	31115.92	$\frac{n\gamma RT_1}{(0.8)(\gamma-1)}$				
W	-5143.34	W				
	5.143337	kW				

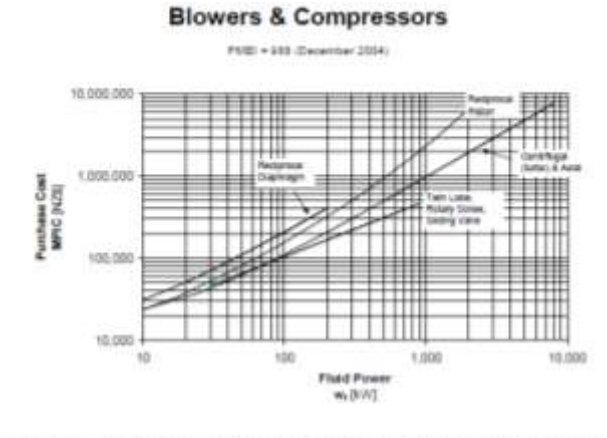

Figure 8.1 Purchased equipment costs of blowers and compressors. Cost of drives are excluded. Note that where $(\dot{W}_s)_p = \dot{m}\left[\frac{g}{n}(n\Delta)\right] = \dot{m}\Delta H_s$, $\dot{W}_s$ = shaft work and η_c = efficiency.

Blower / Compressor Type	Equation
Reciprocal Diaphragm	MPIC = $1.96 \times 10^3 \dot{W}_s + 11.5 \times 10^3$
Reciprocal Piston	MPIC = $0.044 \dot{W}_s^2 + 1.37 \times 10^3 \dot{W}_s + 9.75 \times 10^3$
Centrifugal (turbo) and Axial	MPIC = $362 \dot{W}_s + 14.3 \times 10^3$
Twin Lobe, Rotary Screw, Sliding Vane	MPIC = $4.63 \times 10^3 \dot{W}_s^{0.676}$

Twin Lobe, Rotary Screw, Sliding Vane

MPIC = 4.63 x 103 wf^0.676

MPIC	14008.2	$

H102

N2 heated up

S115	89.88744	kg/hr	89.88744
T1	15	°C	
T2	540	°C	
Cp	1.104	KJ/kgK	*www.engineeringtoolbox.com
Q	52098.76	KW	Q=mCpΔT

MPIC	12000	$

H101

Air heated up

S106	92.78351	kg/hr	92.78351
T1	12	°C	
T2	104	°C	

Cp	1.005	KJ/kgK	*www.engineeringtoolbox.com
Q	8578.763	KW	Q=mCpΔT

Price is included in the Price of the Rotary Drier

E303 + **E304**

MPIC	10000	$	based on an industry bought system

E405	7000	$	ratio control
E404	7000	$	quality tester
E407	2500	$	
E406	2500	$	
E408	6800	$	

P401

	286.3636		
S411	286.3636	kg/hr	
ρ Chemi-			
cal A	1330	kg/m3	
v	0.215311	m3/kg	

Piston-Stainless Steel Pump

MPICx = 458 v + 6.79 x 10^3

MPIC	6889	$

P402

	572.7273		
S412	572.7273	kg/hr	
ρ Bio			
Mix	1167.333	kg/m3	
v	0.490629	m3/kg	

Piston-Stainless Steel Pump

MPICx = 458 v + 6.79 x 10^3

MPIC	7015	$

P404

	389.4545		
S421	389.4545	kg/hr	
ρ Bitu-			
men	970	kg/m3	
v	0.4015	m3/kg	

Piston-Stainless Steel Pump

MPICx = 458 v + 6.79 x 10^3

MPIC	6974	$

Perry's Chemical Engineers' Handbook (7th Edition)/Chapter 10:
Piping may represent as much as 25 percent of the cost of a chemical process plant. The installed cost of piping systems varies widely with the materials of construction and the complexity of the system. A study of piping costs shows that the most economical choice of material for a simple straight piping run may not be the most economical for a complex installation made up of many short runs involving numerous fittings and valves. The economics also depends heavily on the pipe size and fabrication techniques employed. Fabrication methods such as bending to standard long-radius-elbow dimensions and machine-flaring lap joints have a large effect on the cost of fabricating pipe from ductile materials suited to these techniques.

- *C powders* cohesive; small particles (d_p < 30 μm); difficult to fluidize. Channeling occurs readily.
- *A powders* aeratable; relatively small particles (30 < d_p < 150 μm); easy to fluidize. $U_{mf} < U_{mb}$. Homogeneous expansion may occur.
- *B powders* bubbling from the onset of fluidization; larger particles. 150 < d_p < about 500 - 600 μm. Easy to fluidize. $U_{mf} = U_{mb}$.
- *D powders* dense particles. Large particles. d_p > about 500 - 600 μm. $U_{mf} = U_{mb}$.

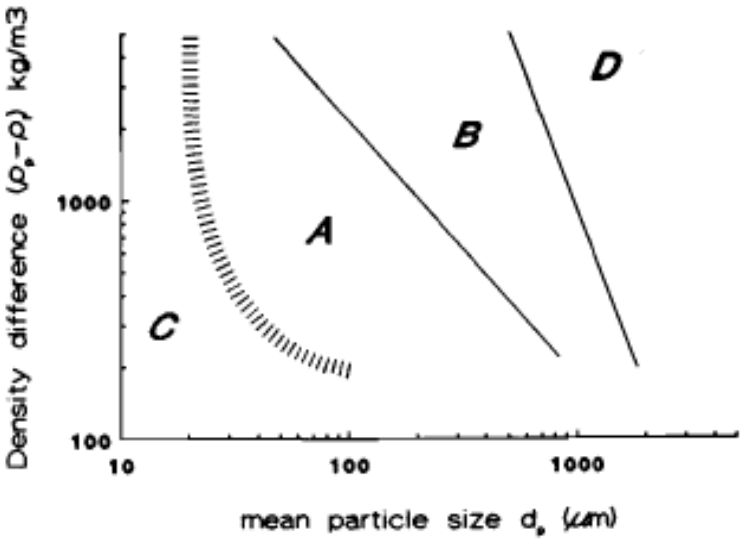

Figure 1.2 *Powder classification according to Geldart (1973).*

$$U_{mf} = \mu \cdot \{ [(33.7)^2 + 0.0408 \cdot Ar]^{1/2} - 33.7 \} / (d_p \cdot \rho_f)$$

$$\text{with } Ar = \frac{d_p^3 \cdot \rho_f \cdot (\rho_p - \rho_f) \cdot g}{\mu^2} .$$

Umf	0.105	Minimum fluidizing velocity	m/s	
B	4.093E-07	*Power-Law Viscosity Law		
		*http://202.118.250.111:8080/fluent/Fluent60_help/html/ug/node28		
n	0.667	2.htm		
μ	3.39E-05	Viscosity in Bed		
dp	0.0004	m sand diameter (0.4 mm=400μm)	B powder	
ρf	280	kg/m3 Density bed		
ρp	2700	kg/m3		
g	9.81			
Voidage at minimum fluid-izing condi-tions, emf:	0.55			
Sphericity	0.67			
T in bed	480	°C		
	753.15	K		
ρ gas	1.27	kg/m3	Ar	2658.902
1-Ɛ	0.45			
Deff	0.0000828	m diameter of one hole		
Ɛ	0.55			
Cd	118.87	Viscous regime assumed		
u	0.14	m/s		
Re	0.32	for viscous regime 0.1<Re<500		
LHS	11913			
RHS	95447			
	697790881			
(LHS-RHS)^2	5			
Dbed	0.18	m given		
π	3.14	constant		
A	0.02	.=D^2*π/4		

$$\frac{\Delta P}{L} = 150\frac{(1-\varepsilon)^2}{\varepsilon^3}\frac{\mu * V_S}{D^2} + 1.75\frac{(1-\varepsilon)}{\varepsilon^3}\frac{\rho_G * V_S^2}{D}$$

$$C_D = \frac{24}{Re}(1 + 0.15 * Re^{0.687})$$

$$u_f^2 = \frac{4Dg(\rho_{part} - \rho_{fluid})}{3C_D\rho_{fluid}}$$

$$Re = \frac{Du\rho}{\mu}$$

$$\frac{\Delta P}{L} = (1-\varepsilon)(\rho_S - \rho_G)g$$

Q	0.0035	m^3/s	.=u*A
Qsecondry	0.21	m^3/hr	in reality will supply 30 m^3/hr to insure that the particles will stay in the column

Qterminal	36.63	m^3/hr	.=Qsecondary-Qmin

Fluidized Bed Rector **R101**

from experemental values:

homogeneous fluidization of current FB with 80mm diameter is 60 l/min of N2 flow in

need to take into account the Ideal Gas Law, as N2 tested under atm conditions, the pyrolysis process occured at 450-480°C

N2 flow	65	l/min	+	5	l/min	
feed	0.7	kg/hr		7.692308	%	
density feed (biomass)	280	kg/m3				
feed volumetric flow rate	0.0025	m3/hr				
Sand particle size	0.4	mm	400	µm		2

Pilot FB design

H reactor	216	mm	reactor height			
H bed	97.2	mm	bed height			
Ddp	75	mm	diameter of distributor plate			
Dh	0.3	mm		300	µm	diameter of distributor plate holes

$$\frac{\Delta P}{L} = 150\frac{(1-\varepsilon)^2}{\varepsilon^3}\frac{\mu * V_S}{D^2} + 1.75\frac{(1-\varepsilon)}{\varepsilon^3}\frac{\rho_G * V_S^2}{D}$$

$$u_f^2 = \frac{4Dg(\rho_{part} - \rho_{fluid})}{3C_D\rho_{fluid}}$$

$$\frac{\Delta P}{L} = (1-\varepsilon)(\rho_S - \rho_G)g$$

Sand & N2

Average particle size of sand, d_s	0.0007	m					
Sand Density, ρ_s	2700	kg/m^3					
N2 Density in Bed, ρ_g	1.27	kg/m^3					
Gravity	9.81	kg/m^2	$\mu = BT^n$	B	4.09E-07	*Power-Law Viscosity Law	
Viscosity in Bed, µ	3.38815E-05	kg/(m.s)		n	0.666667	*http://202.118.250.111:8080/fluent/Fluent60_h	
Voidage at minimum fluidizing conditions, ε_{mf}	0.55			T in bed	480	°C	
Sphericity, ϕ_s	0.67	$Ar = \frac{d_p^3 \cdot \rho_f \cdot (\rho_p - \rho_f) \cdot g}{\mu^2}$			753.15	K	
Ar	10046.17692						21.6
Dbed	0.3	m					
π	3.141592654		constant				
A	0.070685835	m^2	$U_{mf} = \mu \cdot \{ [(33.7)^2 + 0.0408 \cdot Ar]^{1/2} - 33.7\}/(d_p \cdot \rho_f)$				
Minimum fluidizing velocity, U_{mf}	0.213952354	m/s					
Volume flow rate	0.015123401	m^3/s					
	54.44424253	m^3/h					
	907.4040421	l/min	*minimum				
	1179.625255	l/min	.+30%	89.88744	kg/hr	S114	89.9
+	94.37002038	l/min	8% into hopper	7.190996	kg/hr	S113	7.2

Reynolds number

$$C_D = \frac{24}{Re}(1 + 0.15 * Re^{0.687})$$

$$Re = \frac{Du\rho}{\mu}$$

Minimum fluidizing velocity, U_{mf}	0.065106595	m/s
Average particle size of sand, d_s	0.0007	m
N2 Density in Bed, ρ_g	1.27	kg/m^3
Viscosity in Bed, v	3.38815E-05	kg/(m.s)
Reynolds number, Re	0.141586578	for viscous regime 0.1<Re<500

N2:

40	l/min	
2400	l/hr	1000L=1m3
2.4	m3/hr	
1.27	kg/m3	ρ gas
3.048	kg/hr	* currently

3 CAPITAL COST ESTIMATING METHODS

SCENZ

3.4 Scaling Factors

Scaling factors are usually related through a power law relationship. The scaling factor rule, sometimes also known as the power law, six-tenths or two-thirds rule, states that the ratio of the cost of two equivalent pieces of equipment, equals the ratio of the sizes raised to the power of *a*, where *a* is often about $^6/_{10}$ or $^2/_3$ (thus the name), especially for vessels. For some plant however, this may range from 0.3 to 1.0. This is shown by equation 1; where C_S is the cost of the plant or equipment to be estimated at the size, *S*. C_r is the known reference cost of a plant or equipment at the known reference size, S_r.

$$\frac{C_S}{C_r} = \left(\frac{S}{S_r}\right)^a \quad (1)$$

*CRL Energy Ltd Data				
	20	kg/hr	feed	
MPIC		250000	$	
	0.0025	m3/hr	assume 8000hrs/yr operational	
			density	
	280	kg/m3	feed	
	0.7	kg/hr	S109	454.5455
a		0.25		
		108133	$	
MPIC		545854	$	

Distillation Column:		**R401**	refer to S Wang, 2009; redesign if have time	
In				
S414	114.55	kg/hr		114.55
Out				
S419	97.36	kg/hr	85%	97.36
S405	28.64	kg/hr	25%	28.64
S415	31.50	kg/hr	105%	31.50
S417	2.86	kg/hr	5%	2.86

From Research completed known, that 83% processes out of 'usable' material from the Distillation Column and 17% follows as 'waste' to recycle

			* case completed for a previous re-
Total Flow	7205.7	kg/hr	search
Temperature	60	°C	
Pressure	1700		
Tray spacing l_t	0.55	m	
Diameter	1.5	m	
No. Trays	10.0		
Height	5.5	m	
Lang Factor	4.2		
Shell	26625.8	Vertical	
Scaling Factor			
Cost	1.7		
Shell Cost	45263.91		
Tray cost	580.0		
	5800.0	US$	
	7656.0	$NZ	
Total Cost 1			
column	118200	$	Added 30,000 dollars for Boiler and condensor

Cost index 1991/2012		Conversion	
1.666666667			1.32
ρ_l	748.40	kg/m3	
ρ_v	21.83	kg/m3	
u_v	0.28889		
V_w	696.1	Max Vap rate kg/s	
D_c	11.9	m	

L		47.42	m
	7205.67	kg/hr	feed
MPIC		118200	$
			assume 8000hrs/yr op-
	12.5	m3/hr	erational
	280	kg/m3	density feed
	114.55	kg/hr	new plant feed
a		0.1	
MPIC		78117	$

Coulson & Richardson's Chemical Engineering. Vol. 6, Chemical Engineering Design, 4th Ed

Distillation Column: **R401**

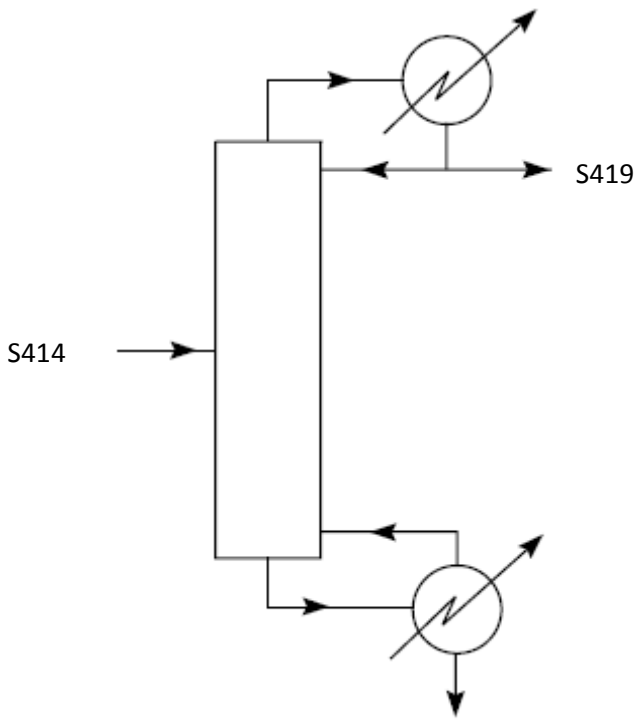

Bio Bitumen

250 °C

Chemical A layer

60 °C

In			
S414	114.5455	kg/hr	114.5455
Out			
S416	97.36	kg/hr	85%
S419	17.18182	kg/hr	15%

From Research completed known, that 83% processes out of 'usable' material from the Distillation Column and 17% follows as 'waste' to recycle

* case completed for a previous research

Total Flow	115	kg/hr
Temperature	60	°C
Pressure	1700	
Tray spacing l_t	0.55	m
Diameter	0.3	m
No. Trays	3.0	
Height	1.7	m
Lang Factor	4.2	
Column Cost	4323	US$
	5707	$NZ
Tray cost	580	$ per tray
	1740	US$
	2297	$NZ

$$\mathbf{MPIC} = 2.64 \times 10^3 \, \mathbf{h}^{0.985}$$

Added 30,000 dollars for Boiler and condensor

Total Cost	43339	$	
Cost index 1991/2012		Conversion	
1.666666667			1.32
ρ_l	748.40	kg/m3	
ρ_v	21.83	kg/m3	
u_v	0.28889		
V_w	696.1	Max Vap rate kg/s	
D_c	11.9	m	
L	47.42	m	

Example 1.1

The optimum proportions for a cylindrical container. A classical example of the optimisation of a simple function.

The surface area, A, of a closed cylinder is:

$$A = \pi \times D \times L + 2\frac{\pi}{4}D^2$$

where D = vessel diameter
L = vessel length (or height)

This will be the objective function which is to be minimised; simplified:

$$f(D \times L) = D \times L + \frac{D^2}{2} \qquad \text{(equation A)}$$

For a given volume, V, the diameter and length are related by:

$$V = \frac{\pi}{4}D^2 \times L$$

and

$$L = \frac{4V}{\pi D^2} \qquad \text{(equation B)}$$

and the objective function becomes

$$f(D) = \frac{4V}{\pi D} + \frac{D^2}{2}$$

Setting the differential of this function zero will give the optimum value for D

$$\frac{-4V}{\pi D^2} + D = 0$$

$$D = \sqrt[3]{\frac{4V}{\pi}}$$

From equation B, the corresponding length will be:

$$L = \sqrt[3]{\frac{4V}{\pi}}$$

So for a cylindrical container the minimum surface area to enclose a given volume is obtained when the length is made equal to the diameter.

In practice, when cost is taken as the objective function, the optimum will be nearer $L = 2D$; the proportions of the ubiquitous tin can, and oil drum. This is because the cost

V	590.9	kg/hr	S414
ρ	1000	kg/m3	
π	3.141593		
V*	0.5909	m3/hr	
D	0.250786	m	Column diameter
L	0.909511	m	Column height

114.5454545	kg/hr	feed
MPIC	43339	$
		assume 8000hrs/yr opera-
12.5	m3/hr	tional
1000	kg/m3	density feed
12500	kg/hr	new plant feed
a	0.1	
MPIC	69291	$

EQUIPMENT LIST

Process	Equipment	
	ID	Name
Biomass Pyrolysis	E101	Pulversier
	E102	Rotary Drier
	E103	4mm Size Grater
	E104	Screw Feeder Auger 1
	E105	Screw Feeder Auger 2
	P101	Pump
	C101	Compressor/Pressure Relief System
	H101	Fired Heater 1
	H102	Fired Heater 2
	R101	Fluidised Bed Reactor
	T101	Log Storage Shed
	T102	Biomass Storage Tank
	T103	Lock Hopper
	M101	Motor for Auger 1
	M102	Motor for Auger 2
Phase Separation Process	E201	Cyclone 1
	E202	Cyclone 2
	E203	Quencher 1
	E204	Quencher 2

Process	Equipment	
	ID	Name
Gas Condensation and Hydrocarbons Production	E301	Electrostatic Precipitator
	E302	Gas Sampling System
	E303	Gas Flare
	E304	Air Compressor
	E305	Oil Separator
	E306	Air Dryer
	E307	Air Filters
	E308	Buffer Tank
	E309	N2 Generator
	E310	N2 Compressor
	E311	Gas Mixer Tank
Bio-Bitumen Production	E401	Mixer 1
	E402	Separation Unit
	E403	Mixer 2 (Heated)
	E404	Recycling Filtration System
	E405	Ratio Controller
	E406	Heat Exchanger 1 /Heater
	E407	Heat Exchanger 2
	T401	Bitumen Storage Tank 1

	E205	Stainless Steel Mesh Condenser

	T402	Dichloromethyl Storage Tank
	T403	Bio-Bitumen Storage Tank 1
	T404	Bio-HydroCarbons Tank
	R401	Distillation Column
	P401	Pump
	P402	Pump
	P403	Pump
	P404	Pump

8.12 Economics

Inputs/ Product

Operating: 8000 hrs/yr

Inputs/ Product	Streams	Flow (kg/hr)	Flow (kg/yr)	Flow (tonne/yr)	$/tonne	$/yr
Wood	S101	531	4247423	4247	$ 50	$ 212,371
Nitrogen	S309 use	106	848000	848	$ 1,500	$ 1,272,000
Bitumen	S406	428	3427200	3427	$ 1,000	$ 3,427,200
Chemical A	S407	14	114545	115	$ 100	$ 11,455
Bio-Bitumen	S423	487	3894545	3895	$ 1,500	$ 5,841,818
Nitrogen	S114 sell	90	719100	719	$ 1,500	$ 1,078,649
Bio-Char	S204+205	68	545455	545	$ 1,000	$ 545,455
						$ 7,465,922
Capital Cost						$ 3,054,435

Utilities

Utilities	Streams	Flow (kg/hr)	Flow (kg/yr)	Flow (tonne/yr)	$/tonne	$/yr
Water	S209	346	2767497	2767	$ 240	$ 664,199

Electricity		$ 36,536
Water		$ 664,199
Total Annual Utilities	$ 700,736	

Labour

Position	Number	Base Salary or Hourly	Total Annual
General Plant Manager	1	$ 85,000	$85,000
Secretary/ Receptionist	1	$ 35,000	$35,000
Laboratory Manager	1	$ 65,000	$65,000
Engineering Technitian	1	$ 65,000	$65,000

I T Support	300 hrs/yr	$ 75/hr	$22,500
Plant Operator	3	$ 80,000	$240,000
Chemical Engineer	1	$ 75,000	$ 75,000
Electrician	300 hrs/yr	$ 75/hr	$ 22,500
Total Annual Labor			$610,000

in	$ 3,651,026
out	$ 6,920,468
η	53

% is the Conversion Efficiency

N2 Cost:

** Based on AirLiquid Quote : N2 $44/10 m3 + $17.50/month bottle rental

* AirLiquid is cheaper then BOC

ManPack is 16 x 10 cm3 cylindersof pure N2 costs $683.51

Rental Cost	17.5	$/month
Gas Cost	4.4	$/m3
ρN2	1.27	kg/m3
Gas Cost	3.464567	$/kg
	3465	$/tonne

Wood:

	per	
$1,400	28	
	tonne	
	$50	$/tonne

Water Cost:

** Based on 'Rotorua District Council Water Supply Rates and Charges'

* and infornmation provided by Rotorua Waste Water Treatment Plant, R Bell

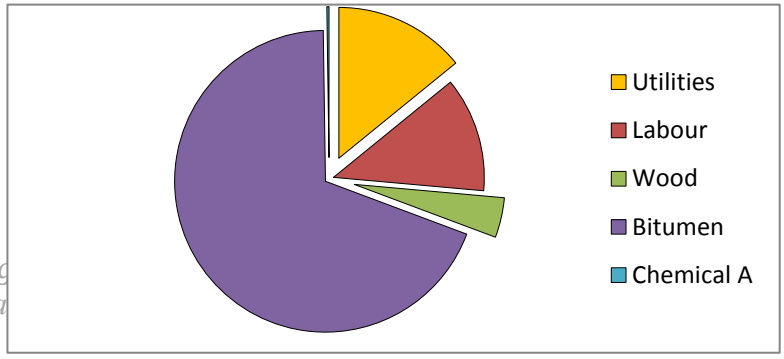

Re: JB's Form

JB's Environmental [jbatjbs@xtra.co.nz]

Good afternoon Olga

We are pleased to offer you the following quotation for supply and delivery of sawdust.
Supply and deliver to Wellington, one x truck and trailer load (70m3) approx. 28 tonne of clean fresh green sawdust from mill. $1400 plus GST per load.

Kind regards
Helen Bak-Bertram
Office Administrator
JB's Environmental Ltd
28 Tararua Road
PO Box 190
LEVIN 5540
Fax 06 367 9019
Mob 021 750 928

-----Original Message-----
From: <oko14@uclive.ac.nz>
Sent: Friday, March 15, 2013 11:46 AM
To: jbatjbs@xtra.co.nz
Subject: JB's Form
The following information was sent from a form on your website:
Name: olga kolokolova
Email: oko14@uclive.ac.nz
Contact number: 570 3713

Message: Good Afternoon. My name is Olga. I am working for a research company in Petone. We are considering a process upgrade, and as a feedstock we are considering to purchase sawdust in a few hundred tonnes a year. In order to complete the techno economic analysis I need some quotes from industry representatives and potential future suppliers. I was wondering if you would be able to give me a quote please. What would be a price for a tonne of pine sawdust? Thank you

Regards,
Olga.

Sent: Tuesday, 19 March 2013 1:37 p.m.

To: Olga Kolokolova

Re: JB's Form Page 1 of 1

https://bluprd0210.outlook.com/owa/?ae=Item&t=IPM.Note&id=RgAAAACc0mivB... 20/03/2013

Main Plant Item Cost

Stage	Equipment	Cost (NZ$)	Proportion of MPIC	Cost (NZ$) Million
Biomass Pyrolysis	Pulversier	$ -	0.00	0.00
	Rotary Drier	$ 24,106	6.93	0.02
	4mm Size Grater	$ 93	0.03	0.00
	Fluidised Bed Reactor	$ -	0.00	0.00
	Delivered Biomass Storage Tank	$ 4,051	1.16	0.00
	Biomass Storage Prior Hopper	$ 3,646	1.05	0.00
			0.00	0.00
	Fired Heater 2	$ -	0.00	0.00
	Lock Hopper, Screw Feeder Auger 1, Screw Feeder Auger 2, Motor for Auger 1, Motor for Auger 2	$ 7,079	2.03	0.01
Phase Separation Process	Cyclone 1	$ 1,267	0.36	0.00
	Cyclone 2	$ 845	0.24	0.00
	Quencher 1	$ 2,565	0.74	0.00
	Quencher 2	$ 3,450	0.99	0.00
	Stainless Steel Mesh Condenser	$ 2,065	0.59	0.00
Gas Condensation and Hydrocar-bons Production	N2 Generator Plant	$ 70,000	20.12	0.07
	Electrostatic Precipitator	$ 55,000	15.81	0.06
	Gas Sampling System, Gas Analysis System	$ 10,000	2.87	0.01
	Gas Flare	$ 10,000	2.87	0.01
	Gas Mixer Tank	$ 21,500	6.18	0.02
Bio-Bitumen Production	Mixer 1	$ 21,690	6.23	0.02
	Separation Unit	$ 7,000	2.01	0.01
	Mixer 2 (Heated)	$ 21,620	6.21	0.02
	Recycling Filtration System	$ 7,000	2.01	0.01
	Ratio Controller	$ 7,000	2.01	0.01
	Heat Exchanger 1 /Heater	$ 2,500	0.72	0.00
	Heat Exchanger 2	$ 2,500	0.72	0.00
	Bitumen Storage Tank 1	$ 10,883	3.13	0.01
	Dichloromethyl Storage Tank	$ 8,557	2.46	0.01

%MPIC	Stage
11.20	**Biomass Pretreatment**
0.00	**Biomass Pyrolysis**
2.93	**Phase Separation Process**
47.85	**Gas Condensation and Hydrocar-bons Production**
38.02	**Bio-Bitumen Production**

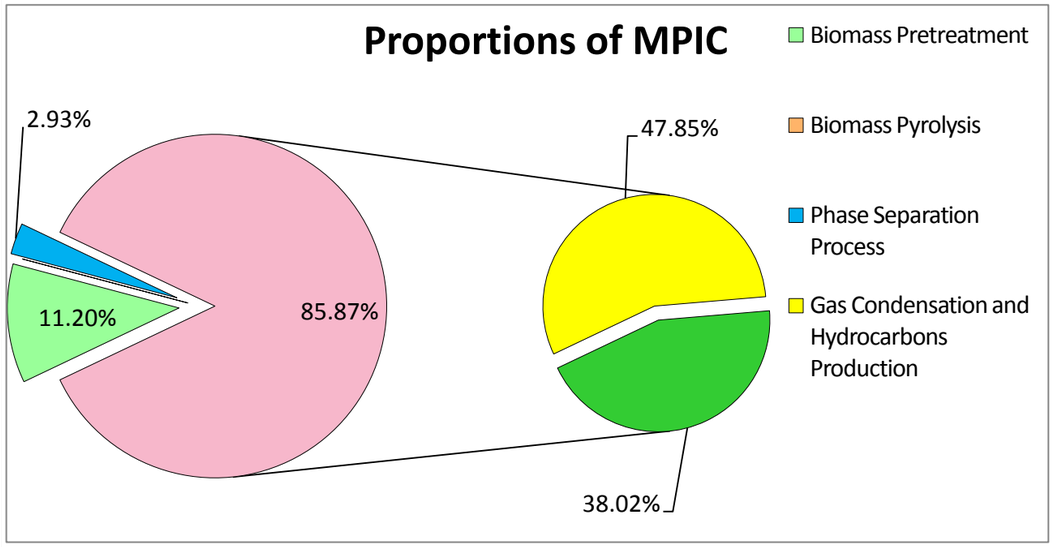

Operating hours per year 8000 hr/yr

Details	%
Total Physical Plant Cost	5.95E+01
Total Direct & Pysical Plant Cost	3.26E+01
Fixed Capital Investment	8.70E+01
Biomass Pretreatment	$38,976
Biomass Pyrolysis	$0
Phase Separation Process	$10,194
Gas Condensation and Hydrocarbons Produc-	$166,500

	Bio-Bitumen Storage Tank 1	$ 11,078	3.18	0.01
	Bio-HydroCarbons Tank	$ 11,589	3.33	0.01
	Distillation Column	$ -	0.00	0.00
	Pump 1	$ 6,889	1.98	0.01
	Pump 2	$ 7,015	2.02	0.01
	Pump 4	$ 6,974	2.00	0.01
Main Plant Item Cost		$ 347,965	100.00	0.35

tion	
Bio-Bitumen Production	$132,295
Pumps	$20,877
Heaters	$0
Compressors	$10,000
Heat Exchangers	$11,016
Total Capex ($Mil)	$0.35

Details	Lang Factor	Cost(NZD$)	Cost (NZ$) Million
Process Equipment Cost	**0.95**	**$ 347,965**	0.35
Delivered Process Equipment Cost	1.00	$ 365,363	0.37
Installation	0.41	$ 149,799	0.15
Instrumentation & Controls	0.13	$ 47,497	0.05
Piping	0.25	$ 91,341	0.09
Electrical	0.10	$ 36,536	0.04
Battery limits and service	0.29	$ 105,955	0.11
Evacuation and site preparation	0.10	$ 36,536	0.04
Auxilliaries	0.50	$ 182,682	0.18
Total Physical Plant Cost	**2.78**	**$ 1,015,709**	1.02
Engineering & Supervision	0.39	$ 142,492	0.14
Construction Expenses (Field Expenses)	0.37	$ 135,184	0.14
Total Direct Plant Cost	0.76	$ 277,676	0.28
Total Direct & Physical Plant Cost	**3.54**	**$ 555,352**	0.56
Contractor's Fee	0.13	$ 47,497	0.05
Contingency	0.39	$ 142,492	0.14
Fixed Capital Investment	**4.06**	**$ 1,483,374**	1.48
Working Capital	0.61	$ 222,506	
Total Capital Investment	**4.67**	**$ 1,705,880**	1.71

Total Physical Plant Cost	$ 1,015,709
Total Direct & Physical Plant Cost	$ 555,352
Fixed Capital Investment	$ 1,483,374
Capital Cost	**$ 3,054,435**
Total Annual Labor	$ 610,000
Total Annual Utilities	$ 700,736

Depreciation of Total Capital Investment

Assuming 15 years of a plant lifetime depreciation

Total Capital Investment $3,054,435 $NZ

Salvage Value is $0

Decreasing Method

Years	Book Value Year Start	Total Cost Depreciable	Depreciation Percent	Depreciation Expense	Accumulated Depreciation	Book Value Year End
1	$3,054,435	$3,054,435	12.50%	$381,804	$381,804	$2,672,631
2	$2,672,631	$3,054,435	11.67%	$311,807	$693,611	$2,360,824
3	$2,360,824	$3,054,435	10.83%	$255,756	$949,367	$2,105,068
4	$2,105,068	$3,054,435	10.00%	$210,507	$1,159,874	$1,894,561
5	$1,894,561	$3,054,435	9.17%	$173,668	$1,333,542	$1,720,893
6	$1,720,893	$3,054,435	8.33%	$143,408	$1,476,950	$1,577,485
7	$1,577,485	$3,054,435	7.50%	$118,311	$1,595,261	$1,459,174
8	$1,459,174	$3,054,435	6.67%	$97,278	$1,692,539	$1,361,896
9	$1,361,896	$3,054,435	5.83%	$79,444	$1,771,983	$1,282,452
10	$1,282,452	$3,054,435	5.00%	$64,123	$1,836,106	$1,218,329
11	$1,218,329	$3,054,435	4.17%	$50,764	$1,886,870	$1,167,565
12	$1,167,565	$3,054,435	3.33%	$38,919	$1,925,788	$1,128,646
13	$1,128,646	$3,054,435	2.50%	$28,216	$1,954,005	$1,100,430
14	$1,100,430	$3,054,435	1.67%	$18,341	$1,972,345	$1,082,090
15	$1,082,090	$3,054,435	0.83%	$9,017	$1,981,363	$0
120			100.00%		$22,611,409	

Straight Line Depreciation

Annual Deppreciation Value $203,629.00 $NZ/yr

Period	Book Value Period Start	Depreciation Expense	Accumulated Depreciation	Book Value Period End
1	$3,054,435	$203,629	$203,629	$2,850,806
2	$2,850,806	$203,629	$407,258	$2,647,177
3	$2,647,177	$203,629	$610,887	$2,443,548
4	$2,443,548	$203,629	$814,516	$2,239,919
5	$2,239,919	$203,629	$1,018,145	$2,036,290
6	$2,036,290	$203,629	$1,221,774	$1,832,661

Depreciable Cost = Original Cost - Salvage Value = (Cost - Salvage)

Salvage Value - The estimated value that an asset will realize upon its sale at the end of its useful life

The sum of years digits method is accelerated depreciation.

Depreciation is taken as a fractional part of a sum of all the years.

The straight line calculation, as the name suggests, is a straight line drop in asset value. The depreciation of an asset is spread evenly across the life.

7	$1,832,661	$203,629	$1,425,403	$1,629,032
8	$1,629,032	$203,629	$1,629,032	$1,425,403
9	$1,425,403	$203,629	$1,832,661	$1,221,774
10	$1,221,774	$203,629	$2,036,290	$1,018,145
11	$1,018,145	$203,629	$2,239,919	$814,516
12	$814,516	$203,629	$2,443,548	$610,887
13	$610,887	$203,629	$2,647,177	$407,258
14	$407,258	$203,629	$2,850,806	$203,629
15	$203,629	$203,629	$3,054,435	$0

Summary of Production Costs:

Variable Costs

			Process Case:
Raw materials, solvent make-up	$	3,651,026	65% bio-oil and tar
Miscellaneous materials, 10% of maintenance cost	$	7,417	15% bio-char
Utilities	$	700,736	
Shipping and packaging	$	-	80% bitumen
Administration Costs	$	183,266	20% bio-mix
Distribution and Selling Costs	$	122,177	
			$
	Sub Total		***4,664,622***
Annual Production Rate of Bio-Bitumen		3895	tonne/yr
Price of Raw Materials	$	937	$/tonne Bio-Bitumen produced

Fixed Cost:

Maintenance, take as 5% of fixed capital	$	74,169		
Operating labour, allow one extra man on days.	$	-		
Supervision, no additional supervision would be needed	$	-		
Plant overheads, take as 50% of operating labour	$	305,000		
Total Annual Labor	$	610,000		
Capital charges, 6% of fixed capital (bank rate 4%)	$	14,834		
Insurance, 1% of fixed capital	$	14,834		
Local taxes	$	-		
Royalties	$	-		
Depreciation	$	203,629		
Rates of Land, Local Taxes and Insurance	$	42,762		
Direct Product Costs	Sub Total		***$***	***1,010,691***

Sales Expense	$	283,766		
Research and Development	$	152,722		
	Sub Total		***$***	***436,487***

Annual Production Cost	***$***	***5,675,313***	$/yr
Annual Production Rate of Bio-Bitumen		4000	tonne/yr
Production Cost	***$***	***1,419***	$/tonne Bio-Bitumen produced

By Olga Kolokolova

7/10/2013

Special Chemical is part of the original investment, as mostly recycled

Nitrogen is part of the original investment, as produced on site.

	Process Flow Case 1	Case 1 tonne/yr	Process Flow Case 2	Case 2 tonne/yr	Process Flow Case 3	Case 3 tonne/yr	Process Flow Case 4	Case 4 tonne/yr	Process Flow Case 5	Case 5 tonne/yr	Process Flow Case 6	Case 6 tonne/yr	Process Flow Case 7	Case 7 tonne/yr	Process Flow Case 8	Case 8 tonne/yr	Process Flow Case 9	Case 9 tonne/yr
Wood feed	100%	4247	100%	4247	100%	4247	100%	4247	100%	4247	100%	4247	100%	4247	100%	4247	100%	4247
Bio-Char	20%	849.4	14%	594.6	14%	594.6	20%	849.4	17%	722.0	17%	722.0	20%	849.4	14%	594.6	17%	722.0
Bio-Oil+Tar	65%	2761	38%	1614	38%	1614	65%	2761	52%	2187	52%	2208	65%	2761	38%	1614	52%	2208
After DCM Extraction	27%	745.3	27%	435.7	27%	435.7	27%	745.3	27%	590.5	27%	596.3	27%	745.3	27%	435.7	27%	596.3
Distillation	86%	641	86%	375	86%	375	86%	641	86%	508	86%	513	86%	641	86%	375	86%	513
Bio-Mix	20%	641.0	10%	374.7	20%	374.7	10%	641.0	20%	507.9	10%	512.8	50%	641.0	50%	374.7	50%	512.8
Bitumen	80%	2564	90%	3373	80%	1499	90%	5769	80%	2031	90%	4615	50%	641	50%	375	50%	513
Bio-Bitumen	100%	3205.0	100%	3747.4	100%	1873.7	100%	6410.0	100%	2539.3	100%	5128.0	100%	1282.0	100%	749.5	100%	1025.6

Inputs/ Product	$/tonne	$/yr	$/yr	$/yr	$/yr	$/yr	$/yr	$/tonne	$/yr	$/yr	$/yr
Wood	$ 50	$ 212,350	$ 212,350	$ 212,350	$ 212,350	$ 212,350	$ 212,350	$ 50	$ 212,350	$ 212,350	$ 212,350
Bitumen	$ 1,000	$2,563,999	$3,372,645	$1,498,953	$5,768,997	$2,031,476	$4,615,198	$ 1,000	$ 641,000	$ 374,738	$ 512,800
Bio-Bitumen	$ 1,200	$3,845,998	$4,496,860	$2,248,430	$7,691,997	$3,047,214	$6,153,597	$ 1,150	$1,538,399	$ 899,372	$1,230,719
Bio-Char	$ 1,000	$ 849,400	$ 594,580	$ 594,580	$ 849,400	$ 721,990	$ 721,990	$ 1,000	$ 849,400	$ 594,580	$ 721,990

Cost		$2,776,349	$3,584,995	$1,711,303	$5,981,347	$2,243,826	$4,827,548		$ 853,350	$ 587,088	$ 725,150
Gain		$4,695,398	$5,091,440	$2,843,010	$8,541,397	$3,769,204	$6,875,587		$2,387,799	$1,493,952	$1,952,709
Total Bio-bitumen	tonnes	3205	3747	1874	6410	2539	5128	tonnes	1282	749	1026
Cost /tonne	$/tonne of Bio-bitumen	$ 866	$ 957	$ 913	$ 933	$ 884	$ 941	$/tonne of Bio-bitumen	$ 666	$ 783	$ 707

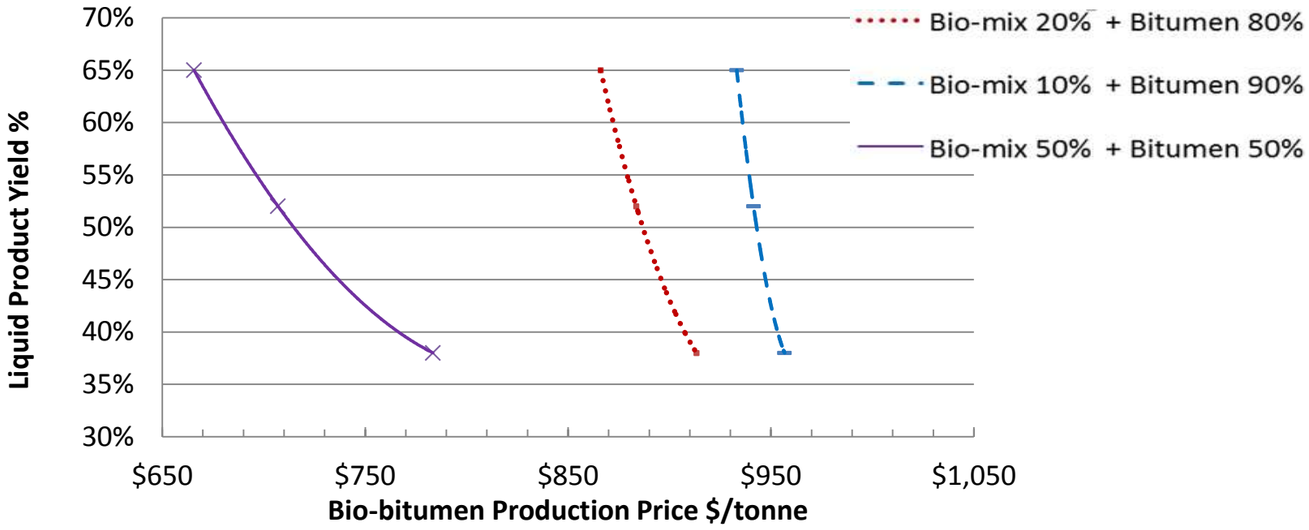
70%
65%
60%
55%
50%
45%
40%
35%
30%
Liquid Product Yield %
$650
$750
$850
$950
$1,050
Bio-bitumen Production Price $/tonne
Bio-mix 20% + Bitumen 80%
Bio-mix 10% + Bitumen 90%
Bio-mix 50% + Bitumen 50%

$$Price = 8.3(Bio-Char) + 93.3(Bio-Oil+Tar) + 411.8(Bio-Mix) + 941(Bitumen)$$

										Constants	
Bio-Char	20%	20%	17%	17%	14%	14%	17%	14%	20%	8.2478	A
Bio-Oil+Tar	65%	65%	52%	52%	38%	38%	52%	38%	65%	93.2586	B
Bio-Mix	20%	10%	20%	10%	10%	20%	50%	50%	50%	411.7778	C
Bitumen	80%	90%	80%	90%	90%	80%	50%	50%	50%	940.9583	D
$/tonne of Bio-bitumen	$ 866	$ 933.13	$ 883.62	$ 941.41	$ 956.67	$ 913.33	$ 707.05	$ 783.33	$ 665.6	P	
	897.39	950.31	884.55	937.94	924.63	871.72	726.26	712.96	738.64		
	-$ 31	-$ 17	-$ 1	$ 3	$ 32	$ 42	-$ 19	$ 70	-$ 73	$ 6	

Bio-mix 20% + Bitumen 80%

Bio-Oil+Tar	$/tonne of bitumen
65%	$ 866.00
52%	$ 883.62
38%	$ 913.33

Bio-mix 50% + Bitumen 50%

Constants Caluclations Iterations

	Constants									Avg
A	8.2474	8.2478	8.2481	8.2482	8.2485	8.2487	8.2469	8.2503	8.2444	8.2478
B	93.1756	93.3418	93.4327	93.4631	93.5939	93.6628	92.9315	94.1070	91.6188	93.2586
C	412.0227	413.0240	413.9750	414.0897	414.7655	415.4778	401.6407	430.5326	390.5	411.7778
D	901.7273	921.6732	939.1323	944.4433	976.0821	991.8608	913.0023	1062.2973	818.4	940.9583

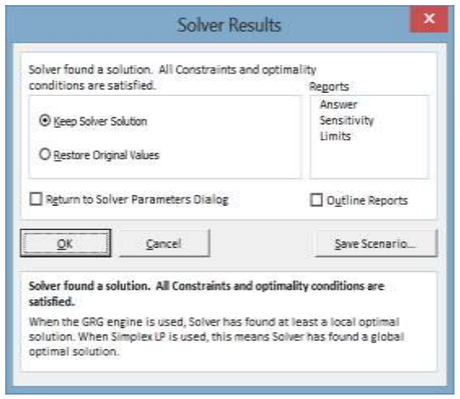

Bio-Oil+Tar	$/tonne of bitumen
65%	$ 665.64
52%	$ 707.05
38%	$ 783.33

Bio-mix 10% + Bitumen 90%

$$Price = 10.1(Bio-Char) + 209.2(Bio-Oil+Tar) + 1010(Bitumen)$$

										Constants
Bio-Char	20%	20%	17%	17%	14%	14%	17%	14%	20%	10.0627827
Bio-Oil+Tar	65%	65%	52%	52%	38%	38%	52%	38%	65%	209.167348
Bitumen	80%	90%	80%	90%	90%	80%	50%	50%	50%	1009.94775
$/tonne of Bio-bitumen	$ 866	$ 933.13	$ 883.62	$ 941.41	$ 956.67	$ 913.33	$ 707.05	$ 783.33	665.64	P
	945.93	1046.92	917.39	1019.43	989.85	888.85	615.45	585.87	642.95	
	-$ 80	-$ 114	-$ 34	-$ 78	-$ 33	$ 24	$ 92	$ 197	$ 23	-$ 2

Bio-Oil+Tar	$/tonne of bitumen
65%	$ 933.13
52%	$ 941.41
38%	$ 956.67

Constants Caluclations Iterations

	Constants									Avg
A	8.5010	9.9999	10.0014	10.0003	10.0008	10.0008	10.6322	10.7306288	10.6979	10.0628
B	92.6339	92.9285	93.3629	93.0489	93.1702	93.1703	380.274	721.916751	240.001	211.1673
C	1000.1107	967.3295	1042.2984	989.9061	1022.4401	1022.4451	1015	1015	1015	1009.9478